Light Perception in Marine Diatoms and Characterization of a Novel Phytochrome from *Phaeodactylum tricornutum*

Thesis

UNRESTRICTED

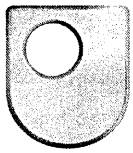

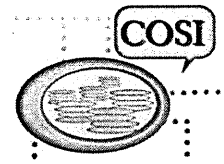

Light Perception in Marine Diatoms and Characterization of a Novel Phytochrome from *Phaeodactylum tricornutum*

Frauke A. Depauw

Thesis submitted for the degree of
Doctor in Philosophy (PhD) in Biological Science

Date of Submission: 28 June 2012
Date of Award: 29 December 2014

Stazione Zoologica 'Anton Dohrn' Napoli, Italy

ProQuest LLC.
789 East Eisenhower Parkway
P.O. Box 1346
Ann Arbor, MI 48106 – 1346

Director of studies:	Dr. Gabriele Procaccini (SZN, Italy)
Co-Director of Studies:	Prof. Dr. Angela Falciatore (UPMC Paris, France)
Internal supervisor:	Prof. Dr. Maria Immacolata Ferrante (SZN, Italy)
Examination panel:	Dr. Marina Montresor (SZN, Italy)
	Dr. Maria Ina Arnone (SZN, Italy)
	Prof. Dr. Philip Gilmartin (UEA, UK)

The most exciting phrase to hear in science, the one that heralds new discoveries, is not "Eureka!" ("I found it!") but rather, "Hmmm... That's funny ..."

Isaac Asimov

Acknowledgements

This PhD thesis has taken me from Belgium to enchanting Naples and the metropolis of Paris, and with every step of the journey my suitcase was filled with more valuable memories and crazy anecdotes. I would never have been able to complete this incredible adventure without the aid and support of countless people.

My first debt of gratitude goes to Dr. Angela Falciatore, my director of studies for giving me the opportunity to work on this thesis in her lab and for patiently guiding my research. I want to thank her for sharing her 'diatom' passion and to encourage me during the tough moments of phytochrome research. My sincere thanks go to Prof. Dr. Maurizio Ribera d'Alcalà, for his invaluable advice and knowledge. Especially our conversations on transpectral processes and Raman scattering will stay in my memories. I want to express my gratefulness also to Prof. Dr. Christian Fankhauser, for his expertise, guidance and helpful suggestions during this PhD project. I would like to thank Dr. Gabriele Procaccini for his guidance and patience in the 'second phase' of the thesis. I appreciated the encouraging and comforting words that all would be well at the end. "The end" took almost two years and you were there every step of the way. Thanks.

I would like to warmly thank all my colleagues from the SZN, with special attention to Monia Russo and Maria Grazia Adelfi for their help and especially for teaching me Neapolitan. Also our lab technician, Alessandro Manfredonia, deserves a big 'thank you' for making liters of all kinds of seawater, hundreds of agar plates and for his friendship. I would like to thank Giovanna Benvenuto for her help with the microscope and Raffaella Raniello for her help during the first months of the thesis.

My colleagues in the diatom lab in Paris deserve my utmost appreciation. Thanks for always being by my side, for your help and company during endless time course experiments, for your enthusiasm in times of joy and for your support when experiments didn't work out. A special thanks goes to Alessandra Rogato for teaching me the basics of diatom biology. I want to express my gratitude also to Antonio Fortunato for always being ready to help me and for the many funny and vivid conversations about our shared interest in GOT. I want to warmly thank also Soizic Cheminant, Carmen and My-Hai for their great help with the phytochrome experiments. I am happy to express my gratitude also toward Amy Kirkham for kindly helping to create the phytochrome knock-down lines in *Thalassiosira* and to Marie Huysman for her' diatom advices' and her friendship. I would like to thank also the 'levure' teams for creating a pleasant atmosphere in the lab and the kitchen with their good mood and jokes. Thank you Nicolas, Alex,

Hélène, Gilles, Ingrid, Frédéric, Mathilde, Sébastien, Geneviève, Jawad and Thierry. Thanks also to all the members of the bioinformatics team of Prof. Dr. Alessandra Carbone, for making me feel welcome in the group and for your good humor during lunch and coffee breaks.

This work would not have been possible without the financial support of the European Commission, Marie Curie Actions. Because I was involved in the Initial Training Network on Chloroplast Signaling (COSI), I want to thank all people of the consortium and especially Dr. Markus Teige, the coordinator of the COSI, for his endless energy and enthusiasm during the COSI meetings and workshops. I also want to thank Prof. Dr. Ute Vothknecht and Agostinho Rocha for giving me the opportunity to help organizing the COSI symposium in Croatia. And of course, last but not least, thanks to all the PhD students and postdocs (Michele, Mikko, Irina, Daniel, Simon, Jenny, Philipp, Chhavi, Judit, Norbert, Sascha, Arianna and Agostinho) in the COSI program, I have had such a wonderful time with all of you during the meetings and workshops all over Europe!

Ik wil mijn vrienden in België bedanken, om toch te blijven contact houden, ook al was ik in het verre Napels of het drukke Parijs. Bedankt om me te komen opzoeken tijdens de afgelopen jaren, als het voor mij te moeilijk was om naar België te komen. Ik doe binnenkort mijn best om weer wat vaker bij de bende te zijn! Een extra dikke mercie aan Brecht, Steffie en Anne! Een special woordje van dank gaat naar Jenny, men dierbare collegaatje, kamergenote op de vele COSI meetings en mijn 'taxi' van België naar Parijs. Bedankt voor alles, je vriendschap heeft enorm veel voor me betekent de afgelopen jaren!

Dit doctoraat was nooit tot een goed einde gekomen zonder de hulp, steun en liefde van het thuisfront. Bedankt, mams en paps, om er voor me te zijn elke stap van de weg en om te blijven geloven in me. Ook een mercietje aan Ybert en Josje, voor de schouderklopjes. Ik ben blij dat we binnenkort de verloren tijd wat kunnen inhalen!

Table of contents

List of Figures and Tables 10

List of abbreviations 12

Abstract 14

Aims of the thesis 15

Chapter I: Biochemical and functional characterization of DPh 17

1.1 Introduction

1.1.1 Diatoms as model species 19

1.1.2 Novel information on diatom biology from the genomes 23

1.1.3 A suite of new molecular resources in diatoms 27

1.1.4 Diatom light sensing 28

1.1.4.1 The underwater light field 28

1.1.4.2 Light sensing molecules in diatoms 30

1.1.4.3 Blue-light sensing 32

1.1.4.4 Red light responses in the ocean 36

1.1.5 General characteristics of the phytochrome superfamily 37

1.1.6 Cyanobacterial phytochromes 46

1.1.7 Bacterial phytochromes 49

1.1.8 Fungal phytochromes 53

1.2. Material and methods

1.2.1 Cell culture conditions for *P. tricornutum* 57

1.2.2 Cell culture conditions for *T. pseudonana* 57

1.2.3 Construction of PtGAF and PtDPh3' silencing vectors 57

1.2.4 Transformation of *P. tricornutum* and selection of resistant clones 59

1.2.5 Colony screening on diatoms 60

1.2.6 Construction of the pBad-DPh-Myc-HisC expression vector and expression in *E. coli* 60

1.2.7 Construction of the pKT270 PebB-PebA expression vector and expression studies in *E. coli* 62

1.2.8 Construction of the codon-optimized DPh expression plasmid and expression studies in *E. coli* 64

1.2.9 Cell culture conditions for prolonged red light treatments in *P. tricornutum* 65

1.2.10 Cell culture conditions for R/FR fluence rate experiments in *P. tricornutum* and *T. pseudonana* 66

1.2.11 Cell culture conditions for R/FR photoreversibility experiments in *P. tricornutum* 66

1.2.12 Protein extraction protocols 67

1.2.13 Western Blotting 68

1.2.14 Preparation and purification of DPh antibodies 68

1.2.15 RNA extraction and cDNA synthesis 69

1.2.16 Quantitative real-time PCR (qRT-PCR) 69

1.3. Results

1.3.1 *In silico* study of the diatom phytochromes 73

1.3.2 Analysis of DPh spectral properties 78

1.3.3 Functional characterization of DPh in diatoms 85

1.3.4 Gene expression profile analysis in different light conditions 88

1/ Red light-induced genes in *P. tricornutum* 88

2/ Red light mediated gene expression in Pt WT and DPh knock-down lines 91

3/ R-FR photoreversibility experiments in P. tricornutum WT and DPh knock-down lines 93

4/ DCMU inhibitor experiment 97

5/ Blue light response experiments in Pt1 and DPh knock-down lines 98

6/ R/FR pulse experiment in *T. pseudonana* 100

7/ DPh regulation: protein studies 102

1.4. Discussion

1.4.1 Existence of phytochromes in the marine environment 105

1.4.2 The diatom phytochrome is a red/far-red light photoreceptor 107

1.4.3 Gene expression profile experiments 109

Chapter II: Study of the role of DPh in life strategy regulation in marine diatoms 119

2.1 Introduction

2.1.1 Why do diatoms aggregate? 120

2.1.2 Mechanisms behind aggregation 123

2.2 Materials and methods

2.2.1 Media and care of diatom cultures 126

2.2.2 Hemocytometer/Malassez slide 126

2.2.3 *P. tricornutum* growth and colony distribution under continuous light and L:D 12h:12h regimes 126

2.2.4 Quantification of transparent exopolymer particles (TEP) 127

2.2.5 Protein extraction and Western Blot 127

2.2.6 Calculations 128

2.2.7 Generation and growth of Tp DPh knock-down lines 129

2.2.8 Construction of the pH4:PtHO silencing vector 131

2.2.9 Silica starvation experiments in *T. pseudonana* 132

2.2.10 Aggregate enrichment experiments in *P. tricornutum* 132

2.3. Results

2.3.1. DPh knock-down lines show aggregation/chain phenotype in *P. tricornutum* 134

2.3.2. Modulation of DPh content in the RNAi lines and under different light conditions 135

2.3.3. Generation and phenotypic characterization of DPh knock-down lines in *T. pseudonana* 141

2.3.4. Specific environmental conditions leading to DPh down-regulation and aggregation phenotypes 143

2.3.5 Generation of Heme Oxygenase (HO) knock-down lines 148

2.4. Discussion

2.4.1 DPh controls colony formation and aggregation in *P. tricornutum.* 151

2.4.2 The generation of a "blind photoreceptor" induces the formation of colony and aggregates in *P. tricornutum* 154

2.4.3 Generation and phenotypic characterization of DPh knock-down lines in *T. pseudonana* 155

2.4.4 Specific environmental conditions leading to DPh down-regulation and aggregation phenotypes 156

Chapter III: Conclusions and perspectives **160**

References 166

Annexes 186

List of Figures and Tables

Chapter I: Biochemical and functional characterization of DPh

Figure 1.1.1: SEM picture of *T. pseudonana* 21

Figure 1.1.2: The pennate diatom *P. tricornutum* 22

Figure 1.1.3: Endosymbiosis in diatoms 24

Figure 1.1.4: Vertical attenuation of light at different wavelengths in two typical water types 25

Figure 1.1.5: The six distinct types of photoreceptors 31

Figure 1.1.6: Domain structures of the photosensory molecules found in *P. tricornutum* (Pt) and *T. pseudonana* (Tp) 32

Figure 1.1.7: Tetrapyrroles biosynthetic pathway 39

Figure 1.1.8: Domain structures of phytochromes 41

Figure 1.1.9: Simplified scheme showing domains and their functions in phytochrome proteins 56

Figure 1.3.1: Domain structures of DPh in *P. tricornutum* and *T. pseudonana* 74

Figure 1.3.2: Amino acid sequence alignment showing domains architecture of phytochrome protein in various species 76

Figure 1.3.3: Nucleotide sequence alignment of the original PtDPh and the PtDPh sequence with the optimized codon usage 81

Figure 1.3.4: SDS-PAGE analysis of different fractions of the DPh-His protein 82

Figure 1.3.5: Absorption spectra upon red/far-red light illumination of the N-terminal and full-length PtDPh protein 83

Figure 1.3.6: Schematic maps of the antisense and the inverted repeat constructs for PtDPh silencing 86

Figure 1.3.7: Western Blot analysis of *P. tricornutum* WT and a selection of DPh transgenic knock-down lines 86

Figure 1.3.8: mRNA levels in *P. tricornutum* WT in set of genes in continuous red light 90

Figure 1.3.9: a) mRNA levels in the Pt1 WT upon continuous red light exposure 92

b) mRNA levels in the DPh knock-down lines upon continuous red light exposure 93

Figure 1.3.10: Scheme with experimental set-up photoreversibility experiment 97

Figure 1.3.11 A1-A2-B: mRNA levels of PT WT cells and DPh knock-down lines in photoreversibility experiment 96-97

Figure 1.3.12: mRNA levels in Pt1 WT cells treated with (+) or without (-) DCMU 98

Figure 1.3.13: mRNA levels in Pt1 WT and two DPh knock-down lines, treated with a blue light pulse 100

Figure 1.3.14: mRNA expression profiles in *T. pseudonana* WT 101

Figure 1.3.15: Western Blot analysis of DPh protein in Pt1 WT in D:L and prolonged darkness for two days 103

Figure 1.3.16: Western Blot analysis of DPh protein in Pt1 WT and DPh knock-down lines grown in D:L or continuous light conditions 104

Table 1.2.1: Primer sequences utilized in the qRT-PCR experiments for *P. tricornutum* 71

Table 1.2.2: Primer sequences utilized in the qRT-PCR experiments for *T. pseudonana* 72

Chapter II: Study of DPh in life strategy regulation in marine diatoms

Figure 2.3.1: Western Blot analysis and pictures of DPh transgenic knock-down lines in *P. tricornutum* 135

Figure 2.3.2: Growth of *P. tricornutum* WT and DPh knock-down lines 138

Figure 2.3.3: Western Blot showing DPh expression in *P. tricornutum* WT and DPh knock-down lines in LD and LL 139

Figure 2.3.4: TEP analysis of *P. tricornutum* WT and DPh knock-down lines 141

Figure 2.3.5. Western blot of DPh expression in *P. tricornutum* WT and DPh knock-down lines 141

Figure 2.3.6 Western blot analysis and phenotypes pictures of *T. pseudonana* WT, inducible DPh knock-down line and two DPh knock-down lines 142

Figure 2.3.7: Western Blot analysis and phenotype pictures of *T. pseudonana* WT and inducible DPh knock-down line in $NO3^-$ and $NH4^+$ 143

Figure 2.3.8: *T. pseudonana* in silica-replete conditions 146

Figure 2.3.9: Pictures of the phenotypes of fusiform and oval aggregating cells of *P. tricornutum* 147

Figure 2.3.10: Information and amino acid sequence alignment of diatom Heme Oxygenase (HO) genes present in *P. tricornutum* 149

Figure 2.3.11: Phenotype pictures of the two HO-2 knock-down lines 150

Figure 2.3.12: Western Blot analysis of Pt1 and five HO-2 knock-down lines 150

Table 2.1: Daily growth rate for *P. tricornutum* WT and DPh knock-down lines grown in LD and LL 138

List of abbreviations

In alphabethic order

3'UTR: 3' untranslated region

Agp1/2: *Agrobacterium tumefaciens* phytochrome 1/2

AOX: Alternative Oxidase

ASW: artificial seawater

Bph: Bacterial phytochrome

BV: Biliverdin

CF1β: Subunit of the chloroplast ATP synthase complex

CHLH1/2: Mg-chelatase H subunit 1/2

Cph: Cyanobacterial phytochrome

Cycs: Cyanochromes

D: Dark

DCMU: (3-(3,4-dichlorophenyl)-1,1-dimethylurea

DL: Dark/Light cycle of 12 hrs:12hrs

DPh: Diatom phytochrome

EAL: Phosphodiesterase domain

EPS: Exopolymeric Substances

Fcp/FcpB: Fucoxanthin Chlorophyll a/c-binding/ Fucoxanthin Chlorophyll a/c-binding Protein B

Fph: Fungal phytochrome

FR: Far-red light

GAF: Vertebrate cGMP-specific phosphodiesterases, cyanobacterial adenylate cyclases and the formate hydrogen lyase transcription activator FhlA

GGDEF: Diguanylate cyclase domain

GSAT: Gutamate 1-semialdehyde aminotransferase

H4: Histone 4

HEMA: Glutamyl-tRNA reductase

HIR: High Irradiance Response

HK: Histidine Kinase

HO: Heme Oxygenase

HY1: *Arabidopsis thaliana* heme oxygenase 1

HY2: *Arabidopsis thaliana* phytochromobilin synthase

LFR: Low Fluence Response

LHCF1/2: Fucoxanthin chlorophyll a/c 1/2

LL: Continuous light

OD: Optical density

PAS: Per-Arnt-Sim

PCB: Phycocyanobilin

PDS: Phytoene desaturase

PEB: Phycoerythrobilin

PebA/B: Bilin reductase A/B

PHY: Phytochrome (domain)

POR1-4: Protochlorophyllide oxidoreductase 1-4

PRD: PAS-related domain

PSI: Photosystem I

PSII: Photosystem II

Pt: *Phaeodactylum tricornutum*

PΦB: Phytochromobilin

R: Red light

RNAi: RNA interference

RR or REC: Response Regulator

Si: Silica

TEP: Transparent Exopolymeric Particles

Tp: *Thalassiosira pseudonana*

VDL1: Violaxanthin de-epoxidase-like 1

VLFR: Very Low Fluence Response

WT: Wild-Type

ZEP2: Zeaxanthin epoxidase 2

Abstract

Phytochromes are a family of red/far-red light photoreceptors widely distributed throughout the plant kingdom, among bacteria, fungi and even some non-photosynthetic bacteria. Because of the fast attenuation of red and far-red light in the water column, the existence of a red/far red light sensor as the phytochrome in marine organisms has long been a subject of discussion. In this thesis, I have started the characterization of the diatom phytochrome through biochemical and spectral approaches, molecular techniques, physiological studies and bio-informatics. This thesis reports the first evidence that the phytochrome, identified in the diatom genomes (named DPh), acts as photoreceptor for perceiving red/far-red light. The biochemical and spectral analyses of DPh from the diatom *Phaeodactylum tricornutum* have revealed that the absorption maxima of the Pr and Pfr forms of DPh (685 and 740 nm respectively) are more shifted toward the red end of the spectrum than the plant phytochromes. Studies through bio-informatic tools have shown that DPh has a domain organization similar to the bacterial phytochromes (Bphs) and that DPh, similarly to this phytochrome photoreceptor class, binds biliverdin as chromophore. The role of DPh as photoreceptor has also been studies by extensive analyses of red light-mediated gene expression. Several genes have been studied for their expression profiles in diverse light regimes (acute light response experiments with red and far red light treatments of different fluences), including genes involved in the chlorophyll and carotenoid biosynthesis, light harvesting and redox regulation. These studies have shown that a number of the studied genes are induced in various red/far-red light treatments, although it was not possible to reach a final and comprehensive conclusion about the role of DPh. In particular, it was not always clear if DPh acts as a photoreceptor and mediator in red/far-red light responses of these genes, although the results obtained offered important first hints into the complex gene regulation by red/far-red light in the marine environment. Preliminary biochemical analyses have also offered a glimpse in the complex regulation of DPh protein synthesis in cells grown in diverse light conditions. Curiously, DPh down-regulation by RNA interference in two diatom species induced the formation of abnormal cell chains and aggregates, possibly through altered cell division and neighbor perception processes. These data raise novel and interesting hypotheses about the role of a red light photoreceptor in controlling growth and life strategies in the oceans.

'OUR ACCEPTANCE

Student details

Your full name: Frauke A. Depauw

Personal identifier (PI): A496299X

Affiliated Research Centre (ARC) (if applicable): Stazione Zoologica 'Anton Dohrn' Naples

Department: Ecology and Evolution of Plankton

Thesis title: Light Perception in Marine Diatoms and Characterization of a Novel Phytochrome from Phaeodactylum tricornutum

Authorisation statement

I confirm that I am willing for my thesis to be made available to readers by The Open University Library, and that it may be photocopied, subject to the discretion of the Librarian

Signed: ... .

British Library Authorisation (PhD and EdD candidates only)

Print name: Frauke Depauw

Date: 21/01/2015 DD/MM/YY

The Open University has agreed that a copy of your thesis can be made available on loan to the British Library Thesis Service on a voluntary basis. The British Library may make the thesis available online. Please indicate your preference below:

☒ I am willing for The Open University to loan the British Library a copy of my thesis

OR

☐ I do not wish The Open University to loan the British Library a copy of my thesis

Aims of the thesis

Diatoms are a key phytoplankton group in our contemporary oceans, as they account for almost one fifth of the primary production on Earth (Smetacek, 1999; Falkowski *et al.*, 2004). A major factor responsible for the success of these autotrophs may be their ability to manage efficiently changes in the underwater light conditions. In fact, it is well known that diatoms can grow over a wide range of light intensities and wavelengths, and have developed specific photo-acclimation and photo-adaptation processes (Lavaud *et al.*, 2007), that we only began to characterize at the molecular level (Depauw *et al.*, 2012). Differently from immobile land plants, diatoms live suspended along the water column where they experience dramatic changes in both the light intensity and color. Because red and far-red light are not as abundant as blue light in the oceans, the presence of a putative red/far-red light photoreceptor, identified in the genome of several diatoms, represents an intriguing and novel question. Moreover, the red/far-red light photoreceptor known as phytochrome was previously thought to be restricted to land plants only. Therefore, the existence of a red/far-red light photoreceptor in marine microalgae might represent an important step to understand the evolutionary history of red/far-red light photoreceptors. Thus, the major aim of this thesis was to gain insights into the mechanisms of light perception in the marine environment and to address their ecological relevance through the characterization of the diatom phytochrome (DPh) from *Phaeodactylum tricornutum*.

The different aspects of this PhD project can be summarized in two main topics. In the first part, the biochemical and functional characterization of DPh was investigated, with the objective to understand whether DPh acts as a photoreceptor and if yes, which colour(s) DPh might absorb. The DPh photoreceptor function has been investigated through a in-depth biochemical and spectral characterization of DPh in the pennate diatom *Phaeodactylum tricornutum*, done in collaboration with the laboratory of Dr. Ikeuchi Masahiko in Japan. During this work, I have contributed to the cloning of the DPh expression plasmid and the optimization of the conditions for DPh expression and purification in *E. coli* whilst the Japanese team provided the spectral

information of the purified DPh protein. In parallel, I have also characterized the function of DPh in the control of red light-mediated gene expression in the wild-type and DPh transgenic lines. For this reason, I performed a detailed study of gene expression patterns under different light regimes in wild-type and DPh trangenic lines in *P. tricornutum*. This work is described in detail in **Chapter I**, starting with an extensive overview of the literature on the information derived from the genomes of several diatom species, the molecular tools that are available to work with diatoms in the field of photobiology and their light sensing capabilities. The last part of the introduction gives a summary on the characteristics of the phytochrome superfamily, in plants, cyanobacteria, bacteria and fungi.

In the second part, I studied the role of DPh in the regulation of life strategies through the characterization of DPh RNAi transgenic lines generated in two different diatom species, *P. tricornutum* and the centric diatom *Thalassiosira pseudonana*. This work became particularly intriguing with the observation that DPh knock-down lines were showing an unusual cellular aggregation or colony formation phenotype. Therefore, understanding the possible link between the DPh photoreceptor function and observed grouping behaviour has taken an important place during this PhD research project. This work, described in **Chapter II**, has provided a possible novel function for DPh in the control of life strategies in marine phytoplankton which might be of great significance since the main factors controlling aggregation in the ocean are mostly unknown. At the beginning of this chapter, an introduction is given on the known factors influencing cellular aggregation and colony formation in the ocean.

The main conclusions and perspectives of this thesis are recapitulated in the summary (**Chapter III**).

At the date of the thesis submission, the following review article has been published:

Depauw, F.A., Rogato, A., Ribera d'Alcala, M., and Falciatore, A. (2012). Exploring the molecular basis of responses to light in marine diatoms. Journal of Experimental Botany (*doi:10.1093/jxb/ers005*). See Annex 2

CHAPTER I

Biochemical and functional characterization of DPh

DPh photoreceptor function has been investigated through an in-depth biochemical and spectral characterization of DPh in the pennate diatom Phaeodactylum tricornutum, in collaboration with the laboratory of Dr. Ikeuchi Masahiko in Japan. In parallel, I have characterized the function of DPh in the control of red light-mediated gene expression in the wild-type and DPh transgenic lines. The biochemical characterization has provided the first evidence that DPh acts as a red/far-red light photoreceptor in diatoms.

1.1 Introduction

The Oceans cover approximately 70% of the Earth's surface and photosynthetic organisms living in the photic zone are responsible for half of global primary productivity (Falkowski and Raven, 2007). Marine photosynthesis is dominated by eukaryotic microalgae, which together with cyanobacteria, are collectively called phytoplankton. These organisms drive most of the major oceanic processes; since more than 3 billion years, they actively influence the composition of Earth's atmosphere, ultimately creating conditions that have allowed multicellular organisms to evolve (Knoll, 2003; Katz *et al.*, 2004). Contributing at least 20% of global CO_2 assimilation and to biogeochemical cycling of important nutrients such as carbon, nitrogen, and silicon (Smetacek, 1999), diatoms are key ecological players in the contemporary oceans. These enormously diverse microalgae (Guillard and Kilham, 1977; Vanormelingen *et al.*, 2008) posses unique biological features (e.g., the silicon frustules) (Kooistra *et al.*, 2007), and complex metabolic pathways (Bowler *et al.*, 2008; Allen *et al.*, 2011), likely obtained from their ancestors via secondary endosymbiosis (Tirichine and Bowler, 2011). Since their radiation 140 My ago, diatoms have shown high plasticity in adapting to different environmental conditions (Kooistra *et al.*, 2007). They proliferate in ice (Thomas and Dieckmann, 2002), generally dominate in upwelling systems (Margalef, 1978), thrive in subsurface layers (Crombet *et al.*, 2011) and are considered the best-fit group in turbulent environments (Margalef, 1978). The basis of their ecological success is still poorly understood, although recent results suggest that diatoms utilize sophisticated mechanisms to respond to environmental changes (Falciatore *et al.*, 2000; Ianora *et al.*, 2004; Vardi *et al.*, 2006; Matsuda *et al.*, 2007; Bowler *et al.*, 2008). In particular, several species can cope with highly variable light conditions, suggesting that diatoms are capable of perceiving, responding and, likely, anticipating light variations and, that they possess suited molecular systems mediating light responses. Notwithstanding, our understanding of light-driven processes in marine diatoms is still

in its infancy and present knowledge on their photobiology is largely based on physiological and *in situ* studies, with less information available at the molecular level in contrast to other aquatic model systems such as cyanobacteria (Grossman *et al.*, 2001) or *Chlamydomonas* (Rochaix, 2002). In the next paragraphs, I have summarized the diatom general characteristics together with the novel information obtained from the recently sequenced genomes of the model species *Phaeodactylum tricornutum* and *Thalassiosira pseudonana*.

1.1.1 Diatoms as model species

The fact that at least 50% of the primary productivity on Earth is carried out by phytoplankton (Field *et al.* 1998, Nelson *et al.* 1995) was observed by remote satellite-based studies of chlorophyll concentrations in oceanic surface waters together with *in situ* recordings (Curtin & Belcher 2008). As mentioned before, about one-fifth of the photosynthesis on Earth is carried out by diatoms (Nelson *et al.*, 1995) which makes that every year, diatom photosynthesis in the sea generates about as much organic carbon as all the terrestrial rainforests combined (Field *et al.*, 1998). Diatoms have also an important role in the biological carbon pump, which not only stores carbon in the ocean interior (Bowler *et al.*, 2009; Karl, 2007) but also transfers energy and electrons to the deep sea and organisms living beneath the photic zone of the water columns (Bowler *et al.*, 2009).

One of the main features of diatoms is their ability to generate a highly patterned external wall composed of amorphous silica, known as the frustule. The frustule consists of two overlapping parts, fitting together like a box and a lid, called hypotheca and epitheca respectively. Pattern design of the frustules is reproduced from generation to generation. These silicified cell walls are responsible for a particular form of cell division in diatoms (see later).

Although prokaryotic phytoplankton such as the marine cyanobacteria *Prochlorococcus* are the most widespread (Moore & Chisholm 1998), diatoms form the most abundant and diversified group of eukaryotic phytoplankton in the ocean (Kooistra *et al.* 2007), with an

estimated 200 000 different species, ranging in size from a few micrometers to a few millimeters and existing either as single cells or as chains of connected cells (Armbrust *et al.*, 2009). Diatoms can exist as planktonic forms, found in all open water masses, and benthic forms that can grow on sediments, attached to rocks or macroalgae. Some species can even be found in soil.

The diatoms are generally divided into two groups depending on the symmetry of their frustules: the centrics (radially symmetrical) and the pennates (bilaterally symmetrical). The latter are further subdivided into raphid pennates, with a raphe, and the araphids, without a raphe. The raphe is a slit along the frustule that is used for movement, via the secretion of polysaccharides (Kooistra *et al.*, 2007). Overall, the fossil records show that centric diatoms evolved first and were then followed 90 Mya by the pennate diatoms (first araphids and then raphids) during the Cretaceous. Although it is worth noting that the centric species *T. pseudonana* (see figure 1.1.1) and the pennate (raphid) species *P. tricornutum* (see figure 1.1.2) are more divergent than fish and humans (Bowler *et al.*, 2010).

Larger diatom species (as *Ditylum brightwellii*) can move up and down the water column by changing the ionic composition of their vacuole (Fisher & Harrison, 1996). Other species (as *Skeletonema costatum* and *Thalassiosira nordenskioldii*) can control their buoyancy by making colonies (Karp-Boss & Jumars, 1998). As mentioned before, some benthic pennate diatoms move by a mechanism involving the secretion of mucilage through their raphe slit (Kooistra *et al.*, 2007). This ability of diatoms to move is very important, not only during sexual reproduction where sexually competent cells have to find each other, but also in the context of perceiving light for optimal photosynthetic efficiency and protecting themselves from photodamage.

Diatom cell division typically proceeds through asexual mitotic divisions to ensure the diploid vegetative state (Chepurnov *et al.*, 2004). The frustule precludes cell growth expansion; Therefore, the two daughter cells must generate inside the parent cell. The hypotheca of the parent cell is used as a guide to build a new hypotheca, whereas the other daughter cell uses the parental hypotheca to create an inner theca, such that the parental hypotheca becomes the

epitheca of the daughter cell. The consequence of the process is the reduction in size during successive mitotic divisions in the daughter cell. Regeneration of the original size typically occurs via sexual reproduction. During the 'gametogenesis', the resulting male and female gametes combine to create a diploid auxospore that is surrounded by a special organic or inorganic silica wall which allows expansion. Auxospore expansion seems to be a well-controlled process (Mann, 1993), during which the shape of the new enlarged cell is generated. In centric diatoms, this process is influenced by external species-specific factors such as light irradiance, day length and temperature (Chepurnov *et al.*, 2002). Centrics form within one clonal culture large egg cells and motile, flagellated sperm cells (oogamy). Although auxosporulation in pennate diatoms is also dependent on environmental factors, the primary determinant of gametogenesis onset seems to be cell-cell interaction between vegetative cells from different sexually compatible clones (mating types). The gametes produced by most pennates are, in contrast to those produced by centric diatoms, non-flagellated and morphologically identical (isogamy) (Chepurnov *et al.*, 2004).

The centric diatom Thalassiosira pseudonana

The diatom *T. pseudonana* (see figure 1.1.1) was the first eukaryotic marine phytoplankton species whose genome was sequenced (Armbrust *et al.*, 2004) and can be considered to be the molecular model species and representative of the centric diatoms. *T. pseudonana* was chosen because this species has served as a model for many diatom physiology studies, the genus *Thalassiosira* is cosmopolitan throughout the world's oceans, and the genome is relatively small with 32,4 mega base pairs. Analysis of the genome of *T. pseudonana* has provided novel insights on the synthesis of the peculiar cell wall of diatoms made essentially of hydrated silica (Chiovitti *et al.*, 2005; Mock *et al.*, 2008).

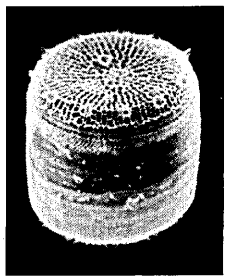

Figure 1.1.1: SEM picture of *T. pseudonana*.

Picture by Nils Kröger, Universität Regensburg.

The pennate diatom Phaeodactylum tricornutum

The marine pennate diatom *P. tricornutum* (see figure 1.1.2) is the second diatom for which a whole genome sequence has been generated. It was primarily chosen because of its small genome size (27,4 Mb), the superior genetic resources available for this diatom and because it has been used in laboratory-based studies of diatom physiology for several decades. Although not considered to be of great ecological significance, it has been found in several locations around the world, typically in coastal areas with wide fluctuations in salinity. Unlike other diatoms, *P. tricornutum* can exist in 3 different morphotypes (see figure 1.1.2) and changes in cell shape can be stimulated by environmental conditions (De Martino *et al.*, 2011). This feature is a useful tool for exploring the molecular basis of cell shape control and morphogenesis. The plasticity of its shape relates to the rather atypical nature of its cell wall, which is mainly organic and only poorly silicified (Borowitzka & Volcani, 1978). As a consequence, *P. tricornutum* does not have an obligate requirement for silica during growth (Brzezinski *et al.*, 1990). Different *P. tricornutum* accessions isolated from several locations worldwide have been characterized and described, allowing the study of natural variation in cellular responses or gene expression (De Martino *et al.*, 2007; Bowler *et al.*, 2008). The strain used during this research project is a fusiform strain called Pt1 and represents the accession that was used for genome sequencing (Bowler *et al.*, 2008).

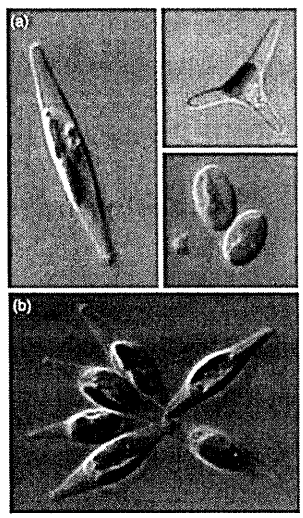

Figure 1.1.2: The pennate diatom *P. tricornutum*.

(a) Light micrographs showing the three morphotypes of *P. tricornutum*: left, fusiform; top right, triradiate; bottom right, oval.

(b) Light micrographs of a small cluster of cells of *P. tricornutum*. Each cell is approximately 15 µm in length. Images courtesy of Alessandra De Martino.

From Vardi *et al.* Genome Biology, 2008.

1.1.2 Novel information on diatom biology from the genomes

The completed genome sequences from diatoms have provided novel information about the evolutionary history of algae (Parker *et al.,* 2008) and offer a blueprint for understanding diatom biology and metabolism. Diatoms are believed to have obtained their plastid from a secondary endosymbiosis between a heterotrophic eukaryote, a green alga and an ancient red alga (see figure 1.1.3) (Bhattacharya *et al.*, 2007; Moustafa *et al.*, 2009). The initial, primary endosymbiosis occurred about 1.5 billion years ago, when a eukaryotic heterotroph engulfed (or was invaded by) a cyanobacterium to form the photosynthetic plastids of the Plantae, the group that includes land plants and red and green algae (Yoon *et al.*, 2004). Genes were subsequently relocated from the symbiotic cyanobacterial genome to the host nucleus. About 500 million years later, a secondary endosymbiosis occurred, in which a different eukaryotic heterotroph captured a red alga. Over time, the red-algal endosymbiont was transformed into the plastids of the Stramenopiles, the group that now includes diatoms, brown macroalgae and plant parasites. Because of the presence of numerous green algal genes present in diatoms, it was proposed that also another endosymbiotic event occurred with a cryptic endosymbiont related to prasinophyte-like green algae (Moustafa *et al.*, 2009). Gene transfer continued from the red-algal nuclear and plastid genomes to the host nucleus (Armbrust *et al.*, 2004). At least 170 red-algal genes have been identified in the nuclear genome of diatoms, most of which seem to encode plastid components (Bowler *et al.*, 2008).

Because of these multiple endosymbiotic events, diatoms contain a unique combination of genes that has permitted novel metabolic innovations and resulted in countless diatom specific features. There is evidence of the presence of genes originating from both the ancestral heterotrophic host and the photosynthetic symbiont (Armbrust *et al.,* 2004). These animal/plant-like origins have been confirmed in both species *Phaeodactylum* and *Thalassiosira*, by the co-existence of metabolisms typically found in plants (such as photosynthesis) and in metazoans

(such as a complete and functional urea cycle and mitochondrial fatty acid oxidation pathways) (Armbrust *et al.*, 2004; Allen *et al.*, 2008; Bowler *et al.*, 2008). The existence of a complete urea cycle was previously thought to be restricted to organisms that consume complex organic nitrogen compounds and excrete nitrogenous waste products. Extensive gene expression studies of several urea cycle genes (Maheswari *et al.*, 2009; Allen *et al.*, 2011) have suggested that the urea cycle in diatoms may be principally involved in the biosynthesis of organic nitrogenous compounds rather than their breakdown, as is the case in animals (Esteban-Pretel *et al.*, 2010). This cycle probably enables diatoms to efficiently use carbon and nitrogen from their environment (Allen *et al.*, 2011). As stated above, diatoms also combine an animal-like ability to generate chemical energy from the breakdown of fat with a plant-like ability to generate metabolic intermediates from the breakdown. This combination probably allows diatoms to survive long periods of darkness, as occurs at the poles (Armbrust *et al.*, 2004).

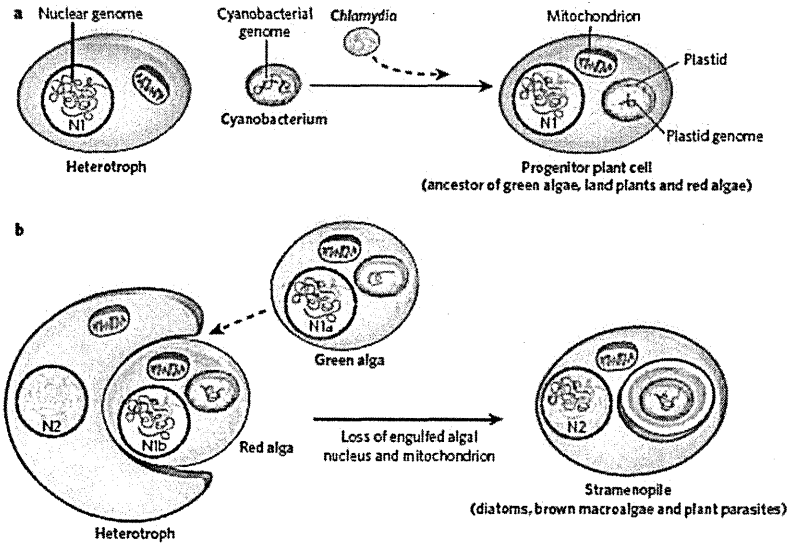

Figure 1.1.3: Endosymbiosis in diatoms. Representation of the origin of diatom plastids through sequential primary (a) and secondary (b) endosymbioses, and their potential effects on genome evolution. Figure from Armbrust, 2009.

It appeared also that hundreds of bacterial genes were spread throughout the diatom genomes (Bowler *et al.*, 2008). This result came as a surprise, because horizontal gene transfer is considered rare in eukaryotes (Keeling & Palmer, 2008) but seemingly, diatoms have mastered the art of bacterial gene transfer, perhaps because of their well-known associations with bacteria (Carpenter & Janson, 2000; Morris *et al.*, 2006; Foster & Zehr 2006). Less than half of the bacterial genes in *P. tricornutum* are shared with *T. pseudonana*, and only 10% are shared between *T. pseudonana* and the distantly related oomycete *Phytophthora* (Bowler *et al.*, 2008). These gene transfers provide novel possibilities for metabolite management and perception of environmental signals (for example by bacterial two-component systems).

On another note, diatoms have developed sophisticated strategies to deal with nutrient a limitation of especially iron, which is often limited in open-ocean regions. *Thalassiosira*, for example, seems to have tailored the photosynthetic apparatus to use less iron (Strzepek & Harrison, 2004). The species has even replaced iron-requiring electron-transport proteins with comparable proteins that require copper (Peers & Price, 2006). *Phaeodactylum* on the other hand, responds to iron-starved conditions with the overall down-regulation of processes that require a lot of iron and the up-regulation of alternative pathways for dealing with oxidative stress and additional iron-acquisition pathways (Allen *et al.*, 2008). Thus, evidence suggests that raphid pennate and centric diatoms have different ways of optimizing their systems for dealing with a shortage of iron. Moreover, centric and pennate diatoms also differ in their capability to store iron. A study from Marchetti *et al.* (2008) has reported the existence of a special iron-storage molecule, ferretin, in several pennate genera (*Pseudo-nitzschia*, *Fragilariopsis* and *Phaeodactylum*). Ferretin is also known to protect the cells against oxidative stress. Interestingly, *Thalassiosira*, does not encode ferretin, so it appears that this gene is privy to a restricted group of pennate diatoms. This suggests that this gene was probably inherited by lateral gene transfer from other species.

The analysis of the genomes also provided novel information in the light absorption capacities of diatoms. It has been revealed that the light-harvesting antennae of the diatom photosynthetic machinery are composed of fucoxanthin chlorophyll a/c binding proteins (FCPs) structured into oligomeric complexes (Büchel, 2003; Beer *et al.*, 2006). These complexes have a large number of carotenoids (Coesel *et al.*, 2008) only found within photosynthetic heterokonts and haptophytes, such as diatom-specific fucoxanthin (Fx), as well as diadinoxanthin (Ddx) and diatoxanthin (Dtx) pigments that are involved in their unique xanthophyll cycle (Lepetit *et al.*, 2010; Photoprotection in diatoms was reviewed in Depauw *et al.*, 2012). Three antenna protein families have been found: Lhcf (the classical light-harvesting proteins), Lhcr (red algal-related proteins), and the less abundant Lhcx proteins (previously known as LHCSR and Li818) (Green & Zhu, 2007; Bailleul *et al.*, 2010; Lepetit *et al.*, 2010).

Diatoms have long been considered as C_3 photosynthesizers, but evidence from metabolic labeling and genome sequencing suggests that photosynthesis in diatoms might result from a form of C_4-like biochemistry (Roberts *et al.*, 2007). This specialized form of photosynthesis allows a more efficient consumption of available CO_2 and is restricted to a few land plants, such as sugar cane and maize. The authors from Roberts *et al.* (2007) provided evidence for a C_3-C_4 intermediate photosynthesis in *T. weissflogii*, but only C_3 photosynthesis in *T. pseudonana*. However, it is possible that their study failed to detect C_4 pathways in *T. pseudonana*, perhaps because the proper organic acids were not tested. Although various genes potentially involved in a C_4-like photosynthesis have been identified in the genome of *P. tricornutum* by Kroth *et al.* (2009), the existence of C_4-based photosynthesis in diatoms has not yet been conclusively demonstrated to date.

As conclusion, the invaluable new information obtained from diatom genomes indicates that these microalgae are chimeras of genes, as a result of their complex evolutionary history and the gene flow that followed between host and endosymbiont.

1.1.3 A suite of new molecular resources in diatoms

Genomic tools and knowledge from the genomes of representative species now permit a deeper exploration of the molecular components regulating diatom biology. A set of molecular tools for functional genomic studies, such as a genetic transformation system are available for *P. tricornutum* (Apt *et al.*, 1996; Siaut *et al.*, 2007), *T. pseudonana* (Poulsen *et al.*, 2006) and for other non-sequenced diatom genomes (Dunahay *et al.*, 1995; Fischer *et al.*, 1999). A range of reporter genes have been used, particularly in *P. tricornutum*, including the *E. coli uidA* (β-glucuronidase) gene, the *cat* (chloramphenicol acetyl transferase) gene, the firefly luciferase, different variants of GFP (green fluorescent proteins) and the jellyfish aequorin gene (Falciatore et al, 1999; Falciatore *et al.*, 2000). More recently, a set of Gateway-based vectors for diatoms has been set-up to allow functional analysis in a more high-throughput manner (Siaut *et al.*, 2007). Efforts have been made in recent years to develop genome-enabled resources such as comprehensive EST libraries (http://www.biologie.ens.fr/diatomics/EST3/) (Montsant *et al.*, 2005; Maheswari *et al.*, 2009) and whole genome microarrays (Mock *et al.*, 2008).

Nevertheless, a major limitation for the study of diatom gene function is the limited amount of tools to generate mutants through forward or reverse genetic approaches. The generation of loss-of-function mutants by insertional mutagenesis appears difficult in a diploid organism such as *P. tricornutum* that seems to lack a sexual cycle. As there is no evidence for homologous recombination events in diatoms (Falciatore *et al.*, 1999), it is also unlikely that targeted gene disruption via homologous recombination can be developed as a standard approach. More recently, it has been shown that inhibition of gene expression by RNA interference (RNAi) is possible in *P. tricornutum* and *T. pseudonana* (De Riso *et al.*, 2009; Kirkham *et al.*, in preparation). The RNAi technique has proven to be a valuable tool during my PhD research project. New available molecular tools for studying diatom photobiology have been summarized in Depauw *et al.*, 2012. (see annex 2, last pages of the thesis).

1.1.4 Diatom light sensing

Because the light conditions in the marine environment differ in many aspects from the terrestrial one and because diatom light sensing molecules are well adapted to their peculiar environment, I have provided in the next paragraphs an introduction on the peculiarities of the underwater light field and summarized the evidences for the presence of photoreceptors in diatoms.

1.1.4.1 The underwater light field

Aquatic environments differ from the terrestrial ones in many aspects and impose different constraints to photosynthetic organisms. Light intensity and nutrient concentrations are definitely lower in aquatic than in terrestrial environments (see figure 1.1.4). By contrast, terrestrial photosynthetic organisms can suffer from water limitation and can be exposed to stronger temperature variations (Margalef, 1974). The intensity of direct light is at least one or two orders of magnitude higher on land, and can decrease to levels comparable with marine conditions only beneath dense canopies. Spectral properties and their spatial and temporal variations are also different. The light spectrum on the land is modified by atmospheric attenuation and by the absorption/reflectance of other plants, the latter resulting in a general bias towards longer wavelengths (Bjorn, 2008). In aquatic environments, light varies not only because of the incident solar radiation and time of the day, but also because of the absorption and scattering processes of the water, the depth of the water column, the presence of colored dissolved organic matter (CDOM) and suspended particles, among which photosynthetic organisms themselves (Kirk, 1994). Water absorption of the light is strong in the red and infra-red wavebands and displays a positive gradient towards UV, which causes a progressive dominance of the blue-green (400-500 nm) spectral components with depth. Nonetheless, despite the strong attenuation of red and infra-red light coming from the sun, these components are still present in the sea, yet at low intensities. This is due to transpectral processes, that are responsible for the

emission of the absorbed light at longer wavelengths, such as in the case of the chlorophyll a fluorescence (Mobley, 1994). All the aforementioned processes combine differently in diverse regions of the hydrosphere (e.g., lacustrine vs. marine, eutrophic vs. oligotrophic) and make the variability of underwater light fields very distinct from the terrestrial ones.

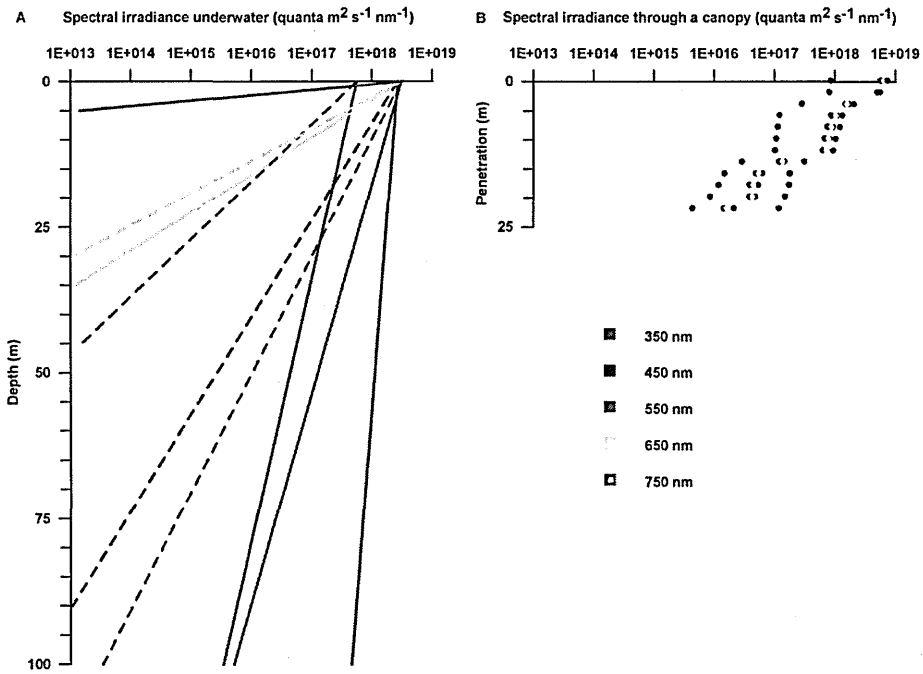

Figure 1.1.4: (A) Vertical attenuation of light at different wavelengths in two typical water types according to Austin and Petzold (1986). Continuous line: type I water (clear water with low phytoplankton concentration); dashed line: type III water (turbid water with high phytoplankton concentration). (B) Vertical attenuation of light at same wavelengths as in A within a canopy of a sub-tropical forest during a similar time period and latitude at increasing distances from the top (De Castro, 2000). Figure from Depauw *et al.* 2012.

Additionally, natural water movements (tides, streams, layer mixing, etc.) cause relevant spatial displacements of marine microorganisms, which have no equivalent in the terrestrial environment (Mann and Lazier, 2006). Consequently, the variation of underwater light field sketched above, in combination with vertical displacements, produce light variations that may significantly impact on cell physiological responses (Esposito *et al.*, 2009). On the other hand, vertical displacement is always coupled with a parallel variation of the light spectrum, which may

allow distinguishing variation in intensity due to clouds or time of the day from the variation produced by the displacement itself. Whether and how marine unicellular phototrophs do discriminate among the different origins of light variations (diurnal, seasonal and global changes both in irradiance and in spectral distribution) is still an open and intriguing question. However, studies support the presence of several diatom photoreceptors, implicated in these light-regulated processes. An overview is given in the next paragraph.

1.1.4.2 Light sensing molecules in diatoms

Light-sensing molecules, such as photoreceptors, allow many organisms to perceive light signals and to initiate a downstream signal pathway. Photosensory proteins are usually modular in their architecture. One or more domains serve as a sensory-input domain and may bind the chromophore, an organic, non-protein component that confers specific photochemical properties. Chromophores undergo physicochemical and structural changes upon light absorption, which are essential for the signal propagation (Moglich *et al.,* 2010). Six main classes of photoreceptors have been identified and classified according to the chemical nature and photochemistry of their chromophores (Moglich *et al.,* 2010; see figure 1.1.5): the light-oxygen-voltage domain (LOV) with a flavin mononucleotide (FMN) as the chromophore; cryptochrome and the blue-light sensor using FAD (BLUF), both using flavin adenine dinucleotide (FAD); photoactive yellow protein (PYP), with a *p*-coumaric acid (*p*CA) chromophore; rhodopsin, with retinal; and the phytochrome class, with a tetrapyrrole as the chromophore. Because of the increased number of sequenced genomes, a variety of photoreceptors are being revealed, in which specific sensory domains are found in novel combination with different effectors. I will focus on the diatom photoreceptors identified in *Phaeodactylum* and *Thalassiosira*, and will discuss their nature and possible function (see figure 1.1.6 for overview of known diatom photosensory proteins).

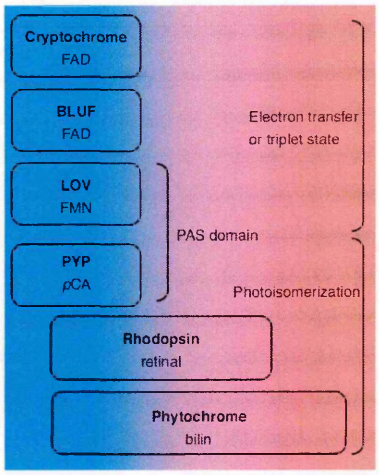

Figure 1.1.5: The six distinct types of photoreceptors.

From Gomelsky & Hoff, 2011.

Diatoms possess multiple putative photoreceptors belonging to the LOV, cryptochrome and phytochrome families. The biochemical and functional characterization of these proteins and their chromophores is still very limited, and the signaling cascades and regulatory processes (e.g., transcriptional and post-transcriptional regulation, secondary messengers, and the role of chromatin remodeling) that they activate are basically unknown. Comparative genomic studies have also revealed that none of the downstream components of plant photoreceptor pathways (Kami *et al.,* 2010) are present in diatoms. However, bacterial histidine-kinase phosphor-relay two-component systems, involved in environmental signaling, also appear to be highly developed in diatoms (Bowler *et al.*, 2008). In both *P. tricornutum* and *T. pseudonana*, a wide range of two-component signaling proteins have been found, sometimes organized in novel domain combinations (see further) and it is likely that they represent novel types of sensing molecules. Therefore, the elucidation of the diatom light-signaling pathways requires novel genetic and biochemical investigations. In the next paragraphs, I have summarized the diatom photoreceptors to respond to blue light and red light.

Diatom photosensory proteins	ID Phatr2	Best NCBI for Pt	ID Thaps3	Putative Chromophore	Description
Plant CRY1 (*A. thaliana*) PHR CCT **A Diatom Cryptochrome/Photolyase family**					
Cry/6-4 PHR CCT	PtCPF1:27429	Cryptochrome 1 (*E. siliculosus*)	TpCPF1:262946	FAD MNTF or HDF	Animal-like Cry with double function (Coesel *et al.*, 2009)
Cry/DASH-like PHR	PtCPF2:34592 PtCPF4:55091	Cry-DASH-like (*O. taun*) Cry-DASH (*D. rerio*)	TpCPF2:35005 TpCPF3:268988 TpCPF4:23500	FAD MNTF or HDF	Unknown
CPD/Photolyase-like PHR	PtCPD1:1947 PtCPD3:51952 PtCPD4:49165	Deoxyribodipyrimidine photolyase (*O. antarcticus*) DNA photolyase (*Salpingoeca*) Deoxyribodipyrimidine photolyases (*R. baltica*)	TpCPD1:14315 TpCPD4:10414 TpCPD3:40995	FAD MNTF or HDF	DNA repair function
PHR CCT	PtCPD2:54342	Cryptochrome-like protein (*O. taun*)	TpCPD2:7368	FAD MNTF or HDF	DNA repair function
B Diatom Aureochrome bZIP LOV	PtAUREO1a:49116 PtAUREO1b:49458 PtAUREO1c:56742 PtAUREO2:56060	Aureochrome 3 (*E. siliculosus*) Aureochrome 4 (*E. siliculosus*) Unknown protein (*E. siliculosus*) Aureochrome 3 (*E. siliculosus*)	TpAUREO1a:33340 TpAUREO1b:20065 TpAUREO1c:37198 TpAUREO2:33407	FMN	Putative blue light sensor and light-regulated transcription factor
Bacterial Phytochrome (BphP) C PAS GAF PHY HK RR					Putative red: far red photoreceptor.
C Diatom Phytochrome C GAF PHY HK RR C PAS GAF PHY HK RR	PtDPh:54330	Phytochrome-like protein 3 (*E. siliculosus*)	TpDPh:22848	Unknown Unknown	Two-component signaling system, bacterial-like

Figure 1.1.6: Domain structures of the photosensory molecules found in the *P. tricornutum* (Pt) and *T. pseudonana* (Tp) domain architecture according to the PFAM database (http://pfam.sanger.ac.uk/). (A) Cryptochrome/photolyase family. (B) Aureochrome. (C) Phytochrome. The protein identification (ID) numbers of the *Phaeodactylum* and *Thalassiosira* genomes, the best hit in the NCBI database for *Phaeodactylum* (the BLASTP searches were performed on the NCBI sequence browser on 19 August 2011), the putative chromophores, and a short protein description are reported in the above figure. The domain abbreviations are as follows: PHR, photolyase-related domain; CCT, cry C-terminal domain; bZIP, basic leucine zipper domain; LOV, light–oxygen–voltage domain; GAF, GAF domain; PHY, phytochrome domain; HK, histidine kinase domain; RR, response regulator; and C, conserved cysteine residue. The chromophore abbreviations are as follows: FAD, flavine adenine dinucleotide; MNTF or pterin, 5,10-methenyl-tetrahydropteroylpolyglutamate; HDF, deazaflavin; and FMN, flavin mononucleotide. The species abbreviations are as follows: E. *siliculosus, Ectocarpus siliculosus*; *O. antarcticus, Octadecabacter antarcticus; O. tauri, Ostreococcus tauri; R. baltica, Rhodospirellula baltica;* and *D. rerio, Danio rerio.* The asterisk in PtDPh corresponds to the conserved cysteine residue for putative chromophore binding. Figure from Depauw *et al.* (2012), Journal of Experimental Botany.

1.1.4.3 Blue-light sensing

Because of the spectral properties of the underwater light field, blue-light sensors are expected to be crucial for controlling the life of marine organisms. Interestingly, despite the fact that diatoms are capable of moving plastids within the cell, diatom genomes lack the gene for phototropin that is widely distributed in the green lineage (Christie, 2007). However, two other

blue light photoreceptors, the cryptochrome and the aureochrome, are present in multiple copies in these organisms.

The cryptochrome/photolyase family

Cryptochromes (crys) are blue/ultraviolet-A (UV-A) light photoreceptors that are widely distributed throughout all of the kingdoms. These receptors mediate various light-induced responses in plants and animals (Chaves *et al.,* 2011), and their function in the generation of circadian rhythms is highly conserved, either as input components in the circadian clock or as transcriptional repressors in the negative feedback loop of the circadian oscillator.

Crys share sequence similarities with photolyases, flavoproteins that catalyze the repair of cyclobutane pyrimidine dimers (CPDs) and 6-4 photoproducts (6-4PP) within UV-damaged DNA (Sancar, 2003). It is generally accepted that the functions of photolyases and cryptochromes differentiated during evolution, with crys losing the DNA-repair activity. However, this assumption has been recently questioned because photolyases exhibiting gene-regulatory activity have been characterized in fungi (Berrocal-Tito *et al.,* 2007; Bayram *et al.,* 2008), in the green alga *Ostreococcus* (Heijde *et al.,* 2010) and in diatoms. Moreover, the recently identified cry-DASH protein, whose signaling and function remains largely unclear (Brudler *et al.,* 2003; Kleine *et al.,* 2003), has also been shown to have DNA-repair activity (Daiyasu *et al.,* 2004; Huang *et al.,* 2006). In agreement with their common origin, photolyases and cryptochromes possess considerable structural similarity in the amino-terminal photolyase-homology region (PHR) that is responsible for chromophore binding and light absorption. All of the members of the family use a flavin-adenine dinucleotide (FAD) and either a pterin (MTHF) or a deazaflavin (HDF) as chromophores. The light activation of these molecules is determined by changes in the flavin redox state and electron transfer (Chaves *et al.,* 2011). Adjacent to the PHR, some crys contain a carboxy-terminal extension (CCT) that can vary in length. The CCT can have a role in signaling when it contains a DAS domain with recognizable motifs (Li and Yang, 2007). By contrast, the animal CCT is less

conserved, and its role in cry function has been established only in a few organisms (Chaves *et al.,* 2011).

The computational analyses of diatom genome sequences have revealed several members of the cryptochrome/photolyase family (see figure 1.1.6) (Coesel *et al.,* 2009). Cry-DASH (CPF2-4) is the most represented, with several members in both *P. tricornutum* and *T. pseudonana.* In addition, these two species possess another member that is phylogenetically closer to the animal 6-4 photolyases (cryptochrome/photolyase family 1; CPF1) but is nonetheless an independent clade. The presence of an animal-type protein can be explained by the evolutionary history of this group of organisms, and by the fact that many diatom proteins are more similar to their animal rather than to their plant counterparts (Bowler *et al.,* 2008). Surprisingly for photosynthetic algae, diatom genomes do not contain a clear ortholog of plant cry genes while several genes encode CPD photolyases. A member of this family has a C-terminal extension, which normally is not present in the photolyases. This extension does not contain the plant DAS domain, and it is not known whether the extension has a role in signaling. Besides CPF1, no additional 6-4 photolyases were found in the diatom genomes. The functional and biochemical characterization of the *P. tricornutum* CPF1 was performed in the laboratory where I did my thesis and has provided novel information regarding the diatom cry family. The primary structure of CPF1 exhibits a high similarity with animal crys. It notably displays residues that are important for cellular circadian regulations (Stanewsky *et al.,* 1998). PtCPF1 also contains a 28-amino-acid C-terminal extension, which is comparable to the extension described in *Drosophila* but lacks the plant DAS domain (Falciatore A, unpublished). On the other hand, the *Phaeodactylum* and the *Thalassiosira* CPF1s both possess residues that are crucial for the (6-4) photolyase activity (Hitomi *et al.,* 2001). This activity was confirmed through biochemical studies. The *P. tricornutum* CPF1 binds and repair 6-4 PPs *in vitro* (Coesel *et al.,* 2009), and transgenic *cpf1* knock-down lines are hypersensitive to UV exposure (De Riso *et al.,* 2009). Additionally, the demonstration that PtCPF1 can act as a circadian

clock transcriptional repressor in a heterologous mammalian cell system, similarly to the mouse cry, provided the first indication of an additional regulatory role for this protein. The function was confirmed by blue-light-dependent gene-expression studies showing that the genes encoding proteins involved in distinct processes (photosynthesis, photoprotection, cell cycle, DNA repair and others) are misregulated in over-expressing CPF1 lines, suggesting a possible function for CPF1 as a photoreceptor (Coesel *et al.,* 2009). Because crys and photolyases share many residues, it is not possible from the sequence alone to predict if the other diatom CPFs (PtCPF2 and PtCPF4) possess DNA-repair activity or a role in light signaling. This limitation also prevents the estimation of the nature of their chromophores. Further biochemical and functional analyses combined with structural studies will be necessary to identify the residues responsible for these different functions and to determine the light properties allowing their specific activity.

The light-oxygen-voltage (LOV) sensors

LOV-containing photoreceptors are widely distributed among prokaryotes and eukaryotes (Krauss *et al.,* 2009; Losi and Gärtner, 2011). The receptors contain a light-oxygen-voltage (LOV) domain that binds the flavin mononucleotide (FMN) as a chromophore and acts as a sensor module. Light induces structural changes in the LOV domain, which has a photochemistry distinct from that of other flavin-based sensors. LOVs can be found associated with different other protein domains, in a variety of combinations, and in tandem as in the phototropins. Among the different LOV photoreceptors identified in eukaryotes (the phototropins and ZEITLUPE family in plants, the white-collar (WC-1) in fungi, the LOV-HKs, and the aureochrome; Moglich *et al.,* 2010), only the aureochromes have been found in diatom genomes.

The aureochromes

The recent finding of the aureochromes as specific blue-light receptors in the Heterokont clade is particularly significant. The discovery suggests the presence of a suite of novel photoreceptors in marine organisms derived from the secondary endosymbiosis event (Krauss *et*

al., 2009; Takahashi *et al.,* 2007) and whose expansion has probably been favored by the predominance of blue light in marine environments.

Initially discovered in the algae *Vaucheria frigida* (Xanthophyceae) and *Fucus distichus* (Phaeophyceae) and the diatom *T. pseudonana,* the aureochromes are blue-light-regulated transcription factors with an N-terminal basic-zipper domain (bZIP) and a C-terminal LOV domain. The LOV domain contains a cysteine residue in a highly conserved sequence motif, which is required for flavin-cysteinyl adduct formation upon light excitation, and blue light increases the affinity of the bZIP domain for DNA (Takahashi *et al.,* 2007). To date, functional studies have only been reported for the *V. frigida* aureochrome. Gene knock-down experiments revealed the role of the aureochrome in mediating blue light-induced branching and sex-organ development, similar to the role of plant photoreceptors for photomorphogenesis (Takahashi *et al.,* 2007).

The biological functions of diatom aureochromes are still unknown. However, by searching for the LOV-domain within the genomes, it is possible to observe an expansion of this protein family. Four aureochrome-like proteins have been identified in both *P. tricornutum* and *T. pseudonana* (see figure 1.1.6), and a recent *in silico* study highlighted them as potential blue-light-regulated transcription factors (Rayko *et al.,* 2010). Although experimental work is still required, it is likely that these molecules, together with the cryptochrome/photolyase family, play major roles in blue-light signaling.

1.1.4.4 Red light responses in the ocean

Although red light is rapidly extinct in the water column and therefore not abundant, it still constitutes an important underwater signal. Importantly, a rapidly decreasing but still detectable flux of red photons is present in the whole photic zone (Ragni and Ribera d'Alcala', 2004). It has been argued that band ratios (e.g., R:FR, B:R and G:R) may act in marine phytoplankton as complex switches controlling relevant processes such as pigments synthesis, photoadaptation, phototaxis, swimming velocity, gravitaxis and chloroplast displacement (Lopez-

Figueroa, 1992). Similar reports also exist for some bacteria and green algae (Kraml and Herrmann, 1991, Sineshchekov *et al.*, 2000), with red light phototaxis being often negative (Kondou *et al.*, 2001). Thus perceiving red light may allow different scopes. It may allow determination of surface proximity, where excessive light can induce photodamage. A more intriguing hypothesis is that red light deriving from chlorophyll autofluorescence may be perceived (Ragni and Ribera d'Alcala, 2004). At a close distance (< 100 μm), notably when cells aggregate or form chains, chlorophyll autofluorescence could overcome the background signal and the red light may then serve for quorum sensing and/or might affect the process of aggregation. As a matter of fact, several evidences support the presence of red light photoperception in diatoms. Several genes are induced by both red and far-red light (Leblanc *et al.*, 1999; Coesel *et al.*, 2008), and red light can accelerate the sinking of diatoms more rapidly than white and blue light (Fisher *et al.*, 1996). It can also induce motility responses in some estuarine species (Mclachlan *et al.*, 2009). The biological importance of red light has finally been reported for the sexual reproduction of the benthic pennate diatom *H. ostrearia*, in which exposure to red wavelengths triggered auxosporulation (Mouget *et al.*, 2009). Interestingly, in the fungus *Aspergillus nidulans* also, a red/far-red light photoreceptor is required for sexual sporulation and sexual development (Blumenstein *et al.*, 2005).

1.1.5 General characteristics of the phytochrome superfamily

The phytochromes constitute a superfamily of photoreceptors that usually allow sensing red and far-red light, enabling organisms to respond optimally to changing light conditions. In addition to absorbing red light, both forms of the phytochrome also absorb light in the blue region of the spectrum, as the phytochrome is known to be a blue protein pigment. Initially discovered in plants in which they play a central role in many developmental processes, phytochromes and phytochrome-like sequences are widely dispersed among bacteria, fungi and even in some non-photosynthetic organisms where they play diverse functions (e.g., chromatic adaptation, pigment

synthesis, phototaxis, sexual development and probably many other metabolic adaptations) (Karniol *et al.,* 2005; Rockwell *et al.,* 2006; Ulijasz and Vierstra, 2011). Because of the complexity of the subject, a simplified scheme of the phytochrome superfamily in plants, cyanobacteria, bacteria, fungi and diatoms is reported in figure 1.1.9.

Structure and function of phytochrome protein

Phytochrome is a soluble protein that occurs as a dimer, with monomer molecular weights of around 125 kDa. Each subunit consists of two components: a light-absorbing pigment molecule called the chromophore, covalently linked to a polypeptide chain called the apoprotein. Together they make up the functional holoprotein known as the phytochrome. The chromophore is a single bilin molecule consisting of an open chain of four pyrrole rings (tetrapyrrole) that absorbs the light and, as a result, changes the conformation of bilin and subsequently that of the apoprotein. All tetrapyrroles are synthesized from a common precursor, 5-aminolevulinic acid (ALA) (see figure 1.1.7, below), that is subsequently converted to protoporphyrin IX, through a highly conserved pathway (Timko, 1998). Protoporphyrin IX is the last common intermediate before the separation of the Fe^{2+} and the Mg^{2+} branches that lead to the formation of heme and chlorophyll, respectively. Heme is then further reduced by a an oxidative reaction catalyzed by heme oxygenase (HO) to yield their characteristic open chain. First, a heme oxygenase (HO1) converts heme into biliverdin (BV), which is directly incorporated as the chromophore of bacterial and fungal phytochromes. In plants and cyanobacteria, however, BV is further reduced to yield phytochromobilin (PΦB) in higher plants and phycocyanobilin (PCB) in cyanobacteria and green algae. Conversion of BV to PΦB is carried out by HY2 (phytochromobilin synthase) in the chloroplast, whereas reduction of BV to yield PCB is carried out by the bilin reductase (Peb). In this thesis, several diatom genes coding for enzymes involved in the tetrapyrrole biosynthetic pathway have been investigated: in the early steps of tetrapyrrole biosynthesis (*HEMA* and *GSAT*), after the Mg^{2+} branching point leading to the production of chlorophyll (*CHLH1, CHLH2 and POR1-*

4) and after the Fe^{2+} branching point leading to the phytochrome chromophores: BV, PΦB, PEB and PEB (*HO-2* and *PebA/B*). In plants, the PΦB is exported to the cytosol where it is autocatalitically linked to the apoprotein through a thioether linkage to a cysteine residue in the GAF domain (Montgomery and Lagarias 2002). The chromophore always binds through a conserved custeine residue, although this residue is not always found in the GAF domain (see figure 1.1.9).

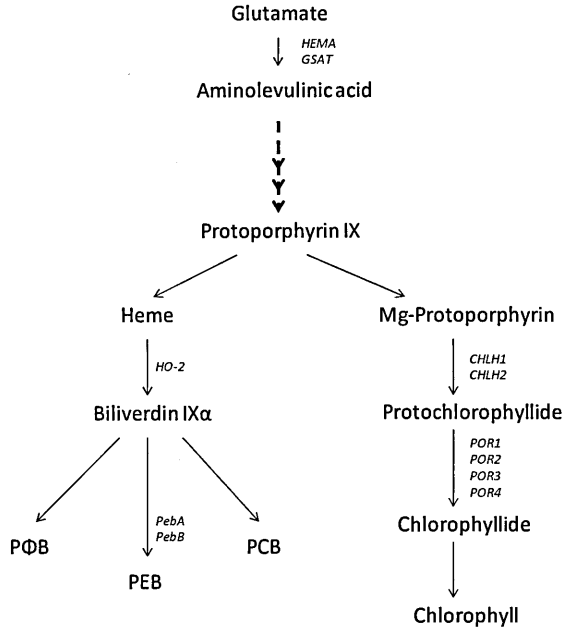

Figure 1.1.7: Tetrapyrroles biosynthetic pathway. Chlorophyll and heme are synthetized from the common precursor, 5-aminolaevulinic acid (ALA). Protoporphyrin IX is the last common intermediate before the separation of the Fe^{2+} and the Mg^{2+} branches that lead to the formation of heme and chlorophyll, respectively. The diatom genes coding for the tetrapyrrole biosynthetic enzymes that were analyzed in this study are reported in red: *HEMA* (glutamyl-tRNA reductase), *GSAT* (glutamate 1-semialdehyde aminotransferase), *CHLH1/2* (Mg-chelatase H subunit), *POR 1-4* (protochlorophyllide oxidoreductase), *HO-2* (heme oxygenase), *PebA-B* (bilin reductase).

Sequence comparison between phytochromes isolated from different species (plant, cyanobacteria and fungi) has enabled the identification of several conserved domains. Phytochromes contain a N-terminal photosensory domain and a less conserved output regulatory domain involved in dimerization and activation of signal transduction (Rockwell, 2006; Fankhauser, 2008; Nagatani, 2010; Ulijasz, 2010), related to the domain found on two-component histidine kinase systems. The N-terminal half usually contains i) a PAS domain, ii) a GAF domain which is the most conserved domain of the phytochrome and displays bilin-lyase activity, necessary for autocatalytic assembly of the chromophore, and iii) a PHY (for phytochrome)

domain, which stabilizes the phytochrome in the Pr forms. PAS domains are structurally related to GAF domains (Zhulin *et al.*, 1997) and are found in large families of transcriptional regulatory proteins including the period clock (PER) protein, the aromatic hydrocarbon receptor nuclear translocator (ARNT) and the single minded (SIM) of *Drosophila* (Aravind & Ponting, 1997). GAF domains are present in vertebrate cGMP-specific phosphodiesterases, in cyanobacterial adenylate cyclases and in the formate hydrogen lyase transcription activator FhlA (Aravind & Ponting, 1997). In higher plants, downstream of the PHY domain are two PAS-related domains (PRD) repeats that mediate phytochrome dimerization (see figure 1.1.8 and 1.1.10).

The C-terminal regulatory output domain varies among different species. It was shown in bacteria and fungi that phytochromes are light regulated histidine-kinases that perform histidine autophosphorylation and transphosphorylation of an aspartate within a response regulator (RR) domain (Yeh *et al.*, 1997; Yeh and Lagarias, 1998). The C-terminal domain of plant phytochromes is only weakly related to histidine kinases (Schneider-Poetsch, 1998; Yeh and Lagarias, 1998) and is therefore called a histidine kinase-related domain (HKRD; see figure 1.1.8). Moreover, mutating several critical residues required for bacterial HK activity did not affect the activity of plant phytochromes, suggesting that plant phytochromes are not active histidine kinases (Quail, 1997). Nevertheless, eukaryotic phytochromes were shown to be HK paralogs with serine/threonine specificity (Yeh and Lagarias, 1998). Consistent with this discovery several substrates of phytochrome kinase activity have been found in plants, such as PKS1 (Fankhauser *et al.*, 1999) and Cry1 (Ahmad *et al.*, 1998) (see later). However, so far, the kinase domain of phytochrome has not been determined. Also the biological function of this kinase activity in inducing light responses is unknown.

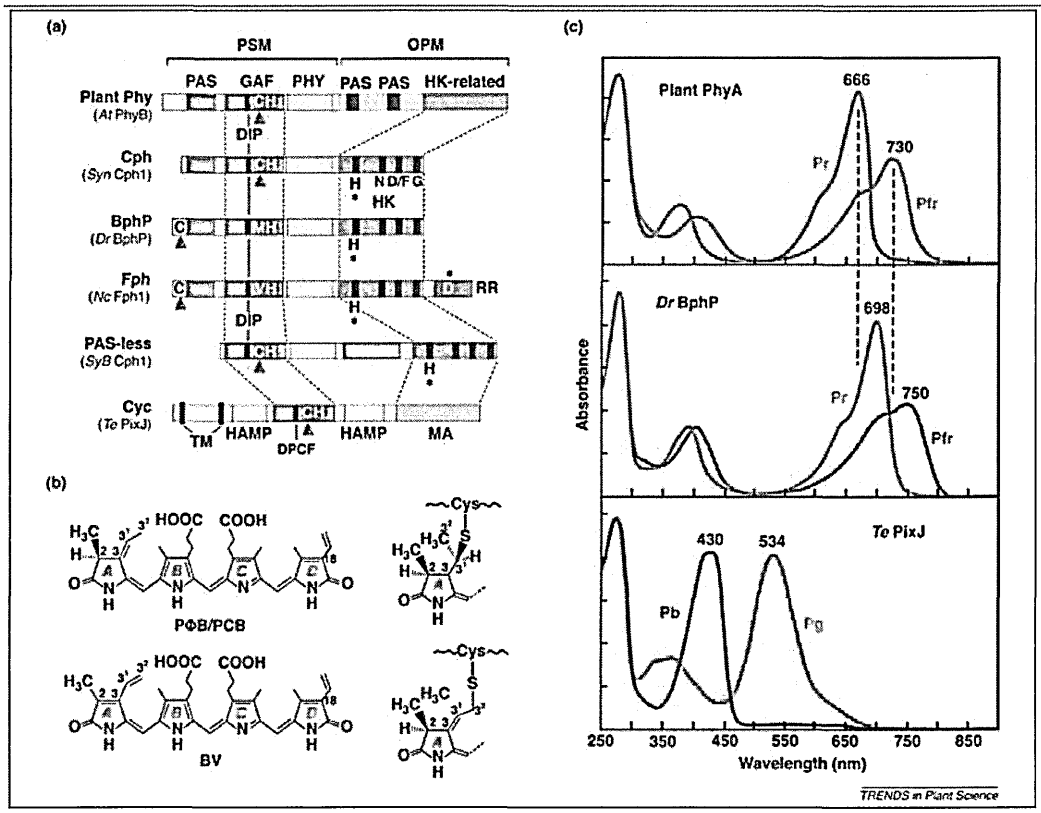

Figure 1.1.8: Domain structures of phytochromes. Description of the phytochrome families from plants (Phy), cyanobacteria (Cph, PAS-less and Cyc), proteobacteria (BphP) and fungi (Fph). **(a)** Domain structures of representative members. Red arrowheads indicate the bilin attachment site(s). **(b)** Structures of phytochromobilin (PΦB), phycocyanobilin (PCB), and biliverdin IXα (BV) in plant, cyanobacterial and proteobacterial/fungal phytochromes, respectively. **(c)** Absorption spectra of a plant phytochrome (full-length oat PhyA), a bacterial BphP [full-length *Deinococcus radiodurans* (*Dr*) BphP], and a cyanochrome [GAF domain from *Thermosynechococcus elongatus* (*Te*) PixJ] assembled with PΦB, BV and PCB, respectively. Figure from Vierstra & Zhang, 2011.

The phytochrome photochemical and biochemical properties

In dark-grown or etiolated plants, phytochrome is present in a red light-absorbing form (λ_{max} 660 nm), referred to as Pr. This inactive form is converted to a far-red light-absorbing form called Pfr (λ_{max} 730 nm), which triggers photomorphogenesis in plants. Pfr, in turn, can be converted back to Pr upon far-red light illumination. This phenomenon was initially observed in lettuce seeds that were stimulated by red light and inhibited by far-red light (Flint and McAlister, 1935). The real breakthrough came years later, in 1952, when lettuce seeds were exposed to alternating treatments of red and far-red light. Almost 100% of the red light-illuminated seeds germinated, whilst the far-red light treated seeds were strongly inhibited in germination

(Borthwick *et al.,* 1952). This conversion property, known as photoreversibility, is the most distinctive property of phytochrome. However, the phytochrome pool is never fully converted to the Pfr or Pr forms after red or far-red light irradiation, therefore the absorption spectra of the Pfr and Pr overlap (see figure 1.1.8 panel C). In plants, the Pfr form can spontaneously convert back to the Pr form in darkness over time. This phytochrome-specific process is called dark reversion. The physiological significance of dark reversion remains uncertain, but it has been proposed that it may protect a fraction of Pfr from degradation (Kendrick & Kronenberg, 1993).

In plants, the apo-protein autocatalitically assembles the bilin chromophore to form a covalent thioether linkage with a conserved cysteine residue in the GAF domain. The Pr-Pfr photointerconversion is mediated by a linear tetrapyrrole prosthetic group (bilin), which undergoes a *cis* to *trans* (*Z* to *E)* isomerization around the C15–C16 double bond. This action results in the far-red light absorbing Pfr form (Andel *et al.*, 1996). Even if the details are still unresolved, the Pr-Pfr phototransformation involves a series of intermediates that appear on the picosecond to millisecond timescales. For example, the bilin undergoes a deprotonation–reprotonation cycle before the appearance of Pfr. These properties together allow phytochrome to function as a red/far-red dependent light switch.

Plant phytochrome responses fall into three categories based on the amount of light required to trigger the response: very-low fluence responses, also known as VLFR (from 0,0001 $\mu mol/m^2$ to 0,05 $\mu mol/m^2$) and are non-photoconvertible; low-fluence responses also known as LFR (from 1,0 $\mu mol/m^2$ to 1000 $\mu mol/m^2$) and display photoreversibility and high-irradiance responses or HIRs which require prolonged or continuous exposure to light of relatively high irradiance and are not photoreversible. In plants, the photolabile phyA mediates the very-low-fluence response and the far-red high-irradiance response, whilst the photostable phyB acts as a typical red light receptor to mediate the low-fluence response and the red light high-irradiance response (Nagatani *et al.,* 1993; Parks and Quail, 1993).

The plant phytochrome signaling pathways

As phytochrome signaling was not the main topic of this thesis, I will only briefly summarize the most important findings on phytochrome signaling components from higher plants. In *Arabidopsis*, phytochromes are encoded by a nuclear gene family of 5 genes, denoted *PHYA-PHYE* (Sharrock and Quail, 1989; Clack *et al.,* 1994). PhyA and phyB are the most prominent phytochromes in *Arabidopsis* and regulate almost every facet of plant development and growth (Kami *et al.,* 2010; Franklin and Quail, 2010). PhyC-phyE are far less abundant (Clack *et al.,* 1994). Although phyA is the predominant phytochrome in etiolated seedlings, it displays unique properties as it rapidly degraded upon red light and accumulates in the dark and upon far-red light. In this way, phyA serves initially as a highly sensitive light 'antenna', enabling the rapid promotion of de-etiolation upon soil emergence. In sunlight, however, phyB is the most abundant phytochrome due to phyA degradation (Sharrock and Clack, 2002) and is the phytochrome that is the most involved in shade-avoidance responses. During the Pr to Pfr conversion, the protein moiety of the holoprotein also undergoes a conformational change resulting in the movement of the phytochrome molecule from the cytosol to the nucleus after its exposure to light for the first time. Once in the nucleus, phytochromes interact with transcriptional regulators to mediate changes in gene expression (Franklin & Quail, 2010). These interaction proteins are localized to the nucleus and can bind to DNA suggesting an intimate association between phytochromes and gene transcription. One of the most well-studied transcription factors that interact with phytochromes are the phytochrome-Interacting Factors (PIFs), that represent a subset of constitutively nuclear, basic helix-loop-helix (bHLH) transcription factors with a PAS domain. Using yeast two-hybrid library screens and co-immunoprecipitation techniques, several PIFs have been identified upon nuclear import with phyB in *Arabidopsis* (Matsushita *et al.,* 2003; Castillon *et al.,* 2007; Oka *et al.,* 2008), from which PIF3 is the most extensively characterized. PIF3 is able to bind G-boxes (Martinez-Garcia *et al.*, 2000), functionally important *cis*-elements within the promoters

of some light-regulated genes (Quail, 2000). Furthermore, the phytochrome/PIF3 interaction is red/far-red light-reversible, and only occurs when phytochrome is in the Pfr form (Ni *et al.*, 1999). This interaction triggers rapid phosphorylation and subsequent degradation of the PIF protein via the ubiquitin proteasome system. Several studies pointed out that PIFs negatively regulate photomorphogenesis (summarized in review from Leivar and Quail, 2011). Furthermore, PIF3 interacts with both phyA and phyB in their Pfr form (Ni *et al.,* 1998), whilst other characterized PIFs similarly bind Pfr-specifically to the phyB (Huq, 2004; Leivar, 2008). The cloning of several COP (constitutive photomorphogenesis)/ DET (de-etiolated)/ FUS (fusca) genes has revealed an essential role for these protein complexes in protein degradation during photomorphogenesis. During the night, COP1 enters the nucleus and the COP1/SPA complex adds ubiquitin to a subset of transcriptional activators. These transcription factors are then degraded by the COP9 signalosome-proteasome complex. During the day, COP1 exists the nucleus, allowing the transcriptional activators to accumulate. COP1 binds to phyA and phyB (Seo *et al.,* 2004; Boccalandro *et al.,* 2004) and also, COP1 has recently been found to bind both cry1 as cry2 (Wang *et al.*, 2001; Yang *et al.*, 2001).

HY5 is another important regulator in the phytochrome signaling pathway. *HY5*, encoding a bZIP transcription factor known as HY5. The mutant, known as *elongated hypocotyl 5* or *hy5 (*Oyama *et al.,* 1997), shows a general reduction of all types of light signaling. The action of HY5 is thought to be repressed by COP1 which induces degradation of HY5 (Osterlund *et al.,* 2000). The severity of this mutant demonstrates that HY5 plays a key role in the control of photomorphogenesis.

Around ten years ago, Jarillo *et al.* (2001) reported their findings on the binding of phyB to a PAS-containing circadian clock protein (ADO1). As the cryptochrome photoreceptor is known to entrain circadian rhythms in the fly *Drosophila*, mammals and *Arabidopsis,* this finding indicated that an *Arabidopsis* circadian clock component interacts with both cry1 and phyB.

In addition to nucleus-localized transcription factors, recent studies have shown that phytochrome also plays an important role in cytosol-mediated responses even if the role of phytochromes in the cytosol is not well understood. Two-hybrid screens revealed cytosolic proteins as potential partners for phytochrome proteins, such as Phytochrome Kinase Substrate 1 (PKS1), a protein of unknown function (Fankhauser *et al.*, 1999). PKS1 is able to interact with phyA and phyB in both the active Pfr and inactive Pr form (Fankhauser *et al.*, 1999). The PKS1 protein accepts a phosphate from phyA. A loss-of-function *pks1* mutant shows enhanced responsiveness to red light, implying that it may negatively regulate phyB signaling (Fankhauser *et al.*, 1999). Moreover, molecular and genetic analyses suggest that PKS1 and the closely related PKS2 act to promote phyA-mediated VLFR. More recently, it was suggested that these proteins are involved in cross-talk between phyA and phototropin signaling pathways (Lariguet *et al.*, 2006). On another note, it has been reported that phytochromes regulate mRNA translation and a number of growth responses even in the absence of nuclear import (Rösler *et al.*, 2007; Paik *et al*, 2012). In particular, Paik *et al.* (2012) showed that the Pfr form interacts with the cytosolic protein PENTA1 (PNT1) and inhibits the translation of protochlorophyllide reductase (*PORA*) mRNA, a chlorophyll biosynthetic gene. Their results demonstrate that phytochromes transmit light signals to regulate not only transcription in the nucleus through PIFs, but also translation in the cytosol through PNT1. Other evidence for phytochrome signaling events localized in the cytoplasm comes from studies that have implicated the involvement of G-proteins, cGMP, calcium and calmodulin in the control of phytochrome-dependent gene expression (Shacklock *et al.*, 1992; Bowler *et al.*, 1994). Reverse genetics approaches have subsequently provided further support for the involvement of G-proteins (Okamoto *et al.*, 2001). A role for calcium in light signaling has been reinforced by the identification of SUB1, a cytoplasmically-localized calcium-binding protein that appears to negatively regulate cryptochrome and phyA responses (Guo *et al.*, 2001).

1.1.6 Cyanobacterial phytochromes

The idea that phytochromes are only present in plants and a few algae, changed drastically with the pioneering work of Kehoe and Grossman (1996), studying complementary chromatic adaptation (CCA) in the cyanobacteria *Fremyella diplosiphon*. CCA occurs primarily in response to green and red light and was first observed in certain cyanobacteria that could change their pigmentation in response to the wavelengths of light in the environment (Engelmann, 1882). This process provides many cyanobacteria with the ability to tailor the properties of their light-harvesting antennae to the spectral distribution of ambient light (Grossman, 2003). The changes that occur during CCA have been well characterized in the freshwater cyanobacterium *Fremyella diplosiphon*, which is also designated Calothrix sp. PCC 7601 (Kehoe & Gutu, 2006).

Kehoe and Grossman identified RcaE for response to chromatic adaptation in a mutant E that was unable to respond to red or green light. It was later proposed that RcaE controls CCA by acting as a red light photoreceptor (Kehoe and Grossman, 1996 and 1997) and that the protein is structurally related to higher plant phytochromes and bacterial histidine kinases. Moreover, the authors also noted that other cyanobacteria, such as *Synechocystis* sp strain PCC6803, contain phytochrome-like sequences.

The cyanobacterial phytochrome, Cph1 from *Synechocystis*, has an overall domain arrangement comparable with that of plant phytochromes and incorporates phycocyanobilin (PCB) as a chromophore. The biochemical and functional characterization confirm that Cph1 is a phytochrome-like photoreceptor capable of binding a chromophore and being red/far-red photochromic (Yeh *et al.*, 1997; Hughes *et al.*, 1997; Park *et al.*, 2000). Many of the cyanobacterial phytochrome family have three highly conserved photosensory domains (PAS, GAF and PHY, with a conserved cysteine residue in the GAF domain for chromophore binding) and a C-terminal HK transmitter module (see figure 1.1.8 and 1.1.9). However, some cyanobacterial phytochromes have been found to bind the chromophore through a conserved cysteine residue in the N-terminal domain, upstream of the PAS domain, similar to the Bphs (see later).

Cph1 goes through reversible photoconversion, with Pr and Pfr absorption spectra. Yeh *et al.* (1997) have demonstrated that only Cph1-Pr exhibits kinase activity, suggesting that Cph1-Pr is the active form that transduces the light signal by phosphate transfer to Rcp1. This is in contrast with data from plants in which the Pfr is the active form transducing the light signals. Cph1 has a blue-shifted spectrum in comparison to the plant phytochromes and this can be explained by the loss of the N-terminal serine-rich domains in Cph1s (Vierstra, 1993), only present in higher plants so far.

Another cyanobacterial phytochrome in *Synechocystis*, Cph2, lacks the N-terminal serine-rich domain and the PAS domain as found in plant phytochromes. Because of the presence of a conserved cysteine residue in the GAF domain in Cph2 its ability for red/far-red reversible photochromicity *in vitro* (Tarutina *et al.,* 2006), it was suggested that this protein behaves as a *bona fide* phytochrome (Park *et al.*, 2000; Wu and Lagarias, 2000). Cph2 was shown to covalently attach a bilin as chromophore (Park *et al.,* 2000). However, Cph2 is unusual because the protein lacks a HK domain and has as alternative output domains as GGDEF and EAL (Montgomery and Lagarias, 2002). Moreover, the protein has two GAF domains with two cysteine-residue bilin binding sites, Cys-129 and Cys-1022 (Rockwell *et al.*, 2006). By *in vitro* mutagenesis and Zn^{2+} fluorescence, it was demonstrated that the Cys-129, not the Cys-1022, was the chromophore binding residue (Park *et al.*, 2000). Furthermore, Wilde *et al.* (2002) proposed that the Cph2 protein is part of a light-stimulated signal transduction chain inhibiting the movement of *Synechocystis* sp. PCC 6803 cells towards blue light. It remains unclear whether Cph2 itself is the photoreceptor that inhibits phototaxis under blue light or whether the interaction of Cph2 with another blue light receptor leads to the observed phenotype. Wilde and colleagues (2002) indeed suggested an involvement of another blue light receptor in motility, as Cph2 mutants are still able to sense blue light and can determine the position of the light source. Recently, Moon and colleagues (2011) suggested that Cph2 is essential for the inhibition of positive phototaxis toward UV-A. Moreover, their results demonstrated that another phytochrome-like protein, PixJ1 (see

later), is required for positive phototaxis toward UV-A and is also involved in suppressing the negative phototaxis.

Sequencing projects are now revealing that many novel phytochrome sequences are present in cyanobacteria, with variants missing the photosensory module PAS domain (Cph2 or PAS-less phytochromes) or both the PAS and PHY domains (Park *et al.*, 2000; Ulijasz *et al.*, 2008). Moreover, also GAF-only photosensory modules are present in cyanobacteria, which are respectively known as Cph2s and cyanobacteriochromes (CBCRs) (Wu *et al.*, 2000; Rockwell *et al.*, 2006; Ulijasz *et al.*, 2009). Also phytochrome-like sequences, called cyanochromes (Cycs), have been found that contain a distinct GAF domain. The Cycs are especially intriguing in that they employ two GAF domain cysteines to bind their chromophore that enables photoconversion between blue and green-light absorbing species (Ishizuka *et al.*, 2006; Ikeuchi & Ishizuka, 2008; Rockwell *et al.*, 2008). I will summarize several examples to demonstrate the variability in the cyanbacterial phytochrome family. For instance, the cyanobacterial phytochrome-like protein, PixJ1, binding to a bilirubin as chromophore (Yoshihara *et al.*, 2004; see figure 1.1.8) has been found in the unicellular cyanobacterium *Synechocystis* sp. PCC 6803. PixJ1 showed unique reversible photoconversion between a 425–435 nm absorbing form (Pb absorbing in the blue region) and a 531–535 nm-absorbing form (Pg absorbing in the green region) (Yoshihara *et al.*, 2004, Ishizuka *et al.*, 2006). This is in contrast with the red-absorbing form (Pr) and far- red absorbing form (Pfr) of plant phytochromes and bacterial phytochromes (Davis *et al.*, 1999, Giraud *et al.*, 2005). PixJ1 has also been reported to mediate positive phototactic motility on solid surfaces (Bhaya *et al.*, 2000; Yoshihara *et al.*, 2000) and is known to be involved in suppressing the negative phototaxis against UV-A (Moon *et al.*, 2011). Interestingly, the putative chromophore-binding GAF domain of a CikA homolog (named Slr1969), shows unique absorption peaks in the UV (≈325 nm) and violet (≈400 nm) regions (Narikawa *et al.*, 2008). The *Synechocystis* cyanochrome ETR1 is another example of the diversity within the cyanobacterial clades and binds

ethylene, implying that ETR1 works as a hybrid receptor to integrate light and hormone signals at once (Ulijasz *et al.,* 2009).

Most of the cyanobacterial phytochromes belong to the family of 'two component regulatory systems' that initiate a signal transduction cascade in response to various environmental signals, including light (Stock *et al.,* 2000). Two-component systems are based on two signal transduction components: a histidine kinase and a response regulator (reviewed by Mascher *et al.,* 2006). In prokaryotes, the genes encoding for these signaling elements are often found in the same operon, resulting in a close correspondence between histidine kinases and response regulators. This is also the case for Cph1 that resides in an operon with a gene encoding its response regulator Rcp1 (Yeh *et al.,* 1997). Cph1 acts as a light-regulated histidine kinase that autophosphorylates in the Pr form and then trans-phosphorylates the response regulator Rcp1 (Kehoe and Grossman, 1997; Esteban *et al.,* 2005; Psakis *et al.,* 2011).

Novel information on the signaling components of cyanobacterial phytochromes was derived from a study with a truncated derivative of Cph2, BphG1, that shows light-dependent c-di-GMP phosphodiesterase activity (Tarutina *et al.,* 2006) and is involved in a blue-light dependent signal transduction pathway. C-di-GMP is a novel second messenger and is involved in complex behavioral responses such as biofilm formation, virulence and many other surface-associated traits in bacteria (reviewed by Ryan *et al.,* 2006; Drepper *et al.,* 2011). The presence of C-di-GMP indicated a light-regulated, non-kinase enzymatic activity for this phytochrome-related molecule.

1.1.7 Bacterial phytochromes

A major breakthrough in phytochrome research was achieved with the discovery of phytochrome-like proteins in two heterotrophic eubacteria, *Deinococcus radiodurans* and *Pseudomonas aeruginosa* (Bhoo *et al.,* 2001). These bacterial phytochromes, or also called bacteriochromes (Bphs), are common among photosynthetic and non-photosynthetic eubacteria and present in some fungi.

In general, also the Bphs possess a typical N-terminal photosensory domain (PAS, GAF and PHY domain) and a HK domain. However, some Bphs can also display various other output domains, such as GGDEF (diguanylate cyclase), EAL (phosphodiesterase), PAS motifs with or without a Che Y-homologuous receiver domains (REC or RR) (Rockwell *et al.* 2006). GGDEF and EAL domain proteins are involved in c-di-GMP synthesis and often brought in correlation with surface attachment and multicellularity, as has also been observed in some cyanobacteria (Gomelsky & Hoff, 2011). Some of the bacterial phytochromes (e.g. *Synechococcus elongatus* CikA, *Pseudomonas putida* BphP2 and *Agrobacterium tumefaciens* BphP2) contain a RR domain appended to the C-terminal end of the HK domain.

A significant difference between plant and bacterial phytochromes lays in the binding site of the bacterial chromophore, which is located in the N-terminal region at the outer upstream border of the PAS domain through a conserved cysteine residue. Thus, Bphs lack the cysteine residue in the GAF domain. However, the adjacent histidine residue in the GAF domain of Bphs is reported to be conserved (Davis *et al.*, 1999) (see figure 1.1.8 and 1.1.9).

Bphs play diverse functions. They can serve as bilin, light and/or oxygen sensors (Montgomery and Lagarias, 2002) and be involved in carotenoid synthesis (Davis *et al.,* 1999; Giraud *et al.,* 2004), chlorophyll synthesis (Giraud *et al.,* 2002), synthesis of the photosynthetic apparatus (Karniol *et al.*, 2005), circadian rhythm (Schmitz *et al.,* 2000) or phototaxis (Yoshihara *et al.*, 2000). For example, it was revealed that Bphs might play an essential role in the regulation of the photosystem synthesis in the *Bradyrhizobium*'s (Giraud *et al.*, 2002). An identical function was shown in the photosynthetic bacterium *Rhodopseudomonas palustris*, in which it appeared that the bacterial photosynthetic apparatus was synthesized in its complete form only when the phytochrome was in its active (far-red-light absorbing) configuration (Giraud *et al.*, 2002). *al.,* 2000) or phototaxis (Yoshihara *et al.,* 2000). Also, a function for the phytochrome in *D. radiodurans Dr*BphP has been postulated in the light-dependent regulation of carotenoid

biosynthesis, to protect the bacterium from UV radiation (Davis *et al.,* 1999). Additionally, an investigation by Vuillet *et al.* (2007) revealed for the first time a Bph without chromophore. This discovery has been done by characterizing the photosynthetic bacterium *R. palustris* that has two distinct types of Bphs-related proteins, depending on the strain considered. The first type binds the chromophore biliverdin and acts as a light-sensitive kinase, thus behaving as a *bona fide* Bphs. But the second type, does not bind the chromophore. The loss of light sensing is replaced by a redox-sensing ability, which is mediated by two specific cysteine residues (Cys422 and Cys722) located in the PHY and HK domains, respectively.

All Bphs studied thus far, except for a new type of Bph found in the aerobic photosynthetic bacterium *Bradyrhizobium* ORS278 that binds phycocyanobilin (PCB), contain a BV as chromophore (Jaubert *et al.*, 2007). Major progress in the field of Bphs was achieved with the three-dimensional structure for the N-terminal phytochrome region bound to its chromophore (BV), from the extremophilic bacterium *D. radiodurans* (Wagner *et al.*, 2005). In particular, X-ray crystallography resolved the 35-kDa structure of the PAS-GAF domain of DrBph1 in its Pr form (Wagner *et al.*, 2005) and revealed how the chromophore is deeply buried in the chromophore pocket formed in the GAF domain. With this came also the discovery of a 'light-sensing knot' formed between the PAS and GAF domain through a lasso loop (reviewed in Vierstra and Zhang, 2011). It has been shown by structural studies that this knot is a general characteristic of PAS-containing phytochromes (Essen *et al.*, 2008; Yang *et al.*, 2007 and 2008). The importance of the knot is unclear: possibilities are that it stabilizes the photosensory module, and/or that it encourages conformational changes in the bilin and protein during photoconversion (Vierstra and Zhang, 2011). Mutations in the PAS and GAF domains of plant phytochromes that result in altered function *in vivo* have been mapped onto the *Dr*BphP structure. Although several loss-of-function mutations cluster about the chromophore-binding pocket as expected, others occur in residues at the interface between the PAS domain and the trefoil knot, such as Gly118, Ser134, and Ile208 in *Arabidopsis* PhyB. Such mutations might affect the proper folding of these domains.

It is conceivable that these helices play a role in signal transduction via light-mediated regulation of either intramolecular interactions or direct intermolecular interactions with downstream signaling components.

The spectral properties of Bphs are more shifted toward the red end of the spectrum in comparison with plant phytochromes (see figure 1.1.8). Information on the Bph spectral properties have been derived from the extensively studied proteobacterium *Agrobacterium tumefaciens*, containing two genes encoding for phytochrome-homologous proteins (Bhoo *et al.*, 2001) termed Agp1 and Agp2 (Lamparter *et al.*, 2002). *In vitro* assembly and chromophore binding of Agp1 with BV showed that the spectrum was red-shifted to 701 nm for Pr and 755 nm for Pfr (Lamparter *et al.*, 2002). Agp1 exhibits strong autophosphorylation activity in the Pr form, although kinase activity has been demonstrated in both the Pr and the Pfr forms (Lamparter *et al.*, 2002). In Bph of *P. aeruginosa*, the HK activity did not differ significantly between the Pr and the Pfr forms (Tasler *et al.*, 2005), whereas for *P. syringae* phytochrome (Bhoo *et al.*, 2001) and for *A. tumefac*iens phytochrome AtBphP2 (Agp2) (Karniol *et al.*, 2003), strong Pfr activity and weak Pr activity have been reported. Interestingly, Bphs that possess far-red absorbance maxima in the thermal ground state with photoconversion to Pr-like species were described in the Rhizobiales, bacteria that live mainy in the soil (Giraud *et al.*, 2002; Karniol and Vierstra, 2003). Whether this spectral inversion proceeds via a reverse of the normal dark reversion pathway or via some other mechanism is not yet clear for any of these bathy Bphs or 'bathy-bacteriophytochromes' ((Rottwinkel *et al.*, 2010). This peculiar feature of the Rhizobiales phytochrome might be due to their light regime in the soil. Some other bacterial phytochromes, from *Rhodopseudomonas* and *Bradyrhizobium,* photoconvert between Pr and a near-red 'Pnr' or orange 'Po' conformation (Jaubert *et al.*, 2007).

Amino acid sequence analysis tools showed that Agp1 has a domain arrangement typical for bacterial phytochromes such as Cph1 from *Synechocystis* or Bph from *D. radiodurans*. Agp2, on the other hand, is unusual as it contains the GAF and PHY domains but no HK module.

Although Agp1 and Agp2 have both been reported to act as light-regulated kinases (Karniol & Vierstra, 2003), Agp2 has been designated to a new class of kinases which are termed HWE histidine kinases, carrying a C-terminal response regulator domain (Karniol & Vierstra, 2004).

1.1.8 Fungal phytochromes

Fungi are capable of responding to radiance from UV-C to far-red light (Purschwitz, J. *et al.,* 2006). Brandt and co-workers (2008) reported the first study of a functional and spectral characterization of the fungal phytochrome FphA in *Aspergillus nidulans.* Several putative fungal phytochrome genes have also been found in the genomes of other ascomycetous fungi such as *Neurospora crassa*, *Gibberella zeae*, *Cochliobolus heterostrophus*, and *Aspergillus fumigatus*, and also in the basidiomycetes *Ustilago maydis* and *Cryptococcus neoformans* (Blumenstein et al, 2005; Karniol *et al.,* 2005). While FphA has been understood to be involved in the control of the sexual and asexual cycle of *A. nidulans*, the function of the *N. crassa* phytochromes, designated as PHY-1 and PHY-2, remains unclear. Though, it has been reported that the abundance of the PHY-1 transcripts are circadian-clock regulated (Froehlich *et al.,* 2005).

All fungal phytochromes share a common domain organization, very similar to bacterial phytochromes. They typically consist of an N-terminal photosensory domain (PAS-GAF-PHY), harboring the bilin chromophore and a C-terminal output module (Brandt *et al.,* 2008) (see figures 1.1.8 and 1.1.9). Particularly, fungal phytochromes possess an N-terminal variable extension (NTE) preceding the PAS domain (Blumenstein *et al.,* 2005; Froehlich *et al.,* 2005), which is not homologous to the serine-rich N-terminal domain (upstream from the PAS domain) of plant phytochromes (Montgomery and Lagarias, 2002). This fungi-specific NTE region is now known to stabilize the Pfr form. Concerning the C-terminal output module, fungal phytochromes are multi-functional proteins combining a histidine kinase domain and a response regulator domain (RR) in one protein (Brandt *et al.,* 2008). Although it was known for a while that *Aspergillus nidulans* requires red light for asexual sporulation (Mooney & Yager, 1990), the involved red light

photoreceptor (Fph) was only characterized a few years ago by Blumenstein *et al.* (2005), because at that time the central dogma was that phytochromes are plant-specific molecules (Rodriguez-Romero *et al.*, 2010). Other work presented by Purschwitz and co-workers (2008) demonstrated that there is a tight interaction between blue and red light sensing in *A. nidulans* for fine-tuning of asexual and sexual reproduction in response to light.

Recombinant FphA from *Aspergillus nidulans* was characterized as a *bona fide* phytochrome with absorbance maxima at 705 and 758 nm for the Pr and Pfr forms, respectively (Brandt *et al.*, 2008). The form initially synthesized in the dark is the Pr form. Neither the Pr nor the Pfr form undergo a defined dark reversion as it is especially found by dicot plant phytochromes to regulate the signal output. In FphA, cysteine 195 within the PAS domain was shown to be the site of attachment for BV (Blumenstein *et al.*, 2005), similarly to bacterial phytochromes. Because no heme oxygenase can be identified in most of the currently available fungal genomes, the nature and synthesis of the bilin chromophore remains cryptic. Although, in *Saccharomyces cerevisiae* and *Candida albicans*, heme oxygenases have been identified. These heme oxygenasese are used to acquire free iron from heme, a process necessary for survival and virulence (Kim *et al.*, 2006; Pendrak *et al.*, 2004). However, these fungi do not possess phytochrome.

FphA most probably integrates the signal light via two-component signaling phosphorelays, fused to the phytochrome protein. FphA is a functional histidine kinase protein, since the Pfr form phosphorylates very efficiently. Thus, the Pfr form appears to be an active HK, but autophosphorylation of the Pr form could also be observed and depends on a functional RR domain of the dimerization partner. These data suggest a functional RR domain is necessary for tuning the kinase activity in both spectral forms.

In contrast to plant phytochrome proteins, fungal phytochromes were initially observed to localize exclusively to the cytosol, irrespective of light conditions (Froehlich *et al.*, 2005; Blumenstein *et al.*, 2005). Further studies have now also identified a fraction of FphA in the

nucleus as well (Purschwitz *et al.,* 2008). The proteins LreA, LreB and VeA have been shown to be FphA-interacting proteins and they have been identified by the purification of light-regulated protein complexes (Purschwitz *et al.,* 2008). These regulatory proteins are White Collar (WC) homologs, that are PAS domain-containing transcription factors and play a dominant role in the blue light perception and the circadian feedback loops in *Neurospora.* FphA appeared to interact directly with both regulator proteins VeA and LreB. These interactions were mapped to the C-terminal output motif of FphA and VeA was found to be a highly phosphorylated protein (Purschwitz *et al.*, 2009), although no downstream phosphotransfer initiated by FphA was shown.

Concluding summary: the phytochrome superfamily

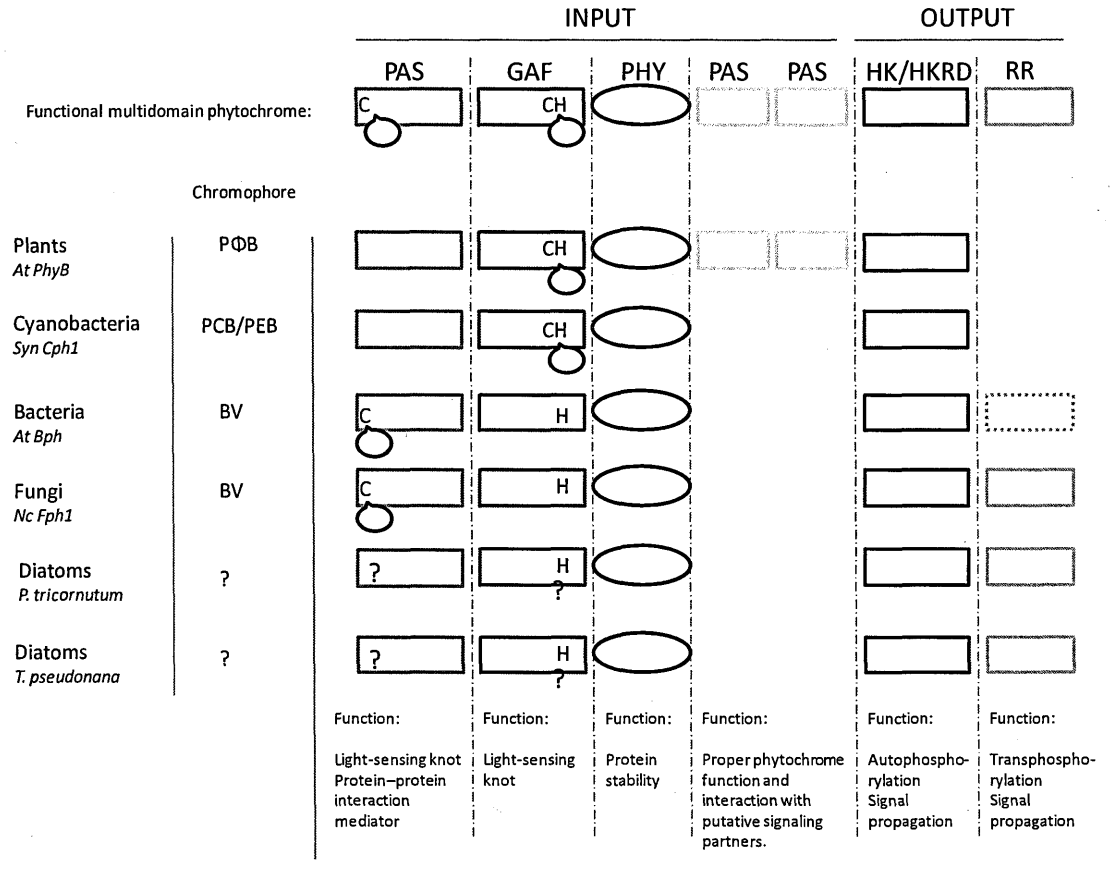

Figure 1.1.9: Simplified scheme showing domains and their functions in phytochrome proteins from plants (*A. thaliana* PhyB), cyanobacteria (*Synechocystis* sp. PCC6803 Cph1), bacteria (*D. radiodurans* Bph), fungi (*N. crassa*) and two diatom species (DPh from *P. tricornutum* and *T. pseudonana*). The structure of DPhs is described in detail in the next paragraph. The figure on top of the scheme represents a fictional phytochrome protein with all the possible domain combinations and sites for chromophore binding from the species above described. The domain abbreviations are: PAS (PAS, domain, PER-ARNT-SIM), GAF (GAF domain), PHY (PHY domain), HK (histidine kinase domain), HKRD (histidine kinase-related domain), RR (response regulator). Chromophore abbreviations are: PΦB (phytochromobilin); PCB (phycocyanobilin); PEB (phycoerythrobilin), BV (biliverdin). The C in the PAS or the GAF domains refers to the conserved cysteine residue for chromophore binding. The balloon cartoon represents the chromophore. The H in the GAF domain refers to the histidine residue that is conserved in all GAF domains throughout the phytochrome superfamily. The dashed line for the RR in bacteria refers to the fact that the RR is not always attached to the phytochrome molecule in bacteria.

1.2. Material and methods

1.2.1 Cell culture conditions for P. tricornutum

Axenic *P. tricornutum* cells were obtained from the Provasoli-Guillard National Center for Culture of Marine Phytoplankton (strain CCMP632, originally isolated by Coughlan in 1956 of the coast of Blackpool, U.K.). Cultures were normally maintained at a temperature of 18 ± 1°C in a 12 hour photoperiod with white light at an intensity of approximately 100 µmols/m^2/s^1 in autoclaved 95% f/2 medium without silica (Guillard, 1975). After selection of positive transformants, the DPh knock-down lines were kept under antibiotic selection with zeocine (100 µg/ml final concentration) on 95% f/2 - silica plates. For the gene expression studies, the cells were grown in artificial seawater (ASW; Vartanian *et al.*, 2009).

1.2.2 Cell culture conditions for T. pseudonana

Axenic *T. pseudonana* cells were obtained from Provasoli-Guillard National Center for Culture of Marine Phytoplankton (strain CCMP1335, originally isolated by Guillard in 1958 from Moriches Bay, Long Island, New York). Cultures were grown at a temperature of 18 ± 1°C in a constant light regime (24 hours light) with a white light intensity of approximately 100 µmols/m^2/s^1. Generally, cells were grown in autoclaved NEPC medium (Kröger *et al.*, 2000).

1.2.3 Construction of PtGAF and PtDPh3' silencing vectors

To obtain DPh knock-down lines in *P. tricornutum*, different constructs were made. Either the DPh silencing plasmid was generated with a fragment against the GAF region as target (called PtGAF) or with a fragment against the 3'UTR region of DPh as target (called PtDPh3'). Both the PtGAF and PtDPh3' plasmids were constructed from the parental PtGUS RNAi vector containing either the antisense *GUS* gene fragment or the inverted repeat *GUS* gene fragment (De Riso *et al.*, 2009).

For generation of the DPh-GAF inverted-repeat vector, a 250 bp fragment (corresponding to the *DPh* gene sequence from 727 bp to 977 bp, Phatr2 ID number 54330) and a 418 bp fragment (corresponding to the *DPh* gene sequence from 727 to 1145 bp) were amplified from the *DPh* cDNA, respectively, with the primers *Gaf1fw* (containing a *Eco*RI site: (5'ACTGAATTCCAGCTATCTTGGCATGC 3')) and *Gaf1rv* (containing a *Xba*I site; (5'ACTTCTAGATCATTGTCGACAACAAT 3')), and *Gaf1fw* and *Gaf2rv* (containing a *Xba*I site). The fragments were digested with *Eco*RI and *Xba*I and ligated in sense and antisense orientations in the *Eco*RI site of the original GUS vector, replacing the *GUS* gene fragments. The PtGAF inverted repeat silencing plasmid was generated with two different promoters, either the FcpB (Fucoxanthin Chlorophyll a/c-binding Protein B) or the H4 (Histone 4) promoter and contain the *sh ble* gene downstream of the H4 or FcpB promoter, conferring resistance to phleomycin. This cloning strategy generated the H4-GAF and FcpB-GAF inverted repeat plasmids.

For the antisense PtGAF construct, a 250 bp fragment from the GAF region (from 727 bp to 977 bp on the *DPh* gene) was amplified from cDNA with the *GAF1fw* (with *Eco*RI; (5'ACTGAATTCCAGCTATCTTGGCATGC 3')) and *Gaf1Rv* (with *Xba*I; (5'ACTTCTAGATCATTGTCGACAACAAT 3')) oligos, digested with *Eco*RI and *Xba*I and subsequently introduced in the antisense orientation between the *sh ble* gene and the FcpA terminator into the *Eco*RI – *Xba*I linearized GUS plasmid with H4 or FcpB promoter, to replace the *GUS* gene fragment with the GAF fragment. With this cloning strategy, H4-GAF and FcpB-GAF antisense silencing plasmids were generated. Also antisense plasmids were made with a 200 bp amplicon (from 3110 bp to 3310 bp on the *DPh* gene) from the 3'UTR region of *DPh*. This PtDPh3' fragment was amplified from cDNA with the following forward oligo *NorrFw1* including an *Eco*RI restriction site (5'ACTGAATTCTGATGTACACTGCTGATGCCA 3') and the following reverse oligo *NorrRv1* including a *Xba*I restriction site (5'ACTTCTAGACGGCCGAAGAATAAACGAAA 3'). The PCR product was digested

with *Eco*RI and *Xba*I and introduced in antisense direction into a the *Eco*RI - *Xba*I linearized GUS plasmid with H4 or FcpB promoter, to replace the *GUS* gene fragment with the *PtDPh3'* gene fragment. This cloning strategy generated the H4-DPh3' and FcpB-DPh3' antisense silencing plasmids. For maps of the generated plasmids, see annex 3.

Subsequently, inverted repeat and antisense PtGAF and antisense PtDPh3' silencing vectors were introduced into a *P. tricornutum* WT strain Pt1 by microparticle bombardment (see later). Putative silenced clones were first selected on 1% agar plates (50% f/2- silica medium) containing 50 µg/mL phleomycin (Invitrogen). The presence of silencing constructs was verified by checking the integration of the *Sh ble* gene with the primers *Sh ble1fw* (5' AGGGTACCCATGGCCAAGTT 3') and *Sh ble1rv* (5' GATGAACAGGGTCACGTCGTC 3'). The obtained DPh knock-down lines were kept under 100 µg/mL zeocine antibiotic (member of the bleomycin/phleomycin family, InvivoGen) selection in liquid media and plates with 95% f/2 - silica. For long-term storage, aliquots from the PtGAF and PtDPh3' knock-down lines were stored in -80°C, after cryopreservation in a 10% DMSO solution.

1.2.4 Transformation of P. tricornutum and selection of resistant clones

The protocol to transform *P. tricornutum* has been described in Falciatore *et al.* (1999). Approximately 5 x 10^7 cells were spread on 1% agar plates (50% f/2 – silica medium). 5 µg of plasmid DNA from the PtGAF, PtDPh3' or PtHO-2 silencing vectors were coated onto M17 tungsten particles of 1.1 µm diameter (Bio-Rad) as described in the manual of the Biolistic PDS-1000/He Particle Delivery system (Bio-Rad) and was used to bombard the cells. Agar plates containing diatoms cells are positioned at level 2 in the Biolistic chamber (around 6 cm for the stopping screen) to be bombarded using a pressure of 1550 psi. After bombardment, the diatoms cells were maintained for 48 hours in the diatom culture room and were then spread on 1% agar plates (50% f/2 – silica medium) containing 50 µg/mL phleomycin (Invitrogen). Resistant colonies

were obtained after 3-4 weeks of incubation at 18°C in a 12 hour dark-light photoperiod. Individual resistant colonies were restreaked on 50% f/2 – silica medium plates with 1% agar and 100 µg/mL zeocine (InvivoGen) for further analysis.

1.2.5 Colony screening on diatoms

Positive transformants were screened for the presence of the introduced plasmid via a colony screening by PCR. Separate tubes were prepared for each clone containing 20 µl of cold lysis buffer (1% Triton X100, 20 mM Tris-HCl pH 8 and 2 mM EDTA). Individual colonies were picked, resuspended in the lysis buffer, vortexed, kept on ice for 15 minutes and subsequently, incubated at 95°C for 10 minutes. Samples were diluted with 1 ml of Milli-Q water and 5 µl of this dilution was used as template for PCR screening with the target primers.

1.2.6 Construction of the pBad-DPh-Myc-HisC expression vector and expression in E. coli

In order to express DPh in *E. coli* for further protein purification and biochemical studies, the bacterial expression vector pBad-DPh-MycHisC was made. The 1089 bp N-terminal region from the *DPh* gene, containing the GAF domain has been amplified by PCR with oligos *Pt2FwSmaI* containing a *SmaI* restriction site (5'CGAACACCCGGGATGAGCGGGGCAAATTATAGAG 3') and *Pt4RvHind3* containing a *HindIII* restriction site (5' GACAAAGCTTACATGAGAGATTCAATACGAAC 3') and was subsequently digested with restriction enzymes *SmaI* and *HindIII*. This fragment was introduced in the pBad-DPh-MycHisC expression plasmid (Gambetta & Lagarias, 2001) harboring the cyanobacterial phytochrome Cph1 from *Synechocystis* sp. PCC6803. The original Cph1 plasmid was digested with *NcoI* and subsequently, the *NcoI* site was made blunt by Klenow fill-in to match with the blunt *SmaI* digested *DPh* gene fragment. Then, the plasmid was digested with *HindIII* to remove the Cph1 fragment and followingly, the *SmaI-HindIII* digested N-terminal *DPh* gene fragment was ligated into the linearized pBad-MycHisC plasmid to yield the pBad-DPh-MycHisC plasmid. For a map of the generated plasmid, see annex 3. *E. coli* strain LMG194 (Invitrogen) was transformed with pBad-DPh-MycHisC by using standard protocols to produce ampicillin-resistant

apophytochrome-expressing strain. Positive transformants were transformed with plasmid pPL-BV, containing the gene operon with a heme oxygenase and a bilin reductase gene for the chromophore biosynthesis, conferring resistance to kanamycin (Gambetta & Lagarias, 2001). Transformants exhibiting both ampicillin and kanamycin resistance were selected. As control, a pBad-Cph1-MycHisC plasmid was transformed with a pPL-PCB plasmid for expressing the cyanobacterial apophytochrome with its chromophore PCB. Both plasmids pPL-PCB and pPL-BV for chromophore biosynthesis were gifts from C. Lagarias. The expression of the vectors was under the control of an inducible system, therefore co-expression experiments were done in several steps. The details of the procedure are described below:

One liter of RM media contains 2% casamino acids, 0,2% glucose, 1 mM MgCl2, 1 x M9 salts. One liter of 10 x M9 salts contains 60 g of Na_2HPO_4, 30 g of KH_2PO_4, 5 g of NaCl, and 10 g of NH4Cl (pH 7.4). *E. coli* strain LMG194 containing both apophytochrome and PCB or BV biosynthetic expression plasmids were grown overnight at 37°C in 2 ml of RM media with 25 µg/ml of kanamycin and 50 µg/ml of ampicillin, to inhibit expression of the pBad vector. Cultures were then diluted to 100 ml of RM media, grown at 37°C till the cultures reached an OD_{600} of 0,5. Cultures were then transferred to 9 ml of Luria-Bertrani (LB) medium with 25 µg/ml of kanamycin and 50 µg/ml of ampicillin.. Followingly, IPTG was added to a final concentration of 1 mM to start the expression of the bilin biosynthetic operon. After incubation for 1 h at 37°C, arabinose was added to a final concentration of 0.002% to induce the expression of the apoDPh and to hyperinduce the expression of the bilin biosynthetic operon. Cultures were grown for 4 hours at 37°C, after which cells were collected by centrifugation and resuspended in 100 µl of Laemmly 1x sample buffer. Samples were boiled at 100°C for 5 minutes and then stored at -20°C till further analysis. As described in Lagarias and Gambetta (2001), Cph1 co-transformants turned deep blue-green within 4 hours of induction as a result of the production of holo-Cph1. In the case of the DPh co-transformants no color changes in the pellets were detected. Protein extracts were

analyzed for holophytochrome expression by SDS-PAGE. After electrophoresis, the 10% acrylamide gel was stained with Coomassie Brilliant Blue staining. The proteins from a second acrylamide gel were electrophoretically transferred to polyvinylidene difluoride (PVDF) membranes at 100 V for 90 min. The PVDF membranes were incubated in 1.3M zinc acetate overnight at 4°C. Fluorescence was visualized with the Transilluminator. The co-expression experiment to induce the formation of a diatom holophytochrome was repeated with an overnight incubation temperature at 18°C in minimal media (RM) to optimize expression conditions. Unfortunately, positive results were only obtained for the positive control with the cyanobacterial pBad-Cph1-MycHisC plasmid.

1.2.7 Construction of the pKT270 PebB-PebA expression vector and expression studies in E. coli

In order to broaden our attempts to express PtDPh, a trial was started to use chromophore biosynthetic genes putatively specific to diatoms. Two genes were found in the genome of *P. tricornutum*, possibly coding for bilin reductase in *P. tricornutum*, known as *PebA* (Phatr2 ID number 33770, chromosome 4) and *PebB* (Phatr2 ID number 45446, chromosome 7). The bilin reductases might produce phycoerythrobilin (PEB) from biliverdin and possibly, diatoms might use PEB as a diatom-specific chromophore. These genes were amplified by PCR, in order to clone into the low-copy number plasmid pKT270, sent to our laboratory from the group of Prof. Dr. Takayuki Kohchi in Japan. The pKT270 plasmid provides an inducible T5 promoter and the *HO1* (Heme Oxygenase) gene. The cloning strategy was performed in accordance with the work of Prof. Dr. Mukougawa *et al.* (2006), allowing the cloning of the *PebB* and *PebA* gene fragments into the pKT270 expression plasmid. *PebA* gene fragment was amplified from cDNA by PCR with the forward oligo *PebAFw* (5' ACGCTCTAG**AGGAGA***AATTAACT*ATGGTCCGCGCCTACCAGGTCCATCGG 3') including a *Xba*I restriction site, the ribosomal binding site sequence (bold) and the Shine-Delgarno sequence (italic) for optimal expression in the bacterial host system, and the reverse oligo *PebARv* (5' ACGCGTCGACCTACTTTTGCGAGAGTGGAAAGAG 3') harboring a *Sal*I restriction

site. The *PebB* gene fragment was amplified from cDNA by PCR with the forward oligo *PebBFw* (5'ACGCGTCGAC**AGGAGA***AATTAACT*ATGAAGTTGGTTCCTGCGTGGACC 3'), including a *Sal*I restriction site, a ribosomal binding site sequence (bold) and the Shine-Delgarno sequence (Italic) as in the PebA forward oligo, and the *PebB* reverse oligo *PebBFw* (5' ACGCTCTAGA CTATGGCGATGGGAATAGCAC 3') with a *Xba*I restriction site. Both PebA and PebB PCR fragments were digested with *Sal*I-*Xba*I restriction enzymes. The parental plasmid was digested with the Sal*I* restriction enzyme and PebB and PebA, both containing *Sal*I restriction sites at the 5' end (PebB) and 3' end (PebA), were ligated to each other in serie (PebB-PebA) by a common *Xba*I restriction site. Positive transformants were selected on Luria-Bertrani plates with chloramphenicol (25 µg/ml). The sequence of the plasmid pKT270-PebB-PebA has been validated by sequencing and were then send to the laboratory of Dr. Masahiko Ikeuchi in Japan. For a map of the generated plasmid, see annex 3. There, the pKT270-PebB-PebA plasmid was used for further expression studies with the diatom apophytochrome expression plasmid in *E. coli.* The N-terminal photosensory region of the *DPh* gene was *Nco*I-*Sal*I restricted, fused to an N-terminal tag and cloned into the expression vector *Nco*I-*Sal*I linearized plasmid pET28a. Subsequently, the pET28a plasmid was introduced into a *E. coli* strain harboring the pKT270-PebB-PebA plasmid. The *E. coli* cells harboring both expression plasmids were grown at 37°C with shaking at 200 rpm for 2 hours till OD_{600} of 0.34 was reached. IPTG was added to a final concentration of 0.1 mM to induce protein expression. The culture was further incubated overnight at 18°C in the dark for 16 hours at 110 rpm. Cells were collected by centrifugation when reaching an OD_{600} of 4.01. After washing with 20 mM HEPES–NaOH, pH 7.5, cells were resuspended in the same buffer and then broken with a French press with three passages at 1,500 kg cm^{-2}. The homogenate was centrifuged at 194100 x g for 30 min at 4°C. The supernatant was applied to an Ni-affinity column (HiTrap HP column; GE Healthcare) equilibrated with 20 mM HEPES-NaOH (pH 7.5), 100 mM NaCl and 10% (w/v) glycerol. The protein was eluted, using a linear gradient of imidazole. Absorbance and difference spectra of DPh were obtained by UV-VIS spectroscopy. For zinc blot analysis, proteins

separated by gel electrophoresis (SDS–PAGE) and were incubated for 30 minutes with 20 µM zinc acetate. Another acrylamide gel was stained with Coomassie Brilliant Blue staining. Fluorescence from the zinc acetate staining was detected using the sensitive FM-BIO II detection system. Absorption spectra were recorded with a UV-2400PC spectrophotometer (Shimadzu, Kyoto, Japan).

1.2.8 Construction of the codon-optimized DPh expression plasmid and expression studies in E. coli

Because previous trials were not very successful in expressing the diatom DPh in *E. coli*, an additional attempt was performed by rewriting the PtDPh full-length sequence for optimizing expression in *E. coli* (see Chapter I, Results, figure 1.3.3). Subsequently, the team of Prof. Dr. Masahiko Ikeuchi in Japan generated two constructs with the optimized sequence for DPh. In one case, the N-terminal photosensory region including the N-terminal photosensory domain including the conserved cysteine for chromophore attachment, and the GAF and PHY domains were introduced into the *Nco*I-*Xho*I restricted pET28a plasmid. In order to introduce *Nco*I and *Sal*I restriction sites for cloning the N-terminal photosensory region, two amino acids in the DPh sequence were altered: a serine on position 2 in the DPh sequence was altered into an alanine and an isoleucine on position 573 was altered into a valine. *Nco*I restriction site was obtained as described above and the *Xho*I restriction site was obtained by adding two amino acids (leucine and glutamic acid) at the C-terminal end of the DPh sequence. The pET28a plasmid containing either the N-terminal or the full-length DPh was introduced in competent *E. coli* strain BL21. Subsequently, kanamycin-positive transformants were co-transformed with cells harboring a pKT270 plasmid, producing biliverdin from the cyanobacterial heme oxygenase gene (*HO1*) from *Synechocystis*. Positive transformants harboring the two expression plasmids were selected on media containing both kanamycin and chloramphenicol. The *E. coli* cells were grown at 37°C with shaking at 200 rpm for 2 hours till to OD_{600} of 0.36 was reached. IPTG was added to a final concentration of 0.1 mM to induce protein expression. The culture was further incubated

over night at 18°C in the dark for 15 hours at 110 rpm. Cells were collected by centrifugation when reaching an OD_{600} of 4.805. After washing with 20 mM HEPES–NaOH, pH 7.5, cells were resuspended in the same buffer and then broken with a French press with three passages at 1,500 kg/cm. The homogenate was centrifuged at 194100 x g for 30 min at 4°C. The supernatant was applied to an Ni-affinity column (HiTrap HP column; GE Healthcare) equilibrated with 20 mM HEPES-NaOH (pH 7.5), 100 mM NaCl and 10% (w/v) glycerol. The protein was eluted, using a linear gradient of imidazole. Absorbance and difference spectra of DPh were obtained by UV-VIS spectroscopy. For zinc blot analysis, proteins were separated by gel electrophoresis (SDS–PAGE) and were incubated for 30 minutes with 20 µM zinc acetate. Another acrylamide gel was stained with Coomassie Brilliant Blue staining. Fluorescence from the zinc acetate staining was detected using the sensitive FM-BIO II detection system. Absorption spectra were recorded with a UV-2400PC spectrophotometer (Shimadzu, Kyoto, Japan).

1.2.9 Cell culture conditions for prolonged red light treatments in P. tricornutum

In order to characterize red light-induced genes in *P. tricornutum*, several time course experiments were performed with WT cells exposed to red light. In a first experiment, WT cells were dark-adapted for 60 hours and exposed to continuous red light (660 nm) for two hours. Cells were exposed to either 0,2 or 2 µE of red light. Samples were taken before the onset of light, and after 30 minutes, 1 hour and 2 hours of red light illumination. Samples were collected on Whatman filters (diameter 40,5 mm) by filtration. The filters were immediately washed with 50 ml of PBS 1x before freezing the filters in liquid nitrogen. *P. tricornutum* WT cells were grown in Artificial Seawater (ASW) to increase to reproducibility of the experiments. Subsequently, this experiment was repeated with Pt1 WT and three DPh knock-down lines (*dph-1, dph-1' and dph-5').* The cells were dark-adapted for 60 hours and subsequently exposed to 0.2 µE, 2µE or 20 µE of continuous red light (660 nm). Samples were taken after 10 minutes, 30 minutes and 1 hour, were collected on Whatman filters and washed with PBS 1x. In both experiments, an extra Pt1 WT

culture was used to test the effect of DCMU (3-(3,4-dichlorophenyl)-1, 1-dimethylurea or also called Diuron, an inhibitor of photosynthetic electron flow from photosystem II to the PQ pool) on the red light gene expression. DCMU was added in a final concentration of 10 µM, 10 minutes before the onset of red light illumination.

1.2.10 Cell culture conditions for R/FR fluence rate experiments in P. tricornutum and T. pseudonana

For testing the range of action of the DPh, time course experiments were first performed in *P. tricornutum* WT cells (WT). WT cells were adapted in the dark for 60 hours and exposed to 1 µmol of red light (685 nm) or far-red light (740 nm) for 5 seconds and 100 seconds (respectively 5 µmols and 100 µmols in total of either red light or far-red light)(see results, figure 1.3.12). No spectral overlap between the red and far-red light was observed. After the illumination, cells were immediately restored to total darkness. 50 ml of culture were collected on Whatman filters (diameter 40,5 mm) before the onset of light and after 20 minutes, 1 hour, 3 hours, 5 hours and 8 hours of the light pulse. The filters were immediately washed with 50 ml of PBS 1x before freezing in liquid nitrogen.

1.2.11 Cell culture conditions for R/FR photoreversibility experiments in P. tricornutum

To test the photoreversibility characteristics of DPh, red/far-red light (R/FR) photoreversibility experiments were performed with WT and two DPh knock-down lines (*dph-2* and *dph-5'*). The cells were adapted in the dark for 60 hours and exposed to 1 µmol of red light (685 nm) or far-red light (740 nm) for 100 seconds (respectively 100 µmols of either red or far-red light). To test photoreversibility, cells were exposed to 1 µmol of red light for 100 seconds, but followed by 1 µmol of far-red light for 100 seconds. The opposite (far-red followed by red light) was also tested in the same conditions. After the illumination, cells were immediately restored to total darkness. Samples were collected on Whatman filters (diameter 40,5 mm) before the onset of light and on 20 minutes, 1 hour, 3 hours and 5 hours after the light pulse. The filters were

immediately washed with 50 ml of PBS 1x before freezing in liquid nitrogen. The photoreversibility was also studied in *T. pseudonana* (Chapter I, Results, Figure 1.3.21). The same experimental set-up and conditions were used as for *P. tricornutum*, with the exception that *T. pseudonana* WT cells were grown in NEPC media. A blue-light experiment (Chapter I, Results, Figure 1.3.20) was performed with the same experimental set-up described above for the red light analysis in WT and DPh knock-down lines. As control, an additional WT culture was used that was kept in darkness during the complete experiment after the sampling with the green safety light to exclude a possible green light effect in the gene induction.

1.2.12 Protein extraction protocols

Proteins were extracted with two different procedures. When cells were collected by centrifugation, proteins were extracted with the following protocol: cell pellets were resuspended for 30 minutes in lysis buffer (50 mM Tris-HCl pH 6,8, 2%SDS) at room temperature. Cells were centrifuged for 30 minutes at 4°C and protein extracts were quantified following the instructions from the BCA™ Protein Assay Kit (Pierce). 6x loading buffer (0,37 M Tris-HCl pH 6,8; 30,3 % glycerol; 3,4 mM SDS; 6,5 mM DTT and 1,8 µM bromophenol blue) was added to the protein dilutions and samples were cooked for 10 minutes at 95°C for protein denaturation.

When cells were collected on filters, an optimized protocol was used from M. Huysman, a colleague from the W. Vyverman laboratory in Ghent. 200 µl of lysis buffer (6,6% glycerol, 1,5% SDS, 41,6 mM Tris-HCl pH 8) was added to the frozen filters, together with proteinase inhibitors. After freezing the samples for a few seconds in liquid nitrogen, they were vortexed at high speed in room temperature to allow cells to lyse. In a next step, filters were squeezed out and removed from the samples. The remaining extract was centrifuged for 15 minutes at 13000 rpm at 4°C to remove cells debris. The supernatant was then transferred to a new and cold Eppendorf. Protein extract were quantified using Bradford assay (Bio-Rad). Samples were incubated for 10 minutes at 95 °C for protein denaturation, together with loading buffer (6x; for protocol see above).

1.2.13 Western Blot analysis

Diatom proteins were analyzed by SDS-PAGE. An acrylamide gel (7.5% for DPh protein analysis) was used for gel electrophoresis and then the gel was transferred to nitrocellulose membranes (Whatman Protran®) with a Bio-Rad® tank transfer system at 300 mM for 1 hour. To check the success of transfer, proteins were visualized with Ponceau Red. Membranes were incubated for the blocking reaction in 5% milk, 0.1% Tween 20, PBS 1X for 45 minutes at room temperature, and overnight at 4°C with the primary antibody (1:500 dilution of purified DPh antibody). The next day, membranes were first washed with 0.1% Tween 20, PBS 1x, for 3 x 10 minutes and then incubated for 45 minutes with the secondary antibody (1: 10 000 dilution of anti-rabbit for α-DPh) in 5% milk, 0.1% Tween 20, PBS 1x. The signal was visualized using the enhanced chemiluminescence kit (ECL kit; Pierce) with the sensitive detection camera LAS4000 from Fujifilm Global (DPh signal detection after 3 minutes). A cleaner DPh signal with less aspecificity was obtained when incubating the membrane with 5% milk, 0.1% Tween 20, PBS 1x blocking reaction overnight.

1.2.14 Preparation and purification of DPh antibodies

Polyclonal antibodies were prepared by Eurogentec for DPh in P. tricornutum (PtDPh) and T. pseudonana (TpDPh). For generating the PtDPh antibody, a PtDPh-specific peptide (EP110002, corresponding to the aa 214-229, C+ GKYDRGMVRFHDDL) was injected in the rabbit and the obtained serum was controlled for DPh-specificity in our laboratory by Western Blot analysis. Subsequently, because of the presence of multiple aspecific bands, the PtDPh antibody was further purified by small affinity purification and analyzed by indirect ELISA. Again, the purity of the antibody was controlled by Western Blot analysis with the newly purified antibody in a dilution of 1:500 and by using the purified PtDPh-His protein as control. The detection of the PtDPh antibody signal revealed a band with an approximate molecular weight of 120 kDa (DPh)

and an aspecific band with an approximate molecular weight of 65 kDa. For generating the TpDPh antibody, exactly the same procedures was done but with two TpDPh-specific peptides: P113617: QPPSKRRVSDDNFLLC and EP113618 : FPASDIPRQARELFMR. Because only the peptide P113617 worked to detect the TpDPh protein, it was subsequently used for small affinity purification and analyzed by indirect ELISA. The purity of the antibody was controlled by Western Blot analysis with the newly purified antibody in a dilution of 1:500. The detection of the purified TpDPh antibody signal revealed a band with an approximate molecular weight of 120 kDa (DPh) and several aspecific bands with a molecular weight between 65-85 kDa.

1.2.15 RNA extraction and cDNA synthesis

To extract RNA, around 50 ml of cells in exponential growth ($1,5.10^6$ cells/ml) were centrifuged at 3200 x g for 10 minutes at 4°C. The cell pellets were washed with 1 mL of PBS 1x before freezing in liquid nitrogen. Subsequent RNA extraction was performed using the TriPure Isolation Reagent (Roche Applied Science, IN, USA) according to the manufacturer's instructions. 1.5 mL of reagent was used for approximately 10^8 diatom cells. For cells collected on poly-carbonate filters, 1,5 ml of TriPure Isolation Reagent was added directly onto the filters. RNA concentration and quality was determined by spectrophotometry at 260 and 280 nm and by agarose gel electrophoresis. Genomic DNA was removed from the RNA sample by gDNA WipeOut treatment (Qiagen QuantiTect^R Reverse Transcription kit) by incubation 500 ng of RNA at 42°C for 10 minutes. cDNA was then generated from the treated RNA by RT-PCR (Reverse Translation-Polymerase Chain Reaction) using random hexamer primers following the protocol of the QuantiTect^R Reverse Transcription kit (Qiagen).

1.2.16 Quantitative real-time PCR (qRT-PCR)

For the gene expression profiling in the WT cells of *P. tricornutum* and *T. pseudonana* and their corresponding DPh knock-down lines, triplicate qRT-PCRs were performed for each selected gene on the same cDNA. Individual reactions contained 1 µl of cDNA (5 ng), 5 µl of SsoAdvanced^{TM}

SYBR^R Green Supermix (Bio-Rad), 3,6 µl of water and 0,2 µl of forward and reverse primers (each 10 µM). Amplifications were conducted on an Real-Time PCR detection system (Bio-Rad®) with the following program: 98°C 30'', 95°C 2'', 60°C 15'', 40 X repeat, 70°C 2'', 95°C 5''. Relative expression levels were calculated by using Ct values from the Bio-Rad® Real-Time Detection system software (Bio-Rad SFX manager V. 1.6) and averaged reaction efficiencies. For *P. tricornutum*, Histone (*H4*) and 30S ribosomal proteins subunit (*RPS*) genes were used as internal controls (Siaut *et al.*, 2007), whilst for *T. pseudonana* the gene Actin was used (Mock *et al.*, 2008). Relative mRNA levels were calculated using the $2^{-\Delta\Delta}C_T$ method, where $\Delta\Delta C_T = (C_T \text{ target} - C_T \text{ control gene})_{\text{Time x}} - (C_T \text{ Target} - C_T \text{ control gene})_{\text{Time 0}}$ (Livak & Schmittgen, 2001). For time course experiments with red, far-red and blue light treatments, mRNA levels were not only normalized against the internal gene but also against the dark point. All primers utilized in the qRT-PCR experiments were designed using the Primer3 software program (http://frodo.wi.mit.edu/) selecting a primer length of 20-23 nucleotides, a melting temperature of 62 +/- 2°C and a resulting PCR fragment of 180-200 bp. All primers were tested by RT-PCR to verify single amplification products of the expected size. The primer pair efficiency was calculated and primer pairs with an efficiency ≥ 1,8 were selected for the studies. Primers used for qPCR analysis are showed in table 2.1 (for *P. tricornutum*) and table 2.2 (for *T. pseudonana*).

Gene	ID n° Phatr2	Protein name	Primer name	Primer sequence
DPh	54330	Phytochrome	phy3 Fw	5' GTTCCGCACGATTTCTACGA 3'
			phy3 Rv	5' GCGTACGCTGAACCATCATA 3'
HO-2	55416	Heme oxygenase	HO2Fw	5' CCGGAATTCAATCGCGTGTGAAGAAGAGC 3'
			HO2Rv	5' CTAGTCTAGATAATTGTGGGGATGCTGACC 3'
HO-4	5902	Heme oxygenase	HO7Fw	5' AAGCTTCGTCTTTTGGCTGT 3'
			HO7Rv	5' CCACATGGCCTTAAAAGGTG 3'
HO-3	35647	Heme oxygenase	HO8Fw	5' TCGTCCGAATTCGAAGAGAT 3'
			HO8Rv	5' CTGCAGGATTACGATGCAAA 3'
PebB	45446	Bilin reductase	PebBfw	5' CCCAGCCAATGACAGAAGAT 3'
			PebBrv	5' GATGCCATACGTGTCCACAG 3'
PebA	33770	Bilin reductase	PebAFw	5' CCGACAAGGTCTTCTGGAAA 3'
			PebARv	5' AAGTCGATGCCCAATACAGG 3'
GSAT	50966	Glutamate 1-semialdehyde aminotransferase	GSATFw	5' AACGCAAATCCCAAAAACTG 3'
			GSATRv	5' TGCCAAATTTTTCGCTATCC 3'
HEMA	32977	Glutamyl-tRNA reductase	HEMAFw	5' TTTCGCAACAAGATTTGCAG 3'
			HEMARv	5' TGGTGATACGTTCGAGTCCA 3'
CHLH1	13265	Protoporphyrin IX magnesium-chelatase, subunit H	CHLH1Fw	5' AGGTGTCCTAACGGATGTCG 3'
			CHLH1Rv	5' AAAGGCGGATTTGACTTCCT 3'
CHLH2	10100	Magnesium-chelatase, subunit H	CHLH2Fw	5' CTGGTCGTATCGTTCGGTTT 3'
			CHLH2Rv	5' GTTGGCAAAAGAATCCCTGA 3'
POR1	20051	NADPH: protochlorophyllide oxidoreductase A	POR1Fw	5' AAGCAAGTCGCCAAAGAAAA 3'
			POR1Rv	5' TGAGGTTGCTCACAAAATCG 3'
POR2	20818	NADPH: protochlorophyllide oxidoreductase A	POR2Fw	5' TACGGGAGGATACGTTGGAG 3'
			POR2Rv	5' TTCTACCCCACGTCCTTCAC 3'
POR3	43164	NADPH: protochlorophyllide oxidoreductase	POR3Fw	5' GCTACAGGAGCCGGTATTGA 3'
			POR3Rv	5' TGAGTCTCACCGCTTTTCCT 3'
POR4	34307	NADPH: protochlorophyllide oxidoreductase	POR4Fw	5' CAACTAGCAACGCGATTGAA 3'
			POR4Rv	5' CGACGAGGATAATGCGATTT 3'
ZEP2	56488	Zeaxanthin epoxidase	ZEP2Fw	5' TCCGCCGATGTTCTAGTAGGAT 3'
			ZEP2Rv	5' TTGCATAGTAGTCCGGGTCTT 3'
VDL1	46155	Violaxanthin de-epoxidase-like 1	VDL1Fw	5' GCCTTTAGATTGCACGGGTA 3'
			VDL1Rv	5' AAGTTATGCCGTGGTTCGT 3'
PDS	45735	phytoene desaturase	PDSFw	5' TCTCATGAACCAGAAAATGCTCA 3'
			PDSRv	5' AAGACTTCTTCGTTGATGCGTTC 3'
LHCF1	18048	Fucoxanthin chlorophyll a/c protein 1	LHCF1Fw	5' GAGTGCTGTGCCTGGAGCCG 3'
			LHCF1Rv	5' GCCGCACGTCCCTGGTTGAG 3'
LHCF2	25172	Fucoxanthin chlorophyll a/c protein 2	LHCF2Fw	5' CCCGCAGGCTGGGCTTATCC 3'
			LHCF2Rv	5' TGAGCGGCACGTCCCTGGTT 3'
AOX	45063	Alternative oxidase	AOXFw	5' AATACGGAACCGTGTTGGAG 3'
			AOXRv	5' TGGCATACTTGAGCAGCAT 3'
H4	34971	Histone 4	H4Fw	5' AGGTCCTTCGCGACAATATC 3'
			H4Rv	5' ACGGAATCACGAATGACGTT 3'
RPS	10847	30S Ribosomal protein subunit	RPSFw	5' CGAAGTCAACCAGGAAACCAA 3'
			RPSRv	5' GTGCAAGAGACCGGACATACC 3'

Table 2.1: Primer sequences utilized in the qRT-PCR experiments for *P. tricornutum*.

Gene	ID n° Thaps3	Protein name	Primer name	Primer sequence
DPh	22848	Phytochrome	TpPHYqPCR Fw	5' GAAATTGCAAAGGAGCTTCG 3'
			TpPHYqPCR Rv	5' GGGATATCAGACGCTGGAAA 3'
GSAT	14861	Glutamate 1-semialdehyde aminotransferase	TpGSATFw	5'AACAACCTGGAGTCCACGAC 3'
			TpGSATRv	5 'TCCCTCGACGAAGTACCATC 3'
HEMA	270328	Glutamyl-tRNA reductase	TpHEMAFw	5' CAATGTTGGTGGTGGTTCAG 3'
			TpHEMARv	5' GACGTTCCTGCTTCGTCTTC 3'
CHLH1	26573	Protoporphyrin IX magnesium-chelatase, subunit H	TpCHLH1Fw	5' TGGGGAACTGACAACATCAA 3'
			TpCHLH1Rv	5' AGGACGACCAAGCTTCTCAA 3'
ZEP2	261390	Zeaxanthin epoxidase	TpZEP2Fw	5' CATCAAATCGTTGCATCAGG 3'
			TpZEP2Rv	5' ACCAATGAGGACGACGTTTC 3'
LHCF1	38583	Fucoxanthin chlorophyll a/c protein 1	TpLHCF1Fw	5' TGGATTCTTCGATCCTTTGG 3'
			TpLHCF1Rv	5' TGTCTCCTGGAAGACGGATT 3'
LHCF2	260392	Fucoxanthin chlorophyll a/c protein 2	TpLHCF2bisFw	5' TGCTCTGCACATCATCAACA 3'
			TpLHCF2bisRv	5' CCAAAGGATCGAAGAATCCA 3'
LHCF5	42962	Fucoxanthin chlorophyll a/c protein 5	Tp LHCF5 Fw	5' ACCGGAGAGGGAGAGTTTGT 3'
			Tp LHCF5 Rv	5' CGCTGCTTACATCTGTCCAA 3'
ACT1	25772	Actin	TpActinFw	5' ACTGGATTGGAGATGGATGG 3'
			TpActinRv	5' CAAAGCCGTAATCTCCTTCG 3'
TF2D2	264095	transcription factor IID, TATA box binding protein	TpTF2D2Fw	5' CCGAATTCAACCCTCGTAGA 3'
			TpTF2D2Rv	5' ACCCCACCCTCTCCAAAATA 3'

Table 2.2: Primer sequences utilized in the qRT-PCR experiments for *T. pseudonana*.

1.3. Results

1.3.1 *In silico* study of the diatom phytochromes

The genomes of the two diatoms *P. tricornutum* (Bowler *et al.*, 2008) and *T. pseudonana* (Armbrust *et al.*, 2004) each contain one gene that code for a phytochrome protein, named DPh. These DPh sequences have been used to investigate the specific domain arrangements in comparison with phytochrome sequences from plants, bacteria, cyanobacteria and fungi.

First, by using SMART and PFAM protein analysis tools to analyze the DPh domain arrangement, I have shown that both DPhs have a domain arrangement similar to the Bphs and Fphs. These DPhs display a N-terminal chromophore-binding domain followed by a 'transmitter' histidine kinase (HK) domain and a response regulator (RR) module at the C-terminus (see later figure 1.3.1 and figure 1.3.2), similar to the two-component system found in bacteria. Therefore, DPhs may act as light-activated kinases.

Second, the analysis of the *T. pseudonana* DPh sequence revealed that the prediction of this protein, done during the first annotation of the genome, was incorrect. Sequence alignment with DPh from *P. tricornutum* and Agp1 from *Agrobacterium tumefaciens* revealed that the conserved cysteine for chromophore binding was not present in the N-terminal region of DPh from *T. pseudonana*. However, a more accurate analysis of the genome allowed to identify another methionine upstream from the originally predicted N-terminal region. By using this longer protein sequence, I discovered that the *T. pseudonana* DPh contains a N-terminal PAS domain, like the plant phys, Bphs and Fphs. Moreover a conserved cysteine residue was identified upstream from the PAS domain, in which Bphs and Fphs have been shown to bind the BV (Ulijasz *et al.*, 2010; Blumenstein *et al.*, 2005). In contrast, the *P. tricornutum* DPh lacks this PAS domain but contains the conserved cysteine residue for the chromophore attachment in the N-terminal region, upstream from the PAS domain.

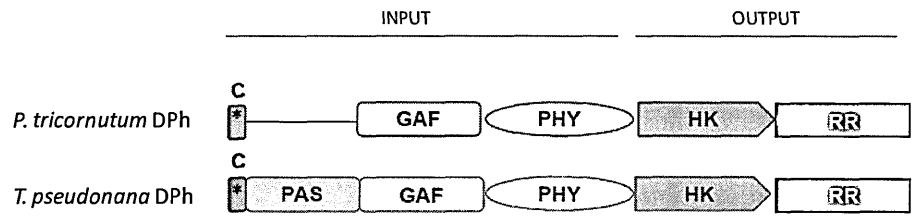

Figure 1.3.1: Domain structures of DPh in *P. tricornutum* and *T. pseudonana*, according to PFAM database (http://pfam.sanger.ac.uk/). Abbreviations are GAF (GAF domain), PHY (phytochrome domain), HK (histidine kinase domain), RR (response regulator), C (conserved cysteine residue). Asterisks correspond to conserved cysteine residue for putative chromophore binding.

Third, the analysis of the output C-terminus region revealed that the DPhs contain the typical residues of the bacterial two-component system, also often referred to as the His-Asp phosphorelay system (Egger *et al.*, 1997). In particular, short blocks of common sequence have been found in the HK domain of DPhs. I refer to these motifs by their characteristic residues as blocks 'H', 'N', 'G1', 'G2', 'G3' and 'F' (see figure 1.3.2). Block H, the most variable of the five regions, is located in the N-terminal half of the HK domain and includes the histidine residue that serves as the site of autophosphorylation. From the protein alignments with bacterial phytochrome sequences, I identified an aspartate residue in the RR domain that may act as the site of transphosphorylation and thus may serve as a molecular switch to control signal propagation.

Fourth, I have also enlarged the DPh sequence list from other marine species. A detailed search in the transcriptomic database from the pennate diatom *Seminavis robusta* revealed 4 putative phytochrome sequences (Personal communication with Vyverman, W.). All four DPh sequences showed a similar domain architecture to *P. tricornutum*. Similarly, the recently sequenced genome of the toxic diatoms *Pseudo-nitzschia multiseries* revealed that at least one possible phytochrome sequence is very similar to the *P. tricornutum* PAS-less DPh. Also the brown alga *Ectocarpus siliculosus*, another member from the Heterokont family, was found to harbor 3 phytochrome sequences. In addition, a phytochrome-like sequences was found in the genome *E.*

siliculosus-specific virus EsV-1-(Cock *et al.,* 2010) and in the genome of the *Feldmania* virus FirrV-1 (see figure 1.3.2). Interestingly, the *E. siliculosus*, the EsV-1 and FirrV-1 phytochrome sequences all lack the N-terminal PAS domain, as in *P. tricornutum*, but contain the conserved cysteine residue in the N-terminal domain similar with other DPhs. The lack of PAS domain in several diatom phytochrome might represent a general feature of several Heterokont phytochromes. It is worth to mention that the two *E. siliculosus* phytochromes contain the N-terminal cysteine found in the DPhs, but also an additional cysteine residue in the GAF domain, that in plants has been shown to bind the chromophore. These data suggests a common origin, but also a possible diversification during the evolution of the DPh protein sequences within the Heterokont clade.

Nonetheless, the *T. pseudonana* and *P. tricornutum* genomes have been thoroughly investigated for genes potentially encoding chromophore biosynthetic enzymes. Both diatom species contain several heme oxygenase (*HO*) genes (see later, chapter II), suggesting that diatoms may produce biliverdin (BV) from heme and use it as a chromophore, similar to Bphs and Fphs. Interestingly, the genomes also contain putative bilin reductase genes (*PebA* and *PebB*), which could mediate the further reduction of BV. However, the proteins encoded by these genes are more closely related to the enzymes involved in phycoerythrobilin (PEB) synthesis than to the ferredoxin-dependent bilin reductases that mediate the conversion of BV to PEB and PCB in cyanobacteria, respectively (Rockwell *et al.,* 2006). Because diatoms do not seem to use PEB as a light-harvesting pigment, an interesting alternative hypothesis is that these genes may be used to produce a diatom-specific chromophore. Thus, the functional identification of the diatom chromophores and clarification of DPh spectral properties was necessary to extend the study of the phytochrome superfamily in other secondary endosymbionts, such as diatoms.

Apart from the phytochrome genes discovered in the Heterokont family, I have also identified a number of genes coding for GAF-containing proteins, suggesting at the existence of novel and yet uncharacterized sensory proteins in diatoms other than the classical phytochrome

photoreceptors. In the species *P. tricornutum*, *T. pseudonana* and *Fragilariopis cylindricus*, a number of GAF-containing proteins coupled with HK and RR have been identified (see table annex 1).

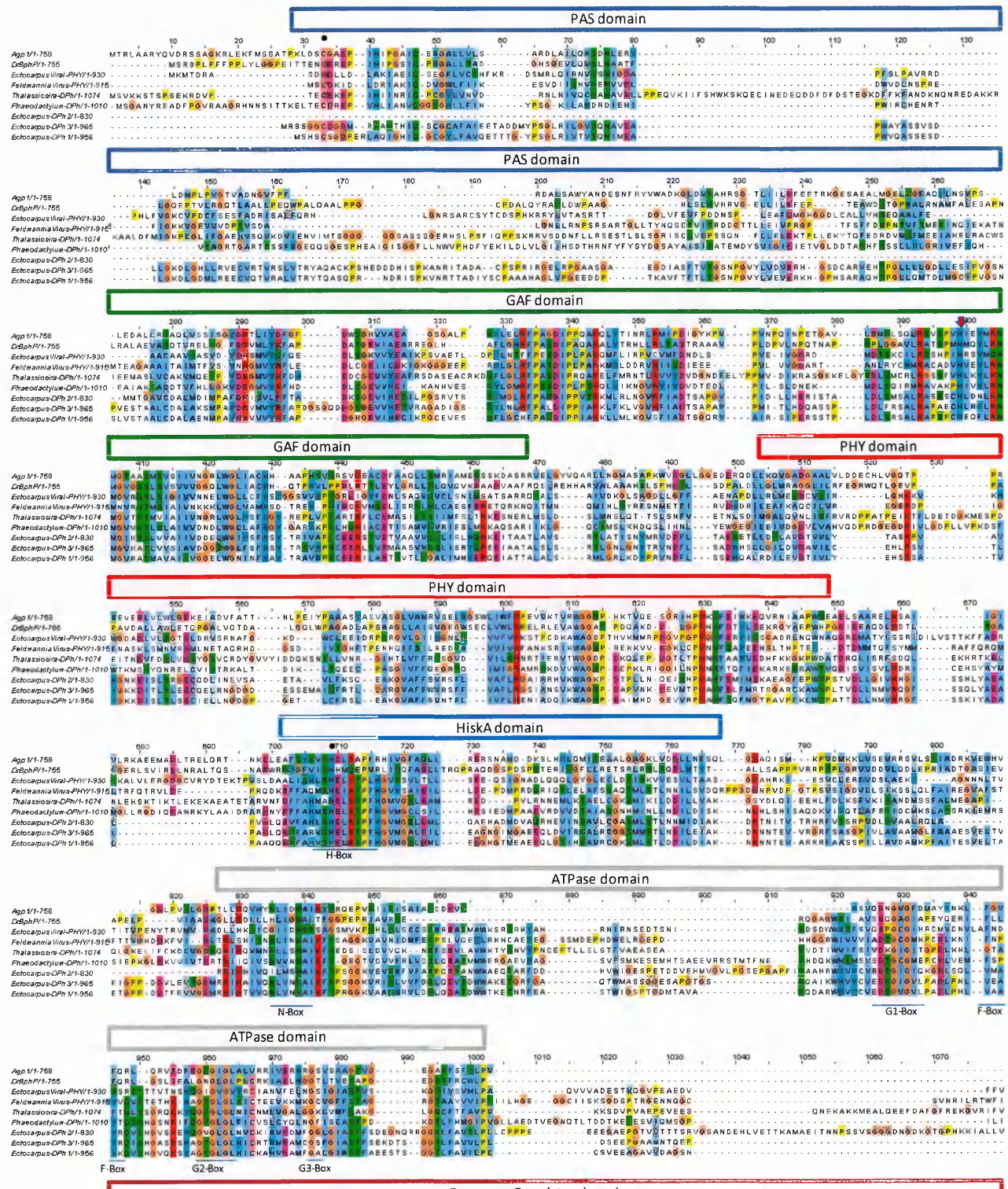
PAS domain
PAS domain
GAF domain
GAF domain
PHY domain
PHY domain
HisKA domain
H-Box
ATPase domain
N-Box
G1-Box
F-Box
ATPase domain
F-Box
G2-Box
G3-Box
Response Regulator domain

Figure 1.3.2 (previous page): Amino acid sequence alignment showing the domains architecture of the phytochrome protein in the following species: *Agrobacterium tumefaciens* (Agp1), *Deinococcus radiodurans* (DrBph), *T. pseudonana* (TpDPh), *P. tricornutum* (PtDPh), *Ectocarpus siliculosus* (with its species-specific virus, noted as '*Ectocarpus* Viral PHY') and the *Feldmania* virus FirrV-1. The PAS, GAF, PHY, Histidine Kinase (HiskA), ATPase and Response Regulator domains are indicated. The black dot at the beginning of the PLD domain indicates the conserved cysteine residue for chromophore binding. The red arrow indicates the conserved histidine residue in the GAF domain. Motifs for autophosphorylation have been assigned 'H', 'N', 'G1', 'G2', 'G3' and 'F' in the Histidine Kinase and ATPase domains, with the black dot in the H-box indicating the conserved histidine residue for autophosphorylation. The red star in the Response Regulator domain shows the site for the conserved aspartate (D) residue for phosphorylation. The sequences were aligned using ClustalW and domains were assigned according to Vierstra & Davis, 2000.

1.3.2 Analysis of DPh spectral properties

Expression of the PtDPh in E. coli

To clarify the function of the phytochrome as photoreceptor in diatoms, it was essential to obtain biochemical and spectral information on DPh. To this aim, I have conducted several trials to express and purify the DPh protein from *P. tricornutum* (PtDPh). As a general strategy, I used a dual-plasmid system to co-express the plasmid containing the apophytochrome (PtDPh) in *E. coli* together with a plasmid containing the heme oxygenase and bilin reductase genes for the chromophore biosynthesis, in order to obtain a photoactive diatom holophytochrome. This strategy was successfully used by Gambetta & Lagarias in 2001 to obtain spectral information of the cyanobacterial phytochrome. The study showed the feasibility of producing photoactive phytochromes in any heme-containing cell. Therefore, I cloned the N-terminal region of PtDPh (covering the first 1090 bps) containing the GAF domain into the high-copy pBad-MycHisC plasmid for a robust inducible protein expression. Firstly, I transformed the *E. coli* strain with the pBad-DPh plasmid. Secondly, I retransformed the transformants with a second plasmid for chromophore biosynthesis, either pPL-PCB or pPL-BV, with PCB coding for phycocyanobilin or BV coding for biliverdin, the latter being the immediate precursor of the biliprotein chromophores (see materials & methods for more details). As control, I used *E. coli* cells containing the expression plasmid for the truncated N-terminal region of the cyanobacterial phytochrome (Cph1) (Gambetta and Lagarias,

2001), in combination with the pPL-PCB expression plasmid for cyanobacterial chromophore biosynthesis. Strains harboring the PtDPh plasmid alone (pBad-DPh-MycHisC) or in combination with the chromophore biosynthesis plasmids (pPL-BV or pPL-PCB) displayed no visible color change. Despite several trials to express pBad-DPh-MycHisC in different treatments (18°C and 37°C) and with two plasmids coding for different chromophore biosynthetic enzymes, the results indicated that the PtDPh protein expression was always too low to be detected by Coomassie Brilliant Blue (CBB) or zinc acetate staining. On the contrary, for the cyanobacterial Cph1, protein analysis revealed the successful expression of protein of 59.8 kDa with its chromophore (data not shown). Because of many unsuccessful trials in the lab, a collaboration was started with Prof. Dr. Ikeuchi Masahiko in Japan as his laboratory is well known for its expertise in the phytochrome spectral analysis and the purification of 'less canonical' phytochromes. Together, the following attempts were taken:

1/ Our collaborator introduced the diatom full-length *DPh* gene into another plasmid for bacterial expression, pET28a carrying the T7 promoter, fused to a N-terminal histidine tag. Subsequently, the team of Prof. Dr. Ikeuchi Masahiko introduced the plasmid into two different *E. coli* strains: one producing BV from a cyanobacterial *HO* gene and another one producing phycoerythrobilin (PEB) in addition to BV. Again, it was concluded that the amount of fluorescent PtDPh was too low to be visualized even with a sensitive detection system. Also the cyanobacterial PEB-producing enzyme from *Synechocystis* expressed in the pKT278 vector was tried but the results were almost identical. Insufficient expression could be due to an unsuitable codon usage for expression in the bacterial *E. coli* system, but could also be due to the possible instability of the PtDPh protein and/or to the use of the false chromophore biosynthetic enzyme since PtDPh chromophore biochemistry is unknown.

2/ The possibility that PtDPh might need a diatom-specific chromophore has been investigated. Because the diatom genome harbors genes coding for bilin reductase enzymes, that could be involved in the synthesis of PEB, we put the hypothesis forward that PEB could be implicated in the

biosynthesis of a diatom-specific chromophore. Therefore, I amplified both diatom bilin reductase genes (*PebA* and *PebB*) from the *P. tricornutum* genome and cloned them into the low-copy number plasmid pKT270. Consequently, the group of Dr. Ikeuchi Masahiko tried the co-expression of PtDPh with the PebA/PebB plasmid but no positive results were obtained. This strategy was not pursued any longer as the presence of a N-terminal conserved cysteine in the PAS domain is not in accordance with the idea that PEB could act as the chromophore of DPh. The PEB has an ethylidene at ring A (Lamparter *et al.*, 2002) and this fits better with the binding to a conserved cysteine residue in the GAF domain. An alternative possibility would be that PebA only catalyzes the conversion of BV to 15,16-dihydrobiliverdin, which might be incorporated into the PtDPh. Since no results were obtained, it was decided to abandon this strategy and to investigate the codon usage of PtDPh in more detail.

3/ A detailed analysis of the PtDPh sequence performed in the laboratory elucidated that its codon usage is significantly different from that of other diatom genes and also from *E. coli* genes (see later figure 1.3.3). Therefore, the Japanese team performed an attempt by rewriting the PtDPh full-length sequence for optimized expression in *E. coli*, with the insertion of a C-terminal histidine-tag for subsequent purification of the protein. This strategy was the successful one, because both the N-terminal photosensory (PAS-GAF-PHY) region and the PtDPh full-length protein were expressed in *E. coli* with a heme oxygenase gene from *Synechocystis.* The Japanese team succeeded in purifying the PtDPh holoprotein by Ni-affinity chromatography (see figure 1.3.4) and absorption spectra were obtained. These spectra of the purified PtDPh protein were evidence of a successful expression and assembly of the protein with its chromophore. In addition, the results were confirmed by the positive zinc acetate staining that allowed the formation of a fluorescent complex between biliproteins and zinc acetate, which is a typical feature of the assembled phytochrome holoprotein.

The results have shown that PtDPh is a red/far-red light photoreceptor, although with a strongly red-shifted spectrum (Pr at 690 nm and Pfr at 740 nm; see later figure 1.3.5) compared to plant phytochromes. A similar red-shifted spectrum was also observed in bacterial phytochromes as *Pseudomonas aeruginosa* (Tasler *et al.*, 2005) and *Agrobacterium tumefaciens* (Lamparter *et al.*, 2002). Both the N-terminal photosensory and the full-length DPh protein showed the same absorption spectra, indicating that the N-terminal domain of DPh by itself is photoactive. In *E. coli*, PtDPh uses BV as chromophore, thus we believe that BV might act as the chromophore of DPh in diatoms as well. This work, performed in collaboration with the laboratory of Dr. Masahiko Ikeuchi in Japan, has provided the first evidence that the diatom phytochrome works as a red/far-red light photoreceptor in marine microalgae.

In addition to the data presented above, supplementary analyses have been conducted by the group of Dr. Masahiko Ikeuchi. First, their data support the two-directional photoreversibility of PtDPh *in vitro*. Secondly, dark reversion of PtDPh was observed, with 80% of the Pfr form being converted to the Pr after a prolonged dark treatment.

Figure 1.3.3: Nucleotide sequence alignment of the original PtDPh and the PtDPh sequence with the optimized codon usage for bacterial expression. The sequences were aligned with ClustalW. Asterisks indicate the conserved nucleotides.

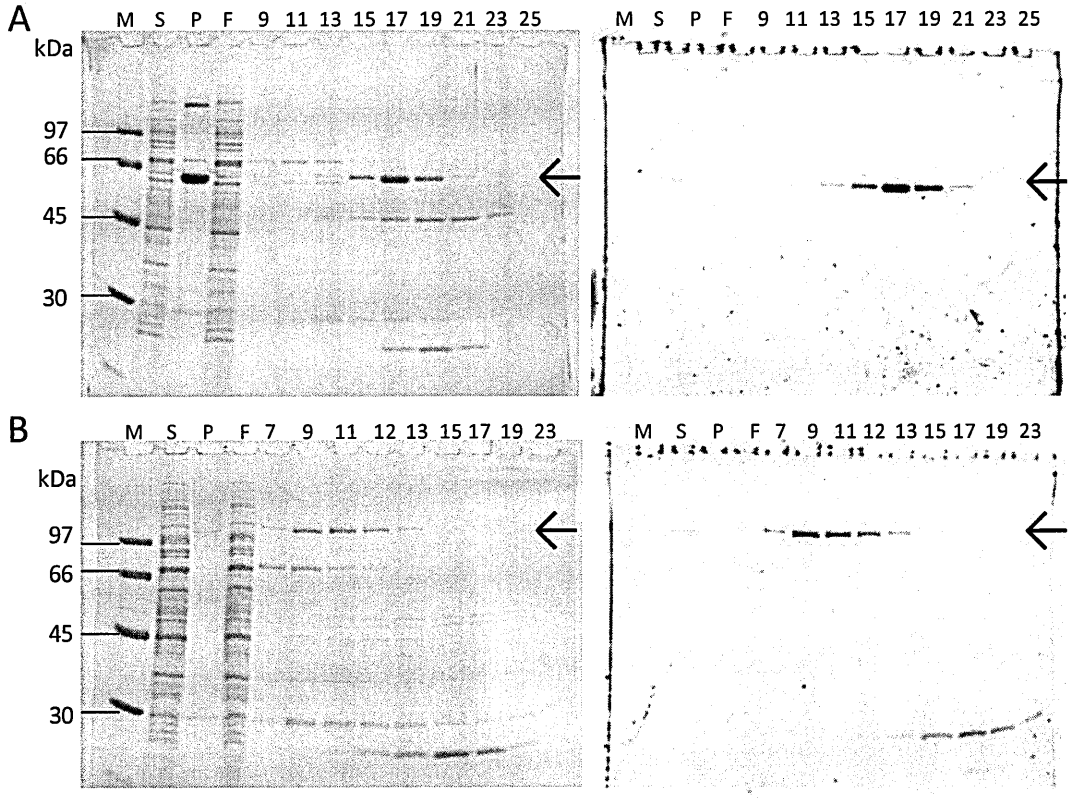

Figure 1.3.4: SDS-PAGE analysis of different fractions of the DPh-His protein, purified by Ni-affinity chromatography. After electrophoretic separation, proteins were transferred on the PVDF membranes and stained with Coomassie Blue Staining (left) and zinc acetate staining (right). Zinc-staining was performed with 20 µM ZnAc. Panel A: SDS-PAGE analysis of the assembled DPh photosensory domain (PLD-GAF-PHY), with a C-terminal His-tag. M: protein marker; S: supernatant fraction; P: membrane fraction; F: flow-through; numbers 9-25: Ni-affinity chromatography fractions. For the spectral analysis of the full-length DPh, fractions 9-25 were pooled and concentrated. Panel B : SDS-PAGE analysis of the assembled DPh full-length protein, with a C-terminal His-tag. M: protein marker; S: supernatant; P: membrane; F: flow-through; numbers 7-23: Ni-affinity chromatography fractions. For the spectral analysis of the full-length DPh, fractions 7-13 were pooled and concentrated. The arrows indicate the expressed DPh protein of 65,4 kDa (panel A) and 113,9 kDa (panel B), respectively.

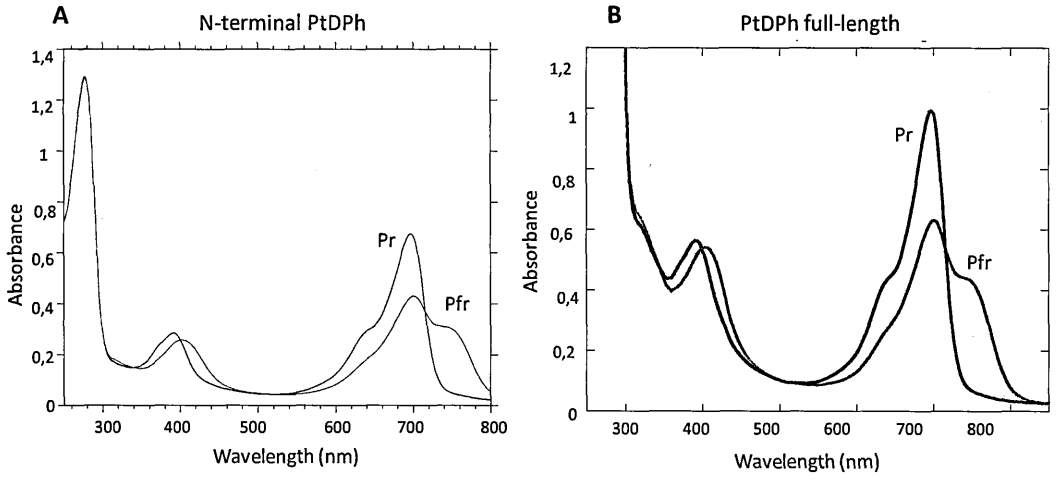

Figure 1.3.5: Absorption spectra upon red/far-red light illumination of the N-terminal and full-length PtDPh protein obtained after expression in *E. coli* and purification by Ni-affinity chromatography as reported for figure 1.3.4. (Panel A) showing Pr (Black) and Pfr (Red) spectral forms of N-terminal photosensory domain of DPh. (Panel B) showing Pr (Black) and Pfr (Red) spectral forms of full-length DPh.

1.3.3 Functional characterization of DPh in diatoms

Generation and characterization of PtDPh knock-down lines

The function of DPh has been investigated by generating transgenic knock-down lines by RNA interference (RNAi) (De Riso *et al.*, 2009) in *P. tricornutum*. These clones have been obtained by introducing a vector with an inverted repeat or an antisense sequence from DPh, by particle bombardment in *P. tricornutum* WT cells. The targeted DPh regions corresponded to either the GAF domain or the 3'UTR region of DPh (see annex 4 for an overview of the DPh sequence and the targeted regions). The fragments for the silencing were cloned in RNAi plasmids and to drive transcript expression, two different *P. tricornutum* promoters were used, FcpB and H4, from the Fucoxanthin Chlorophyll a/c-binding Protein B and a Histone (*H4*) gene, respectively. Both promoters have been proven to drive robust expression of transgenes in *P. tricornutum* and have been routinely used for generating knock-down lines in the laboratory (De Riso *et al.*, 2009). During the first trials, I have introduced the different constructs with DPh-GAF antisense and inverted repeat fragments in the WT (see figure 1.3.6 and see annex 4). However, on more than 80 analyzed clones by Western Blot, only 3 transgenes showed a reduced protein content (2 clones with inverted GAF repeats and 1 clone with antisense GAF) (see figure 1.3.7), suggesting that either the efficiency of the silencing was quite low or that the silencing of DPh might be problematic for the cell growth. Although few clones were obtained, all three of these clones displayed a rare chain or aggregation phenotype. The matter of chain and aggregation phenotypes observed in the DPh knock-down lines will be discussed in detail in chapter II. Nevertheless, novel constructs were made in order to obtain novel independent silencing and achieve higher efficiency rates of silencing, in which the 3'UTR region of DPh was used as target (see figure 1.3.6 and see annex 4). This region was chosen because of its high specificity as other regions in the gene (such as the HK domain) were also present in other proteins and might generate an aspecific silencing. After transforming new WT cells with the DPh3' plasmid and extensive Western Blot analyses of the positive transformants, a higher number (8 silenced clones on a total of 35 transgenes analyzed) of DPh knock-down lines were identified (see figure 1.3.7; a selection of those 8 knock-down lines was performed at random, therefore 5 knock-

down lines were shown in the figure). In general, most of the obtained DPh knock-down lines displayed a DPh protein content between 25% and 50 % in comparison to the WT, with the exception of *dph-3*, which showed a more dramatic reduction in DPh protein content (see figure 1.3.7). Interestingly, some of these newly identified clones displayed a chain phenotype, although in a less obvious manner than for the clones targeted in the GAF domain during the first trial (see Chapter II, Results, figure 2.3.1). Both types of targeting, GAF or 3' UTR, proved to be suitable to generate DPh knock-down lines although in the case of 3' UTR silencing a higher number of positive although less DPh-repressed lines were generated. The fact that both GAF and 3'UTR knock-down lines showed an impaired (chain/aggregation) phenotype confirmed the consistency of the silencing.

As already shown in De Riso *et al.* (2009), analysis of mRNA levels in the WT and DPh knock-down lines revealed that the DPh transcript levels in the DPh knock-down lines were slightly higher (up to two fold) than in the WT. These data suggest that the reduction in protein content in the DPh knock-down lines is due to a post-transcriptional regulation. In addition, these results also indicate that the reduction of DPh protein may have an effect on its own RNA synthesis, direct or indirect, via a tight regulatory feedback loop.

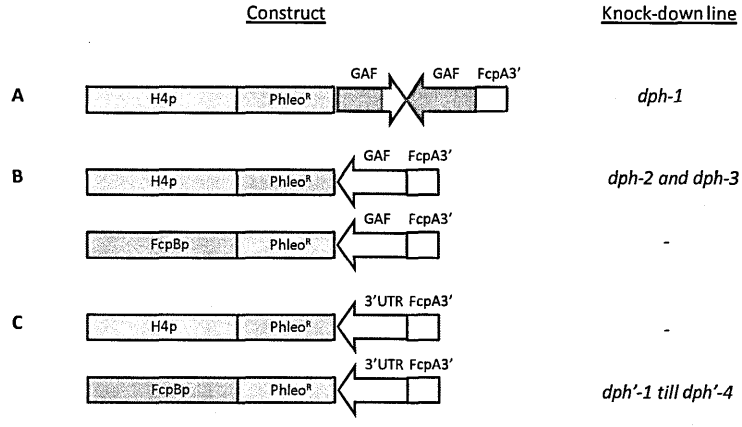

Figure 1.3.6: Schematic maps of the antisense and the inverted repeat constructs for PtDPh silencing. (A) Inverted-repeat construct: the DPh GAF fragments were cloned in sense and anti-sense orientation under the H4 promoter, to generate the *dph-1* transgenic line. (B) GAF anti-sense constructs: DPh-GAF fragment of 250 bp was cloned in antisense orientation under the FcpB or H4 promoter, generating the *dph-2* and *dph-3* transgenic lines both containing the H4 promotor. (C) Anti-sense constructs covering DPh3' fragments

of 250 bp in antisense orientation, under the FcpB or H4 promoter. *dph'-1* till *dph'-4* transgenic lines were generated with the DPh3' antisense construct containing the FcpB promoter. H4 (Histone 4 promoter), FcpB (Fucoxanthin Chlorophyll a/c-binding Protein B promoter). *Sh Ble* gene confers resistance to the antibiotic phleomycin. FcpA3' refers to the diatom FcpA terminator region.

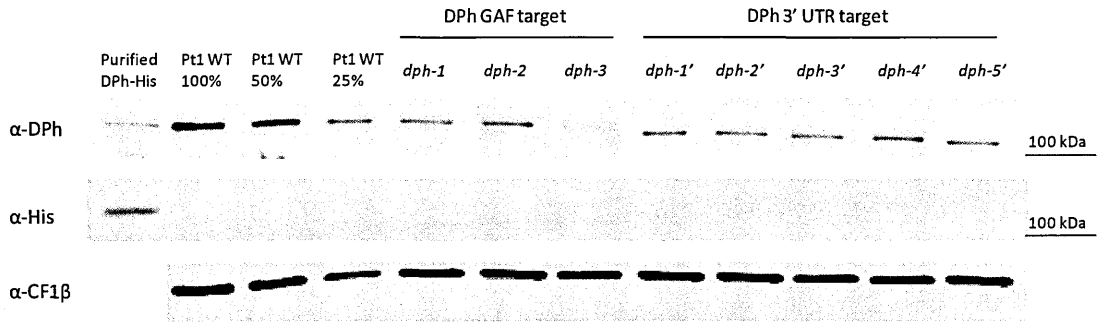

Figure 1.3.7: Western Blot analysis of *P. tricornutum* WT and a selection of DPh transgenic knock-down lines. 50 µg of proteins from each extract was used and the level of DPh was quantified using a serial dilution of proteins from WT cells as standard. The level of DPh was tested with the α-DPh antibody, targeted to the GAF domain of the protein (see annex 4). The antibody α-CF1β, subunit of the chloroplast ATP synthase complex, was used as loading control. The purified DPh with a His-tag was used as control to test the specificity of the DPh antibody. Transgenic lines targeted in the GAF domain are *dph-1*, *dph-2* and *dph-3*. Transgenic lines targeted in the 3'UTR region are *dph-1'* till *dph-5'*.

1.3.4 Gene expression profile analysis in different light conditions

1/ Red light-induced genes in P. tricornutum

Information about red light-mediated gene expression in diatoms and the possible role of DPh in the process of red light sensing and regulation is still very limited, therefore obtaining insights into the red light-mediated gene expression in diatoms might clarify the importance and mechanisms of red light sensing in the marine environment on the molecular level. To enrich our knowledge and understanding in this subject, I studied the gene expression profiles of several diatom genes in different light conditions. A preliminary analysis was started in the WT of *P. tricornutum* (strain Pt1) in red light, with 2 µE or 20 µE continuous red light (660 nm). The gene expression of *DPh* in red light was investigated to understand the role of red light in the function of DPh as a putative photoreceptor. But besides *DPh*, also other genes were chosen. First of all, genes putatively involved in the DPh chromophore biosynthesis were selected (heme oxygenase (*HO-2*) and bilin reductases (*PebA* and *PebB*), see figure 1.1.7 for scheme tetrapyrrole biosynthetic pathway). Then, also genes encoding for enzymes of the chlorophyll biosynthetic pathway were included in our analysis as some of these genes are known to be regulated by light in plants and algae (Ilag *et al.*, 1994; Matters &Beale, 1994) and to be downstream from *PHYA* and *PHYB* signaling in plants (Huang *et al.*, 1989; McCormack & Terry 2002). In particular, I selected genes coding for the glutamate-1-semialdehyde-2,1-aminomutase (*GSAT*) and the glutamyl-trna reductase (*HEMA*); two genes for protoporphyrin IX magnesium chelatase subunit H (*CHLH1* and *CHLH2*) and 4 genes coding for protochlorophyllide oxidoreductases (*POR1, POR2, POR3 and POR4*). Finally, also markers of the cellular redox state (alternative oxidase, *AOX*) and genes coding for pigment biosynthesis (violaxanthin de-epoxidase-like 1 (*VDL1*); phytoene desaturase (*PDS*); zeaxanthin epoxidase (*ZEP2*)) were included in this analysis. The latter are known to be induced by red light in diatoms (Coesel *et al.*, 2008).

In a first experiment, cells were dark-adapted for 60 hours and subsequently exposed to either 2 µE or 20 µE of red light (660 nm). Samples were collected before the onset of light and after 30 minutes, 1 hour and 2 hours of red light illumination. The results of the experiment are shown in Figure 1.3.8.

The transcript levels of the *DPh* gene were minimally affected during continuous exposure to 2 and 20 µE of red light. The heme oxygenase gene (*HO-2*), putatively involved in the DPh chromophore biosynthesis from heme to BV (see figure 1.3.7 in Introduction), also showed a minimal induction with a maximum of transcript levels after 30 minutes in both 2 and 20 µE of red light. Bilin reductase *PebA* seemed to have an increased expression after a longer exposure to red light, especially at 2 µE. *PebB* on the other hand, showed very high transcript levels at higher red light intensities (20 µE), and almost no induction in lower light conditions. The transcript levels of the marker gene of the cellular redox state (*AOX*) increased immediately upon 20 µE red light exposure, after 30 minutes of continuous red light. The effect of 2 µE red light was minimal, except for a small increase after 2 hours of continuous red light. Among genes implicated in pigment biosynthesis (*VDL1*, *PDS* and *ZEP), PDS and ZEP2* showed an increased expression at longer exposure times and to higher red light (20 µE), while *VDL1* showed its highest expression levels after 1 hour of continuous 2 µE red light. All of the investigated genes of the chlorophyll biosynthetic pathway, except *CHLH2* and *POR1*, were induced by red light, although the different genes were displaying dissimilar behaviors. *GSAT* showed the strongest induction among all other genes, especially in 20 µE red light, with the highest transcript levels after 1 hour of continuous 20 µE red light. *CHLH1* was also strongly induced, although at lower levels than *GSAT* and at lower red light intensity (2 µE) after 1 and 2 hours, while it displayed a smaller induction after prolonged exposure to 20 µE of red light. *CHLH2* showed a moderate to minimal induction after 30 minutes in both red light conditions. *HEMA,* on the other hand, is moderately expressed in prolonged exposure to low red light (2 µE) and less to higher red light intensities (20 µE). Interestingly, *POR2* transcript levels demonstrated a dramatic increase to

low red light (2 µE), after 1 hours of irradiation, whilst *POR1* transcript levels did not show any induction to red light at all. The two other *POR* genes (*POR3* and *POR4*) have also been investigated but the raw data proofed to be of insufficient quality to assess the analysis. Because three *POR* genes are present in *Arabidopsis*, the presence of four *POR* genes in diatoms suggests an expansion of this gene family. Additionally, their different gene expression profiles suggest that they might play various roles in chlorophyll biosynthesis in different light conditions. The fact that most of the investigated chlorophyll biosynthetic genes are induced by red light, suggests that they might be regulated by a red light photoreceptor in diatoms as well. The generation of DPh knock-down lines allowed us to test this hypothesis.

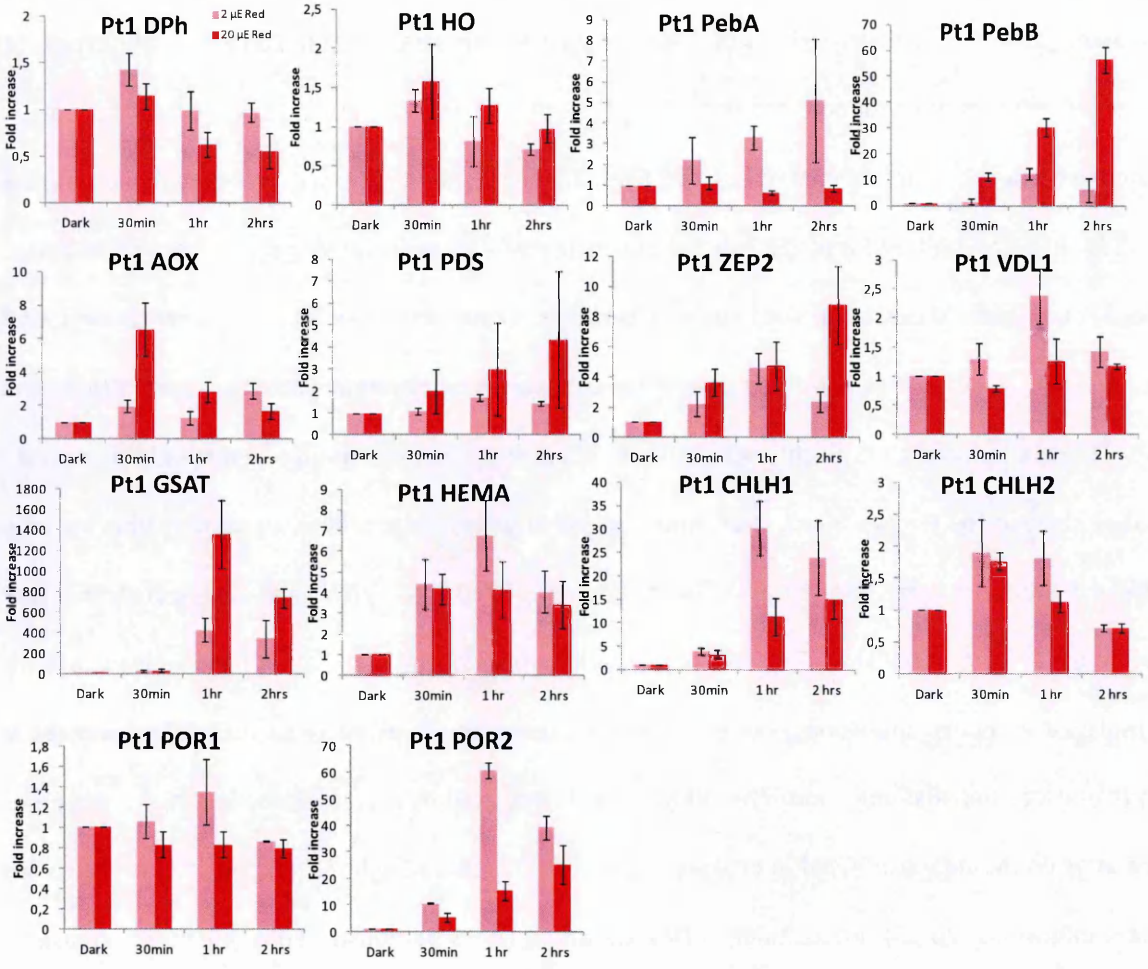

Figure 1.3.8 (previous page): mRNA levels of the following genes upon red light illumination: phytochrome (*DPh*), heme oxygenase (*HO*), bilin reductases (*Peba* and *PebB*), alternative oxidase (*AOX),* violaxanthin de-epoxidase-like 1 (*VDL1*), phytoene desaturase (*PDS*), zeaxanthin epoxidase (*ZEP2*), glutamate-1-semialdehyde-2,1-aminomutase (*GSAT*), glutamyl-trna-reductase (*HEMA),* protoporphyrin IX magnesium chelatase subunit H (*CHLH1, CHLH2*) and protochlorophyllide oxidoreductases (*POR1, POR2*). Pt1 WT cells illuminated with 2 µE or 20 µE continuous red light (660 nm) after dark adaptation. Relative transcript levels were determined after 30 minutes, 1 hour and 2 hours by qRT-PCR using *H4* and *RPS* as a reference gene. The values were normalized to the transcript levels in the dark. These data are averages from triplicate measurements on the same cDNA samples, and error bars indicate standard deviations. All raw Ct values are listed in Annex V.

2/ Red light mediated gene expression in Pt WT and DPh knock-down lines

A comparative analysis of red-light mediated gene expression was performed in Pt1 WT. The cells were dark-adapted for 60 hours and subsequently exposed to continuous red light (660 nm). In addition to the previously tested fluencies of 2 and 20 µE of red light, I also tested variation in gene expression under very low red light illumination (0,2 µE) and shorter sampling points (10 minutes, 30 minutes and 1 hour), to better comprehend the role of DPh as photoreceptor in these responses and to reduce the possible involvement of chloroplast and photosynthetic activity. As shown in figure 1.3.9, the *GSAT* transcript levels of the Pt1 WT showed an increase, especially with higher red light intensities (20 µE) after 30 minutes and 1 hour. The transcript levels of *ZEP2* showed only a very dramatic increase after 1 hour in 20 µE red light treatment. Transcript levels of *CHLH1* kept steady-state levels upon exposure to 0,2 µE of red light. *AOX* transcript levels increased in a moderate way in 2 µE red light and increased then dramatically after 1 hr in 20 µE red light. It can be generally stated that most genes react to higher fluency rates, and increase their expression over time. When investigating the transcript levels in the DPh knock-down lines, it seems that gene expression is almost always higher, even much higher in some cases, than for Pt1 WT, especially in higher red light intensities (see Figure 1.3.9b). Unfortunately, the data with the knock-down lines was more variable, therefore the standard deviation shows quite high values in the graph with the knock-down lines, making it difficult to draw strong conclusions. Transcript levels of *GSAT* in the DPh knock-down lines are increasing to highest levels observed for all tested genes in 2 and 20 µE of red light, in two out of

three knock-down lines (*dph1'* and *dph5'*). In *ZEP2*, the transcript levels in the knock-down lines in 0.2 µE do not differ from the WT but keep on increasing in 2 µE in *dph1'* and *dph5'* and even more in 20 µE in *dph-1*, *dph1'* and *dph5'*. In *AOX*, the transcript levels in the knock-down lines are quite similar than the WT in the lowest red light condition (0,2 µE). In the intermediate red light condition (2 µE) only *dph1'* showed an increased expression at 30 min and 1 hr exposure. The other two knock-down lines showed similar transcript levels than the WT. In the highest red light condition (20 µE) especially *dph-1* showed high transcript levels after 1 hour, followed by *dph1'*. *Dph5'* transcript levels were similar to the WT. In *CHLH1*, transcript levels in 2 µE were already quite elevated for *dph5'* after 30 minutes and keep on increasing in 2 µE. In 20 µE, *dph5'* levels were similar to the WT. The other two knock-down lines show elevated transcript levels in 2 and 20 µE, especially *dph-1* levels increase strongly in 2 µE after 1 hour. In general, all DPh knock-down lines show higher and much elevated transcript levels in comparison to the WT, in 2 and 20 µE red light.

a)

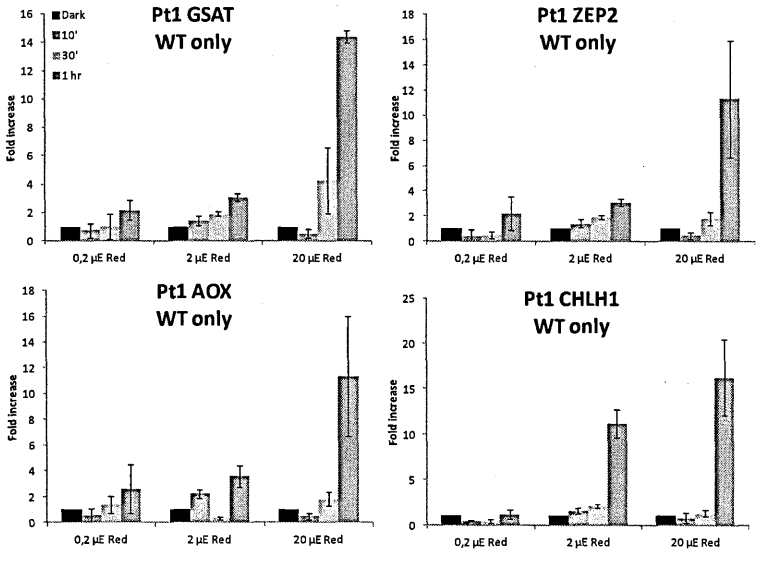

b)

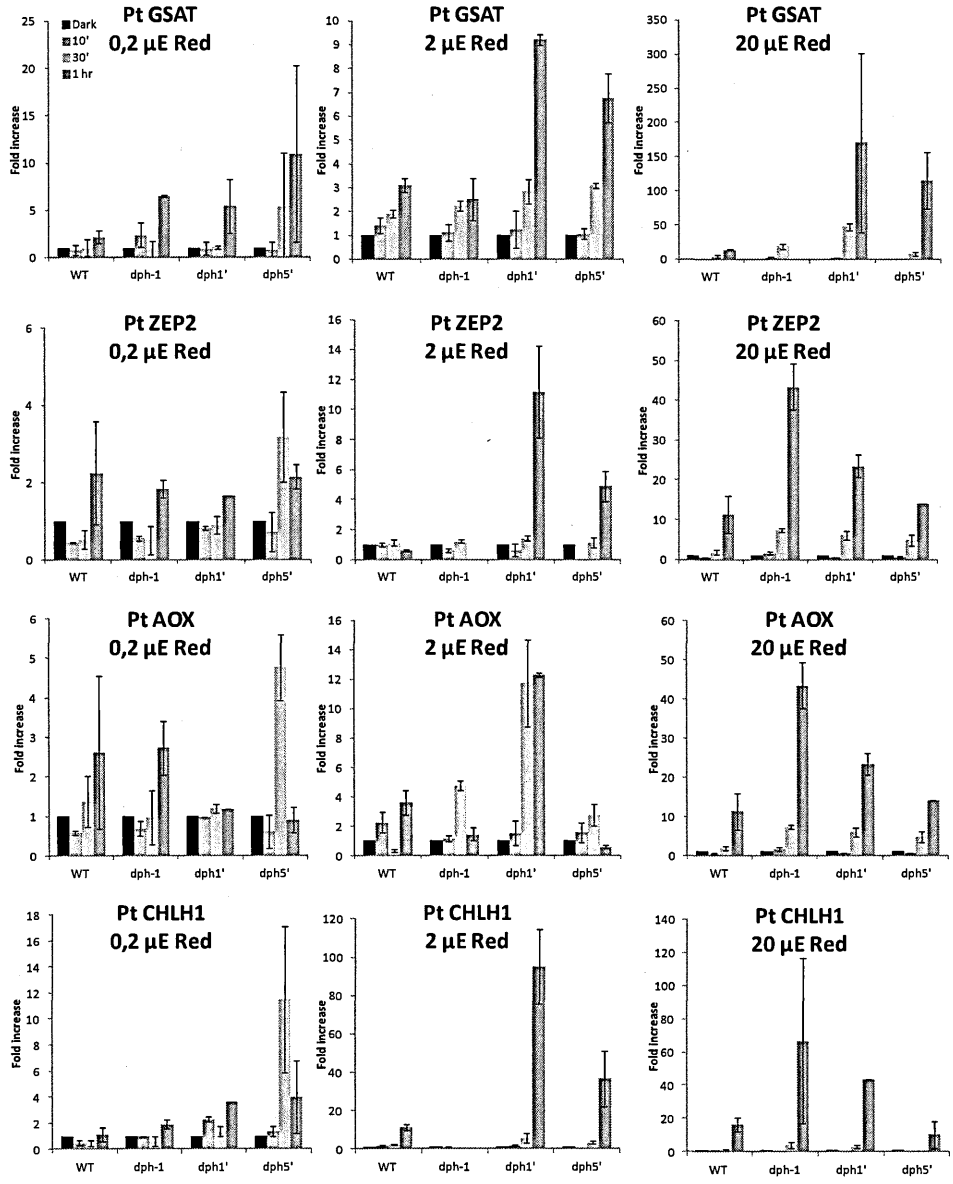

Figure 1.3.9: mRNA levels in the Pt1 WT upon continuous red light exposure (0,2 µE, 2 µE and 20 µE) with wild type cells (a – previous page) and DPh knock- down lines (b). The following genes were tested: Glutamate-1-semialdehyde-2,1-aminomutase (*GSAT*), zeaxanthin epoxidase (*ZEP2*), alternative oxidase (*AOX*) and protoporphyrin IX magnesium chelatase subunit H (*CHLH1*). Relative transcript levels were determined after 10 minutes, 30 minutes and 1 hour by qRT-PCR using *H4* as a reference gene. The values were normalized to the transcript levels in the dark. These data are averages from triplicate measurements on the same cDNA samples (repeated twice), and error bars indicate standard deviations. All raw Ct values are listed in Annex V.

3/ R-FR photoreversibility experiments in P. tricornutum WT and DPh knock-down lines

As mentioned in the introduction, the canonical phytochrome is a photoswitch with two conformations, Pr and Pfr. In plants, the Pr form is converted to the active Pfr form upon red light illumination, triggering further downstream components for biological activity. On the contrary, the Pfr form is converted to Pr upon far-red light illumination. This sensitive equilibrium between Pr and Pfr forms is often tested with red/far-red (R/FR) light photoreversibility experiments. Thus, with the knowledge obtained from the previous analysis, additional experiments were performed to test a possible photoreversibility in the DPh mediated responses, with Pt1 WT and one DPh knock-down line (*dph-2*). First, 100 µmols/m² of red and far-red light was used with earlier sampling points to increase the resolution of the gene expression profiles. Second, to test photoreversibility events in *P. tricornutum*, Pt1 WT and DPh knock-down cells were also exposed to either 100 µmols/m² of red light followed by 100 µmols/m² of far-red light (R+FR) or 100 µmols/m² of far-red light followed by 100 µmols/m² of red light treatment (FR+R). After the light treatment, cells were immediately restored to complete darkness. Samples were taken before the light treatment, and after 20 minutes, 1 hour, 3 hours and 5 hours (see figure 1.3.10 below) following the pulse. We tested only a couple of genes that previously showed interesting reactions (*GSAT* and *CHLH1*) and we added also *LHCF2*, a classical light harvesting protein and homologue of the plant *CAB* gene, as *LHCF2* was previously tested in the lab on Pt1 and showed interesting results (data not shown). Unfortunately, *DPh* gene was also tested but raw data proofed to be of too bad quality to assess the analysis and it was therefore not included in below graphics.

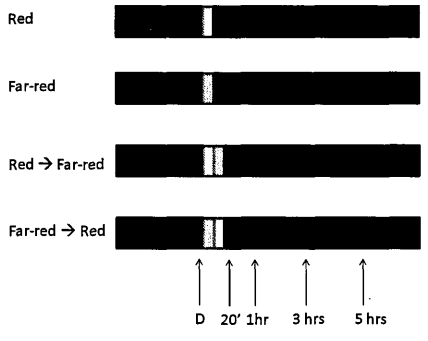

Figure 1.3.10: Scheme with the experimental set-up. Pt1 WT cells were dark-adapted for 60 hours and exposed to different treatments (100 µmols/m² R; 100 µmols/m² FR; 100 µmols/m² R + 100 µmols/m² FR; 100 µmols/m² FR + 100 µmols/m² R). Samples were collected before illumination and 20 minutes, 1 hour, 3 hours and 5 hours after illumination.

The gene expression data indicate stable levels of Pt1 WT transcripts in *GSAT*, *CHLH1* and *LHCF2* at 100 µmols/m² of R light pulse. In this experiment, all genes showed in average the same gradually increased expression to the far-red light-only treatment. Both *GSAT* and *CHLH1* were even more induced by the R+FR and FR+R light treatments as an additive effect than the single-color treatments (R or FR light). *LHCF2* however did not react in a particular way to either R or FR light alone but reacted very strongly to the FR+R light treatment after 5 hours, indicating here that there is an additive effect of FR with R light. The effect is also visible in the R+FR light treatment, although the *LHCF2* expression is less in the R+FR light treatment.

I analyzed also the response in one knock-down line, *dph*-2, for the genes *GSAT*, *CHLH1* and *LHCF2*. Unfortunately, the data for *GSAT* was of insufficient quality to perform a qualitative analysis on the expression levels. In *CHLH1* and *LHCF2*, the DPh knock-down line showed a reduction of their transcript levels in both R and FR light treatments (see figure 1.3.11 panel b).

Figure 1.3.11: **Panels A1 and A2** (next page) show mRNA levels in Pt1 WT, treated with (A) 100 µmols/m² red light, (B) 100 µmols/m² far-red light, (C) 100 µmols/m² red light followed by 100 µmols/m² far-red light and (D) 100 µmols/m² far-red light followed by 100 µmols/m² red light. After the light treatments, cells were restored to complete darkness. Tested genes are *GSAT*, *CHLH1*, *LHCF2* and *DPh*. Samples were collected before the light treatment (Dark) and 20 minutes, 1 hour, 3 hours and 5 hours after light pulse. Panel A2 is a detailed view of the lower mRNA levels with smaller scale to appreciate the smaller mRNA differences in 20', 1 hour and 2 hours time points. **Panel B –** next page) shows mRNA levels in Pt1 WT and DPh knock-down lines (*dph-2* and *dph-5'*), treated with (A) 100 µmols/m² red light, (B) 100 µmols/m² far-red light, (C) 100 µmols/m² red light followed by 100 µmols/m² far-red light and (D) 100 µmols/m² far-red light followed by 100 µmols/m² red light. The results were normalized against an internal gene standard, the *H4* gene and to the transcript levels in the dark. These data are averages from triplicate measurements on the same cDNA samples, and error bars indicate standard deviations. mRNA levels were only normalized against the internal gene standard, the *H4* gene. These data are averages from triplicate measurements on the same cDNA samples, and error bars indicate standard deviations. All raw Ct values are listed in Annex V.

A1

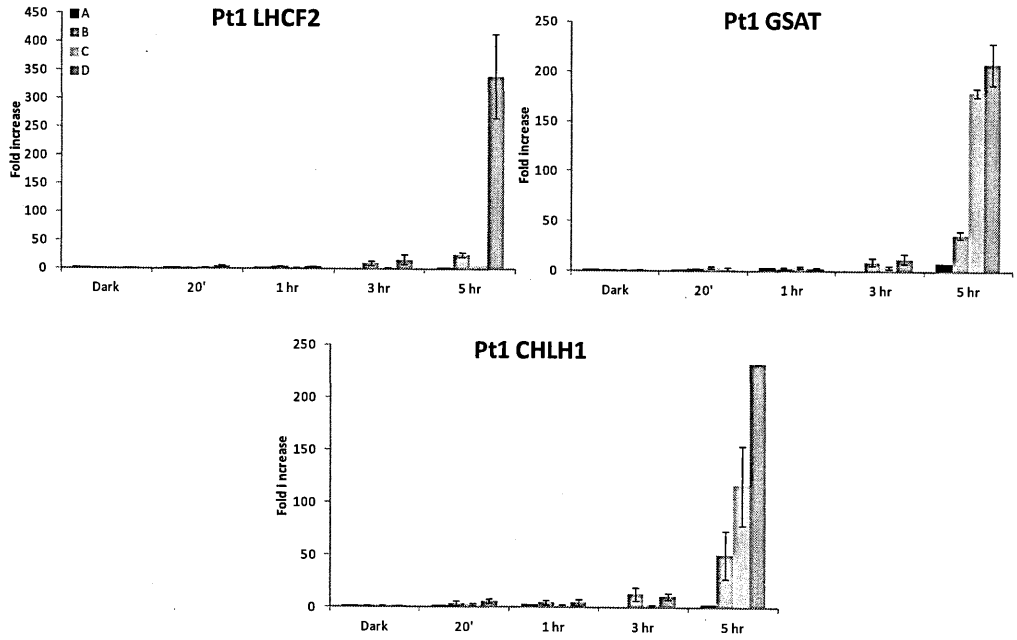
Pt1 LHCF2
Fold increase
A
B
C
D
Dark
20'
1 hr
3 hr
5 hr
Pt1 GSAT
Fold Increase
Pt1 CHLH1
Fold I ncrease

A2

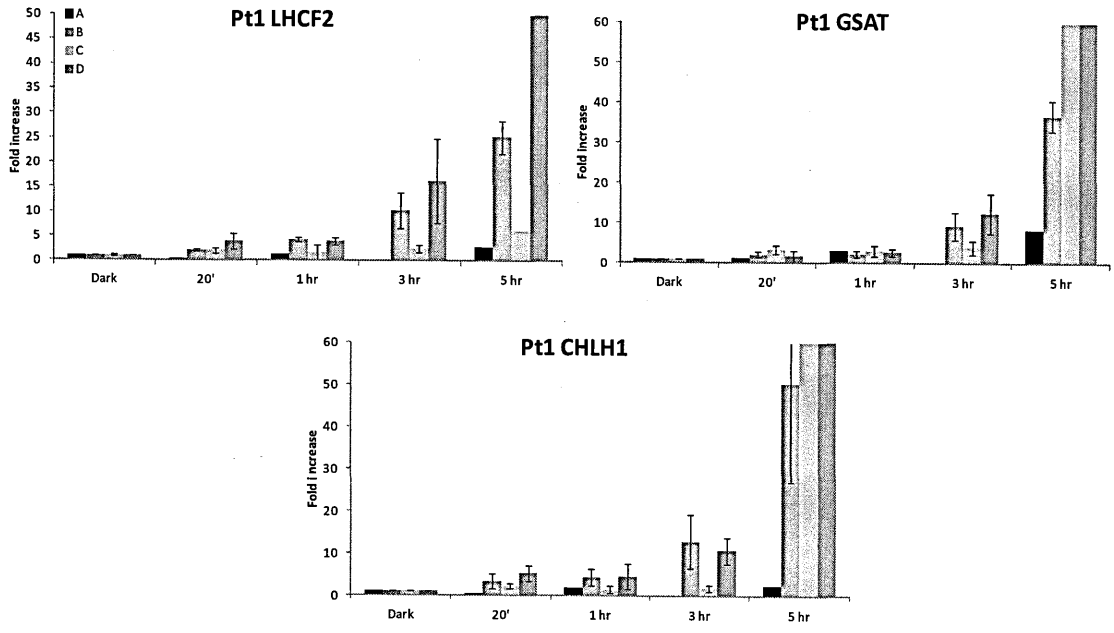
Pt1 LHCF2
Fold increase
A
B
C
D
Dark
20'
1 hr
3 hr
5 hr
Pt1 GSAT
Fold Increase
Pt1 CHLH1
Fold I ncrease

B

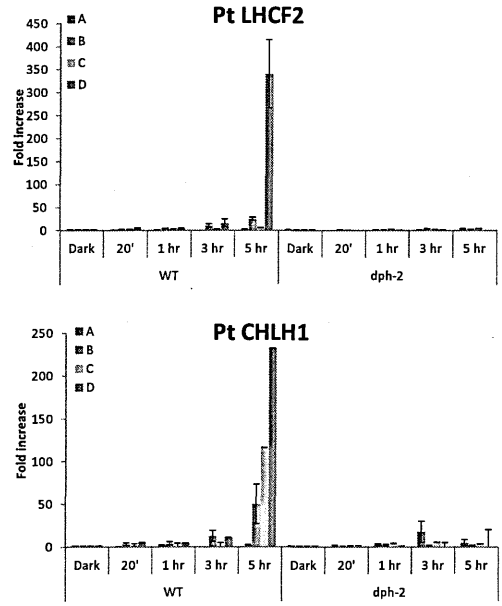

4/ DCMU inhibitor experiments

I also investigated whether the observed changes in gene expression in red light were due to a regulation through chloroplast activity. For this reason, I performed gene expression studies in Pt1 WT cells treated with or without DCMU or also called Diuron (3-(3,4-dichlorophenyl)-1,1- dimethyl-urea), an inhibitor of photosynthesis that prevents electron transfer between the two photosystems and in particular between PSII and the plastoquinone pool (Trebst, 1980). To this aim, WT cells were dark-adapted for 60 hours and illuminated with various red light fluencies (2 and 20 µE), as described for the experiment in figure 1.3.8 (in Results). Duplicate cultures (A-B) were used, in which a cultures A received DCMU (10 µM final concentration) before the light treatment and the other cultures B functioned as control cultures without the addition of DCMU. Surprisingly, the addition of DCMU blocked almost completely the light mediated induction in gene expression in *HEMA, AOX* and *CHLH1*, especially in 20 µE red light conditions (see figure 1.3.12), indicating a chloroplast regulation.

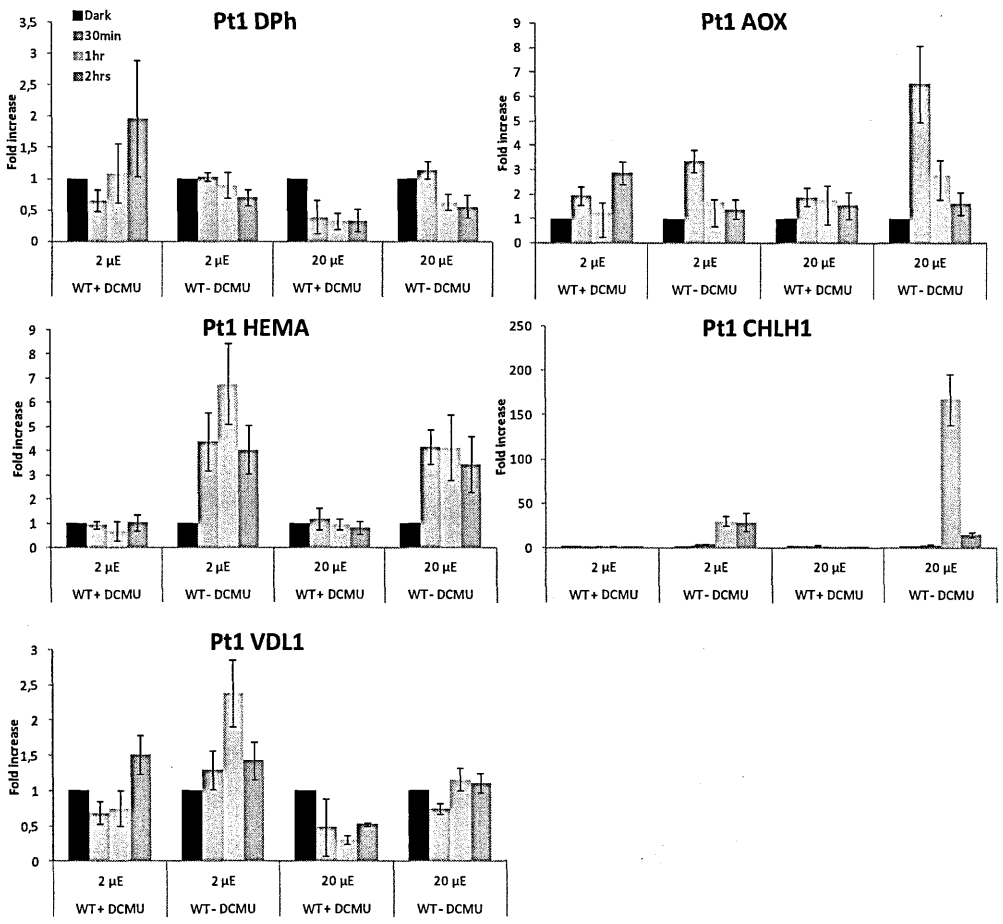

Figure 1.3.12: mRNA levels in Pt1 WT cells treated with or without DCMU, in continuous red light (2 and 20 µE). Tested genes are *DPh, AOX, GSAT, HEMA, CHLH1 and VDL1*. All the mRNA expression values were normalized against an internal gene standard, the *H4* gene (Histone 4). The values were normalized to the transcript levels in the dark. These data are averages from triplicate measurements on the same cDNA samples, and error bars indicate standard deviations. All raw Ct values are listed in Annex V.

5/ Blue light response experiments in Pt1 and DPh knock-down lines

In order to test the specificity of DPh in the regulation of red light-mediated responses, additional experiments were performed in which Pt1 WT and two DPh knock-down lines (*dph-2* and *dph-5'*) were illuminated with a blue light pulse of 5 µmols/m^2. Cells were first pre-adapted to a 60 hour-period of darkness and then treated with blue light following complete darkness. Samples were collected before the onset of light and after 20 minutes, 1 hour, 3 hours and 5 hours of light treatment. As a weak green safety light was used during the dark samplings in all the experiments

described so far, a control was done by exposing cells to the same green light but without any additional illumination with blue or red light, in order to exclude a possible green light effect in the gene expression. The same set of genes was investigated for their relative mRNA levels as for the R/FR photoreversibility experiments described in paragraph 4. The quality of the raw data was not of the best and as a result, high standard deviations were observed. However, transcript levels of *GSAT* in the WT were higher in blue light than in red light (see figure 1.3.13), suggesting a regulation of this gene also by blue light. *CHLH1* transcript levels did not show a relevant increase in expression in comparison to previous red light treatment, as well as *LHCF2* transcript levels in the WT. The expression pattern in the DPh knock-down lines is not straight forward, as the two knock-down lines do not behave in the same way to the blue light treatment. The *dph-2* knock-down line shows a similar expression profile as the WT for *LHCF2* and *CHLH1*. In *GSAT*, the *dph-2* knock-down line shows a strong inhibition of expression, as well as the other knock-down line *dph-5'* where the inhibition in expression is even more clear. Knock-down line *dph-5'* showed a slight decrease in expression for *LHCF2* and *CHLH1*, in comparison to the WT. This effect could be explained either by a role of DPh also in blue light perception or to a deregulation of DPh downstream components, that are also implicated in the blue light pathway mediating the gene expression responses. The control that was kept in permanent darkness, showed mostly unaffected expression profiles in all the tested genes.

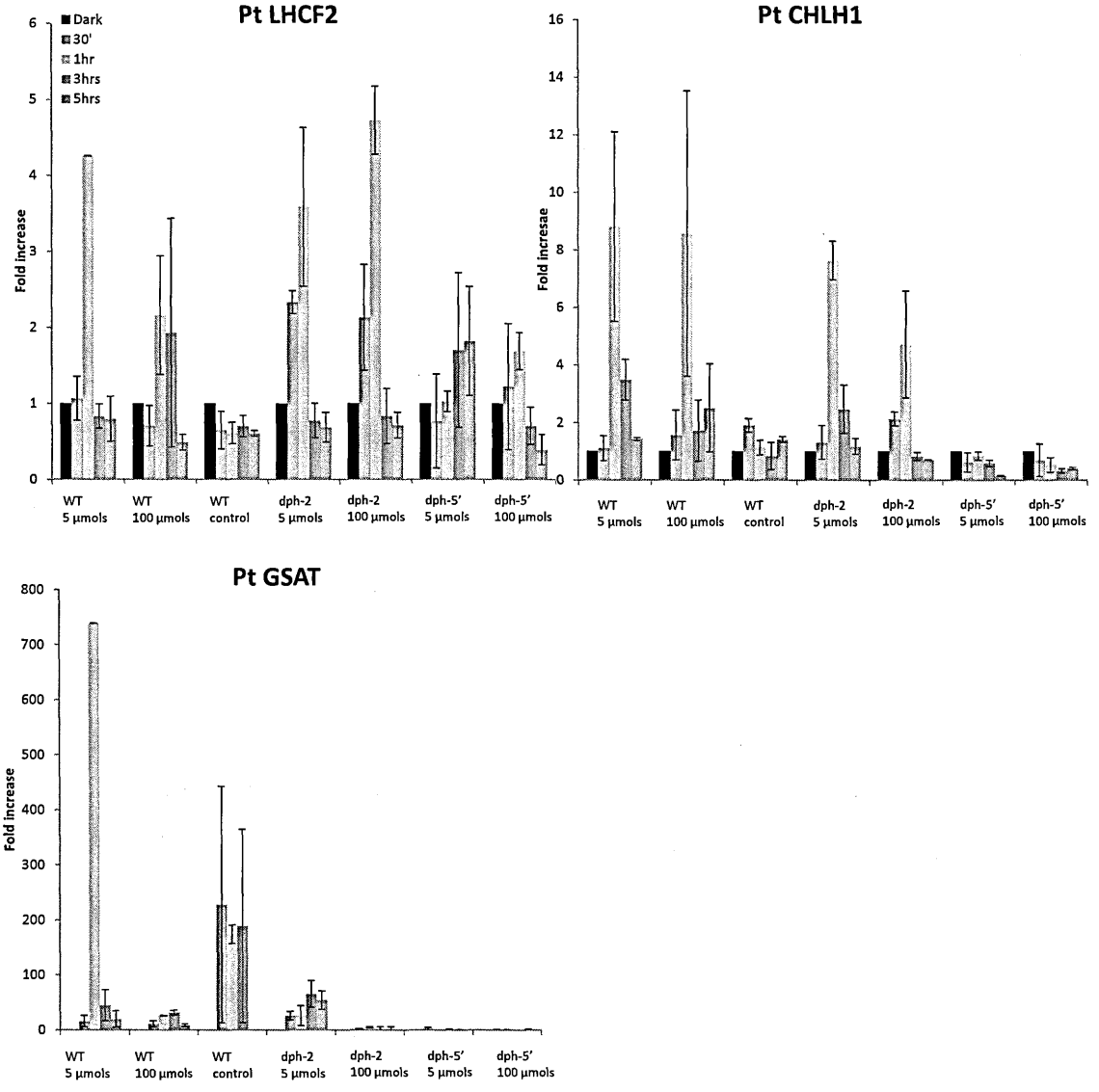

Figure 1.3.13: mRNA levels in Pt1 WT and two DPh knock-down lines (*dph-2* and *dph-5'*), treated with a blue light pulse (5 µmols/m² and 100 µmols/m²). Samples were also taken from cells kept in the dark permanently, after the dark point sampling as control (WT Dark control). Tested genes are *GSAT*, *CHLH1* and *LHCF2*. All the mRNA expression values were normalized against an internal gene standard, the *H4* gene. The values were normalized to the transcript levels in the dark. These data are averages from triplicate measurements on the same cDNA samples, and error bars indicate standard deviations. All raw Ct values are listed in Annex V.

6/ R/FR pulse experiment in T. pseudonana

With a set of red or far-red light regulated genes observed in *P. tricornutum* in those genes, we wanted also to test the generality of DPh-mediated responses in another diatom, *T. pseudonana,*

available in the lab. For this reason, cells from *T. pseudonana* were dark-adapted for 60 hours and treated with a total of 100 µmols/m² red (R) or far-red (FR) light. To test photoreversibility, cultures were also exposed to either 100 µmols/m² of red light followed by 100 µmols/m² of far-red light (R+FR) or 100 µmols/m² of far-red light followed by 100 µmols/m² of red light treatment (FR+R) (see Figure 1.3.14). After the light treatment, cells were immediately restored to complete darkness. Samples were taken before the onset of light and after 3 hours and 5 hours. *LHCF1* and *LHCF2* genes were investigated for their relative mRNA levels in *T. pseudonana*. Also the genes *CHLH1* and *GSAT* were tested initially, but re-analysis of the data has suggested that the quality of these raw data sets was insufficient to report in the thesis. In general, no clear responses for these two genes to red, far-red light or photoreversibility experiments were observed as in comparison with the *Phaeodactylum* cells. However, a slight additive effect was observed in the R+FR light conditions, as the transcript levels always increased after 5 hours.

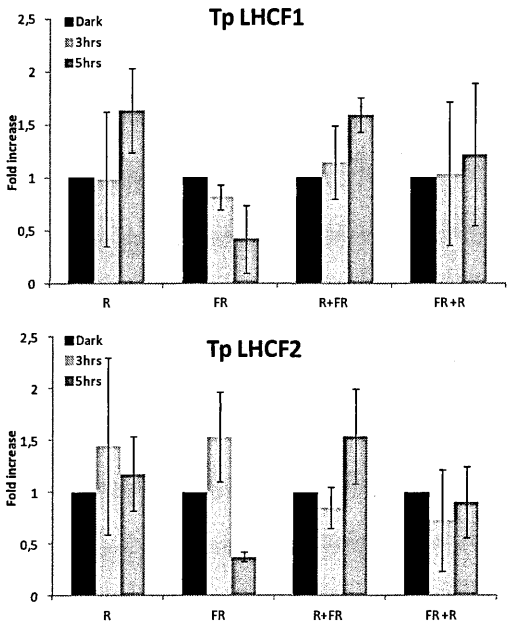

Figure 1.3.14: Relative mRNA expression profiles in *T. pseudonana* WT, on cells treated with red light (R), far-red light (FR), red light followed by far-red light (R+FR) and far-red light followed by red light (FR+R). Tested genes are *LHCF1* and *LHCF2*. All the mRNA expression values were normalized against an internal gene standard, the *Actine* gene. The values were normalized to the transcript levels in the dark.

These data are averages from triplicate measurements on the same cDNA samples, and error bars indicate standard deviations. All raw Ct values are listed in Annex V.

7/ DPh regulation: protein studies

In order to understand the balance between RNA synthesis (from the photoreversibility experiment, see figure 1.3.11) and DPh protein accumulation, I characterized more in detail the expression and possible degradation of DPh under different light conditions. Therefore, to test a possible diurnal and circadian regulation of DPh expression, the following experiment was performed. Pt1 WT cells were pre-adapted for several days to a D:L (12hrs:12hrs) regime (40 µE of white light) and then exposed to either D:L (12hrs:12hrs) or continuous darkness for 2 days. Samples were taken every 4 hours from the beginning of the experiment. As shown in figure 1.3.15, the DPh protein content seems increase to its maximum concentration at the end of the light period (6:00 PM), pointing toward the existence of a diurnal expression pattern in DPh. Interestingly, a small induction of DPh protein content is observed in day 1 at 6:00 PM of the continuous darkness condition, suggesting a possible circadian regulation in DPh. These results are in line with previous *DPh* gene expression analyses done in the laboratory, which pointed toward a diurnal expression of *DPh* at RNA level. During prolonged darkness, DPh seems to decay in time, especially after 36 hours of darkness. However, a certain amount of DPh protein is still present after prolonged darkness, suggesting that light is needed for the *de novo* synthesis of DPh but that the protein is also quite stable in the dark.

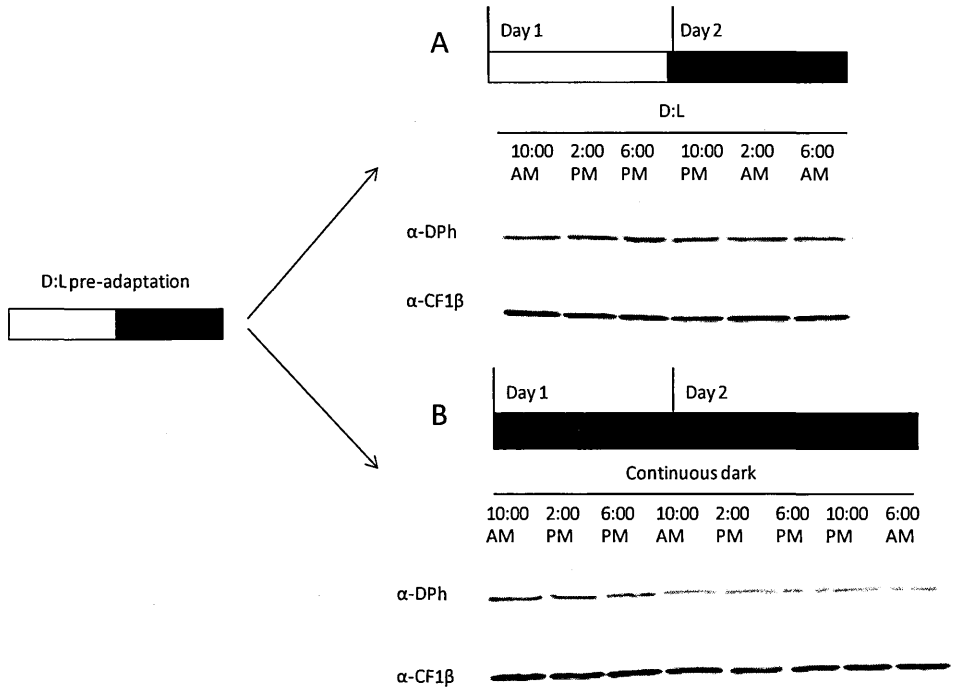

Figure 1.3.15: Western Blot analysis of Pt1 WT in D:L (12hrs:12hrs, Panel A) and prolonged darkness (Panel B) for two days. Cultures were first pre-adapted to a D:L (12hrs:12hrs) regime for several days and then shifted either D:L or continuous darkness. Samples were taken every 4 hours from the onset of light. DPh levels were studied with the α-DPh antibody. The antibody α-CF1β was used as loading control.

Then, I also tested DPh content in cells adapted to continuous light for 3 days, in order to compare the DPh expression levels with those from cells grown in D:L (12 hrs:12hrs, with samples taken at mid-day). As seen in figure 1.3.16, the content of DPh decreased in the prolonged light treatment, suggesting a possible degradation of DPh by light. Interestingly, the level of silencing in the DPh knock-down lines became even more pronounced. This exciting result correlates with the observed increase in the colony phenotype, as will be described in chapter II (Results, figure 2.3.5). These experiments all together have shown that there is a complex regulation of the DPh protein by light and point toward the existence of a delicate balance between DPh synthesis (at RNA and protein level) and DPh degradation. All these aspects are momentarily under investigation in the laboratory.

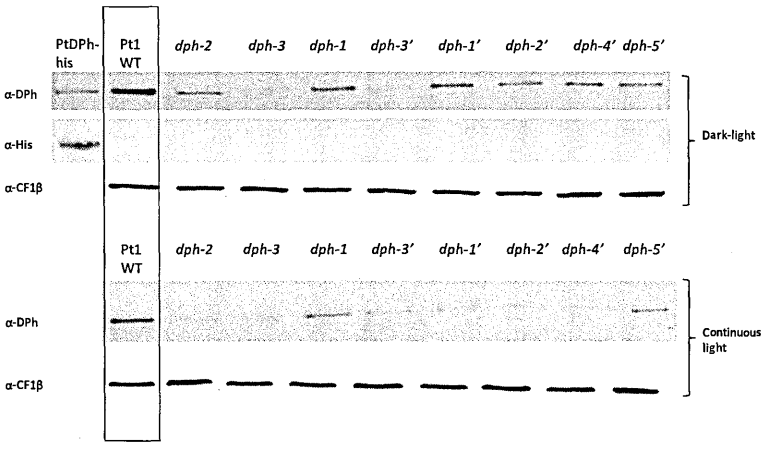

Figure 1.3.16: Western Blot analysis of DPh protein in Pt1 WT and DPh knock-down lines (*dph-2, dph-3, dph-1, dph-3', dph-1', dph-4'* and *dph-5'*) grown in D:L (12hrs:12hrs) or continuous light conditions (both 40 μE). The purified PtDPh protein with histidine tag was used as control for the identification of the endogenous DPh, with the α-his antibody. The antibody α-CF1β was used as loading control.

1.4. DISCUSSION

1.4.1 Existence of phytochromes in the marine environment

Until 1996, it was believed that phytochrome proteins were a specific feature of higher plants. This changed with the discovery of the phytochrome RcaE photoreceptor in *Fremyella* (Kehoe & Grossman, 1996) and phytochrome-like sequences in the cyanobacterium *Synechocystis* (Yeh *et al.,* 1997a). Later, phytochromes have not only been found in many other lower plants, algae, cyanobacteria and purple bacteria, but also in other prokaryotes including the non-photosynthetic *Deinococcus radiodurans* and *Agrobacterium tumefaciens*, suggesting that the existence of phytochromes is not restricted to photosynthetic organisms. A few years ago, when the diatom genomes became available, the discovery of phytochrome sequences in marine diatoms was astonishing and unexpected. Because of the low abundance of red and far-red light in the oceans, the ecological significance of red/far-red light responses through a phytochrome photoreceptor in these organisms became an intriguing and novel question. To date, these proteins represent the only putative red light sensor identified in these marine organisms.

The analysis performed during my PhD work has allowed enlarging further the phytochrome family, revealing the presence of novel phytochrome-like sequences in different members of the Heterokont family to which also diatoms belong, all displaying a common evolutionary history. Several pennate diatom species, as *P. tricornu*tum, *P. multiseries* and *S. robusta* contain a phytochrome sequence, as well as the centric diatom *T. pseudonana.* Also the genome of the brown alga *E. siliculosus* displays three phytochrome sequences and interestingly, several marine viruses, EsV-1 and FirrV-1 were found to harbor a phytochrome. It is worth noting that the analysis of the recently sequenced genome of the diatom *Fragilariopsis cylindrus* (genome.jgi-psf.org/Fracy1/), a sea-ice species that experiences a very low attenuation for red light in ice, revealed that this species does not possess any DPh. Thus, this diatom seems to have well evolved to adapt to its red light-free environment in the ice where there is no need for a red/far-red light sensor.

The phytochrome sequences from the Heterokont family all share common domain architecture. These sequences display GAF and PHY domains in the N-terminal photosensory input domain and HK and RR in the C-terminal output domain, like bacterial and fungal phytochromes. Despite these similarities, variations are present at the N-terminal end of these phytochromes. DPhs from the pennate diatoms *P. tricornutum* and *S. robusta,* and from the brown alga *E. siliculosus* all lack the PAS domain at the N-terminal photosensory domain, whilst this PAS domain is present in the centric diatom *T. pseudonana*. The presence of PAS domain in *T. pseudonana*, which is almost 90 million years older than *P. tricornutum*, and the loss of PAS domain in all the other Heterokont species, may suggest that the PAS domain was present in the common ancestors of the Heterokont family, but was lost in pennate diatoms and multicellular brown algae later. The lack of this domain, shown to be important for the formation of the PAS-GAF light sensing knot domain and protein stability and signaling in bacteria and plants, may also suggest that the Heterokont phytochromes may show different light-sensing properties. On another note, the fact that the *E. siliculosus* phytochromes have two putative cysteine residues for the chromophore binding, one in the N terminal domain and one in the GAF domain (as in plants), suggests that several rearrangements in specific residues have occurred during the evolution of the phytochromes also in the Heterokont clade. All together these studies confirm previous observations indicating that domain arrangements and losses of domains have been responsible for the generation of new phytochromes during evolution, as previously shown from the analysis of a number of bacterial phytochromes that lack HK domains and other catalytic/regulatory domains that have been inserted in their place. Also, domain exchanges have occurred more recently in primitive plants to yield the neochromes, which are functional chimeras of a plant phytochrome photosensory domains and a blue-light-sensing phototropin (Suetsugu *et al.*, 2005). Functional and biochemical studies will be needed to better understand the implication of all these variations in the novel phytochromes found in the Heterokont clade.

Previous phylogenetic analyses have already indicated that DPhs form an independent clade with two brown-algal viruses, EsV-1 and FirrV-1 (Montsant *et al.*, 2007). This lead to the hypothesis that a possible 'brown clade' of phytochromes may exist, in which virus-mediated lateral transfer would have contributed to spread phytochrome-like genes among Heterokonts. The novel sequences identified in this thesis are now used to perform new phylogenetic analyses. Preliminary data performed in the laboratory (not shown in this thesis) already indicated that beside the differences summarized above, all these phytochromes form a new and enlarged clade of Heterokont phytochromes, underlining a common evolutionary history.

1.4.2 The diatom phytochrome is a red/far-red light photoreceptor

The main goal of this thesis project was to understand whether DPh in *P. tricornutum* acts as a photoreceptor, by investigating its spectral and biochemical properties, and its function in *vivo*. For the first time since many years of diatom phytochrome research, a clear answer has been provided with the acquired absorption spectra of the recombinant DPh holoprotein. These have clearly demonstrated that DPh is a red/far-red light photoreceptor with red-shifted spectra (Pr at 690 nm and Pfr at 740 nm) compared to plants, and similar to the reported absorption spectra from bacterial phytochromes such as the Agp1 from *A. tumefaciens*. Analysis performed by our collaborators indicated that the two DPh forms are photoconvertible (Pr to Pfr and Pfr to Pr), following irradiation with red and far-red light, respectively. The formation of a photoactive holophytochrome following co-expression of *DPh* and the cyanobacterial *HO* genes in *E. coli* indicated that both proteins were successfully expressed in the bacterial system, allowing the synthesis of the biliverdin (BV) chromophore and its assembly with the apophytochrome DPh. Considering the similarity between DPh and Bph, it is very likely that BV may also act as the chromophore of DPh in diatoms, by binding to the conserved cysteine residue in the N-terminal region. However, final evidences about the endogenous DPh chromophore are still missing. The obtained DPh spectra with BV do not imply that BV is necessarily the chromophore in diatoms,

because also in *Arabidopsis* red/far-red absorption spectra were obtained by expression of the phytochrome from *Arabidopsis* in *E. coli* with BV and PCB as chromophores, other than its natural chromophore which is PΦB. By searching in the diatom genomes, I indeed found endogenous *HO* genes that could be responsible for the BV synthesis. One of these *HO* genes has also been characterized during this thesis, as described in chapter II. Analysis of HO knock-down lines also revealed a deregulation of DPh synthesis, as also shown in plants, strongly supporting a role for this protein in chromophore biosynthesis. However, it is still possible that BV is not the chromophore in *P. tricornutum*, because bilin reductase genes (*PebA* and *PebB)* are present in the genome and show increased expression levels upon red light in *P. tricornutum* (see results, figure 1.3.8), which could point toward an implication of these genes in the further conversion of BV to phycoerythrobilin (PEB). Therefore, during these years I have also investigated the possibility that *PebB* and *PebA* could be implicated in the generation of a diatom specific chromophore (PEB). To this aim, the *DPh* gene from diatoms has been expressed in *E. coli*, together with a bacterial *HO* gene (for the BV synthesis) and the *PebB* and *PebA* genes (for the conversion of BV in PEB). Data from our collaborator in Japan indicated that the resulting holoprotein did not show any spectral differences compared to the expression of the *HO* alone. This suggests that the photoactive DPh might rather use BV as chromophore. As fact, if absorption spectra were obtained for the expression of DPh with bilin reductase gene indicating that DPh uses PEB as chromophore, shorter wavelengths would be expected. These data, together with the lack of evidences that diatoms might produce PEB as pigment, indicate that BV is still the most likely endogenous chromophore of DPh.

1.4.3 Gene expression profile experiments (Figures 1.3.8 and 1.3.9)

Red and far-red light mediated gene expression in the Pt WT

In order to better clarify the role of DPh as photoreceptor in diatoms, I focused on the possible role of this protein in the regulation of red light-mediated gene expression. To this aim, efforts have been diverted during this PhD to identify and characterize red light regulated genes in *P. tricornutum*. Acute light response experiments, performed on cells adapted to the dark and then exposed to red light of different intensities (0.2, 2 and 20 µmols/m^2/sec) for several hours allowed to identify several genes that are red or far-red light mediated.

The most important observation of the red light mediated gene expression can be summarized as follows: several genes coding enzymes of the carotenoid biosynthesis (*VDL1*, *PDS* and *ZEP2*) and a cellular redox state marker (*AOX*) all showed a clear red light regulation, with specific expression patterns that have been described in detail in the Results section, figure 1.3.8. The observed red light-mediated response of *PDS* and the two genes *VDL1* and *ZEP2*, confirmed results previously obtained in the laboratory (Coesel *et al.*, 2008), in particular that the transcript levels of these genes were induced in red light. The *AOX* gene did not show a clear signal of induction at increasing exposure times to red light, but showed a red light-mediated gene expression with an increased expression with increasing light intensities (see Results, figure 1.3.8 and 1.3.9). This is particularly clear after 30 min exposure. AOX is known to play a role in optimizing photosynthesis in the mitochondria (Yoshida *et al.* 2008) and moreover, it has been suggested that it can prevent the production of reactive oxygen species (ROS) (Pasqualini *et al.* 2007; Van Aken *et al.* 2009; Vanlerberghe *et al.* 2009), therefore AOX might also protect chloroplasts against photodamage in plants. In plants, AOX acts as an alternative to the cytochrome pathway to transfer electrons from the respiratory chain to molecular oxygen (Van Aken *et al.*, 2009). The AOX proteins found in *P. tricornutum* and *T. pseudonana* contain the redox-sensitive residues that are potential targets of the thioredoxin regulation, as in AOX proteins from all other organisms examined to date (Van Aken *et al.*, 2009). In addition, the

diatom AOX sequences also contain calmodulin-like calcium-binding motifs (EF hands), suggesting a calcium-mediated regulation of AOX activity (Prihoda *et al.*, 2012). As observed in these experiments in *P. tricornutum*, the increased *AOX* transcripts levels with increased light intensities would be expected from a protein that is involved in protecting the cells from photodamage.

Particular attention has been also diverted to the analysis of several genes of the tetrapyrole biosynthetic pathway. As described in the introduction of this chapter, tetrapyrroles are co-factors for essential proteins involved in a wide variety of cellular functions (Mochizuki *et al.*, 2010). Additionally, all the different tetrapyrroles (chlorophyll, heme, siroheme and phytochromobilin) are synthesized in the chloroplast from a common precursor (5-aminolevulinic acid (ALA)). Their synthesis requires tight regulation because misregulation of the tetrapyrrole metabolism can lead to severe photo-oxidative stress (see Introduction, figure 1.3.7). During this PhD, I have analyzed the expression of several genes acting at different steps in this pathway. The *HEMA* and *GSAT* genes, both at the beginning steps of the tetrapyrrole biosynthesis, are both regulated by red light, but with a very different expression pattern at different light intensities (see the Results section, figure 1.3.8 and 1.3.9). *GSAT* showed the highest transcript levels between all the analyzed genes, already at very low light intensity (see the Results section, figure 1.3.8), and the transcript levels increased with higher light treatments, like already observed in the green alga *C. reinhardtii* (Im *et al.*, 2006). Although the existence of a phytochrome in *C. reinhardtii* is not supported yet, there is evidence that a putative red/far-red light photoreceptor influences expression of *GSAT* (Im *et al.*, 2006). The diatom *HEMA* gene, on the contrary, appeared to show slightly higher levels of induction in 2 μE than 20 μE. Therefore, our data on the diatom *GSAT* and *HEMA* gene expression seem in contrast with what is observed in higher plant where *HEMA1* is highly light-regulated to meet an increased demand for chlorophyll by the chloroplast (McCormac & Terry, 2001), whilst *GSAT* genes only respond weakly to these signals. Although, since *HEMA* is known to be the rate limiting step in the chlorophyll biosynthesis in different organisms, it might be that the reduced *HEMA* expression observed in higher red light in

diatoms serves to prevent the production of chlorophyll in conditions that might be experienced as stressful and harmful for the diatom cells. Once this critical regulatory point is passed in the pathway, it might be that the high expression of the other downstream genes such as *GSAT* is necessary to generate as much chlorophyll as possible. An important branch point of the pathway involves the insertion of either Mg^{2+} or Fe^{2+}, by Mg-chelatase and Fe-chelatase, respectively, thereby directing protoporphyrin IX into the chlorophyll or heme biosynthetic pathways. In the chlorophyll branch, Mg-protoporphyrin IX is sequentially modified to form protochlorophyllide, which in higher plants accumulates in the dark, because the next enzyme, NADPH:protochlorophyllide oxidoreductase (POR), requires light to reduce protochlorophyllide to chlorophyllide a (see Introduction, figure 1.1.7). Between the diatom chlorophyll specific genes analyzed, the two *CHLH1* and *CHLH2* genes encoding for the Mg-chelatase subunit H only slightly showed higher transcript levels in lower red light intensities (2 µE) although the two genes displayed slightly different kinetics of transcript increase. Whilst *CHLH1* showed a sudden increase in 2 µE red light after 1 hour followed by a slow decrease after 2 hours and a lower but steady increase in transcript levels in 20 µE, *CHLH2* demonstrated only a very subtle increase in both light conditions after 30 minutes and 1 hour. These results indicate that the *CHLH* genes in *P. tricornutum* react in a very different way to various light conditions. *CHlH* in *A. thaliana* was shown to be light-regulated by continuous white, red, far-red and blue light, with an initial peak of expression after 2-4 hours light (Stephenson & Terry, 2008). As the diatom *CHLH* genes are clearly expressed by red light as is the case in plants, this may suggest that the diatom *CHLH1* might also be highly expressed in light conditions other than red light.

Interestingly, diatoms possess four *POR* genes, with *POR1* and *POR2* showing very different expression profiles in red light. *POR1* did not show a significant red light-mediated gene expression; whilst *POR2* showed a very fast and strong increase of transcript levels after 1 hour in 2 µE of red light. In angiosperms, the expression of *POR* genes is known to be tightly regulated by light, which results in the production of chlorophyll in light conditions but not in the dark, where

the chlorophyll synthesis pathway is blocked at the level of protochlorophyllide. Once a critical level of this intermediate has been reached in the dark, the early step of the pathway is inhibited at the level of ALA synthesis, preventing the accumulation of protochlorophyllide, which would cause photobleaching when the plants are illuminated. The FLU protein of *Arabidopsis* was identified as a key component of this negative feedback loop through its interaction with GluTR (Meskauskiene *et al.*, 2001; Meskauskiene and Apel, 2002). On the other hand, anoxygenic bacteria, cyanobacteria, green algae, nonvascular plants, ferns, and gymnosperms are able to convert protochlorophyllide to chlorophyllide through a light-independent reaction, and are thus capable to produce chlorophyll in the dark (Timko, 1998). Given the fact that also diatoms seem to produce chlorophyll in the dark and that genes implicated in the light-independent reactions have not been found in the genomes, we questioned if the differently light-regulated *POR* genes may play a role in chlorophyll synthesis under diverse light conditions. Because of the complexity of the pathway, this matter can only be elucidated by the further investigation of the chlorophyll biosynthetic pathway in diatoms and with functional studies of the genes encoding for these enzymes.

During the analysis of the red light-regulated genes of the tetrapyrrole pathway, I also studied genes downstream of heme and possibly involved in the DPh chromophore biosynthesis. The heme oxygenase (*HO*), coding for the enzyme involved in the conversion of heme to BV, was only moderately induced after 30 minutes in both red light conditions. Additionally, I also analyzed the two bilin reductase genes (*PebA* and *PebB*) that, as previously described, might be implicated in the synthesis of a diatom specific chromophore. The two genes showed a progressive induction in transcript levels upon red light with *PebA* showing higher transcript levels after 2 hours in 2 µE whereas *PebB* displayed much higher transcript levels in 20 µE. Thus, bilin reductase genes in *P. tricornutum* seem to be regulated by a red light sensor. However, the role of the bilin reductase genes in diatoms remains unclear (see 1.4.2 of the Discussion section).

In this analysis of the gene expression profiling under different red light conditions, I also included the *DPh* gene. The transcript levels of *DPh* did not change following dark to red light transition, and a very slight induction was reported only after 30 minutes upon 2 μE of red light. However, it might be that the experimental set-up and delayed sampling points (as reported for figure 1.3.8 in the Results section) did not allow us to detect an early induction in DPh expression levels, and/or that continuous light treatment may generates a repression of DPh synthesis, as it will be further discussed in the next paragraphs.

Also the DPh knock-down lines have been included in the experiment as reported in Figure 1.3.9 and the interpretation of the results will be discussed in a later paragraph together with other experiments in which the DPh knock-down lines were also used.

Photoreversibility experiments (Figure 1.3.11)

Phytochrome-mediated responses typically show a photoreversible behavior: either red or far-red light stimulates a response, which can be inhibited by a treatment with the other light color (red/far-red or far-red/red). To address a possible photoreversibility in the DPh-mediated responses, the genes *GSAT*, *CHLH1* and *LHCF2* were subjected to an analysis of photoreversibility, as described in figure 1.3.11 of the Results section. Also *DPh* was subjected to the analysis but the raw data was of insufficient quality to perform a qualitative analysis.

In none of the analyzed genes a red/far-red light photoreversibility event was observed. In all genes it was clear that the gene expression started to increase after 3 hours and then increased dramatically after 5 hours. Expression was always the highest in FR+R treatment, followed by R+FR treatment and then the FR light treatment, indicating that first, there is an additive effect of the two light colors and second, especially FR+R is the most effective light treatment to stimulate the expression in those genes. The reason behind that is not clear. We are aware that more experiments with cells exposed to different light treatments are necessary to clarify all these aspects, as it might be that the experimental set-up did not allow us to capture

the frame in which photoreversibility might occur. As mentioned in the previous paragraph, the difficulty might lay in the fact that we are working with a dynamic cell population with the additional difficulty that maybe not all cells perceived the same amount of light during the experiment. It might also be that we were not looking at the right set of genes involved in this process; this might be particularly true when looking at the reaction of the DPh knock-down line in the light experiments. This will be discussed further in a next paragraph (Experiments with the knock-down lines). Additionally, a more extended biochemical analysis of the DPh protein in the WT and the DPh knock-down lines is also necessary, because the emerging picture is that DPh is subjected to a complex regulation.

Specificity of the red light responses (Figure 1.3.13)

In order to test the specificity of DPh responses in red and far-red light, gene expression analysis have been performed with a blue light pulse of 5 and 100 µmols/m^2 (see Results, figure 1.3.13). The three tested genes showed a stronger induction after 1 hour blue light treatment. In *LHCF2* and *CHLH1*, induction was lower than in red light, and comparable between 5 and 100 µmols/m^2 treatments. *GSAT*, instead, showed a much stronger induction at lower light intensity. The fact that *GSAT*, a gene of the chlorophyll biosynthetic pathway, showed a larger induction upon blue light than in red light supports the regulation of these genes also through a blue light photoreceptor, as already observed in *C. reinhardtii* (Im *et al.*, 2006). However, the level of induction of *GSAT* in blue light was higher in the lower intensity (5 µmols/m^2) than the higher intensity (100 µmols/m^2) whilst the level of *GSAT* induction is red light is increasing with the intensity. In *LHCF2* and *CHLH1* the light control did not show any major gene activity but in *GSAT* the light control showed more transcript levels than for the 100µmols/m^2 red light condition. This could indicate that the light conditions were maybe not always as optimal and well distributed as they should be. However, it could also be that *GSAT* is active in very low red light conditions but not in high red light conditions, also seen the fact that the light control was 'not active' in the

other two genes. To date, different blue light sensors of the cryptochrome and aureochrome family have been found in diatoms (Depauw *et al.,* 2012). It is therefore very likely that a possible crosstalk between phytochrome and blue light sensors occurs in diatoms as well for the regulation and optimization of different responses to light.

Experiments with the DPh knock-down lines and methodology (Figures 1.3.9, 1.3.11 and 1.3.13)

In order to better understand the functional role of DPh on the red light regulated genes, we have used three different *P. tricornutum* DPh knock-down lines (*dph-1*, *dph-1'* and *dph-5'*) together with the WT. The results obtained cannot always be clearly interpreted, and in some cases they appear to be in contrast. The main reason for that could rely in the fact that the experiments that have been carried out were not always fully replicable, possibly due to the experimental set-up, and in the problems related to the response of cell populations. The response of cell populations, in fact, can be not completely uniform and can vary among replicates. Moreover, as resulting from the results obtained, the role of DPh is not as clear as we would hypothesize at the beginning, and the genes included in the analysis could not be the real targets for its specific action. Nevertheless, I try here to summarize the main results obtained using mutant lines. As reported for figure 1.3.9 in the Results section, the DPh knock-down lines were included to analyze their *GSAT, ZEP2, AOX* and *CHLH1* transcript levels in comparison to the WT. In general, the expression profiles of all three DPh knock-down lines were either similar to the WT or showed an over-expression, but no significant down-regulation was observed for the tested genes. These results indicate that DPh is not involved in the tested pathways and that DPh's role as a photoreceptor is not supported (see figure 1.3.9 b). This seems to be confusing, since the DPh protein studies (see Figure 1.3.7 in the Results section) have shown that DPh protein content is reduced in the knock-down lines. An over-expression in the knock-down lines could be explained by a repressor function but not a photoreceptor function. Therefore, this experiment leads to the conclusion that DPh is not the photoreceptor mediating the red light responses of the analyzed genes.

A DPh knock-down line, *dph-2*, was also used in the photoreversibility experiment described in Figure 1.3.11 in which 3 genes (*LHCF2*, *GSAT* and *CHLH1*) were tested with the WT alone and 2 genes (*LHCF2* and *CHLH1*) were tested with the DPh knock-down line. In both genes, transcript levels of *dph-2* were strongly down-regulated in comparison to the WT. The down-regulation of *dph-2* is in contrast with the results obtained for Figure 1.3.9, that DPh is not involved in the regulation of the red light regulated genes, especially the genes of the chlorophyll biosynthetic pathway. The results of this experiment with the knock-down line suggest however an involvement of DPh in the tested genes, although no photoreversibility was observed. However, *dph-2* was not used in the experiment described in Figure 1.3.9b making it difficult to compare the two experiments and the observed trends. Also the light conditions were different between the two discussed experiments above and may have caused the knock-down line to behave differently to the set light conditions than the other knock-down lines used in the experiment described in Figure 1.3.9.

The *dph-2* knock-down line was also used for the blue light experiment as described in Figure 1.3.13, together with knock-down line *dph-5'*. The knock-down lines did not display a uniform reaction in the tested genes: *dph-2* knock-down line showed a similar expression profile in *LHCF2* and *CHLH1* than in the WT. In *GSAT* on the other hand, *dph-2* showed a down-regulated response in comparison to the WT. *dph-5'* reacted in a down-regulated manner in all tested genes, but especially in *CHLH1* and *GSAT*. Setting the variability aside, the reaction in the knock-down lines in general shows a reduction of the expression profile in comparison to the WT, indicating an overlap of blue and red light responses in the same set of genes. However, the role of DPh in this process is not clear yet.

These light experiments, especially with the knock-down lines, have highlighted the need to repeat this type of experiments under more controlled light and culture conditions. But beside the difficult-to-interpret data with the knock-down lines, also the reproducibility of the level of induction in the WT genes in red light shows the need for repetition and additional validation of

the conditions. For example, the red light experiments performed in this thesis have shown that *GSAT* is red light regulated in *P. tricornutum*, however the level of induction is not always the same throughout the experiments (see Results, figure 1.3.8 and 1.3.9). The fact that the induction in red light induction is only weakly reproduced, could be due to, first, the type of material (cell populations) and second, the experimental set-up. This last point could be problematic in reproducing the data if the cells did not always receive the same amount of red light. Therefore, experiments with additional light distribution validation studies could attribute to the reproducibility of the induction in red light.

Also, as a last point, the DPh knock down lines are known to show aggregation phenotypes (see chapter II). Therefore it is also possible that the variability of the gene expression data is due to the aggregation behavior in DPh knock-down lines. In conclusion, the influence of DPh on the aggregation behavious in algal cells may have impacted the reproducibility of gene expression date in this chaper. Despite the variability that was observed in the gene expression data and the inconclusive nature of some of the experiments, the data provided insighths into the differences of phytochrome-regulated gene expression behavior, compared to those observed in terrestrial plants.

Regulation by chloroplast? (Figure 1.3.12)

Light experiments performed in the presence and absence of chloroplast inhibitors as DCMU indicated that some genes (chlorophyll biosynthesis genes *CHLH1*, *HEMA* in both light conditions and alternative oxidase gene *AOX*, only in 20 µE red light) were also repressed by chloroplast inhibition (see Results, figure 1.3.12). DPh RNA levels were not affected by the DCMU treatment. A chloroplast involvement was not really expected at the low light intensities used in the different experiments, but the observation is very interesting as the regulation through the chloroplast adds another piece to the complex puzzle of red light regulation in *P. tricornutum*. It seems that these genes are regulated by the chloroplast and therefore photosynthesis, however it

would not be straightforward to say that DPh is involved in the regulation of these genes through the chloroplast as the regulative role of DPh on the tested genes is not clear yet. The data of the DCMU experiment can even serve to support the lack of response in the DPh knock-down lines in the previous experiments. Because, if these genes are not regulated by a DPh or not exclusively, it is not surprising that the data with the knock-down lines do not show a suppression of the response because of the involvement of other processes (chloroplast, blue or other receptors,...). Additional experiments are necessary to understand this issue and other unclear observation done during these years. My work has highlighted that DPh is subjected to a complex and tight regulation by internal and external signals and I have just started to unveil this complex regulation at the molecular level.

Chapter II

Study of DPh in life strategy regulation in marine diatoms

The role of DPh in life strategy regulation has been studied through the characterization of DPh knock-down lines generated in two different diatom species, P. tricornutum and T. pseudonana. Because a number of DPh knock-down lines were showing an unusual aggregation or colony formation phenotype, the possible link between DPh photoreceptor function and observed grouping behaviour was investigated. This work, described in the next chapter, has provided a possible novel function for DPh in the control of life strategies in marine phytoplankton.

II. Study of DPh in life strategy regulation in marine diatoms

2.1. Introduction

This chapter focusses on the characterization of DPh function in the wild-type and DPh knock-down lines in both *P. tricornutum* and *T. pseudonana*. One of the most exciting results derived from the DPh characterization is the evidence of a role of this photoreceptor in the control of colony formation and cellular aggregation in diatoms. These two processes are quite different at the cellular level and they are likely triggered by multiple environmental stimuli. Although the mechanisms regulating these complex life strategies are still completely unknown, these processes are often correlated with an increased EPS/TEP (Extracellular Polymeric Substances/Transparent Exopolymer Particles) production. Therefore, we have hypothesized that DPh might control cellular aggregation and colony formation in diatoms by regulating EPS/TEP production. In the following paragraph, I will give a short overview on the known factors influencing cellular aggregation and colony formation in the ocean. It is worth noting that the bibliographic information on the topic is rather limited and do not allow to obtain a conclusive idea on the factors controlling life strategy regulation in diatoms and other phytoplankton species.

2.1.1 Why do diatoms aggregate?

When light and nutrient conditions are optimal, phytoplankton cells often produce large-scale blooms. Such blooms are frequently terminated by aggregation and subsequent sedimentation (Alldredge & Gotschalk, 1989). The formation of large, fast sinking aggregates was proposed to be an integral part of the life cycle of many diatom species (Smetacek, 1985) but contributes also significantly to the carbon flux thus being important for the global carbon cycle (Fowler and Knauer, 1986; Kahl, Vardi & Schofield, 2008). Veldhuis *et al.* (2005) provided evidence that the colonial cells of two species of *Phaeocystis* possess higher growth rates than single cells when grown under identical conditions. Thus, the dominance of colonies in blooms of *Phaeocystis*

can therefore be primarily due to their significantly high growth rate allowing a rapid bloom formation.

Although it is well established that diatom aggregation and the mass sinking of blooms is an important aspect of our ocean's ecosystem function, it is still unclear how and why phytoplankton cells decide to shift from a single cell life to a group behavior life. One common hypothesis is the 'multi-purpose strategy', indicating that aggregation or chain formation of algal cells may provide many advantages. One on these advantages is the ability to escape from predators that feed on algae. In this case, the aggregation or colony formation of algal cells induces their sinking to lower levels of the ocean and therefore, the algal cells escape their predators. This hypothesis, called the adaptive anti-herbivore strategy, was proposed by Lampert *et al.* (1994) by studying the green microalgae *Scenedesmus* and *Desmodesmus* and its grazer, the crustacean *Daphnia magnus*. The hypothesis was reinforced with the observation that colony formation was induced in the algae by a chemical cue released by its predator *D. magna* (Hessen and Vandonk 1993, Lampert *et al.* 1994, Lürling 1999). Interestingly, colonies could only be induced in growing cells, meaning that the colony formation is not clogging of individual cells, but the result of a reproductive process. In addition to escape through sinking which implies a well suited life cycle, there is the more direct hypothesis of size-escape, meaning that colonies are larger and cannot be handled by smaller grazers (Riegman *et al.* 1993; Mazzocchi *et al.* 2009). This effect was extensively studied in *Phaeocystis globosa*, where it was suggested that colony formation and colony enlargement are defense mechanisms against small grazers (Tang *et al.*, 2008).

Different studies also highlight a correlation between the occurrence of aggregates and chain formation and nutrient availability. Karp-Boss and Jumars (1998) proposed that chain-formation in diatoms might also be an advantageous mechanism to allow increase nutrient uptake by a rotating in a shear flow. It has also been reported that algae simply use their

aggregation state to float along the water column and thus localize their optimal nutrient layer in the ocean to maintain optimum growth rates (Peperzak, 1993). Another study aimed to provide novel insights into the transcriptional and translational basis for the generation of the cell wall in the centric diatom *T. pseudonana* (Mock *et al.,* 2008), the authors reported that silica starvation induced the formation of cellular aggregation and sinking. The effect of nutrient concentration on colony formation has also been studied by Takabayashi *et al.* (2006), reporting that in the diatom *Skeletonema costatum* the increasing nutrient concentrations of nitrate induced high growth rates and dominance by longer chains in natural populations from enclosure experiments (San Francisco Bay) in comparison to batch cultures in the laboratory. A positive correlation between growth rate and chain length was observed in both natural populations and batch cultures. Earlier observations were made by Smayda and Boleyn (1966) that longer chains assist diatoms to remain in the euphotic zone by decreasing their sedimentation rate, which is achieved by increased surface area to volume ratio. Therefore, the authors Takabayashi *et al.* concluded that longer chains affected sinking rates in *Skeletonema costatum* and thus likely helped the diatom to remain suspended in the upper part of the water column where physical and chemical parameters are more favorable for growth.

Bacteria, on the other hand, may play a crucial role in regulating the algal stickiness by generating bacterial enzymes and extra-cellular products (Smith *et al.*, 1995; Grossart *et al.*, 2006; Alderkamp *et al.*, 2007) showed that heterotrophic bacteria influence the development and aggregation of marine diatoms such as *Thalassiosira rotula* and *Skeletonema costatum.* Also for *Thalassiosira weissflogii,* it was hypothesized that formation rates, size-dependent densities and settling velocities of diatom aggregates differ in dependence of the physiological state and are influenced by presence of specific bacterial strains (Gärdes *et al.*, 2011).

2.1.2 The mechanisms behind aggregation

Diatoms are especially well known for excreting abundant quantities of polysaccharides during all phases of their growth (Williams, 1990). Such extracellular exopolymeric substances, or EPS, range in structure from being loose slimes to tight capsules surrounding the cells. EPS are primarily composed of sulphated polysaccharides and proteoglucans (Hoagland *et al.*, 1993). The production of EPS in the ocean is of ecological relevance because EPS and other carbohydrate-rich exudates can be used as a carbon source by bacteria, meiofauna and macrofauna (Van Duyl *et al.*, 1999; Middelburg *et al.*, 2000). Moreover, EPS can increase the stability of the marine sediments (Paterson *et al.*, 2000; Widdows *et al.*, 2000). For diatoms, the production of EPS allows them to increase their motility and adhesion, both giving them an ecological advantage because they are able to move in response to changing environmental conditions (Underwood and Paterson, 2003).

One type of EPS, the transparent exopolymer particles, called TEP, has received increasing attention because TEP exist as individual particles rather than as cell coatings or dissolved slimes (Alldredge *et al.*, 1993). This form was first identified in diatom cultures and natural seawater by using polysaccharide-specific staining techniques such as alcian blue staining and it was demonstrated that TEP are a major agent of aggregation in the diatom *Chaetoceros gracilis* (Alldredge *et al.*, 1993). Another work from Passow *et al.* (2000) has reported that high concentrations of TEP are usually associated with phytoplankton blooms (especially with blooms dominated by diatoms), even if not every diatom bloom causes high TEP concentrations (Kiorboe *et al.*, 1993; Radic *et al.*, 2005). As elevated levels of TEP result in enhanced aggregation in diatoms (Alldredge *et al.*, 1993; Gärdes *et al.*, 2011) and as aggregated diatoms remain longer viable in comparison to non-aggregated cells, it was also proposed that aggregation seems to increase the ability of diatoms to maintain their protective membrane. The protective membrane surrounds their frustule and effectively reduces or completely inhibits dissolution of the frustule for some time (Passow *et al.*, 2011) and is of importance to avoid bacterial activity compromising

the diatom community. Thus, the role of TEP as a regulating factor of aggregation formation is two-fold: (1) they increase the concentration of particles and, thus, collision frequency, and (2) they increase particle stickiness and, thus, coagulation efficiency (Jackson, 1995). The sticky nature of TEP is linked to the presence of a high fraction of polysaccharides with sulfate ester groups (Zhou *et al.*, 1998), which give them the ability to form cation bridges (Kloareg and Quatrano, 1988) and hydrogen bonds.

Additionally, it was shown that an elevated temperature led to more and longer chains in diatom cells (Takabayashi *et al.*, 2006) and interestingly, a more recent study demonstrated that the involved mechanisms for this enhanced chain formation is the production of TEP (Piontek *et al.*, 2009). Fukao *et al.* (2010) have studied TEP concentration released by four diatoms species (*Coscinodiscus granii, Eucampia zodiacus, Rhizosolenia setigera*, and *Skeletonema* sp.) and their results suggest that the mechanisms of TEP production differ with growth stage and diatom species. Therefore, it is likely that the differences in TEP production among the diatom species influence the complexity of TEP dynamics in aquatic environments. However, not only diatoms produce TEP when reaching the stationary phase and blooming. Also *Emiliania huxleyi,* the most prominent coccolithophore, has been studied for the secretion of TEP before and during the bloom. De La Rocha & Passow (2007) reported that TEP production during coccolithophorid blooms may control aggregate formation and enhance organic matter export. It was also observed that TEP sticking properties increase toward high salinities in estuaries, enhancing the aggregation/sedimentation process and affecting the vertical export in these environments (Mari *et al.*, 2012).

In the laboratory, the release of extracellular polysaccharides is often associated with senescent cultures and nutrient limitations (Drapeau *et al.*, 1994). An interesting study of Stanley and Callow (2007) demonstrated that diatom cells, cultured on different substrates, can alter their surface properties and subsequently their stickiness according to their physiological state.

The study showed that the oval cell morphotype of *P. tricornutum* is highly enriched (85-90%) if the cells are allowed to adhere to a glass surface of a flask. The authors hypothesize that altered EPS/TEP concentrations are at the basis of this morphological change, on the basis of earlier work done by Abdullahi *et al.* (2006) reporting that significant differences in the proportions of various saccharides may influence EPS/TEP adhesive properties. The work of Stanley & Callow has also been used as a reference during this PhD to enrich a wild-type culture with aggregated cells (see Results, paragraph 2.3.4).

2.2 Materials and methods

2.2.1 Media and care of diatom cultures

Axenic *P. tricornutum* cells were grown in 95% f/2 media (Guillard *et al.*, 1975) and *T. pseudonana* cells in NEPC media (Kröger *et al.*, 2000). Cells were diluted every 2-3 days to keep cells in the exponential growth phase. Contamination tests (with peptone 1 g/L) were carried out with every new dilution to check for the presence of bacteria in diatom cultures.

2.2.2 Hemocytometer/Malassez slide

Cell concentration was calculated by counting the cells from a 100 µL aliquot of culture pipetted onto a Malassez slide. The slide is engraved with a pair of precise grids of known dimensions. Together with the cover slip 0,1 mm above the surface of the grid, each square has a precise volume. Cells were counted only in rows with secondary gridlines. The number of cells counted in 10 rows, multiplied by 10^3, corresponds to the number of cells per ml. Cells were diluted in f/2 media for counting, in case of highly concentrated cultures (1:2 or 1:10 dilution). The aliquot's dilution factor, if any, was taken in account to calculate the cell concentration of the culture. Chain number and the length of each chain were also counted by this method. Cells were normally counted in duplicate. The average of two independent measurements is used for the analysis of the data described below. If the two counts resulted in numbers at varied drastically, the counting was repeated a third time.

2.2.3 P. tricornutum growth and colony distribution under continuous light and L:D 12h:12h regimes

To perform the growth analysis, *P. tricornutum* WT and different DPh knock-down lines (*dph-2*, *dph-1'*, *dph-3'*, and *dph-4'*) were kept in exponential phase of growth by consistent dilution and pre-adapted for three days to two different light regimes: constant light (LL) and a 12h:12h light:dark cycle (LD). Because of the rectangular shape of the flasks and placement of the

lamps in both incubators, light intensity was not entirely homogeneous, but each culture was positioned to receive a gradient from 38 – 42 µE of white light. At the beginning of the experiment, each culture was diluted into volumes of 150 mL f/2 without silica at a starting concentration of $1.5x10^5$ cells/mL. They were then returned to their respective pre-adapted light conditions to grow for a week. Cell concentration and colony size and frequency were measured by daily observations of two independent, undiluted, 50 µL aliquots of culture on a single Malassez slide.

2.2.4 Quantification of transparent exopolymer particles (TEP)

TEP concentrations in diatom cultures were measured by a spectrophotometric method (Passow and Alldredge 1995). Three aliquots of 20 mL per culture strain were filtered onto polycarbonate filters, stained with alcian blue (0,02% alcian blue, 0,06% acetic acid) and then resuspended for two hours in 4 mL of 80% sulfuric acid. A 1 mL aliquot of each resuspension was pipetted into a cuvette and its optical density (OD) at 787 nm was read by spectrophotometer. OD values were converted into µg of TEP, by using the OD values of the xanthan gum standards as reference. The xanthan gum standard of 0, 50, 100, 200, 400 and 600 µg of xanthan gum was prepared in 100% EtOH, with a 1 mg/ml of xanthan gum stock solution. To all standards, 2 ml of alcian blue solution was added. Subsequently, standards were centrifuged for 30 minutes at 3200 x g. Supernatant with excess of alcian blue dye was removed and standards were dried overnight at 30°C. TEP values were then normalized both by cell concentration and protein concentration to obtain relative TEP values.

2.2.5 Protein extraction and Western Blot

See material and methods as described in Chapter I.

2.2.6 Calculations

Growth curves were generated to obtain information about the diatom division rate, by reporting the cell concentration of each strain (WT and DPh knock-down lines) for each day the experiment was conducted. Most of our experiments have been performed when the cells were in exponential or logarithmic phase, the period characterized by cells doubling. The diatom growth curve is plotted as L = log (numbers of cells per ml), versus time.

The growth rate of cultures was calculated over three days, when cultures were clearly in exponential phase. Growth rate is defined as the difference between cell concentrations of the first and the third day, divided by the time elapsed. Therefore Growth rate G = (log (number of cells/mL on Day 3) – log (number of cells/mL on Day 1))/2.

Chains counted in a culture in one day were first grouped into three size classes according to chain length: 3-5 cells long, 6-10 cells long, and >10 cells long. Colonies of two cells were put in the single-cell size class under the assumption that they were simply sister cells that had not had the chance to separate after a recent cell division. The number of individual cells in each of these size classes was calculated by multiplying the number counted of a given chain-length by that chain length. For example, the total number of cells in small chains is calculated as: Sm = [(number chains 3 cells long)*3 + (number chains 4 cells long)*4 + (number chains 5 cells long)*5].

Relative growth rate was generated to see how DPh knock-down lines grew compared to the WT. Relative growth rate of each mutant in a given light treatment was calculated by dividing total mutant growth rate by total WT growth rate of the corresponding light treatment. Relative growth is shown as Rel. G = G(mutant in LL or LD)/G(Pt1 in LL or LD), expressed as a percentage.

Chain distribution shows the composition of a culture by presenting the percent frequency of each chain size class in a culture. In this way we can see if a culture is made up almost entirely of single cells, or contains only certain types of chains. To determine chain distribution, the number of individual cells in each size class (calculated above) was divided by the

total number of cells counted to calculate the percentage of cells in a given size class. For a given size class, relative frequency = number of cells in size class/total cells in culture. The frequency of single and double cells was not shown, but adding this value would bring the sum of all size class percentages up to 100%, since this frequency is simply the remaining, non-chain cells in the population.

2.2.7 Generation and growth of Tp DPh know down lines

The DPh antisense expression vectors for *T. pseudonana* were constructed using vectors pTp-fcp and pTp-NR (Poulsen *et al.*, 2006) as parent vectors. Vector pTp-fcp provided a constitutive expression cassette, whereas vector pTp-NR provided an inducible cassette with the nitrate reductase promoter which is switched on in the presence of nitrate, but switched off in the absence of nitrate and presence of ammonium. The parent vector pTp-fcp also contained the *nat1* gene from *Steptomyces noursei* which conveys resistance to the antibiotic nourseothricin, whereas the parent vector pTp-NR contains the *GFP* gene.

For the construction of the constitutive DPh antisense vector, a *Not*I site between the *nat1* gene and the pTp-fcp terminator was exploited for the insertion of the antisense DPh fragment. A 389bp fragment of the *DPh* gene was amplified from extracted genomic *T. pseudonana* DNA using primers *ASPHYF1* 5' ataagaatGCGGCCGC**AAGCTT**CGTGCCTCTGGGGAGAAGGAACTAG 3' introducing the restriction sites *Not*I (underlined) and *Hind*III (underlined, bold) and *ASPHYR2* 5' ataagaatGCGGCCGC**GATATC**GAAATGAGATTCACCTGCAAAGCAC 3', introducing the restriction sites *Not*I (underlined) and *Eco*RV (underlined, bold). The resulting PCR product was purified (Qiaquick purification kit, Qiagen), the fragment and the parent vector digested with *Not*I and the vector was dephosphorylated (rAPId alkaline phosphatase, Roche) before being purified by gel extraction (Qiaquick purification kit, Qiagen). Ligations were carried out overnight at 16°C using T4 DNA

ligase (Promega), and the resulting vectors were transformed into *E. coli*. The *E. coli* colonies that grew on selective ampicillin plates were screened by PCR using primers *ASPHYF1* and *ASPHYR2* to confirm the presence of the fragment, then the orientation of the insert in the vectors was determined by performing miniprep plasmid purification on overnight cultures of putative transgenic *E. coli* clones. Then restriction digestion reactions were performed with *Eco*RV (present in the *ASPHYR2* primer) and *Bgl*II present 109 bp into the FCP terminator. If the fragment was in the antisense orientation, this double digestion would result in the excision of a 501 bp fragment from the vector, whereas if the fragment was in the sense orientation, a fragment of only 116 bp would be excised.

For the construction of the inducible DPh antisense vector, the *GFP* gene was removed from the parent vector pTp-NR-GFP using restriction enzymes *Not*I and *Eco*RV, as restriction sites for these enzymes flanked the gene (the *Not*I site being between the promoter and *GFP* and the *Eco*RV site being between *GFP* and the terminator). The PCR product from the primer pair reported above was this time digested with *Eco*RV, then *Not*I was added to the digestion reaction for a further 3 hours before purification of the fragment. This resulted in the fragment being cut with *Eco*RV in the forward primer (*ASPHYF1*) site and *Not*I in the reverse primer site. Ligations were carried out as described above and the orientation of the fragment was confirmed by digesting resulting vectors with *Not*I (in the reverse primer) and *Bam*HI (with a site 536 bp into the terminator) resulting in excision of a 928 bp fragment, whereas if the fragment had been in the sense direction the a 543 bp fragment would have been excised. However, as expected resulting vectors were shown to contain the fragment in the antisense direction since for the inducible vector the cloning was directional (using a different restriction site at either end of the insert). The vectors were transformed into *T. pseudonana* WT using microparticle bombardment (Biorad Biolistics system) according to the procedure described by Poulsen *et al.*(2006). The inducible vector (pTp-NR DPh) was cotransformed with the original vector (pTp-fcp) in order to convey

resistance to nourseothricin. Selection of transformants was performed on 50% NEPC plates containing 100 ug/ml nourseothricin.See annex 3 for the plasmid map.

For the DPh reversibility experiments with the Tp-NR DPh line, NEPC medium was used either with $NaNO_3$ (47 mg/L) or NH_4Cl (29,4 mg/L) at a pH of 8.1 with a starting cell concentration of $5x10^5$ cells/ml. Because cells were originally growing in NEPC with nitrate, cells were spun down and washed with NH_4^+ NEPC media before changing the NO_3^- media to NH_4^+ media in the culture. Subsequently, when two separate cultures were obtained with either cells in NO_3^- or NH_4^+, the cultures were grown for three days before taking 50 ml of cultures from both conditions to analyze DPh protein content by Western Blot.

2.2.8 Construction of the pH4:PtHO silencing vector

A silencing vector was generated against the diatom homologue of the *A. thaliana* heme *oxygenase 1* (*HO-2*, Phatr2 ID number 55416). A 148 bp amplicon of the 3'UTR region of the *HO-2* gene (from 760 bps to 907 bps in the gene) was amplified with the forward oligo *HO2Fw* including an *Eco*RI restriction site (5'CCGGAATTCACCACGTGAACCCTATACCCCGA 3') and the reverse oligo *HO2Rv* including a *Xba*I restriction site (5' CTAGTCTAGAAAACGGGGCCAGCTCTTCGC 3'). The PCR product was digested with *Eco*RI and *Xba*I and was introduced in antisense direction into the *Eco*RI - *Xba*I linearized PtGAF antisense vector, with the H4 promotor sequence and the *sh ble* gene for antibiotic resistance to phleomycine. See annex 3 for the plasmid map.

Subsequently, H4-HO-2 antisense silencing vectors were introduced into a *P. tricornutum* WT strain Pt1 by microparticle bombardment. Putative silenced clones were first selected on 1% agar plates (50% f/2 – silica medium) containing 50 µg/mL phleomycin (Invitrogen). The presence of silencing constructs was verified by checking the integration of the *Sh ble* gene with the primers *Sh ble1fw* and *Sh ble1rv* (see chapter I, materials and methods). The obtained knock-down lines

were kept in the same media and antibiotic selection as the PtGAF and PtDPh3' knock-down lines. Also for these lines, aliquots were stored in at -80°C in a 10% DMSO solution.

2.2.9 Silica starvation experiments in T. pseudonana

During the silica starvation experiments, *T. pseudonana* was grown in 95% f/2 media with 2 x f/2 nutrients to ensure that the cells were grown in sufficient nutrients. For the depletion/ repletion experiments, the cells were first grown in media containing silica 100 µM and then resuspended after centrifugation either in a media containing silica or without silica according to the treatment. In both media with and without silica, pH was measured and brought to 8.1. The silica-replete culture (named here Si+(2)) was grown in f/2 -Si for two days in continuous light (40 µE), and then silica was added to the culture at the end of the second day. Each culture (120 mL) had a starting concentration of $5x10^5$ cells/mL and were grown under constant white light at 35 µE. The experiment was conducted over three days. Cell concentration was measured over the three days with a single 100 µL aliquot of undiluted culture on Malassez slides. For cultures growing in silica-starved and silica-restored conditions, where cells were aggregated and too clumped to count individually, a 1 mL aliquot was prepared with 200 µL EDTA 0.5M and 800 µL culture. EDTA disassociates polysaccharides and as a consequence aggregates, so that single cells could be counted by Malassez slide (Zatz, 1984). TEP analysis, cell count in triplicate, and protein extraction for normalization and a Western blot were performed on the third day.

2.2.10 Aggregate enrichment experiments in P. tricornutum

The method used for enriching the Pt1 WT culture with aggregated/oval cells was found in the literature (Stanley and Callow, 2007). To obtain cultures predominantly oval in morphology forming aggregates, the *P. tricornutum* WT cultures were grown under the same growth and light conditions, in both plastic flasks and Pyrex conical glass bottles containing 100 ml media. After 3–5 days, the bases of the flasks were examined for the presence of oval cells. If present, the culture

medium was removed, the flasks were 2-3 times rinsed with f/2 medium to remove any remaining fusiform cells, and then 100 ml of fresh medium were added to each flask/bottle. Every 2 days the washing process was repeated until the cultures contained only aggregates of oval cells. After 2 weeks of repeating this process, the treated culture contained 100% oval cells in aggregations, attached to the bottom of the glass bottle. Cells were harvested by shaking the culture with glass bead for 10 minutes, followed by centrifugation and subsequent freezing of the cell pellets in liquid nitrogen. The cells in the control culture remained 100% fusiform and were harvested in the same way. Cell pellets of the untreated and treated cultures were used for Western Blot analysis to investigate DPh protein.

2.3 Results

2.3.1. DPh knock-down lines show aggregation/chain phenotype in *P. tricornutum*

A most intriguing observation during this Ph.D. project was the fact that some of the *P. tricornutum* DPh knock-down lines were displaying a chain or aggregation phenotype (see figure 2.3.1 next page). As chain or aggregation phenotypes are not commonly observed in *P. tricornutum,* only in very old cell cultures, the observation of these phenotypes in the DPh knock-down lines has drawn our immediate attention. First, this has been observed in the DPh knock-down lines targeted in the GAF domain, where three lines showed three very strong but slightly different phenotypes: *dph-1* showed a strong chain phenotype with almost unrecognizable individual cells and considerable smaller cells as they were very tightly merged with their neighboring cells; *dph-2* equally had a phenotype with long chains but was identified as a weaker phenotype as individual cells were still identifiable and kept their fusiform shape; *dph-3* on the other hand, formed bigger aggregates of oval cells. However, also in this line, the cells seemed to form long chains of oval cells closely attached to each other. Moreover, the interesting chain phenotype has been observed again in the DPh knock-down lines targeting the 3' UTR region of the *DPh* gene. Four of these DPh3' knock-down lines (named *dph-1'* till *dph-4'*) clearly showed a DPh down-regulation and a chain phenotype, although the chain phenotype was determined to be weaker than observed before for the clone *dph-2*. These new clones showed shorter and less abundant chains. Also another DPh3' knock-down line (*dph-5'*) was obtained with a clear DPh protein reduction, but not showing an aggregation or chain phenotype. On the contrary, cells were behaving similar to the WT and sometimes even showing fusiform cells attached to each other at the tips of their arms (in the lab called a star-phenotype). Pictures of the different phenotypes are shown in figure 2.3.1 panel B, with the levels of DPh silencing analyzed by Western Blot in panel A. Since it was the first time that such phenotypes were observed in diatom

gene silencing lines, it was proposed that DPh might be involved in the regulation of grouping behavior in marine diatoms.

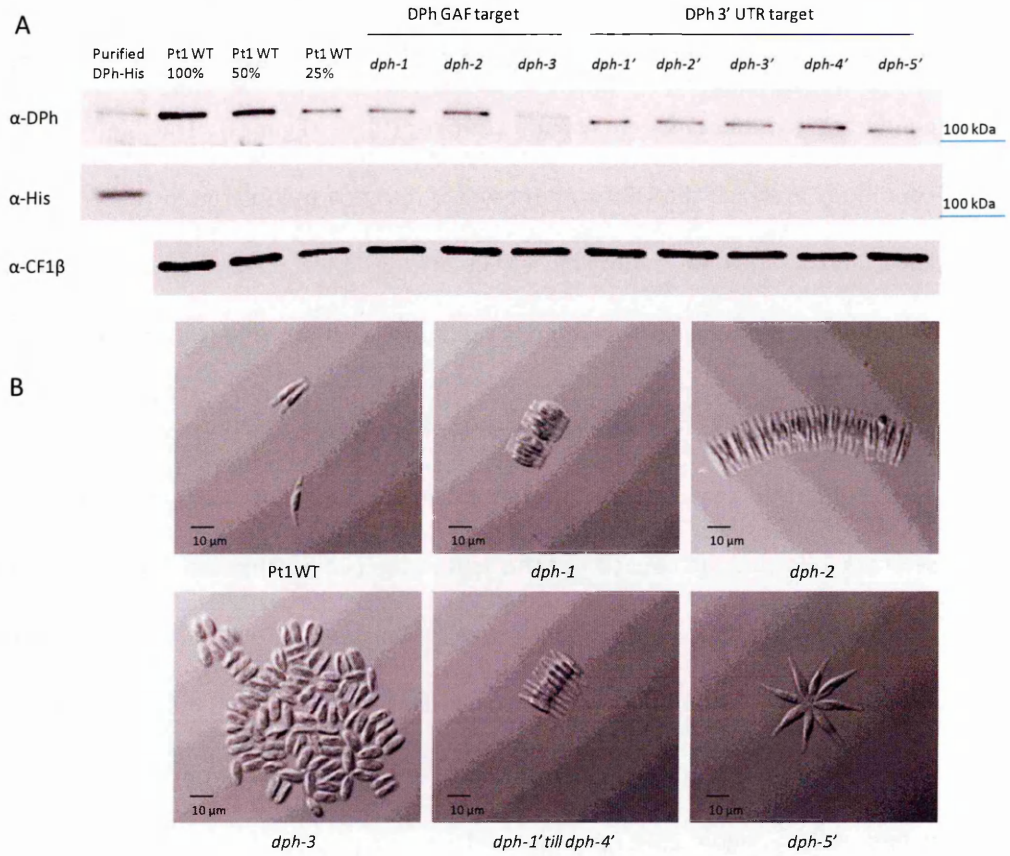

Figure 2.3.1 (Panel A): Western Blot analysis of DPh transgenic knock-down lines in *P. tricornutum* WT Pt1. The level of DPh was tested with the α-DPh antibody. As positive control for DPh protein size, the purified PtDPh with histidine-tag was loaded on the same membrane and revealed with the α-DPh and α-His antibodies. The antibody α-CF1β was used as loading control. Transgenic lines targeted in the *DPh* GAF domain are *dph-1*, *dph-2* and *dph-3*. Also transgenic lines targeted in the 3'UTR region of *DPh* were obtained: *dph-1'* till *dph-4'* on figure above. (Panel B): Phenotypes observed in WT cells of *P. tricornutum* (single cells) and the DPh knock-down transgenic lines with a light microscope (Olympus).

2.3.2. Modulation of DPh content in the RNAi lines and under different light conditions and analysis of the effect on chain formation.

The discovery of the chain forming phenotype in the DPh knock-down lines seemed particularly interesting. For this reason, we wanted to provide more evidence on the regulatory role of DPh in chain formation. This was done by quantitatively characterizing growth rates,

colony size and frequency in *P. tricornutum* WT and DPh knock-down lines, by My-Hai Ha (master 1 student) in the laboratory. Because the analysis of DPh indicated that the protein is partially degraded in cells grown under continuous light conditions (see chapter I, Results, figure 1.3.17), the analysis was performed on two sets of cultures grown in parallel under different light conditions (continuous light or 12h:12h light:dark regimes). The aim was to have different conditions in which the DPh content was differently modulated in the WT and also in the RNAi lines, and to look for a possible effect on the chain phenotype. In parallel with the growth experiments, I have also determined TEP concentrations under different conditions, to assess a possible role of TEP in the chain formation in the DPh knock-down lines.

For this analysis, only the knock-down lines that had a less drastic phenotype were selected, allowing the counting of the cells in the chains (the clone *dph-2* for the DPh-GAF knock-down lines and the clones *dph-1'*, *dph-3'* and *dph-4'* for the DPh3' knock-down lines). The experiment was carried out twice and the results confirmed a similar trend. However, because of the noisiness in the first experiment's data, only the results of the second experiment are shown in figures 2.3.2, figure 2.3.3, and table 2.1.

Analysis of the growth rate indicated that all strains grew faster in LL than in LD. All knock-down strains had a relative growth rate slightly lower than WT in both LD and LL conditions, but in LL the difference between knock-down lines and WT growth rates was not as large. *dph-2,* the strain making the longest chains between those analyzed, showed the slowest growth rate in both LD (46% relative to the WT) and LL (61% relative to the WT), as shown in table 2.1 and figure 2.3.2 A and B. Chain distribution in each culture over the duration of the experiment was plotted in figure 2.3.2 panel C to see how prevalent chains of different sizes were in a culture. This histogram shows analysis only from Day 2 to Day 3, because cultures appeared to enter stationary phase on Day 4, especially in LL (figure 2.3.2 B). The WT was almost entirely chain-free for all three days, and the few chains present were in the small size class in cells grown in LD.

Interestingly, when grown in LL, also the WT started to reveal small chains, that were never observed previously in cells grown in LD cycle (Day 3, WT LL: 6,49%; WT LD: 1,25%). All the knock-down lines formed chains in LD. Remarkably a clear increase in both the percentage of cells in chains and also the length of the chains was observed under LL conditions. *dph-2* displayed the strongest chain-producing phenotype, with 68,24% of cells in chains on Day 3 in LD, and 83,82% in LL. Unlike the WT, *dph-2* in LL had a higher percentage of larger chains. The DPh3' knock-down lines all showed a moderate chain phenotype in LD, forming only small and medium chains. In LL, DPh3' knock-down lines formed large chains, and formed more chains overall than in LD.

In order to test if there was a correlation between the chain variations and the content of DPh proteins, 50 ml of culture was taken on Day 2 from each culture for protein extraction and Western Blot analysis. As shown in figure 2.3.3, the DPh knock-down lines always have a lower content of DPh compared to the WT. Interestingly, all cultures grown in LL, including the WT, showed stronger DPh reduction compared to LD. These data provide a clear correlation between the reduction of DPh and the appearance of colony phenotype in WT, and in the increase of both chain prevalence and chain length in the DPh knock-down lines compared to the WT when in LL. One thing to note is that even if the *dph-2* showed the strongest chain-forming phenotype, the level of protein reduction is still comparable between all the DPh knock-down lines. This suggests that there is only a partial correlation between DPh protein content and strength of the phenotype.

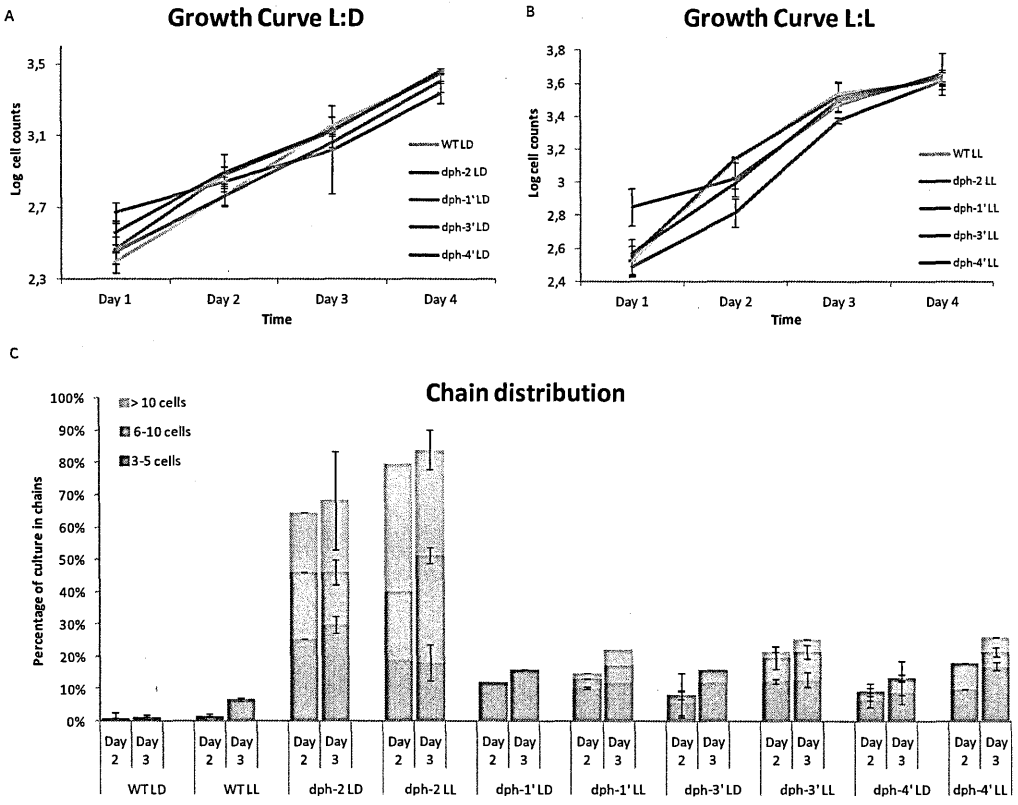

Figure 2.3.2: Growth of *P. tricornutum* WT and DPh knock-down lines (*dph-2, dph-1', dph-3'* and *dph-4'*). Growth curves of cultures grown in (A) 12h:12h light:dark cycle (LD) and (B) continuous light (LL) over four days, calculated from cell counts of two independent half-aliquots on Malassez slide. (C) Chain distribution. The percentage of each chain size class was the number of cells in that size class divided by the total number of cells. Single cells are not shown but make up the remaining percentage. Error bars are standard deviation.

	Day 1-Day 3
Strain	Growth Rate Relative to WT
WT LD	100%
WT LL	100%
dph-2 LD	46%
dph-2 LL	61%
dph-1' LD	81%
dph-1' LL	87%
dph-3' LD	87%
dph-3' LL	95%
dph-4' LD	75%
dph-4' LL	91%

Table 2.1: Daily growth rate from Day 1 to Day 3 for *P. tricornutum* WT and DPh knock-down lines (*dph-2, dph-1', dph-3'* and *dph-4'*) grown in 12h:12h light dark cycle (LD) and continuous light (LL).

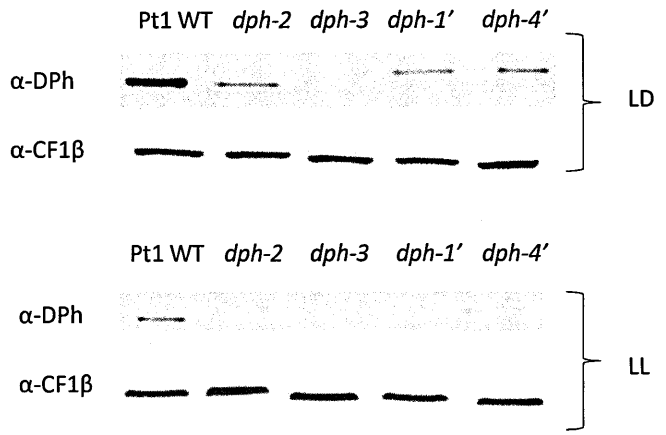

Figure 2.3.3: Western Blot showing DPh expression in *P. tricornutum* WT and DPh knock-down lines (*dph-2, dph-1', dph-3'* and *dph-4'*) grown in 12h:12h light dark cycle (DL) and continuous light (LL). The α-DPh antibody has been used to visualize the DPh protein and the anti-CF1β for the loading control CF1β protein.

A major limitation of the analyses described above was the method by which cells were counted, that was too time-consuming to count all cultures tested in multiple replicates. Despite this statistical weakness, trends in cell growth and colony formation are clear. The recent acquisition by the laboratory of a video camera mounted on the microscope will allow for many pictures of cultures to be taken in a short amount of time to be analyzed on the computer through programs like ImageJ. This will solve both problems of the lack of replicates and different measuring times, and allow for statistical analysis and modeling of the growth and chain-formation.

TEP Analysis of P. tricornutum WT *and DPh knock-down lines*

Previous analyses reported in the literature suggested that TEP played a role in aggregation and colony formation, so this experiment tested whether an increase in the TEP levels was observed in the DPh knock-down lines compared to the WT, and if this corresponded with the intensity of their chain-forming phenotype. To this aim, WT, *dph-2, dph-1', dph-3'*, and *dph-4'* cultures were kept in exponential phase by consistent dilution. TEP levels in each strain were

normalized by cell concentration (figure 2.3.4 panel A) and protein concentration (figure 2.3.4 panel B). Relative TEP normalized for cells was higher in the DPh knock-down lines than the WT, but not in a way that corresponds linearly with levels of chain-formation and level of DPh silencing in the knock-down lines. Despite a lower relative TEP level, *dph-2* displayed a stronger chain-forming phenotype than the DPh3' knock-down lines (figure 2.3.1 panel C). The DPh3' knock-down lines showed variable levels of TEP between themselves, despite the fact that their chain-forming phenotypes were quite comparable.

TEP normalized by protein showed slightly different trends. While *dph-2* and *dph-1'* still displayed higher relative TEP concentrations than the WT, *dph-3'* and *dph-4'* did not. There are possible reasons for the discrepancy between normalization methods. Cells for protein extraction were collected by centrifugation, where a portion of cells is likely left behind in the last drops of supernatant. Moreover, because TEP contains proteins as well as polysaccharides, TEP may have been included in the protein extraction, leading to a misleading effect in the normalization. Counting cells by Malassez slide also presented some problems, since replicate counts for statistical strength were not possible. Another limitation is that living and dead cells are not distinguishable on a Malassez slide. TEP itself was collected by filtration, where loss of material remaining in the tube was less likely. All of these difference methodological factors may have served in generating noise in this data.

Western blot analysis was performed to see if DPh silencing correlated with TEP levels (figure 2.3.5). All DPh knock-down lines are partially silenced for DPh compared to WT. *dph-3'* appeared somewhat less silenced, but there was not a clear link between its level of silencing and TEP levels. It is also worth noting that the relative level of silencing detected by Western Blot in the knock-down lines is also quite variable compared. All together, these results indicate that there is only a moderate increase of TEP in the knock-down lines making chains.

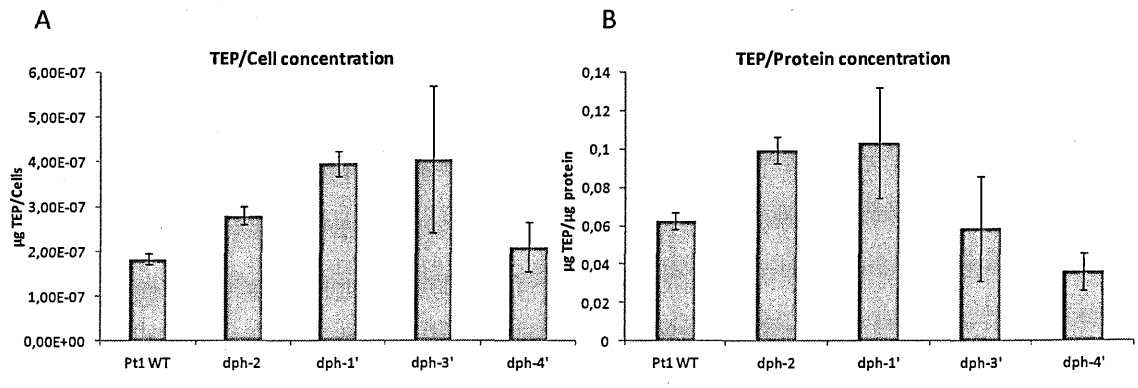

Figure 2.3.4: TEP analysis of *P. tricornutum* WT and DPh knock-down lines (*dph-2, dph-1', dph-3'* and *dph-4'*) normalized for (A) cell concentration and (B) protein. Error bars represent standard deviation.

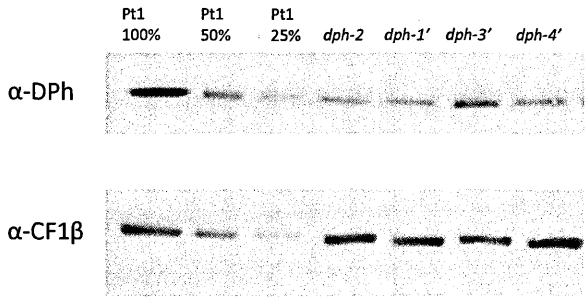

Figure 2.3.5. Western blot of DPh expression in *P. tricornutum* WT and DPh knock-down lines (*dph-2, dph-1', dph-3'* and *dph-4'*). Progressive dilutions of Pt1 WT protein (50 µg correspond to Pt 100%) and 50 µg of proteins from all DPh knock-down lines. The anti-DPh antibody has been used to visualize the DPh protein and the anti-CF1β for the loading control CF1β protein.

2.3.3. Generation and phenotypic characterization of DPh knock-down lines in *T. pseudonana*

Recently, the laboratory has succeeded to set up the RNAi strategy in the ecologically relevant species *T. pseudonana*, in collaboration with the laboratory of Dr. Thomas Mock in Norwich. In particular, the DPh knock-down lines were generated by Dr. Amy Kirkham and I performed the characterization of the obtained knock-down lines. An inducible RNAi system was generated with an inducible RNAi vector under the control of the Nitrate Reductase (NR) promoter. This promoter allows to switch on and back off the silencing, respectively by growing the cells in NO_3 (RNAi ON) or NH_4^+ (RNAi OFF). The silencing mediated by the RNAi is completely

reversible (Kirkham, Mock and Falciatore, in preparation). Also, two independent knock-down lines harboring an antisense DPh vector under the FcpB promoter were obtained. A antibody against the DPh protein from *T. pseudonana* was generated to investigate endogenous DPh levels in the DPh silenced clones. The knock-down line *nr-dph*, as well as the two knock-down lines *fcpb-dph 1* and *2* showed a clear reduction in DPh protein content (see figure 2.3.6 panel A).

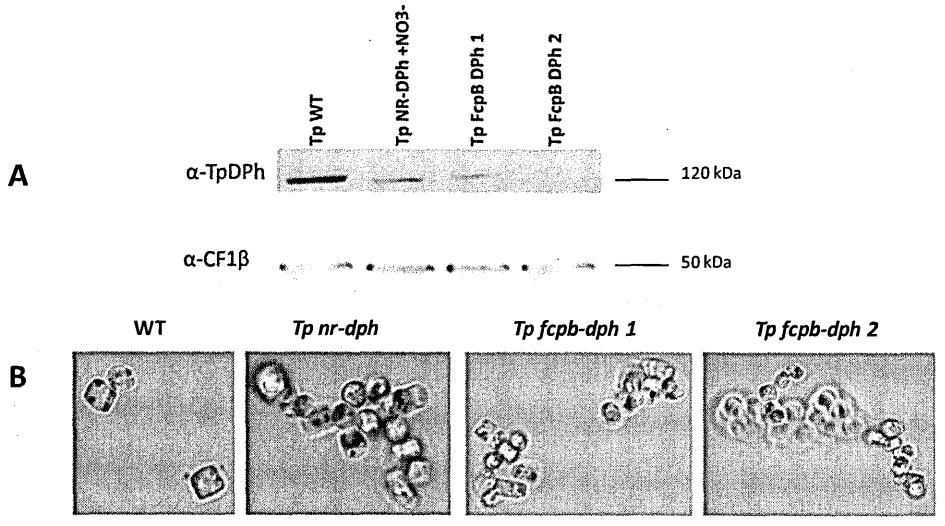

Figure 2.3.6 (Panel A): Western blot analysis of *T. pseudonana* WT, inducible DPh knock-down line (*nr-dph* with the silencing on, in NEPC media with NO_3^-) and two DPh knock-down lines under the FcpB promoter (f*cpb-dph 1* and *2*). TpDPh was detected with the α-TpDPh antibody. The α-CF1β antibody was used as loading control. (Panel B): Phenotypes of the *T. pseudonana* WT, *nr-dph* and the *fcpb-dph 1* and *2*.

Interestingly, the *nr-dph* clone showed an aggregation phenotype when the silencing of DPh was switched on, thus in NO_3^- conditions. It was also possible to switch off the silencing and to revert back its phenotype from aggregation to single cells in media containing NH_4^+. By switching between those two nutrient conditions, the protein levels of the DPh were either reduced (with the aggregation phenotype in NO_3^-) or normal (with the single cells in NH_4^+) (see figure 2.3.7). Moreover, also two independent clones *fcpb-dph 1* and *2* were forming aggregated cells. This observed aggregation phenotype in the DPh knock-down lines from *T. pseudonana* is

different from the phenotypes observed in the DPh knock-down lines from *P. tricornutum*, that are forming chains and/or making aggregates. All the DPh knock-down lines in *P. tricornutum* and *T. pseudonana* with a phenotype share a common ground: cells remain very closely together instead of being dispersed.

Unfortunately, recent analysis has revealed that all the DPh knock-down lines in *T. pseudonana* showing an aggregation phenotype have lost the aggregation phenotype, although DPh still seemed to be silenced. Interestingly, the loss of the phenotype was also observed in the most silenced PtDPh knock-down lines that was making big aggregates of oval cells (see clone *dph-3* in figure 2.3.1). It might be that the cells could overcome the aggregation phenotype, for still unknown reasons. However, these results in *T. pseudonana* have been a major breakthrough in this study. These experiments have shown that DPh might play a role in the life strategy regulation in two diatom species. Additionally, they have also shown that the aggregation phenotype is reversible when levels of DPh are altered, strongly supporting the key regulatory role of DPh in these processes.

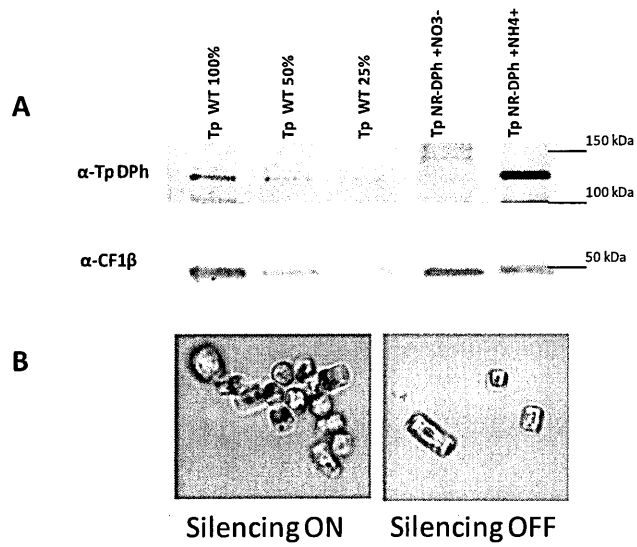

Figure 2.3.7 (Panel A): Western Blot analysis of the *T. pseudonana* WT and the inducible DPh knock-down line (*tp nr-dph*) in both $NO3^-$ (DPh silencing ON) and $NH4^+$ (DPh silencing OFF) conditions. (Panel B): The reversibility of DPh induced the gain/loss of the aggregation phenotype.

2.3.4. Specific environmental conditions leading to DPh down-regulation and aggregation phenotypes

It is well known that diatom aggregates can be observed in the marine environment and that this life strategy is often linked to different stress factors. Therefore, several conditions that could lead to cellular aggregation have been tested in both *T. pseudonana* and *P. tricornutum*, in order to test the levels of DPh in those conditions and to further establish a link between DPh deregulation and cellular chain/aggregation formation in diatoms.

Silica starvation experiments in T. pseudonana

Silica depletion had been previously observed to induce cellular aggregation in *T. pseudonana* (Mock *et al.*, 2008). This process can occur in the natural environment at the end of a bloom. Therefore, I have tried to mimic a bloom termination process by growing *T. pseudonana* WT in silica depleted conditions, to see if silica starvation-induced aggregation correlated with a rise in transparent exopolymer particle (TEP) levels, and a modulation of DPh content when cells were aggregated. Also the effect of restoring silica to a previously silica-starved culture was also tested. During this experiment, the concentration of the cells and the percentage of aggregated cells were calculated, TEP concentration were quantified and DPh protein expression levels were analyzed by Western Blot.

Figure 2.3.8 panel A shows the concentration of cells over the duration of the experiment. Cells in silica-replete conditions doubled in concentration after one day of growth, but became less concentrated on the third day. Silica-starved cells became progressively less concentrated; these cells were seen stuck to the bottom and sides of the flask due to the large amount of polysaccharides being produced. It might be that, in this case, cell counts showed an underestimation of the total cell concentration. The restored silica culture decreased in concentration between the first and second day comparable with those starved for silica, but starting growing exponentially between the second and third day after silica repletion, indicating

that cells were able to grow when nutrient conditions became favorable again, although they were clearly stressed as unusual cell shapes were observed.

TEP concentrations were quantified to determine the possible correlation between aggregation and TEP production. TEP normalized for cell (figure 2.3.8 panel C) and protein concentration (figure 2.3.8 panel D) both show that in the disaggregated, replete condition, relative TEP concentrations are low; in the aggregated, silica-starved condition, relative TEP concentration are high; in the silica-restored condition relative TEP concentrations are at an intermediate level between the two controls, demonstrating that cell aggregation and TEP concentration are strongly correlated. The difference in these two normalizing methods is the scale at which TEP concentrations change between treatments. TEP levels in the restored silica condition appears to be closer to silica-starved TEP levels when normalized for cell concentration, while it drops down almost completely to original replete TEP levels when normalized for protein concentration. Remarkably, this latter trend is supported by the Western blot, where silica-starved cells show a reduced DPh content but silica-restored cells show DPh bands comparable to repleted conditions (figure 2.3.8 panel B). This suggests that diatoms are able to sense changes in nutrient conditions, and are able to disaggregate when conditions become favorable. DPh may work as a regulator in this behavior because DPh expression was linked to silica levels and aggregation, despite the fact that the variable at play here is not light but nutrients.

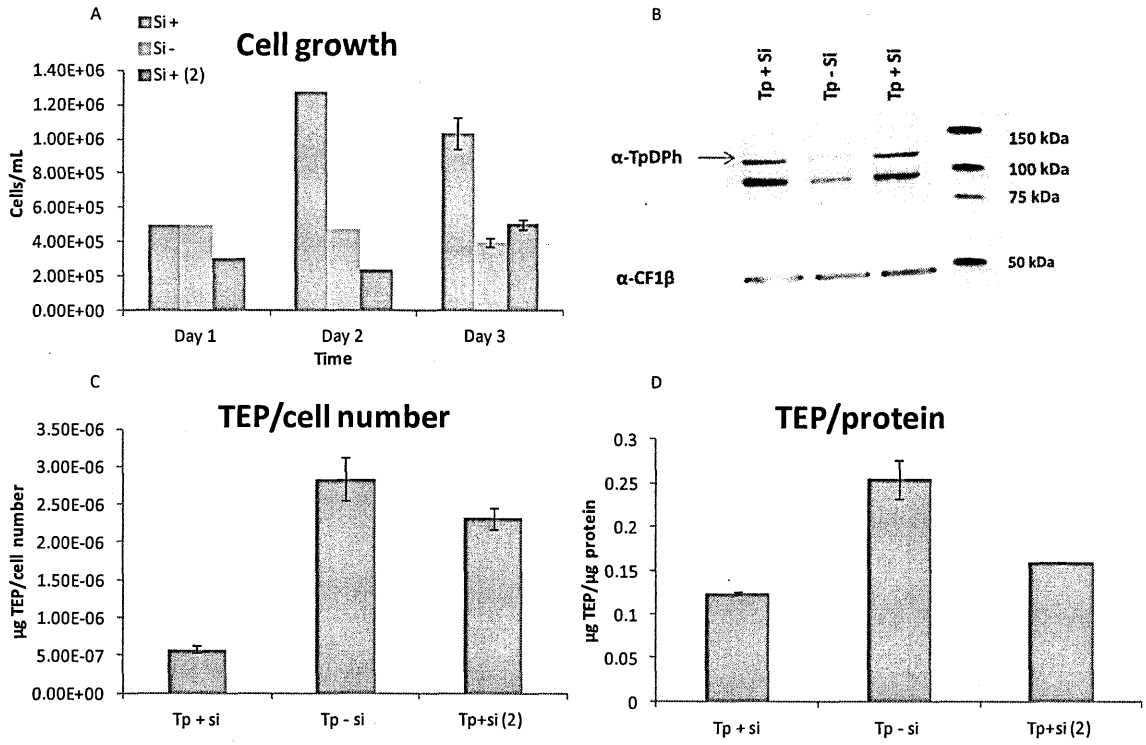

Figure 2.3.8: *T. pseudonana* in silica-replete conditions (+Si), after two days of silica starvations (-Si), and after one day of silica restoration (+Si(2)). (A) Cell concentration over three days. (B) Western blot analysis of DPh protein content. The α-DPh antibody has been used to visualize the DPh protein (120kDa) and the α-CF1β antibody for the loading control. (C) TEP normalized for cell concentration. (D) TEP normalized for protein concentration. Standard deviations were obtained with three independent TEP extractions.

Aggregate cell enrichment in P. tricornutum WT cultures

Unlike other diatoms *P. tricornutum* can exist in different morphotypes (fusiform, triradiate, and oval), and changes in cell shape can be stimulated by environmental conditions (De Martino *et al.*, 2007). As *P. tricornutum* can grow in the absence of silica and the biogenesis of silicified frustules is facultative, similar silica depletion experiments as in *Thalassiosira* could not be performed in *P. tricornutum,* so an alternative strategy had to be sought for inducing an aggregation phenotype in the WT. However, a technique was found to revert fusiform cells into oval and aggregating cells. The method used for enriching the Pt1 WT culture with aggregated/oval cells was found in the literature (Stanley and Callow, 2007). The authors describe that diatoms clearly have the ability to distinguish the properties of a surface and modulate their

adhesiveness accordingly. The mechanism of surface perception and response is unknown, although it presumably lies in quantity and/or quality of EPS produced (Stanley and Callow, 2007). To obtain cultures predominantly oval in morphology, *P. tricornutum* WT was grown in both plastic flasks and Pyrex glass bottles containing 100 ml media. Every 2-3 days, both flasks and bottles were rinsed with media and fresh media was added to all of them. This process was repeated till the cultures in the Pyrex glass bottles contained only aggregated/oval cells. The WT cultures grown in the plastic flasks remained 100% fusiform, even after the extensive rinsing process. The enrichment process was thus confirmed for our WT culture and was followed by the Western Blot analysis to visualize the level of DPh protein in both fusiform and oval WT cells (see figure 2.3.9). The level of DPh seemed significantly lower in cells displaying the oval/aggregation phenotype in comparison to the fusiform WT cells. This experiment proved to be very successful to establish a comparison of two morphotype states in the same WT and to investigate their effect on the DPh level.

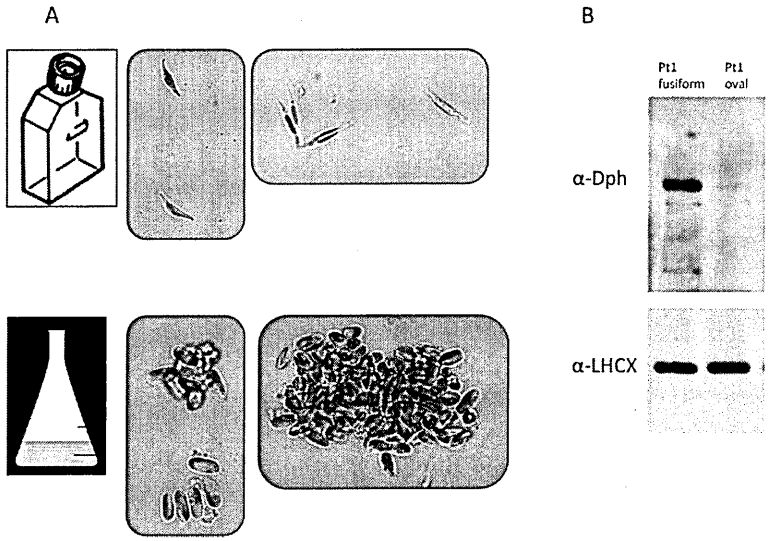

Figure 2.3.9: (Panel A) Pictures of the phenotypes of fusiform and oval aggregating cells, grown in plastic flasks or in glass Pyrex bottles, respectively. (Panel B): Western blot analysis of Pt1 WT fusiform and oval aggregated cell types. The level of DPh was investigated with the α-DPh antibody. The antibody for α-LHCX was used as loading control.

2.3.5 Generation of Heme Oxygenase knock-down lines

Long before the absorption spectra of DPh became available, heme oxygenase (HO) knock-down lines in *P. tricornutum* WT were generated via reverse genetics, to confirm the role of DPh as red/far-red light photoreceptor. The working hypothesis is that the HO-enzyme is involved in the PtDPh chromophore biosynthesis, by producing biliverdin from heme. By silencing the HO-homologue in *P. tricornutum*, we were hoping to produce a "blind" non-functional photoreceptor and to mimic the phenotypes observed in the DPh knock-down lines. This work was started by searching for HO-homologues in the Pt1 WT genomic database. Based on genomic analysis (http://genome.jgi-psf.org/Phatr2/Phatr2.home.html), 4 putative genes were found encoding for HO-like proteins in our species on chromosomes 9, 2, 8 and 7 (see figure 2.3.10 panel A). They were named respectively *HO-1*, *HO-2*, *HO-3* and *HO-4*. From the analysis in the *P. tricornutum* EST-library, it became evident that *HO-2* is constitutively expressed whereas *HO-4* is mostly expressed in silica and iron minus conditions. At the end of this analysis, our attention was focused on the *HO-2* gene, that is most similar to the plant-like *HO* gene and that is targeted to the chloroplast (see figure 2.3.10 panel A and B). The *HO-2* gene seemed the most likely candidate for DPh chromophore biosynthesis in our diatom species. Constructs were made with an antisense fragment of the *HO-2* gene, with the FcpB and H4 promoter. A number of the obtained HO-2 knock-down lines were obtained with the H4 promoter. No positive clones were obtained for the construct with the FcpB promoter. Interestingly, the HO-2 knock-down lines displayed less DPh protein (see figure 2.3.12), as is also observed in *ho* mutants in plants. Therefore, the data suggest the existence of a tight cross talk between the diatom chromophore synthesis and DPh regulation. Based on these results, an analysis of the phenotype was also performed in the HO-2 knock-down lines. Remarkably, some, but not all, of the obtained HO-2 knock-down lines showed a showed a chain or aggregation phenotype as observed previously in DPh knock-down lines (see figure 2.3.12). Because, our HO-2 knock-down lines also display reduced levels of DPh and hereby the

previous observations in the DPh knock-down lines, the aggregation phenotype can be the result of DPh repression and consequent deregulation of the processes downstream of DPh, inducing these particular phenotypes.

A

Protein	ID Phatr2	Length (aa)	EST (Y/N)	Signal P (ChloroP)	Best Hit NCBI	Accession	Id/sim %
HO-1	12588	207	Y	0.000 (0.440)	*Mus musculus* heme oxygenase 1	NP_034572	39/78
HO-2	55416	264	Y	0.925 (0.530)	*Arabidopsis thaliana* heme oxygenase 1 (HO1) (HY1)	AT2G26670	42/71
HO-3	35647	267	Y	0,000(0.439)	*Guillardia theta* heme oxygenase	O78497	33/27
HO-4	5902	213	Y	0,000(0.494)	*Thermosynechococcus elongatus* BP-1 HO-1	BAC07917	46/89

B

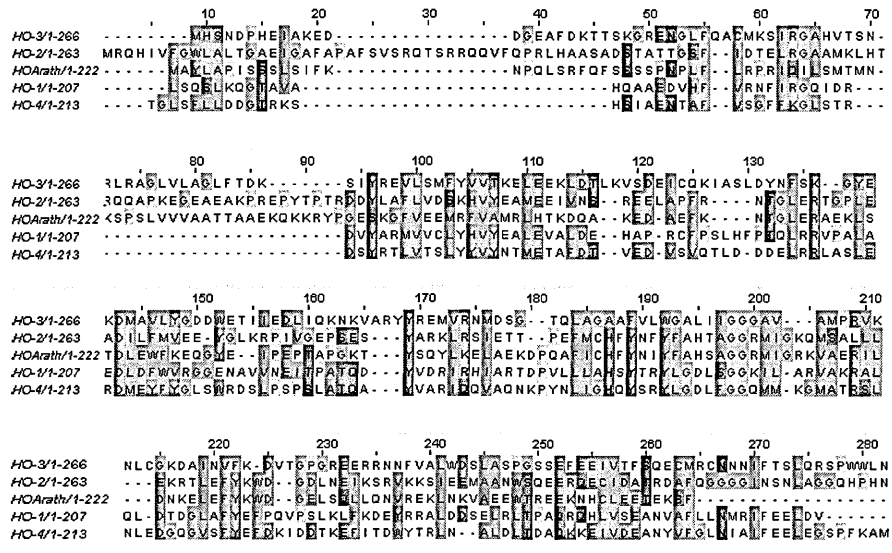

Figure 2.3.10: Panel A showing the diatom Heme Oxygenase (*HO*) genes present in *P. tricornutum*. The Phatr2 genome browser was used to identify *P. tricornutum* gene models encoding heme oxygenase and the following parameters are given: the protein identification number (ID) of the best gene model, the length of the protein, the probability of the presence of a signal peptide as determined by SignalP v3.0 and, in parentheses, the chloroplast targeting prediction score as determined with ChloroP v1.1; the NCBI accession number, species best hit and identity/similarity with the respective *P. tricornutum* genes are given. Panel B shows the amino acid sequence alignment of the four homologues for Heme Oxygenase in *P. tricornutum* and the *Arabidopsis thaliana* heme oxygenase (*HO* Arath in above alignment) (ClustalW). Colors highlight the different conserved regions of the alignment.

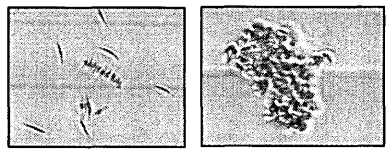

ho2-1 *ho2-2*

Figure 2.3.11 Pictures of the phenotypes are shown, with *ho2-1* showing a chain phenotype and *ho2-2* showing an aggregation phenotype.

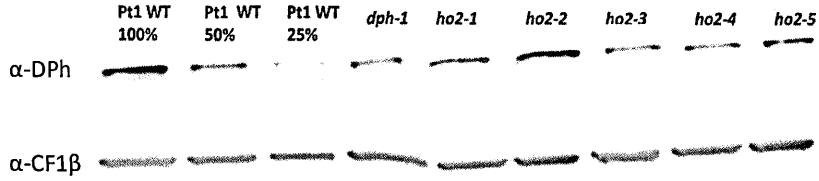

Figure 2.3.12: Western Blot analysis of Pt1 WT (100%, 50% and 25% of total protein extract), a DPh knock-down line (*dph-1*) and five HO-2 knock-down lines (*ho2-1* till *ho2-5*). DPh levels were studied with the α-DPh antibody. The antibody α-CF1β was used as loading control.

2.4. Discussion

2.4.1 DPh controls colony formation and aggregation in *P. tricornutum.*

During this thesis project, several DPh apoprotein knock-down lines were generated to study DPh function and regulation. A number of those DPh knock-down lines showed an unusual phenotype: chain formation or aggregation of cells. These phenotypes were observed in independent knock-down lines, generated with two different vectors harboring antisense fragments against the GAF domain (PtGAF) or the 3'UTR (PtDPh3') of the *DPh* gene. Most of the lines showed a chain phenotype, with the exception of one of the PtGAF lined (the clone *dph-3*) that showed also a change in the morphotype (long chain of oval cells) and the formation of big aggregates. This clone is also showing the strongest level of DPh silencing at protein level. For the other clones, a clear correlation between the level of reduction of the DPh protein and the strength of the phenotype (chain length) was not always observed. Overall, all the PtGAF knock-down lines showed a strong phenotype and the PtDPh3' lines a moderate phenotype that became more evident under specific growth condition affecting the DPh level (see below). We think that the variability of DPh proteins and observed phenotypes in the different knock-down lines might be due to i) the different RNAi processes activated by the different vectors; ii) the complex regulation of the DPh protein synthesis, which seems to be regulated through a complex autoregulative feedback loop; (see chapter I, Results, figure 1.3.8), iii) not yet optimal protein extraction methods generating a certain variability in the Western Blot analysis. All these aspects represent the subject for future investigations.

However, the fact that not all the knock-down lines showed a phenotype had also an advantage, because one DPh knock-down line without a phenotype (*dph-5'*) was used in the gene expression studies next to the DPh knock-down lines with an aggregation phenotype to rule out any side effects of the aggregation phenotype on its gene expression. To better clarify the link between DPh and the chain phenotype, a detailed analysis of the growth rate and chain

distribution of WT and DPh knock-down lines has been performed. As mentioned in chapter I, evidence was found that DPh may by degraded by light. With this aspect in mind, WT and DPh knock-down lines of *P. tricornutum* were grown in different light conditions (dark:light (12hrs:12hrs) versus continuous light), to investigate the effect of both the RNAi and the light dependent phytochrome content modulation on the observed phenotypes. Higher growth rates were observed for cells grown in continuous light than cells grown in light-dark cycles. This increase in light energy over a given day allowed cells to grow and divide more quickly. However, the growth rates did not double between treatments, despite that light exposure was doubled from 12 hours a day to 24 hours. This is not surprising because of factors other than the amount of light energy accessible to cells is involved in determining the rate of cell division. Growth rates of the DPh knock-down lines were slightly lower (less then division per day) than WT growth rate in both treatments, indicating that DPh may control a step in cell division. Analysis are now in progress in the laboratory to better investigate this aspect. However, preliminary data seem to indicate that the knock-down lines are not affected during their cell cycle progression, but are rather affected in the cellular separation during the mitosis, a process that is critical for the chain generation. This unfavorable effect on growth rate, although not dramatic, is almost lost in constant light. Increased light exposure may work to equalize growth rate between WT and DPh knock-down lines, but the cells still do not succeed to complete the cell separation and to generate individual single cells after duplication. The level of DPh silencing was exaggerated in the continuous light condition for all strains, including WT, and strongly correlates with the degradation of DPh protein under continuous light exposure. The fact that chains started to appear also in the WT cells under this condition, and that both the percentage and the length of the chains increased in the knock-down lines, allowed us to establish a clear link between the modulation of DPh content and the observed chain phenotype. The current hypothesis is that DPh might play a role in assuring normal cell division, effectively inhibiting colony formation. Red light is very limited in the water column in depths below 5 meters, but diatoms are able to live as single

cells at depths far deeper than this. If DPh, a red/far-red light photoreceptor, is a regulator of cell separation, there must be more red light present in the water column than what comes from the sun. The laboratory is currently working to test the hypothesis that DPh might control cell division by sensing red light autofluorescence emitted by the cell's own chloroplast. In diatoms, chloroplast duplication is strongly synchronized with nuclear duplication (Chepurnov *et al.*, 2002; Gillard *et al.*, 2008), and therefore the increase in internal red light by this organelle's doubling may function as signal to activate the DPh controlled cellular separation after mitosis. Time lapse video and fluorescence measurements are in progress to investigate whether there is indeed an increase in autofluorescence following chloroplast division and before cellular separation.

TEP Analysis of P. tricornutum WT and DPh knock-down lines

As EPS and particularly TEP are known to play a role in aggregation and colony formation, we were interested to investigate whether the DPh knock-down lines displayed increased TEP levels compared to the WT, in order to better understand the mechanism behind the chain formation or aggregation in the DPh knock-down lines. To this aim, a spectrophotometric assay by coloring TEP with alcian blue was optimized together with two normalization methods (cell concentration and protein content). Relative TEP levels for DPh knock-down lines *dph-2* and *dph-1'* were higher than for the WT when normalized for both cell concentration and protein content, while *dph-3'* and *dph-4'* showed conflicting results depending on the normalization method. Overall, these analyses did not show a conclusive correlation between chain phenotype, level of DPh and TEP content. However, we believe that the TEP detection protocol for *P. tricornutum* needs to be optimized because it is not sufficiently sensitive to detect small TEP variations. It is worth noting that this analysis was only conducted for cultures grown under light:dark conditions, when DPh3' knock-down lines only displayed moderate chain phenotypes. The analysis will be performed now for cultures grown in continuous light to see if a better correlation between TEP increase, DPh silencing and chain phenotype can be established. However, it is also possible that if

chain formation is controlled through an arrest in cell separation, TEP may not be a primary factor responsible for chain formation in the same way that it is for aggregation formation.

2.4.2 The generation of a "blind photoreceptor" induces the formation of colony and aggregates in *P. tricornutum.*

In order to confirm the role of DPh as photoreceptor and better understand its role in the colony and aggregates formation, we used an alternative strategy. In particular, we decided to generate Heme Oxygenase (HO) knock-down lines, to disable the chromophore biosynthesis of the phytochrome. Because a photoactive phytochrome needs its chromophore for light capture, it was expected that the down-regulation of its own chromophore might lead to less photoactive phytochrome. If DPh is involved in the generation of the aggregation/chain phenotypes, it was expected to observe the appearance of the same phenotypes in the chromophore deficient mutants. To this aim, I performed a bioinformatic analysis that revealed the presence of four heme oxygenase (*HO*) genes in the diatom genomes, putative implicated in the synthesis of the biliverdin chromophore. Because of the high similarity with the *HO* from plant and the presence of a chloroplast localization signal, I generated knock-down line for the *HO-2* gene. The phenotypic analysis of the HO-2 lines revealed that two of these lines also displayed a chain (knock-down line *ho2-1*) and aggregation (knock-down line *ho2-2*) phenotypes as the DPh knock-down lines. A similar phenomenon is observed in the plant *hy1* mutant, that does not respond to red and far-red light, although the phytochrome apoprotein is synthesized normally (Chory *et al.*, 1989). The *HY1* gene encodes a heme oxygenase that localizes to chloroplasts and catalyzes the conversion of heme to a biliverdin precursor of phytochromobilin (PΦB) (Muramoto *et al.*, 1999). Interestingly, the *hy1* mutant phenotype is only obvious at the seedling stage; later in the plant development, the mutant plants appear fairly healthy. This could be due to an alternate pathway for chromophore biosynthesis that is activated later in development. Moreover, the *Arabidopsis* genome contains other genes that are similar to *HY1* (Muramoto *et al.*, 1999; Kohchi *et al.*, 2001).

The fact that the diatom HO-2 knock-down lines showed a reduced DPh protein content and a phenotype similar to the DPh knock-down lines provided us with an additional and independent evidence of the role of the DPh photoreceptor in this process. However, it is worth mentioning that not all the analyzed HO-2 knock-down lines showed a chain or aggregation phenotype and not always a clear correlation between the *HO* silencing, DPh reduction and colony/aggregation phenotype was observed. In the case of the HO-2 knock-down lines, we may think that other *HO* genes may replace the affected function in the knock-down lines and that the deregulation of DPh expression and function as holophytochrome is only partially affected in the knock-down lines. The further characterization of the HO-2 knock-down lines is in progress and will be an important research line of the lab in the future. Moreover, a collaboration was started with the laboratory of Prof. Dr. Bernhard Grimm in Berlin to identify and quantify tetrapyrroles in *P. tricornutum* WT, DPh and HO-2 knock-down lines. This will provide novel information on the tetrapyrrole and chlorophyll biosynthesis in diatoms, that are still completely unknown.

2.4.3 Generation and phenotypic characterization of DPh knock-down lines in *T. pseudonana*

Because of the relevance of the results obtained in *P. tricornutum*, we have considered to explore DPh function in the centric species *T. pseudonana*. To this aim, the laboratory set up the RNAi technology by generating silencing plasmids similar to that used in *P. tricornutum* (RNAi vector under FcpB promotor). In addition, we succeed to generate an inducible RNAi system for this species, by putting the RNAi vector under the control of the Nitrogen Reductase promoter, that can be switched on and off, by growing the cells in either NO_3^- or NH_4^+, respectively. Interestingly, a reduction in DPh protein was observed in *T. pseudonana* cells harboring the constitutively expressed RNAi vector. An inducible and reversible reduction of DPh was observed by Western Blot analysis in cells transformed with the inducible RNAi vector: DPh was low in cells grown in NO_3^- containing media, whilst a restored DPh protein content was visible when the DPh silencing machinery was basically off in NH_4^+ containing medium. Intriguingly, an aggregation

phenotype was observed to go hand in hand with the level of silencing; the culture with DPh silenced cells displayed rather large aggregates till the culture was washed with NH_4^+ media and cells lost the aggregation phenotype over the course of a few days. Besides the fact that these observations confirm the role of DPh in life strategies in *T. pseudonana*, these results also indicate that the DPh silencing and the correlated phenotype were reversible. These results open now the way for completely novel investigations to understand the mechanism controlling not only cellular aggregation, but also disaggregation. Disaggregation is probably the greatest unknown of the physical processes that affect marine particles, because there is little understanding or knowledge of crucial pieces of information, such as the size distribution of daughter particles and the forces required to break these particles apart (Burd & Jackson, 2009). Also in the case of aggregating *T. pseudonana* cells, the mechanism(s) involved in the process of aggregation and disaggregation is still unknown.

However, the fact that the aggregation phenotype in all the above mentioned knock-down lines was lost over time, indicates that the cells might have lost (or have overcome) the intrinsic molecular component that leads to their aggregation in the knock-down lines. In general, the aggregation phenotype observed in *T. pseudonana* is less stable than the colony forming phenotype reported in *P. tricornutum*. New inducible DPh knock-down lines are currently being generated in the laboratory of Dr. Thomas Mock with hopefully a similar reversible phenotype to continue the phenotypic analysis in these lines.

2.4.4 Specific environmental conditions leading to DPh down-regulation and aggregation phenotypes

Analysis of cellular aggregation in T. pseudonana induced by silica starvation followed by silica repletion

Because Mock *et al.* (2008) already reported that silica depletion induces cellular aggregation in *T. pseudonana*, an experiment was conducted to investigate whether silica starvation induced

aggregation correlated with a modulation of DPh protein content and rise in TEP levels in *T. pseudonana* WT cells. TEP analysis of *T. pseudonana* in differing nutrient conditions showed that TEP increased when cells were starved for silica and that TEP decreased when cells were returned to silica-replete conditions. TEP levels matched visually observed levels of aggregation. Microscopic observations showed that cells turned to replete conditions were still aggregated, but to a lesser extent than silica-starved cells. A quantitative measurement of the percent aggregation of cultures in these different nutrient conditions was not done in this experiment, but would be valuable data in future trials. Cells were less aggregated when returned to replete conditions have being silica-starved, but it would be interesting to investigate whether this disaggregation rate is the same as the aggregation rate when cells are starved for silica. By analyzing DPh protein content in the different nutrient conditions, we observed that DPh silencing increased during silica-starvation and returned to original levels when cells were replete with silica. Our results indicated that, in *T. pseudonana*, aggregation levels correlated with DPh deregulation. Therefore, a cross-talk between nutrient and light signal pathways can be envisaged on the regulation of DPh because this protein appears from our studies a key regulator of aggregation processes.

Cells returned to repleted conditions showed slightly higher TEP levels than control cells grown under normal, not stressful conditions. There are several possible explanations for this observation. Cells may be able to dissolve TEP to disaggregate when conditions become favorable, however this process may take time and requires different changes of the growth media to be visible. Another hypothesis is that the total TEP produced when cells were stressed is still present even when silica was added back to the culture, and that the drop in relative TEP is due to the increase in cell concentration, and decrease in TEP production, after repletion. Both possibilities suggest interesting mechanisms. The first suggests that cells are able to break down or reabsorb TEP in the surrounding environment. The second suggests that cells are able to grow as single cells despite the presence of TEP, so they must somehow no longer be affected by the sticky

characteristics of TEP, perhaps by changing the composition of their cellular membranes. It may be of interest to investigate the effect of TEP concentrations on aggregation levels by moving cells of known aggregation levels to media inoculated with different concentrations of TEP, to see if TEP already present in the environment can affect aggregation and TEP production in cells. Either way, it is clear that aggregation is not a permanent process, and diatoms can change their level of aggregation according to nutrient conditions.

Oval cell enrichment in P. tricornutum WT cultures

In order to find a correlation between DPh protein levels and cellular aggregation, we examined the possibility to manipulate the oval and aggregating morphotype in *P. tricornutum* WT. Stanley and Callow (2007) reported that every isolate or morphotypes of *P. tricornutum* displays different cell adhesion properties in relation to the surface 'wettability' and that especially the oval morphotype of *P. tricornutum* can be induced by growing the culture on a hydrophobic surface, such as a Pyrex glass bottle. The fact that diatoms can distinguish the properties of surface and modulate their adhesiveness accordingly has not only been shown in *P. tricornutum*; other rapid diatom species also exhibit differential adhesiveness in relation to the wettability of the substrate. Finlay *et al.* (2002) showed that *Amphora coffeaeformis* adheres more strongly to hydrophobic model surfaces in the form of self-assembled monolayers of methyl-terminated alkanethiols, than to OH-terminated alkanethiols, and Holland *et al.* (2004) showed that *Navicula perminuta*, *A. coffeaeformis* and *Craspedostauros australis* adhered more strongly to hydrophobic surfaces in the form of silicone elastomers than to hydrophilic surfaces such as acid-washed glass.

With the article of Stanley and Callow as reference, *P. tricornutum* WT cultures were grown with either a fusiform or an oval/aggregating phenotype on different substrates. As expected for a possible regulatory role in the process, DPh protein levels seemed significantly

lower in cells displaying the oval/aggregation morphotype in comparison to the (normal) fusiform cells. Thus, a link was observed between oval/aggregated cells and a reduced DPh protein content in the *P. tricornutum* WT. This experiment provided an independent evidence that a strong correlation exists between the content of DPh and the appearance of the grouping behavior.

The signal cascades linking DPh and aggregation/chain formation in diatoms is still completely unknown. It is very likely that many factors such as the EPS/TEP concentrations, cell division components, regulators of the diatom specific cell wall, and still many unknown biotic and abiotic triggers are implicated in the complex life strategy regulation. It is possible that not all these unknown components are affected in the HO-2 and DPh know down lines, contributing to the observed variability in the phenotype (colonies versus aggregates) and in the different level of alteration (% percentage and length of the chains).

The data presented in this chapter have important ecological implications, making DPh the first known molecular regulator of the life strategies in diatoms. The discovery that DPh acts as photoreceptor, made this story even more intriguing, although it remains unclear whether the phenotype is directly related to the red light perception function. At the moment, the only clear data derived by these studies is that, when DPh protein content is low, cells tend to stick together, either as aggregates or making chains. The mechanism or the biological reason behind this phenomenon is still open for discussion. It might be that DPh acts as dept detector, by measuring red/far-red light intensities at the water's surface, and regulating together with other signals (e.g., nutrients) aggregation and sinking processes at the end of algal bloom. Alternatively, DPh could be implicated in neighbor perception, by sensing the red light emitted by the phytoplankton autofluorescence. It is important to mention that a recent work of Barkovits *et al.* (2011) revealed that the bacterial phytochrome (Bph) is involved in the regulation of quorum sensing through the regulator LasR in the RPoS/Las quorum sensing network from the bacteria *Pseudomonas aeruginosa*.

Chapter III

Conclusions and perspectives

III. Conclusions and perspectives

Although other studies have hinted in the past toward the possibility of red light sensing in diatoms (Leblanc et al., 1999; Ragni & Ribera d'Alcalà, 2004), this study has provided the first clues that DPh acts as a red/far-red light photoreceptor in diatoms. Furthermore, this study has revealed an important regulative function of DPh in diatoms.

By expressing plasmids containing DPh of *P. tricornutum* and bilin biosynthetic genes in *E. coli*, we have shown that DPh can become a red/far-red light photoreceptor through the binding of biliverdin as chromophore. The spectral analyses have revealed that the Pr-Pfr absorbance of DPh is red-shifted toward 690 nm and 740 nm respectively, similarly to the bacterial phytochromes such as Agp1 from *A. tumefaciens*. In addition, the domain architecture of DPh shares many similarities with bacterial or fungal phytochrome sequences, including a two-component histidine kinase and response regulator. However, the biliverdin binding *in vitro* does not conclusively demonstrate that biliverdin is the chromophore of DPh *in vivo*. In fact, *P. tricornutum* also has the metabolic pathway to synthesize bilin reductases, PebA and PebB, which can further reduce biliverdin to phycoerythrobilin (PEB) and which might be a diatom-specific chromophore. Though, there are two lines of evidence supporting the hypothesis that DPh might use biliverdin as chromophore: DPh has a conserved cysteine residue upstream of the N-terminal PAS-domain similarly to bacterial phytochromes that rather binds biliverdin. On the other hand, the question is raised why diatoms kept the full metabolic pathway to produce enzymes as PebA and PebB, and which function they may play. This prompts for further investigations which can be based on coupling molecular and photobiological approaches. The presence of a bacteria-like phytochrome in diatoms, functioning as red/far-red light sensor, also raises questions on the evolutionary origins of DPh. Phylogenetic analyses have been carried out in the laboratory and are based on sequences from various marine diatoms, marine bacteria and fungi and novel phytochrome sequences from metagenomic databases. The preliminary results indicate that

phytochromes from the Heterokont family represent a separate 'brown' clade with a common origin (Falciatore A. and Carbone A., personal communication).

During this thesis, I also initiated the characterization of the role of DPh by analyzing red light-mediated gene expression profiles in diatoms. I focused on the expression of genes coding for pigment proteins (*VDL1, ZEP2* and *PDS*) and putative chromophore biosynthetic enzymes (*PebB* and *PebA*). Both groups appeared to be red light-mediated. In addition, also genes involved in the chlorophyll biosynthetic pathway (*GSAT, CHLH1* and *HEMA*) and the diatom homologue of the plant *CAB* gene (*LHCF2*) showed elevated transcript levels upon red/far-red light illumination. These gene expression analyses did not offer a conclusive answer on whether DPh acts as a photoreceptor in this process and if the regulation of the tested genes involves DPh as mediator. The blue-light pulse experiments have shown that the genes *GSAT, CHLH1* and *LHCF2* are also induced by blue light, indicating a possible crosstalk between phytochrome and blue light sensors in diatoms. The generality of red light-mediated gene expression was tested in another diatom species, *T. pseudonana*, but no clear responses for the tested genes to red/far-red or photoreversibility conditions were observed. However, this finding does not exclude the existence of such light-regulated processes in *T. pseudonana*, as only one experiment was performed and the number of tested genes was low. The inconclusive nature of the gene expression experiments may be due to technical issue and problems with the synchronization of the cell populations, but it could also be due to the fact the DPh knock-down lines show a specific aggregation phenotype that could influence the results of the gene expression analysis.

The analysis of DPh protein did not resolve the question on which form is the active form of DPh. DPh protein synthesis seemed to be tightly balanced between light, diurnal and circadian regulations, besides the complex regulation of DPh by an autoregulative feedback loop. DPh protein content decreased in cells grown in continuous light in comparison to cells grown in dark, pointing toward a mechanism of DPh degradation by light. These results show that DPh is subject

to an extremely complex regulation, but do not clarify which form of DPh is the one that leads to a biological response. Therefore, further experiments are needed to address this question.

The possibility that the chloroplast might be involved in the regulation of DPh has been explored in *P. tricornutum*, by analyzing red light-mediated gene expression in cells treated with DCMU. In most tested genes (*AOX*, *HEMA* and *CHLH1*) DCMU blocked the responses, indicating that the chloroplast and thus the photosynthesis is involved in the regulation these genes, mainly from the chlorophyll biosynthetic pathway. Further experiments with photosynthesis and proteasome inhibitors might shed light on the role of the chloroplast in the regulation and stability of these red-light regulated processes.

A very interesting observation during this study was the fact that some of the DPh knockdown lines showed a chain or aggregation phenotype. Although there are dissimilarities among the way in which they form chains or aggregate, the functional analyses of the DPh knock-down lines during this thesis has elucidated a peculiar role of DPh in diatom life strategies, because colony formation in pennate diatoms and centric diatoms have shown a correlation with DPh silencing. In the pennate diatom *P. tricornutum*, next to DPh down-regulation inducing chain formation and aggregation, also the quality of the substrate caused cells to change morphotype and aggregate, and a clear reduction of DPh protein in those cells was observed. In the centric diatom *T. pseudonana*, DPh down-regulation gave rise to aggregated cells and moreover, aggregation and a reduced DPh protein content was observed to occur in WT cells grown in particular nutrient depleted conditions. As anticipated above, colony formation and aggregation are not the same behaviors; colonies are genetically similar cells that remain together after cell division, while aggregations may be cells of different lineages that come into contact through random collisions in the water column and stay together via sticky materials such as TEP. During this study, the role of TEP in the process of aggregation was investigated, as TEP has often been postulated to play a major role in aggregation and algal blooms. The results of the TEP

quantification in *P. tricornutum* WT and DPh knock-down lines were rather inconclusive as the TEP levels, DPh silencing and chain phenotypes did not show a convincing correlation. Thus, it might be that TEP is not a major factor involved in the chain formation. On the contrary, TEP was observed to be correlated with aggregation in *T. pseudonana*, as increased TEP concentrations were found in aggregated cultures that were starved for silica. Thus, TEP might be an important regulator in the aggregation mechanism but not in chain formation.

Because the aquatic environment differs completely from the terrestrial environment in its light quality and quantity, with the rapid attenuation of red and far-red light, it was expected that DPh, if characterized as a photoreceptor, might absorb also shorter wavelengths as already shown for less canonical phytochromes isolated from cyanobacteria (reviewed in Ikeuchi and Ishizuka, 2008). The fact that DPh absorbs red and far-red light was not expected, given the low abundance of these colors at sea. Alternatively, most of the red light below the first 5 meters in the ocean originates from chlorophyll a fluorescence (Mobley, 1994), caused by the natural reemission of red light by the chloroplast after light absorption. Therefore, we hypothesize that DPh might perceive an alternative source of red light other than solar red light, locally from neighboring photosynthesizing cells. Consequently, diatoms might use DPh as a neighbor detector, although, it has been reported that perceiving such red light signals could only be relevant on short distances (10-100 µm), thus in the case of extremely proximal cells (Ragni & Ribera d'Alcalà, 2004). Thus, it might be that DPh rather senses red light coming from its own chloroplast than from the neighboring cells, that emit negligible intensities of red light in comparison to cell's own chloroplast. With this in mind, DPh might monitor the division of the chloroplast, that is one of the early steps in the division process in diatoms. If needed, it could be that DPh is able to interrupt the cell separation, that is one of the last phases of cell division, to cause a chain phenotype that might be an advantageous strategy for survival in particular conditions. This intriguing hypothesis opens many new questions and is under investigation in the

laboratory by combining molecular, cellular and physiological approaches, because the biological factors implicated in algal aggregation are of vast ecological importance for understanding processes as algal bloom and aggregation in today's oceans. Algal blooms causing diatom aggregation do not only influence our ocean's worldwide through the release of chemical cue that affect fishery and human well fare, this process has also a high biogeochemical significance as a means of transporting carbon and other nutrients from the euphotic zone to the seabed. Because this study has revealed DPh as red/far-red light sensor and as important regulator in diatom aggregation, promising directions have been provided for research towards characterizing the mechanisms controlling the switch between life strategies.

Bibliography

Abdullahi, A. S., Underwood, G. J. C. *et al.* (2006). "Extracellular matrix assembly in diatoms (bacillariophyceae). V. Environmental effects on polysaccharide synthesis in the model diatom, *Phaeodactylum tricornutum*." Journal of Phycology 42(2): 363-378.

Ahmad, M., Jarillo, J. A. *et al.* (1998). "The CRY1 blue light photoreceptor of *Arabidopsis* interacts with phytochrome A *in vitro*." Molecular Cell 1(7): 939-948.

Alderkamp, A. C., van Rijssel, M. *et al.* (2007). "Characterization of marine bacteria and the activity of their enzyme systems involved in degradation of the algal storage glucan laminarin." FEMS Microbiology Ecology 59(1): 108-117.

Alldredge, A. L. and Gotschalk C. C. (1989). "Direct observations of the mass flocculation of diatom blooms - characteristics, settling velocities and formation of diatom aggregates." Deep-Sea Research Part I-Oceanographic Research Papers 36(2): 159-171.

Alldredge, A. L., Passow, U. *et al.* (1993). "The abundance and significance of a class of large, transparent organic particles in the ocean." Deep-Sea Research Part I-Oceanographic Research Papers 40(6): 1131-1140.

Allen, A. E., LaRoche, J., Maheswari, U., Lommer, M., Schauer, N. *et al.* (2008). "Whole-cell response of the pennate diatom *Phaeodactylum tricornutum* to iron starvation." Proceedings of the National Academy of Sciences of the United States of America 105(30): 10438-10443.

Allen, A. E., Dupont, C. L., Obornik, M., Horak, A., Nunes-Nesi, A. *et al.* (2011). "Evolution and metabolic significance of the urea cycle in photosynthetic diatoms." Nature 473(7346): 203-207.

Al-Sady, B., Ni, W. M. *et al.* (2006). "Photoactivated phytochrome induces rapid PIF3 phosphorylation prior to proteasorne-mediated degradation." Molecular Cell 23(3): 439-446.

Andel, F., Lagarias, J. C. *et al.* (1996). "Resonance Raman analysis of chromophore structure in the lumi-R photoproduct of phytochrome." Biochemistry 35(50): 15997-16008.

Ang, L. H., Chattopadhyay, S. *et al.* (1998). "Molecular interaction between COP1 and HY5 defines a regulatory switch for light control of *Arabidopsis* development." Molecular Cell 1(2): 213-222.

Apt, K. E., Kroth-Pancic, P.G., Grossman, A.R. (1996). "Stable nuclear transformation of the diatom *Phaeodactylum tricornutum* ." Molecular and General Genetics 252: 572–579.

Aravind, L. and Ponting C. P. (1997). "The GAF domain: an evolutionary link between diverse phototransducing proteins." Trends in Biochemical Sciences 22(12): 458-459.

Armbrust, E. V., Berges, J.A., *et al.* (2004). "The genome of the diatom *Thalassiosira pseudonana*: ecology, evolution, and metabolism." Science 306(5693): 79-86.

Armbrust, E. V. (2009). "The life of diatoms in the world's oceans." Nature 459(7244): 185-192.

Austin, R. W. and Petzold T. J. (1986). "Spectral dependence of the diffuse attenuation coefficient of light in ocean waters." Optical Engineering 25(3): 471-479.

Frankland, B. (1972). "Biosynthesis and dark transformations of phytochrome." In Phytochrome, ed. K Mitrakos, W Shropshire, New York: Academic 195–225.

Bailleul, B., Rogato, A., de Martino, A., Coesel, S., Cardol, P., *et al.* (2010). "An atypical member of the light-harvesting complex stress-related protein family modulates diatom responses to light." Proceedings of the National Academy of Sciences of the United States of America 107(42): 18214-18219.

Ballesteros, M. L., Bolle, C. *et al.* (2001). "LAF1, a MYB transcription activator for phytochrome A signaling." Genes & Development 15(19): 2613-2625.

Barkovits, K., Schubert, B. *et al.* (2011). "Function of the bacteriophytochrome BphP in the RpoS/Las quorum-sensing network of *Pseudomonas aeruginosa*." Microbiology-Sgm 157: 1651-1664.

Bauer, D., Viczian, A. *et al.* (2004). "Constitutive photomorphogenesis 1 and multiple photoreceptors control degradation of PHYTOCHROME INTERACTING FACTOR 3, a transcription factor required for light signaling in *Arabidopsis*." Plant Cell 16(6): 1433-1445.

Bayram, O., Biesemann, C., Krappmann, S., Galland, P., Braus, G. H. (2008). "More than a Repair Enzyme: *Aspergillus nidulans* photolyase-like CryA Is a Regulator of Sexual Development." Molecular Biology of the Cell 19(8): 3254-3262.

Beale, S. I. (1999). "Enzymes of chlorophyll biosynthesis." Photosynthesis Research 60(1): 43-73.

Beer, A., Gundermann, K., Beckmann, J., Buchel, C. (2006). "Subunit composition and pigmentation of fucoxanthin-chlorophyll proteins in diatoms: Evidence for a subunit involved in diadinoxanthin and diatoxanthin binding." Biochemistry 45(43): 13046-13053.

Berrocal-Tito, G. M., Esquivel-Naranjo, E. U., Horwitz, B. A., Herrera-Estrella, A. (2007). "*Trichoderma atroviride* PHR1, a fungal photolyase responsible for DNA repair, autoregulates its own photoinduction." Eukaryotic Cell 6(9): 1682-1692.

Bhattacharya, D. E. A. (2007). "How do endosymbionts become organelles? Understanding early events in plastid evolution." Bioessays 29: 1239-1246.

Bhaya, D., Bianco, N. R. *et al.* (2000). "Type IV pilus biogenesis and motility in the cyanobacterium *Synechocystis* sp PCC6803." Molecular Microbiology 37(4): 941-951.

Bhoo, S. H., Davis, S. J. *et al.* (2001). "Bacteriophytochromes are photochromic histidine kinases using a biliverdin chromophore." Nature 414(6865): 776-779.

Björn, L. O. (2008). Photobiology: the science of life and light, 2nd edn., New York: Springer.

Blumenstein, A., Vienken, K. *et al.* (2005). "The *Aspergillus nidulans* phytochrome FphA represses sexual development in red light." Current Biology 15(20): 1833-1838.

Boccalandro, H. E., Rossi, M. C. *et al.* (2004). "Promotion of photomorphogenesis by COP1." Plant Molecular Biology 56(6): 905-915.

Borowitzka, M. A. and Volcani B. E. (1978). "Polymorphic diatom *Phaeodactylum tricornutum* - ultrastructure of its morphotypes." Journal of Phycology 14(1): 10-21.

Borthwick, H. A., Hendricks, S. B. *et al.* (1952). "A reversible photoreaction controlling seed germination." Proceedings of the National Academy of Sciences of the United States of America 38(8): 662-666.

Bowler, C., Allen, A.E., Badger, J.H., *et al.* (2008). "The *Phaeodactylum* genome reveals the evolutionary history of diatom genomes." Nature(456): 239-244.

Bowler, C., *et al.* (2009). "Microbial oceanography in a sea of opportunity." Nature 459: 180–184.

Bowler, C., de Martino, A., Falciatore, A. (2010). "Diatom cell division in an environmental context." Current Opinion in Plant Biology 13: 623–630.

Bowler, C., Neuhaus, G. *et al.* (1994). "Cyclic-GMP and calcium mediate phytochrome phototransduction." Journal of Cellular Biochemistry: 76-76.

Brandt, S., von Stetten, D. *et al.* (2008). "The Fungal Phytochrome FphA from *Aspergillus nidulans*." Journal of Biological Chemistry 283(50): 34605-34614.

Brudler, R., Hitomi, K., Daiyasu, H., Toh, H., Kucho, K., *et al.* (2003). "Identification of a new cryptochrome class. Structure, function, and evolution." Molecular Cell 11(1): 59-67.

Brzezinski, M. A., Olson, R. J. *et al.* (1990). "Silicon availability and cell-cycle progression in marine diatoms." Marine Ecology-Progress Series 67(1): 83-96.

Buchel, C. (2003). "Fucoxanthin-chlorophyll proteins in diatoms: 18 and 19 kDa subunits assemble into different oligomeric states." Biochemistry 42(44): 13027-13034.

Burd, A. B. and Jackson G. A. (2009). "Particle Aggregation". Annual Review of Marine Science. 1: 65-90.

Carpenter, E. J., Janson, S. (2000). "Intracellular cyanobacterial symbionts in the marine diatom *Climacodium frauenfeldianum* (Bacillariophyceae)." Journal of Phycology 36: 540–544.

Casal, J. J. and Boccalandro H. (1995). "Co-action between phytochrome B and hy4 in *Arabidopsis-thaliana*." Planta 197(2): 213-218.

Castillon, A., Shen, H. *et al.* (2007). "PHYTOCHROME INTERACTING FACTORS: central players in phytochrome-mediated light signaling networks." Trends in Plant Science 12(11): 514-521.

Chaves, I., Pokorny, R., Byrdin, M., Hoang, N., Ritz, T., *et al.*, (2011). "The cryptochromes: blue light photoreceptors in plants and animals." Annual Review of Plant Biology 62: 335–364.

Chen, M., Galvao, R. M. *et al.* (2010). "*Arabidopsis* HEMERA/pTAC12 Initiates Photomorphogenesis by Phytochromes." Cell 141(7): 1230-U1237.

Chen, M., Schwabb, R.*et al.* (2003). "Characterization of the requirements for localization of phytochrome B to nuclear bodies." Proceedings of the National Academy of Sciences of the United States of America 100(24): 14493-14498.

Chepurnov, V. A., Mann, D. G. *et al.* (2004). "Experimental studies an sexual reproduction in diatoms." International Review of Cytology - a Survey of Cell Biology, Vol. 237. K. W. Jeon. San Diego, Elsevier Academic Press Inc.

Chepurnov, V. A., Mann, D. G. *et al.* (2002). "Sexual reproduction, mating system, and protoplast dynamics of *Seminavis* (Bacillariophyceae)." Journal of Phycology 38(5): 1004-1019.

Chiovitti, A., Harper, R.E., Willis, A., Bacic, A., Mulvaney, P., Wetherbee, R. (2005). "The complex polysaccharides of the raphid diatom *Pinnularia viridis* (Bacillariophyceae)." Journal of Phycology
41: 1154–1161.

Chory, J., Peto, C. *et al.* (1989). "*Arabidopsis thaliana* mutant that develops as a light-grown plant in the absence of light." Cell 58(5): 991-999.

Christie, J. M. (2007). "Phototropin blue-light receptors." Annual Review of Plant Biology 58: 21–45.

Clack, T., Mathews, S. *et al.* (1994). "The phytochrome apoprotein family in *Arabidopsis* is encoded by 5 genes - the sequences and expression of phyD and phyE." Plant Molecular Biology 25(3): 413-427.

Cock, J. M., Sterck, L. *et al.* (2010). "The *Ectocarpus* genome and the independent evolution of multicellularity in brown algae." Nature 465(7298): 617-621.

Coesel, S., Obornik, M., Varela, J., Falciatore, A., Bowler, C. (2008). "Evolutionary origins and functions of the carotenoid biosynthetic pathway in marine diatoms." PLoS One 3: e2896.

Coesel, S., Mangogna, M., Ishikawa, T., Heijde, M., Rogato, A., Finazzi, G., Todo, T., Bowler, C., Falciatore, A. (2009). "Diatom PtCPF1 is a new cryptochrome/photolyase family member with DNA repair and transcription regulation activity." EMBO Reports(10): 655–661.

Crombet, Y., Leblanc, K., Queguiner, B., Moutin, T., Rimmelin, P., Ras, J., Claustre, H., Leblond, N., Orio, L., Pujo-Pay, M. (2011). "Deep silicon maxima in the stratified oligotrophic Mediterranean Sea." Biogeosciences 8: 459–475.

Curtin, T. B., Belcher, E.O. (2008). "Innovation in oceanographic instrumentation. ." Oceanography 21: 44–53.

Daiyasu, H., Ishikawa, T. *et al.* (2004). "Identification of cryptochrome DASH from vertebrates." Genes Cells 9(5): 479-495.

Davis, S.J., Vener, A.V. *et al.* (1999). "Bacteriophytochromes: Phytochrome-like photoreceptors from nonphotosynthetic eubacteria." Science 286(5449): 2517-2520.

De Castro, F. (2000). "Light spectral composition in a tropical forest: measurements and model." Tree Physiology 20(1): 49-56.

De La Rocha, C. L. and Passow, U. (2007). "Factors influencing the sinking of POC and the efficiency of the biological carbon pump." Deep-Sea Research Part Ii-Topical Studies in Oceanography 54(5-7): 639-658.

De Martino, A., Bartual, A. *et al.* (2011). "Physiological and Molecular Evidence that Environmental Changes Elicit Morphological Interconversion in the Model Diatom *Phaeodactylum tricornutum*." Protist 162(3): 462-481.

De Martino, A., Meichenin, A. *et al.* (2007). "Genetic and phenotypic characterization of *Phaeodactylum tricornutum* (Bacillariophyceae) accessions." Journal of Phycology 43(5): 992-1009.

De Riso, V., Raniello, R., Maumus, F., Rogato, A., Bowler, C., Falciatore, A. (2009). "Gene silencing in the marine diatom *Phaeodactylum tricornutum*." Nucleic Acids Research 37: e96.

Deng, X. W. and Quail P. H. (1992). "Genetic and phenotypic characterization of *cop1* mutants of *Arabidopsis thaliana*." Plant Journal 2(1): 83-95.

Depauw, F. A., Rogato, A. *et al.* (2012). "Exploring the molecular basis of responses to light in marine diatoms." Journal of Experimental Botany 63(4): 1575-1591.

Desnos, T., Puente, P. *et al.* (2001). "FHY1: a phytochrome A-specific signal transducer." Genes & Development 15(22): 2980-2990.

Drapeau, D. T., Dam, H. G. *et al.* (1994). "An improved flocculator design for use in particle aggregation experiments." Limnology and Oceanography 39(3): 723-729.

Drepper, T., Krauss, U. *et al.* (2011). "Lights on and action! Controlling microbial gene expression by light." Applied Microbiology and Biotechnology 90(1): 23-40.

Dunahay, T., Jarvis, E., Roessler, P. (1995). "Genetic transformation of the diatoms *Cyclotella cryptica* and *Navicula saprophita*." Journal of Phycology 31: 1004–1012.

Egger, L. A., Park, H. *et al.* (1997). "Signal transduction via the histidyl-aspartyl phosphorelay." Genes to Cells 2(3): 167-184.

Elich, T. D. and Chory J. (1997). "Biochemical characterization of *Arabidopsis* wild-type and mutant phytochrome B holoproteins." Plant Cell 9(12): 2271-2280.

Engelmann, T. W. (1882). "Uber Sauerstoffausscheidung von Pflanzzellen im Mikrospektrum." Bot. Zeitung 40: 419-414.

Esposito, S., Botte, V., Iudicone, D., Ribera d'Alcala´, M. (2009). "Numerical analysis of cumulative impact of phytoplankton photoresponses to light variation on carbon assimilation." Journal of Theoretical Biology 261: 361–371.

Essen, L. O., Mailliet, J. *et al.* (2008). "The structure of a complete phytochrome sensory module in the Pr ground state." Proceedings of the National Academy of Sciences of the United States of America 105(38): 14709-14714.

Esteban, B., Carrascal, M. *et al.* (2005). "Light-induced conformational changes of cyanobacterial phytochrome Cph1 probed by limited proteolysis and autophosphorylation." Biochemistry 44(2): 450-461.

Esteban-Pretel, G., Marin, M. P. *et al.* (2010). "Vitamin A Deficiency Increases Protein Catabolism and Induces Urea Cycle Enzymes in Rats." Journal of Nutrition 140(4): 792-798.

Fairchild, C. D., Schumaker, M. A. *et al.* (2000). "HFR1 encodes an atypical bHLH protein that acts in phytochrome A signal transduction." Genes & Development 14(18): 2377-2391.

Falciatore, A., Casotti, R., Leblanc, C., Abrescia, C., Bowler, C. (1999). "Transformation of nonselectable reporter genes in marine diatoms." Marine Biotechnology(1): 239–251.

Falciatore, A., Ribera d'Alcala, M., Croot, P., Bowler, C. (2000). "Perception of environmental signals by a marine diatom." Science 288: 2363–2366.

Falkowski, P. G., Raven, J.A. (2007)." Aquatic Photosynthesis". Second Edition, Princeton Univeristy Press.

Falkowski, P. G., Katz, M. E. *et al.* (2004). "The evolution of modern eukaryotic phytoplankton." Science 305(5682): 354-360.

Fankhauser, C. and Chen M. (2008). "Transposing phytochrome into the nucleus." Trends in Plant Science 13(11): 596-601.

Fankhauser, C., Yeh, K. C. *et al.* (1999). "PKS1, a substrate phosphorylated by phytochrome that modulates light signaling in *Arabidopsis*." Science 284(5419): 1539-1541.

Field, C. B., Behrenfeld, M.J., Randerson, J.T., Falkowski, P. (1998). "Primary production of the biosphere: integrating terrestrial and oceanic components." Science 281: 237–240.

Finlay, J. A., Callow, M. E. *et al.* (2002). "The influence of surface wettability on the adhesion strength of settled spores of the green alga *Enteromorpha* and the diatom *Amphora*." Integrative and Comparative Biology 42(6): 1116-1122.

Fischer, H., Robl, I. *et al.* (1999). "Targeting and covalent modification of cell wall and membrane proteins heterologously expressed in the diatom *Cylindrotheca fusiformis* (Bacillariophyceae)." Journal of Phycology 35(1): 113-120.

Fisher, A. E., Berges, J.A., Harrison, P.J. (1996). "Does light quality affect the sinking rates of marine diatoms?" Journal of Phycology(32): 353–360.

Flint, L. H., and McAlister, E. D. (1935). "Wavelengths of radiation in the visible spectrum inhibiting the germination of light-sensitive lettuce seed." Smithsonian Inst. Publs, Misc. Collections 94: 1-11.

Foster, R. A., Zehr, J.P. (2006). "Characterization of diatom-cyanobacteria symbioses on the basis of nifH, hetR and 16S rRNA sequences." Environmental Microbiology 8: 1913–1925.

Fowler, S. W. and Knauer, G. A. (1986). "Role of large particles in the transport of elements and organic-compounds through the oceanic water column." Progress in Oceanography 16(3): 147-194.

Franklin, K. A. and Quail, P. H. (2010). "Phytochrome functions in *Arabidopsis* development." Journal of Experimental Botany 61(1): 11-24.

Froehlich, A. C., Noh, B. *et al.* (2005). "Genetic and molecular analysis of phytochromes from the filamentous fungus *Neurospora crassa*." Eukaryotic Cell 4(12): 2140-2152.

Fukao, T., Kimoto, K. *et al.* (2010). "Production of transparent exopolymer particles by four diatom species." Fisheries Science 76(5): 755-760.

Furuya, M. and Schafer, E. (1996). "Photoperception and signalling of induction reactions by different phytochromes." Trends in Plant Science 1(9): 301-307.

Gambetta, G. A. and Lagarias, J. C. (2001). "Genetic engineering of phytochrome biosynthesis in bacteria." Proceedings of the National Academy of Sciences of the United States of America 98(19): 10566-10571.

Gärdes, A., Iversen, M.H. *et al.* (2011). "Diatom-associated bacteria are required for aggregation of *Thalassiosira weissflogii*." Isme Journal 5(3): 436-445.

Gill, R. T., Katsoulakis, E., Schmitt, W., Taroncher-Oldenburg, G., Misra, J., Stephanopoulos, G. (2002). "Genome-wide dynamic transcriptional profiling of the light-to-dark transition in *Synechocystis* sp. strain PCC 6803." Journal of Bacteriology 184: 3671–3681.

Gillard, J., Devos, V., Huysman, M.J., *et al.* (2008). "Physiological and transcriptomic evidence for a close coupling between chloroplast ontogeny and cell cycle progression in the pennate diatom *Seminavis robusta*." Journal of Plant Physiology 148: 1394–1411.

Giraud, E., Fardoux, L. *et al.* (2002). "Bacteriophytochrome controls photosystem synthesis in anoxygenic bacteria." Nature 417(6885): 202-205.

Giraud, E. and Fleischman, D. (2004). "Nitrogen-fixing symbiosis between photosynthetic bacteria and legumes." Photosynthesis Research 82(2): 115-130.

Giraud, E., Zappa, S. *et al.* (2005). "A new type of bacteriophytochrome acts in tandem with a classical bacteriophytochrome to control the antennae synthesis in *Rhodopseudomonas palustris*." Journal of Biological Chemistry 280(37): 32389-32397.

Gomelsky, M. and Hoff, W. D. (2011). "Light helps bacteria make important lifestyle decisions." Trends in Microbiology 19(9): 441-448.

Green, B. and Zhu, S. (2007). "Light-harvesting and photoprotection in diatoms: Identification and role of L818-like proteins and a novel member of the LHC superfamily." Photosynthesis Research 91(2-3): 167-167.

Green, B. R. (2011). "Chloroplast genomes of photosynthetic eukaryotes." The Plant Journal 66: 34–44.

Grossart, H. P., Czub, G. *et al.* (2006). "Algae-bacteria interactions and their effects on aggregation and organic matter flux in the sea." Environmental Microbiology 8(6): 1074-1084.

Grossman, A.R., Bhaya, D., He, Q. (2001). "Tracking the light environment by cyanobacteria and the dynamic nature of light harvesting. " Journal of Biological Chemistry 276: 11449–11452.

Grossman, A.R. (2003). "A molecular understanding of complementary chromatic adaptation." Photosynthesis Research 76(1-3): 207-215.

Grouneva, I., Rokka, A., Aro, E.M. (2011). "The thylakoid membrane proteome of two marine diatoms outlines both diatom-specific and species-specific features of the photosynthetic machinery." Journal of Proteome Research 10: 5338–5353.

Gruber, A., Vugrinec, S., Hempel, F., Gould, S.B., Maier, U.G., Kroth, P.G. (2007). "Protein targeting into complex diatom plastids: functional characterisation of a specific targeting motif." Plant Molecular Biology 64: 519–530.

Guillard, R. R. L., Kilham, P. (1977)." The ecology of marine planktonic diatoms. In: Werner D, ed. The biology of diatoms". Oxford: Blackwell Scientific Publications.

Guillard, R.R.L. (1975). "Culture of phytoplankton for feeding marine invertebrates." in Plenum Press, New York, USA. .

Guo, H. W., Mockler, T. *et al.* (2001). "SUB1, an *Arabidopsis* Ca^{2+}-binding protein involved in cryptochrome and phytochrome coaction." Science 291(5503): 487-490.

Hamazato, F., Shinomura, T. *et al.* (1997). "Fluence and wavelength requirements for *Arabidopsis CAB* gene induction by different phytochromes." Plant Physiology 115(4): 1533-1540.

Heijde, M., Zabulon, G. *et al.* (2010). "Characterization of two members of the cryptochrome/photolyase family from *Ostreococcus tauri* provides insights into the origin and evolution of cryptochromes." Plant Cell and Environment 33(10): 1614-1626.

Hennig, L. and Schafer, E. (2001). "Both subunits of the dimeric plant photoreceptor phytochrome require chromophore for stability of the far-red light-absorbing form." Journal of Biological Chemistry 276(11): 7913-7918.

Herdman, M., Coursin, T. *et al.* (2000). "A new appraisal of the prokaryotic origin of eukaryotic phytochromes." Journal of Molecular Evolution 51(3): 205-213.

Hessen, D. O. and Vandonk, E. (1993). "Morphological-changes in *Scenedesmus* induced by substances released from *Daphnia*." Archiv Fur Hydrobiologie 127(2): 129-140.

Hitomi, K., Nakamura, H., Kim, S.T., Mizukoshi, T., Ishikawa, T., Iwai, S., Todo, T. (2001). "Role of two histidines in the (6–4) photolyase reaction." Journal of Biological Chemistry 276: 10103–10109.

Hoagland, K. D., Rosowski, J. R. *et al.* (1993). "Diatom extracellular polymeric substances - function, fine-structure, chemistry, and physiology." Journal of Phycology 29(5): 537-566.

Holland, R., Dugdale, T. M. *et al.* (2004). "Adhesion and motility of fouling diatoms on a silicone elastomer." Biofouling 20(6): 323-329.

Huang, L. Q., Bonner, B. A. *et al.* (1989). "Regulation of 5-aminolevulinic acid (ALA) synthesis in developing chloroplasts. Regulation of ALA-synthesizing capacity by phytochrome." Plant Physiology 90(3): 1003-1008.

Huang, Y., Baxter, R. *et al.* (2006). "Crystal structure of cryptochrome 3 from *Arabidopsis thaliana* and its implications for photolyase activity." Proceedings of the National Academy of Sciences of the United States of America 103(47): 17701-17706.

Hudson, M., Ringli, C. *et al.* (1999). "The FAR1 locus encodes a novel nuclear protein specific to phytochrome A signaling." Genes & Development 13(15): 2017-2027.

Hudson, M. E. (2000). "The genetics of phytochrome signalling in *Arabidopsis*." Seminars in Cell & Developmental Biology 11(6): 475-483.

Hughes, J., Lamparter, T. *et al.* (1997). "A prokaryotic phytochrome." Nature 386(6626): 663-663.

Huq, E., Al-Sady, B. *et al.* (2004). "PHYTOCHROME-INTERACTING FACTOR 1 is a critical bHLH regulator of chlorophyll biosynthesis." Science 305(5692): 1937-1941.

Huysman, M. J., Martens, C., Vandepoele, K., *et al.* (2010). "Genome-wide analysis of the diatom cell cycle unveils a novel type of cyclins involved in environmental signaling." Genome Biology 11: R17.

Ianora, A. e. a. (2004). "Aldehyde suppression of copepod recruitement in blooms of a ubiquitous planktonic diatom." Nature 429: 403-407.

Ikeuchi, M. and Ishizuka, T. (2008). "Cyanobacteriochromes: a new superfamily of tetrapyrrole-binding photoreceptors in cyanobacteria." Photochemical & Photobiological Sciences 7(10): 1159-1167.

Ilag, L. L., Kumar, A. M. *et al.* (1994). "Light regulation of chlorophyll biosynthesis at the level of 5-aminolevulinate formation in *Arabidopsis*." Plant Cell 6(2): 265-275.

Im, C. S., Eberhard, S. *et al.* (2006). "Phototropin involvement in the expression of genes encoding chlorophyll and carotenoid biosynthesis enzymes and LHC apoproteins in *Chlamydomonas reinhardtii*." Plant Journal 48(1): 1-16.

Ishizuka, T., Shimada, T. *et al.* (2006). "Characterization of cyanobacteriochrome TePixJ from a thermophilic cyanobacterium *Thermosynechococcus elongatus* strain BP-1." Plant and Cell Physiology 47(9): 1251-1261.

Jackson, G. A. (1995). "TEP and coagulation during a mesocosm experiment." Deep-Sea Research Part Ii-Topical Studies in Oceanography 42(1): 215-222.

Jang, I. C., Yang, J. Y. *et al.* (2005). "HFR1 is targeted by COP1 E3 ligase for post-translational proteolysis during phytochrome A signaling." Genes & Development 19(5): 593-602.

Jarillo, J. A., Capel, J. *et al.* (2001). "An *Arabidopsis* circadian clock component interacts with both CRY1 and phyB." Nature 410(6827): 487-490.

Jaubert, M., Lavergne, J. *et al.* (2007). "A singular bacteriophytochrome acquired by lateral gene transfer." Journal of Biological Chemistry 282(10): 7320-7328.

Jiao, Y., Lau, O.S., Deng, X.W. (2007). "Light-regulated transcriptional networks in higher plants." Nature Reviews Genetics(8): 217–230.

Kadota, A., Sato, Y. *et al.* (2000). "Intracellular chloroplast photorelocation in the moss *Physcomitrella patens* is mediated by phytochrome as well as by a blue-light receptor." Planta 210(6): 932-937.

Kahl, A. L., Vardi, A., Schofield, O. (2008). "The effect of phytoplankton physiology on export flux." Marine Ecology Progress Series 354: 3-19.

Kami, C., Lorrain, S., Hornitschek, P., Fankhauser, C. (2010). "Light-regulated plant growth and development. ." Current Topics in Developmental Biology 91: 29–66.

Karl, D. M. (2007). "Microbial oceanography: paradigms, processes and promise." Nature Reviews Microbiology 5: 759–769.

Karniol, B., Wagner, J.R., Walker, J.M., Vierstra, R.D. (2005). "Phylogenetic analysis of the phytochrome superfamily reveals distinct microbial subfamilies of photoreceptors." Biochemical Journal 392: 103-116.

Karniol, B. and Vierstra, R. D. (2003). "The pair of bacteriophytochromes from *Agrobacterium tumefaciens* are histidine kinases with opposing photobiological properties." Proceedings of the National Academy of Sciences of the United States of America 100(5): 2807-2812.

Karniol, B. and Vierstra, R. D. (2004). "The HWE histidine kinases, a new family of bacterial two-component sensor kinases with potentially diverse roles in environmental signaling." Journal of Bacteriology 186(2): 445-453.

Karp-Boss, L. and Jumars, P. A. (1998). "Motion of diatom chains in steady shear flow." Limnology and Oceanography 43(8): 1767-1773.

Katz, M. E., Finkel, Z.V., Grzebyk, D., Knoll, A.H., Falkowski, P.G. (2004). "Evolutionary trajectories and biogeochemical impacts of marine eukaryotic phytoplankton." Annual Review of Ecology, Evolution and Systematics(35): 523–556.

Keeling, P.J. and Palmer, J.D. (2008). "Horizontal gene transfer in eukaryotic evolution." Nature Reviews Genetics(9): 605–618.

Kehoe, D. M. and Grossman, A. R. (1996). "Similarity of a chromatic adaptation sensor to phytochrome and ethylene receptors." Science 273(5280): 1409-1412.

Kehoe, D. M. and Grossman, A. R. (1997). "New classes of mutants in complementary chromatic adaptation provide evidence for a novel four-step phosphorelay system." Journal of Bacteriology 179(12): 3914-3921.

Kehoe, D. M. and Gutu A. (2006). "Responding to color: The regulation of complementary chromatic adaptation". Annual Review of Plant Biology. 57: 127-150.

Kendrick, R.E. and Kronenberg, K. (1993). "Photomorphogenesis in Plants", 2nd edition, Kluwer Academic Publishers.

Kikis, E. A., Oka, Y. *et al.* (2009). "Residues Clustered in the Light-Sensing Knot of Phytochrome B are Necessary for Conformer-Specific Binding to Signaling Partner PIF3." PLoS Genetics 5(1).

Kim, D., Yukl, E. T. *et al.* (2006). "Fungal heme oxygenases: Functional expression and characterization of Hmx1 from *Saccharomyces cerevisiae* and CaHmx1 from *Candida albicans*." Biochemistry 45(49): 14772-14780.

Kiorboe, T. and Hansen, J. L. S. (1993). "Phytoplankton aggregate formation - observations of patterns and mechanisms of cell sticking and the significance of exopolymeric material." Journal of Plankton Research 15(9): 993-1018.

Kircher, S., Gil, P. *et al.* (2002). "Nucleocytoplasmic partitioning of the plant photoreceptors phytochrome A, B, C, D, and E is regulated differentially by light and exhibits a diurnal rhythm." Plant Cell 14(7): 1541-1555.

Kirk, J. T. O., ed. (1994). "Light and photosynthesis in aquatic ecosystems", New York: Cambridge University Press.

Kleine, T., Lockhart, P. *et al.* (2003). "An *Arabidopsis* protein closely related to *Synechocystis* cryptochrome is targeted to organelles." Plant Journal 35(1): 93-103.

Kloareg, B. and Quatrano, R. S. (1988). "Structure of the cell-walls of marine-algae and ecophysiological functions of the matrix polysaccharides." Oceanography and Marine Biology 26: 259-315.

Knoll, A. H. (2003). "Life on a young planet: the first three billion years of evolution on earth", Princeton, NJ: Princeton University Press.

Kohchi, T., Mukougawa, K. *et al.* (2001). "The *Arabidopsis* HY2 gene encodes phytochromobilin synthase, a ferredoxin-dependent biliverdin reductase." Plant Cell 13(2): 425-436.

Kolber, Z. (2007). "Energy cycle in the ocean: powering the microbial world." Oceanography 20: 79–87.

Kondou, Y., Nakazawa, M., Higashi, S., Watanabe, M., Manabe, K. (2001). "Equal-quantum action spectra indicate fluence-rate-selective action of multiple photoreceptors for photomovement of the thermophilic cyanobacterium *Synechococcus elongatus*." Photochemistry and Photobiology 73: 90–95.

Kooistra, W. H. C. F., Gersonde, R., Medlin, L.K., Mann, D. (2007). "The origin and evolution of the diatoms: their adaptation to a planktonic existence. In: Falkowski PG, Knoll AH, eds. Evolution of planktonic photoautotrophs." Burlington, MA: Academic Press: 207–249.

Kowallik, K. V., Stoebe, B., Schaffran, I., Kroth-Pancic, P., Freier, U. (1995). "The chloroplast genome of a chlorophyll a+c-containing alga, *Odontella sinensis*." Plant Molecular Biology Reporter 13: 336–342.

Kraml, M., Herrmann, H. (1991). "Red-blue interaction in *Mesotaenium* chloroplast movement—blue seems to stabilize the transient memory of the phytochrome signal." Photochemistry and Photobiology 53: 255–259.

Krauss, U., Minh, B.Q. *et al.* (2009). "Distribution and Phylogeny of Light-Oxygen-Voltage-Blue-Light-Signaling Proteins in the Three Kingdoms of Life." Journal of Bacteriology 191(23): 7234-7242.

Kroger, N., Deutzmann, R. *et al.* (2000). "Species-specific polyamines from diatoms control silica morphology." Proceedings of the National Academy of Sciences of the United States of America 97(26): 14133-14138.

Kroth, P. G., Weber, T. *et al.* (2009). "Carbohydrate metabolism in diatoms from a genomic perspective." Phycologia 48(4): 68-68.

Kruse, E., Grimm, B. *et al.* (1997). "Developmental and circadian control of the capacity for delta-aminolevulinic acid synthesis in green barley." Planta 202(2): 235-241.

Lamparter, T., Esteban, B. *et al.* (2001). "Phytochrome Cph1 from the cyanobacterium *Synechocystis* PCC6803 - Purification, assembly, and quaternary structure." European Journal of Biochemistry 268(17): 4720-4730.

Lamparter, T. and Michael, N. (2005). "*Agrobacterium* phytochrome as an enzyme for the production of ZZE bilins." Biochemistry 44(23): 8461-8469.

Lamparter, T., Michael, N. *et al.* (2002). "Phytochrome from *Agrobacterium tumefaciens* has unusual spectral properties and reveals an N-terminal chromophore attachment site." Proceedings of the National Academy of Sciences of the United States of America 99(18): 11628-11633.

Lampert, W., Rothhaupt, K. O. *et al.* (1994). "Chemical induction of colony formation in a green-alga *Scenedesmus-acutus*) by grazers (*Daphnia*)." Limnology and Oceanography 39(7): 1543-1550.

Lariguet, P., Schepens, I. *et al.* (2006). "PHYTOCHROME KINASE SUBSTRATE 1 is a phototropin 1 binding protein required for phototropism." Proceedings of the National Academy of Sciences of the United States of America 103(26): 10134-10139.

Laubinger, S., Fittinghoff, K. *et al.* (2004). "The SPA quartet: A family of WD-repeat proteins with a central role in suppression of photomorphogenesis in *Arabidopsis*." Plant Cell 16(9): 2293-2306.

Lavaud, J., Strzepek, R. F. *et al.* (2007). "Photoprotection capacity differs among diatoms: Possible consequences on the spatial distribution of diatoms related to fluctuations in the underwater light climate." Limnology and Oceanography 52(3): 1188-1194.

Leblanc, C., Falciatore, A., Watanabe, M., Bowler, C. (1999). "Semiquantitative RT-PCR analysis of photoregulated gene expression in marine diatoms." Plant Molecular Biology 40: 1031–1044.

Leivar, P., Monte, E. *et al.* (2008). "Multiple Phytochrome-Interacting bHLH Transcription Factors Repress Premature Seedling Photomorphogenesis in Darkness." Current Biology 18(23): 1815-1823.

Leivar, P. and Quail, P. H. (2011). "PIFs: pivotal components in a cellular signaling hub." Trends in Plant Science 16(1): 19-28.

Leivar, P., Tepperman, J. M. *et al.* (2009). "Definition of Early Transcriptional Circuitry Involved in Light-Induced Reversal of PIF-Imposed Repression of Photomorphogenesis in Young *Arabidopsis* Seedlings." Plant Cell 21(11): 3535-3553.

Lepetit, B., Volke, D. *et al.* (2010). "Evidence for the Existence of One Antenna-Associated, Lipid-Dissolved and Two Protein-Bound Pools of Diadinoxanthin Cycle Pigments in Diatoms." Plant Physiology 154(4): 1905-1920.

Li, L. M. and Lagarias, J. C. (1992). "Phytochrome assembly - defining chromophore structural requirements for covalent attachment and photoreversibility." Journal of Biological Chemistry 267(27): 19204-19210.

Li, Q. H. and Yang, H. Q. (2007). "Cryptochrome signaling in plants." Photochemistry and Photobiology 83(1): 94-101.

Livak, K. J. and Schmittgen, T. D. (2001). "Analysis of relative gene expression data using real-time quantitative PCR and the 2(T)(-Delta Delta C) method." Methods 25(4): 402-408.

Longhurst, A. R. (1998). "Ecological Geography of the Sea." Academic Press.

Lopez-Figueroa, F. (1992). "Diurnal variation in pigment content in *Porphyra laciniata* and *Chondrus crispus* and its relation to the diurnal changes of underwater light quality and quantity." Marine Ecology(13): 285–230.

Losi, A. and Gartner, W. (2011). "Old Chromophores, New Photoactivation Paradigms, Trendy Applications: Flavins in Blue Light-Sensing Photoreceptors." Photochemistry and Photobiology 87(3): 491-510.

Lurling, M. (1999). "Grazer-induced coenobial formation in clonal cultures of *Scenendesmus obliquus* (Chlorococcales, Chlorophyceae)." Journal of Phycology 35(1): 19-23.

Maheswari, U., Mock, T. *et al.* (2009). "Update of the Diatom EST Database: a new tool for digital transcriptomics." Nucleic Acids Research 37: D1001-D1005.

Mann, D. G. (1993). "Patterns of sexual reproduction in diatoms." Hydrobiologia 269: 11-20.

Mann, K. H., Lazier, J.R.N., eds. (2006). "Dynamics of marine ecosystems: biological–physical interactions in the oceans." USA: Blackwell Publishing.

Marchetti, A., Lundholm, N. *et al.* (2008). "Identification and assessment of domoic acid production in oceanic *Pseudo-nitzschia* (Bacillariophyceae) from iron-limited waters in the northeast subarctic Pacific." Journal of Phycology 44(3): 650-661.

Margalef, R., ed. (1974). Ecologıa, Barcelona: Omega.

Margalef, R. (1978). "Phytoplankton communities in upwelling areas." Oecologia Aquatica 3: 97–132.

Mari, X., Torreton, J. P. *et al.* (2012). "Aggregation dynamics along a salinity gradient in the Bach Dang estuary, North Vietnam." Estuarine Coastal and Shelf Science 96: 151-158.

Martinez-Garcia, J. F., Huq, E. *et al.* (2000). "Direct targeting of light signals to a promoter element-bound transcription factor." Science 288(5467): 859-863.

Mascher, T., Helmann, J. D. *et al.* (2006). "Stimulus perception in bacterial signal-transducing histidine kinases." Microbiology and Molecular Biology Reviews 70(4): 910-938.

Masuda, T., Ohta, H. *et al.* (1995). "Stimulation of glutamyl-transfer-rna reductase-activity by benzyladenine in greening cucumber cotyledons." Plant and Cell Physiology 36(7): 1237-1243.

Materna, A. C., Sturm, S., Kroth, P.G., Lavaud, J. (2009). "First induced plastid genome mutations in an alga with secondary plastids: psba mutations in the diatom *Phaeodactylum tricornutum* (Bacillariophyceae) reveal consequences on the regulation of photosynthesis. ." Journal of Phycology 45: 838–846.

Matsuda, Y., Harada, H., Nakajima, K., Colman, B. (2007). "Sensing of elevating CO(2) in a marine diatom: molecular mechanisms and implications. ." Plant Signaling and Behavior 2(109-111).

Matsushita, T., Mochizuki, N. *et al.* (2003). "Dimers of the N-terminal domain of phytochrome B are functional in the nucleus." Nature 424(6948): 571-574.

Matters, G.L. and Beale, S.I. (1994). "Biosynthesis of delta-aminolevulinic-acid from glutamate by sulfolobus-solfataricus." Archives of Microbiology 161(3): 272-276.

Mazzocchi, M. G., González, H.E., Vandromme, P., Borrione, I., DeAlcala, M., Gauns, M., Assmy, P., Fuchs, B., Klaas, C., and Martin, P. (2009). "A non-diatom plankton bloom controlled by copepod grazing and amphipod predation: preliminary results from the LOHAFEX iron-fertilisation experiment. ." GLOBEC International Newsletter 15: 3–6.

McCormac, A. C., Fischer, A. *et al.* (2001). "Regulation of *HEMA1* expression by phytochrome and a plastid signal during de-etiolation in *Arabidopsis thaliana*." Plant Journal 25(5): 549-561.

McCormac, A. C. and Terry, M. J. (2002). "Light-signalling pathways leading to the co-ordinated expression of *HEMA1* and *Lhcb* during chloroplast development in *Arabidopsis thaliana*." Plant Journal 32(4): 549-559.

McCormac, A. C. and Terry, M. J. (2002). "Loss of nuclear gene expression during the phytochrome A-mediated far-red block of greening response." Plant Physiology 130(1): 402-414.

Mclachlan, D. H., Brownlee, C., Taylor, A.R., Geider, R.J., Underwood, G.J.C. (2009). "Light-induced motile responses of the estuarine benthic diatoms *Navicula Perminuta* and *Cylindrotheca Closterium* (Bacillariophyceae)." Journal of Phycology 45: 592–599.

Medlin, L. K., Kooistra, W.H.C.F., Potter, D., Saunders, G.W., Anderson, R.A. (1997). "Phylogenetic relationships of the 'golden algae' (hepatophytes, heterokont chrysophytes) and their plastids." Plant Systematics and Evolution(11):187–210.

Merchant, S. S. *et al.* (2007). "The *Chlamydomonas* genome reveals the evolution of key animal and plant functions." Science(318): 245–250.

Meskauskiene, R. and Apel, K. (2002). "Interaction of FLU, a negative regulator of tetrapyrrole biosynthesis, with the glutamyl-tRNA reductase requires the tetratricopeptide repeat domain of FLU." Febs Letters 532(1-2): 27-30.

Meskauskiene, R., Nater, M. *et al.* (2001). "FLU: A negative regulator of chlorophyll biosynthesis in *Arabidopsis thaliana*." Proceedings of the National Academy of Sciences of the United States of America 98(22): 12826-12831.

Middelburg, J. J., Barranguet, C. *et al.* (2000). "The fate of intertidal microphytobenthos carbon: An in situ C-13-labeling study." Limnology and Oceanography 45(6): 1224-1234.

Millar, A. J. and Kay S. A. (1991). "Circadian control of *CAB* gene-transcription and messenger-RNA accumulation in *Arabidopsis*." Plant Cell 3(5): 541-550.

Miyagawa-Yamaguchi, A., Okami, T., Kira, N., Yamaguchi, H., Ohnishi, K., Adachi, M. (2011). "Stable nuclear transformation of the diatom *Chaetoceros* sp." Phycology Research 59: 113–119.

Mobley, C. D. (1994). "Light and water: radiative transfer in natural waters." San Diego: Academic Press.

Mochizuki, N., Tanaka, R. *et al.* (2010). "The cell biology of tetrapyrroles: a life and death struggle." Trends in Plant Science 15(9): 488-498.

Mock, T. *et al.* (2008). "Whole-genome expression profiling of the marine diatom *Thalassiosira pseudonana* identifies genes involved in silicon bioprocesses." PNAS 105(5): 1579–1584.

Moglich, A., Yang, X., Ayers, R.A., Moffat, K. (2010). "Structure and function of plant photoreceptors." Annual Review of Plant Biology 61: 21–47.

Moller, S. G., Ingles, P. J. *et al.* (2002). "The cell biology of phytochrome signalling." New Phytologist 154(3): 553-590.

Montgomery, B. L. and Lagarias, J. C. (2002). "Phytochrome ancestry: sensors of bilins and light." Trends in Plant Science 7(8): 357-366.

Montsant, A., Allen, A. E. *et al.* (2007). "Identification and comparative genomic analysis of signaling and regulatory components in the diatom *Thalassiosira pseudonana*." Journal of Phycology 43(3): 585-604.

Montsant, A., Jabbari, K. *et al.* (2005). "Comparative genomics of the pennate diatom *Phaeodactylum tricornutum*." Plant Physiology 137(2): 500-513.

Moon, Y. J., Kim, S. Y. *et al.* (2011). "Cyanobacterial phytochrome Cph2 is a negative regulator in phototaxis toward UV-A." FEBS Letters 585(2): 335-340.

Mooney, J. L. and Yager, L. N. (1990). "Light is required for conidiation in *Aspergillus nidulans*." Genes & Development 4(9): 1473-1482.

Moore, L. R. R. G., Chisholm, S.W. (1998). "Physiology and molecular phylogeny of coexisting *Prochlorococcus* ecotypes." Nature 393: 464–467.

Morris, R. M., Longnecker, K., Giovannoni, S.J. (2006). "Pirellula and OM43 are among the dominant lineages identified in an Oregon coast diatom bloom. ." Environmental Microbiology 8: 1361–1370

Mouget, J. L., Gastineau, R., Davidovich, O., Gaudin, P., Davidovich, N.A. (2009). "Light is a key factor in triggering sexual reproduction in the pennate diatom *Haslea ostrearia*." FEMS Microbiology Ecology 69: 194–201.

Moustafa, A., Beszteri, B. *et al.* (2009). "Genomic Footprints of a Cryptic Plastid Endosymbiosis in Diatoms." Science 324(5935): 1724-1726.

Mukougawa, K., Kanamoto, H. *et al.* (2006). "Metabolic engineering to produce phytochromes with phytochromobilin, phycocyanobilin, or phycoerythrobilin chromophore in *Escherichia coli*." FEBS Letters 580(5): 1333-1338.

Muramoto, T., Kohchi, T. *et al.* (1999). "The *Arabidopsis* photomorphogenic mutant *hy1* is deficient in phytochrome chromophore biosynthesis as a result of a mutation in a plastid heme oxygenase." Plant Cell 11(3): 335-347.

Murphy, J.T., Lagarias, J.C. (1997)."The phytofluors: a new class of fluorescent protein probes." Current Biology 7, 870–876.

Nagatani, A. (2010). "Phytochrome: structural basis for its functions." Current Opinion in Plant Biology 13(5): 565-570.

Nagatani, A., Reed, J. W. *et al.* (1993). "Isolation and initial characterization of A*rabidopsis* mutants that are deficient in phytochrome-a." Plant Physiology 102(1): 269-277.

Nagy, F. and Schafer, E. (2002). "Phytochromes control photomorphogenesis by differentially regulated, interacting signaling pathways in higher plants." Annual Review of Plant Biology 53: 329-355.

Nagy, G., Posselt, D., Kovacs, L., Holm, J.K., Szabo, M., *et al.*, (2011). "Reversible membrane reorganizations during photosynthesis in vivo: revealed by small-angle neutron scattering." Biochemical Journal 436: 225–230.

Narikawa, R., Kohchi, T. *et al.* (2008). "Characterization of the photoactive GAF domain of the CikA homolog (SyCikA, Slr1969) of the cyanobacterium *Synechocystis* sp PCC 6803." Photochemical & Photobiological Sciences 7(10): 1253-1259.

Nelson, D. M., Treguer, P., Brzezinski, M.A., Leynaert, A., Queguiner, B. (1995). "Production and dissolution of biogenic silica in the ocean: revised global estimates, comparison with regional data and relationship to biogenic sedimentation." Global Biogeochemical Cycles 9(359-372).

Ni, M., Tepperman, J. M. *et al.* (1998). "PIF3, a phytochrome-interacting factor necessary for normal photoinduced signal transduction, is a novel basic helix-loop-helix protein." Cell 95(5): 657-667.

Ni, M., Tepperman, J. M. *et al.* (1999). "Binding of phytochrome B to its nuclear signalling partner PIF3 is reversibly induced by light." Nature 400(6746): 781-784.

Nureki, O., Shirouzu, M. *et al.* (2002). "An enzyme with a deep trefoil knot for the active-site architecture." Acta Crystallographica Section D-Biological Crystallography 58: 1129-1137.

Nymark, M., Valle, K.C., Brembu, T., Hancke, K., Winge, P., *et al.*, (2009). "An integrated analysis of molecular acclimation to high light in the marine diatom *Phaeodactylum tricornutum*." PLoS One 4: e7743.

Oka, Y., Matsushita, T., *et al.* (2008). "Mutant screen distinguishes between residues necessary for light-signal perception and signal transfer by phytochrome B." PLoS Genetics 4(8): e1000158.

Okamoto, H., Matsui, M. *et al.* (2001). "Overexpression of the heterotrimeric G-protein alpha-subunit enhances phytochrome-mediated inhibition of hypocotyl elongation in *Arabidopsis*." Plant Cell 13(7): 1639-1651.

Osterlund, M. T., Wei, N. *et al.* (2000). "The roles of photoreceptor systems and the COP1-targeted destabilization of HY5 in light control of *Arabidopsis* seedling development." Plant Physiology 124(4): 1520-1524.

Oudot-Le Secq, M. P., Grimwood, J., Shapiro, H., Armbrust, E.V., Bowler, C., Green, B.R. (2007). "Chloroplast genomes of the diatoms *Phaeodactylum tricornutum* and *Thalassiosira pseudonana*: comparison with other plastid genomes of the red lineage." Molecular Genetics and Genomics 277: 427–439.

Oyama, T., Shimura, Y. *et al.* (1997). "The *Arabidopsis* HY5 gene encodes a bZIP protein that regulates stimulus-induced development of root and hypocotyl." Genes & Development 11(22): 2983-2995.

Paik, I., Yang, S. *et al.* (2012). "Phytochrome regulates translation of mRNA in the cytosol." Proceedings of the National Academy of Sciences of the United States of America 109(4): 1335-1340.

Park, C. M., Kim, J. I. *et al.* (2000). "A second photochromic bacteriophytochrome from *Synechocystis* sp PCC 6803: Spectral analysis and down-regulation by light." Biochemistry 39(35): 10840-10847.

Parker, M. S. *et al.* (2008). "Genomic insights into marine microalgae." Annual Reviews Genetics 42: 619–645.

Parks, B. M. and Quail, P. H. (1991). "Phytochrome-deficient *hy1* and *hy2* long hypocotyl mutants of *Arabidopsis* are defective in phytochrome chromophore biosynthesis." Plant Cell 3(11): 1177-1186.

Parks, B. M. and Quail, P. H. (1993). "*hy8*, a new class of *Arabidopsis* long hypocotyl mutants deficient in functional phytochrome-a." Plant Cell 5(1): 39-48.

Pasqualini, S., Paolocci, F. *et al.* (2007). "The overexpression of an alternative oxidase gene triggers ozone sensitivity in tobacco plants." Plant Cell and Environment 30(12): 1545-1556.

Passow, U. (2000). "Formation of transparent exopolymer particles, TEP, from dissolved precursor material." Marine Ecology-Progress Series 192: 1-11.

Passow, U. and Alldredge, A. L. (1995). "Aggregation of a diatom bloom in a mesocosm - the role of transparent exopolymer particles (tep)." Deep-Sea Research Part Ii-Topical Studies in Oceanography 42(1): 99-109.

Passow, U., French, M. A. *et al.* (2011). "Biological controls on dissolution of diatom frustules during their descent to the deep ocean: Lessons learned from controlled laboratory experiments." Deep-Sea Research Part I-Oceanographic Research Papers 58(12): 1147-1157.

Paterson, D. M., and Black, K.S. (1999). "Water flow, sediment dynamics and benthic biology." Advances in Ecological Research 29: 155-193.

Paterson, D. M., Tolhurst, T. J. *et al.* (2000). "Variations in sediment properties, Skeffling mudflat, Humber Estuary, UK." Continental Shelf Research 20(10-11): 1373-1396.

Peers, G. and Price, N. M. (2006). "Copper-containing plastocyanin used for electron transport by an oceanic diatom." Nature 441(7091): 341-344.

Pendrak, M. L., Chao, M. P. *et al.* (2004). "Heme oxygenase in *Candida albicans* is regulated by hemoglobin and is necessary for metabolism of exogenous heme and hemoglobin to alpha-biliverdin." Journal of Biological Chemistry 279(5): 3426-3433.

Peperzak, L. (1993). "Daily irradiance governs growth-rate and colony formation of *Phaeocystis* (Prymnesiophyceae)." Journal of Plankton Research 15(7): 809-821.

Peschke, F., Kretsch, T. (2011). "Genome-wide analysis of light dependent transcript accumulation patterns during early stages of *Arabidopsis* seedling deetiolation." Plant Physiology 155: 1353–1366.

Piontek, J., Handel, N. *et al.* (2009). "Effects of rising temperature on the formation and microbial degradation of marine diatom aggregates." Aquatic Microbial Ecology 54(3): 305-318.

Pontoppidan, B. and Kannangara, C. G. (1994). "Purification and partial characterization of barley glutamyl-tRNA(glu) reductase, the enzyme that directs glutamate to chlorophyll biosynthesis." European Journal of Biochemistry 225(2): 529-537.

Poulsen, N., Chesley, P.M., Kroger, N. (2006). "Molecular genetic manipulation of the diatom *Thalassiosira pseudonana* (Bacillariophyceae)." Journal of Phycology 42(5): 1059-1065.

Prihoda, J., Tanaka, A. *et al.* (2012). "Chloroplast-mitochondria cross-talk in diatoms." Journal of Experimental Botany 63(4): 1543-1557.

Psakis, G., Mailliet, J. *et al.* (2011). "Signaling Kinetics of Cyanobacterial Phytochrome Cph1, a Light Regulated Histidine Kinase." Biochemistry 50(28): 6178-6188.

Purschwitz, J., Mueller, S. *et al.* (2008). "Functional and physical interaction of blue- and red-light sensors in *Aspergillus nidulans*." Current Biology 18(4): 255-259.

Purschwitz, J., Muller, S. *et al.* (2009). "Mapping the interaction sites of *Aspergillus nidulans* phytochrome FphA with the global regulator VeA and the White Collar protein LreB." Molecular Genetics and Genomics 281(1): 35-42.

Purschwitz, J., Muller, S. *et al.* (2006). "Seeing the rainbow: light sensing in fungi." Current Opinion in Microbiology 9(6): 566-571.

Quail, P. H. (1997). "The phytochromes: A biochemical mechanism of signaling in sight?" Bioessays 19(7): 571-579.

Quail, P. H. (2000). "Phytochrome-interacting factors." Seminars in Cell & Developmental Biology 11(6): 457-466.

Radic, T., Kraus, R. *et al.* (2005). "Transparent exopolymeric particles' distribution in the northern Adriatic and their relation to microphytoplankton biomass and composition." Science of the Total Environment 353(1-3): 151-161.

Ragni, M., Ribera d'Alcala, M. (2004). "Light as an information carrier underwater." Journal of Plankton Research 26: 433–443.

Rausenberger, J., Hussong, A. *et al.* (2010). "An Integrative Model for Phytochrome B Mediated Photomorphogenesis: From Protein Dynamics to Physiology." PLoS One 5(5).

Rayko, E., Maumus, F., Maheswari, U., Jabbari, K., Bowler, C. (2010). "Transcription factor families inferred from genome sequences of photosynthetic stramenopiles." New Phytologist 188(1): 52–66.

Reed, J. W., Nagatani, A. *et al.* (1994). "Phytochrome-a and phytochrome-b have overlapping but distinct functions in *Arabidopsis* development." Plant Physiology 104(4): 1139-1149.

Riegman, R., Kuipers, B. R. *et al.* (1993). "Size-differential control of phytoplankton and the structure of plankton communities." Netherlands Journal of Sea Research 31(3): 255-265.

Roberts, K., Granum, E., Leegood, R.C., Raven, J.A. (2007). "C-3 and C-4 pathways of photosynthetic carbon assimilation in marine diatoms are under genetic, not environmental, control." Plant Physiology(145): 230–235.

Rochaix, J. D. (2002). "*Chlamydomonas*, a model system for studying the assembly and dynamics of photosynthetic complexes." FEBS Letters 529: 34–38.

Rockwell, N. C., Njuguna, S. L. *et al.* (2008). "A second conserved GAF domain cysteine is required for the blue/green photoreversibility of cyanobacteriochrome Tlr0924 from *Thermosynechococcus elongatus*." Biochemistry 47(27): 7304-7316.

Rockwell, N. C., Su, Y. S. *et al.* (2006). "Phytochrome structure and signaling mechanisms." Annual Review of Plant Biology. 57: 837-858.

Rodriguez-Romero, J., Hedtke, M. *et al.* (2010). "Fungi, Hidden in Soil or Up in the Air: Light Makes a Difference." Annual Review of Microbiology, 64: 585-610.

Rosler, J., Klein, I. *et al.* (2007). "*Arabidopsis fhl/fhy1* double mutant reveals a distinct cytoplasmic action of phytochrome A." Proceedings of the National Academy of Sciences of the United States of America 104(25): 10737-10742.

Rottwinkel, G., Oberpichler, I. *et al.* (2010). "Bathy Phytochromes in Rhizobial Soil Bacteria." Journal of Bacteriology 192(19): 5124-5133.

Ryan, R. P., Fouhy, Y. *et al.* (2006). "Cyclic Di-GMP signaling in bacteria: Recent advances and new puzzles." Journal of Bacteriology 188(24): 8327-8334.

Sancar, A. (2003). "Structure and function of DNA photolyase and cryptochrome blue-light photoreceptors." Chemical Reviews 103: 2203–2237.

Sanchez-Puerta, M. and Delwiche, C.F. (2008). "A hypothesis for plastid evolution in chromalveolates." Journal of Phycology 44: 1097–1107.

Sato, Y., Wada, M. *et al.* (2001). "Choice of tracks, microtubules and/or actin filaments for chloroplast photo-movement is differentially controlled by phytochrome and a blue light receptor." Journal of Cell Science 114(2): 269-279.

Schafer, E. and Bowler, C. (2002). "Phytochrome-mediated photoperception and signal transduction in higher plants." EMBO Reports 3(11): 1042-1048.

Schmitz, O., Katayama, M. *et al.* (2000). "CikA, a bacteriophytochrome that resets the cyanobacterial circadian clock." Science 289(5480): 765-768.

Schneider-Poetsch, H. A. W., Kolukisaoglu, U. *et al.* (1998). "Non-angiosperm phytochromes and the evolution of vascular plants." Physiologia Plantarum 102(4): 612-622.

Seo, H. S., Watanabe, E. *et al.* (2004). "Photoreceptor ubiquitination by COP1 E3 ligase desensitizes phytochrome A signaling." Genes & Development 18(6): 617-622.

Seo, H. S., Yang, J. Y. *et al.* (2003). "LAF1 ubiquitination by COP1 controls photomorphogenesis and is stimulated by SPA1." Nature 423(6943): 995-999.

Serino, G. and Deng, X. W. (2003). "The COP9 signalosome: Regulating plant development through the control of proteolysis." Annual Review of Plant Biology 54: 165-182.

Shacklock, P. S., Read, N. D. *et al.* (1992). "Cytosolic free calcium mediates red light-induced photomorphogenesis." Nature 358(6389): 753-755.

Shanklin, J., Jabben, M. *et al.* (1987). "Red light-induced formation of ubiquitin-phytochrome conjugates - identification of possible intermediates of phytochrome degradation." Proceedings of the National Academy of Sciences of the United States of America 84(2): 359-363.

Sharrock, R. A. and Clack, T. (2002). "Patterns of expression and normalized levels of the five *Arabidopsis* phytochromes." Plant Physiology 130(1): 442-456.

Sharrock, R. A. and Quail, P. H. (1989). "Novel phytochrome sequences in *Arabidopsis thaliana* structure, evolution, and differential expression of a plant regulatory photoreceptor family." Genes & Development 3(11): 1745-1757.

Shin, J., Kim, K. *et al.* (2009). "Phytochromes promote seedling light responses by inhibiting four negatively-acting phytochrome-interacting factors." Proceedings of the National Academy of Sciences of the United States of America 106(18): 7660-7665.

Siaut, M., Heijde, M., Mangogna, M., Montsant, A., Coesel, *et al.*, (2007). "Molecular toolbox for studying diatom biology in *Phaeodactylum tricornutum*." Gene 406: 23–35.

Silverthorne, J. and Tobin, E. M. (1984). "Demonstration of transcriptional regulation of specific genes by phytochrome action." Proceedings of the National Academy of Sciences of the United States of America-Biological Sciences 81(4): 1112-1116.

Sineshchekov, O., Lebert, M., Hader, D.P. (2000). "Effects of light on gravitaxis and velocity in *Chlamydomonas reinhardtii*." Journal of Plant Physiology 157: 247–254.

Smayda, T. J. and Boleyn, B. J. (1966). "Experimental observations on flotation of marine diatoms 2. *Skeletonema costatum* and *Rhizosolenia setigera*." Limnology and Oceanography 11(1): 18-34.

Smetacek, V. (1999). "Diatoms and the ocean carbon cycle." Protist(150): 25-32.

Smetacek, V. (1985). "Role of sinking in diatom life-history cycles - ecological, evolutionary and geological significance." Marine Biology 84(3): 239-251.

Smith, D. C., Steward, G. F. *et al.* (1995). "Bacterial mediation of carbon fluxes during a diatom bloom in a mesocosm." Deep-Sea Research Part Ii-Topical Studies in Oceanography 42(1): 75-97.

Stanewsky, R., Kaneko, M. *et al.* (1998). "The *cryb* mutation identifies cryptochrome as a circadian photoreceptor in *Drosophila*." Cell 95(5): 681-692.

Stanley, M. S. and Callow, J. A. (2007). "Whole cell adhesion strength of morphotypes and isolates of *Phaeodactylum tricornutum* (Bacillariophyceae)." European Journal of Phycology 42(2): 191-197.

Starostzik, C. and Marwan, W. (1995). "A photoreceptor with characteristics of phytochrome triggers sporulation in the true slime-mold *Physarum polycephalum*." Febs Letters 370(1-2): 146-148.

Stephenson, P. G. and Terry, M. J. (2008). "Light signalling pathways regulating the Mg-chelatase branchpoint of chlorophyll synthesis during de-etiolation in *Arabidopsis thaliana*." Photochemical & Photobiological Sciences 7(10): 1243-1252.

Stock, A. M., Robinson, V. L. *et al.* (2000). "Two-component signal transduction." Annual Review of Biochemistry 69: 183-215.

Strasser, B., Sanchez-Lamas, M. *et al.* (2010). "*Arabidopsis thaliana* life without phytochromes." Proceedings of the National Academy of Sciences of the United States of America 107(10): 4776-4781.

Strzepek, R. F. and Harrison, P. J. (2004). "Photosynthetic architecture differs in coastal and oceanic diatoms." Nature 431(7009): 689-692.

Suetsugu, N., Mittmann, F. *et al.* (2005). "A chimeric photoreceptor gene, NEOCHROME, has arisen twice during plant evolution." Proceedings of the National Academy of Sciences of the United States of America 102(38): 13705-13709.

Suetsugu, N. and Wada, M. (2005). "Photoreceptor Gene Families in Lower Plants, in Handbook of Photosensory Receptors (eds W. R. Briggs and J. L. Spudich)". Wiley-VCH Verlag GmbH & Co. KGaA, Weinheim, FRG. doi: 10.1002/352760510X.ch17.

Sweere, U., Eichenberg, K. *et al.* (2001). "Interaction of the response regulator ARR4 with phytochrome B in modulating red light signaling." Science 294(5544): 1108-1111.

Takabayashi, M., Lew, K. *et al.* (2006). "The effect of nutrient availability and temperature on chain length of the diatom, *Skeletonema costatum*." Journal of Plankton Research 28(9): 831-840.

Takahashi, F., Yamagata, D., Ishikawa, M., Fukamatsu, Y., Ogura, Y., *et al.*, (2007). "AUREOCHROME, a photoreceptor required for photomorphogenesis in stramenopiles." Proceedings of the National Academy of Sciences of the United States of America 104(49): 19625-19630.

Tanaka, R. and Tanaka, A. (2007). Tetrapyrrole biosynthesis in higher plants. Annual Review of Plant Biology. 58: 321-346.

Tang, K. W., Smith, W. O. *et al.* (2008). "Colony size of *Phaeocystis antarctica* (Prymnesiophyceae) as influenced by zooplankton grazers." Journal of Phycology 44(6): 1372-1378.

Tarutina, M., Ryjenkov, D. A. *et al.* (2006). "An unorthodox bacteriophytochrome *from Rhodobacter sphaeroides* involved in turnover of the second messenger c-di-GMP." Journal of Biological Chemistry 281(46): 34751-34758.

Tasler, R., Moises, T. *et al.* (2005). "Biochemical and spectroscopic characterization of the bacterial phytochrome of *Pseudomonas aeruginosa*." FEBS Journal 272(8): 1927-1936.

Taylor, W. R. (2000). "A deeply knotted protein structure and how it might fold." Nature 406(6798): 916-919.

Terry, M. J. and Kendrick, R. E. (1999). "Feedback inhibition of chlorophyll synthesis in the phytochrome chromophore-deficient aurea and yellow-green-2 mutants of tomato." Plant Physiology 119(1): 143-152.

Thomas, D. N., Dieckmann, G.S. (2002). "Antarctic Sea ice—a habitat for extremophiles. ." Science 295(641-644).

Timko, M. P. (1998). "Pigment biosynthesis: Chlorophylls, heme, and carotenoids." Kluwer Academic Publishers, Dordrecht, The Netherlands.

Tirichine, L., Bowler, C. (2011). "Decoding algal genomes: tracing back the history of photosynthetic life on Earth." The Plant Journal 66: 45-57.

Trebst, A. (1980). " Inhibitors in electron flow: tools for the functional and structural localization of carriers and energy conservation sites." Methods in Enzymology (69): 675-715.

Ulijasz, A.T., Cornilescu, G. *et al.* (2010). "Structural basis for the photoconversion of a phytochrome to the activated Pfr form." Nature 463(7278): 250-254.

Ulijasz, A. T., Cornilescu, G. *et al.* (2009). "Cyanochromes Are Blue/Green Light Photoreversible Photoreceptors Defined by a Stable Double Cysteine Linkage to a Phycoviolobilin-type Chromophore." Journal of Biological Chemistry 284(43): 29757-29772.

Ulijasz, A. T., Cornilescu, G. *et al.* (2008). "Characterization of two thermostable cyanobacterial phytochromes reveals global movements in the chromophore-binding domain during photoconversion." Journal of Biological Chemistry 283(30): 21251-21266.

Ulijasz, A. T. and Vierstra, R. D. (2011). "Phytochrome structure and photochemistry: recent advances toward a complete molecular picture." Current Opinion in Plant Biology 14(5): 498-506.

Underwood, G. J. C. and Paterson, D. M. (2003). "The importance of extracellular carbohydrate production by marine epipelic diatoms." Advances in Botanical Research, Vol 40 40: 183-240.

Van Aken, O., Giraud, E. *et al.* (2009). "Alternative oxidase: a target and regulator of stress responses." Physiologia Plantarum 137(4): 354-361.

Van Duyl, F. C., De Winder, B. *et al.* (1999). "Tidal coupling between carbohydrate concentrations and bacterial activities in diatom-inhabited intertidal mudflats." Marine Ecology-Progress Series 191: 19-32.

Vanlerberghe, G. C., Cvetkovska, M. *et al.* (2009). "Is the maintenance of homeostatic mitochondrial signaling during stress a physiological role for alternative oxidase?" Physiologia Plantarum 137(4): 392-406.

Vanormelingen, P., Verleyen, E., Vyverman, W. (2008). "The diversity and distribution of diatoms: from cosmopolitanism to narrow endemism." Biodiversity and Conservation 17: 393–340.

Vardi, A., Formiggini, F., Casotti, R., De Martino, A., Ribalet, F., Miralto, A., Bowler, C. (2006). "A stress surveillance system based on calcium and nitric oxide in marine diatoms." PLoS Biology 4: e60.

Vardi, A., Thamatrakoln, K. *et al.* (2008). "Diatom genomes come of age." Genome Biology 9(12).

Vardi, A. *et al.* (2008). "A diatom gene regulating nitric-oxide signalling and susceptibility to diatoms-derived aldehydes." Current Biology 18: 895-899.

Vartanian, M., Descles, J. *et al.* (2009). "Plasticity and robustness of pattern formation in the model diatom *Phaeodactylum tricornutum*." New Phytologist 182(2): 429-442.

Veldhuis, M. J. W., Brussaard, C. P. D. *et al.* (2005). "Living in a *Phaeocystis* colony: a way to be a successful algal species." Harmful Algae 4(5): 841-858.

Vierstra, R. D. (1993). "Illuminating phytochrome functions." Plant Physiology 103(3): 679-684.

Vierstra, R. D. and Davis, S. J. (2000). "Bacteriophytochromes: new tools for understanding phytochrome signal transduction." Seminars in Cell & Developmental Biology 11(6): 511-521.

Vierstra, R. D. and Zhang, J. R. (2011). "Phytochrome signaling: solving the Gordian knot with microbial relatives." Trends in Plant Science 16(8): 417-426.

Vuillet, L., Kojadinovic, M. *et al.* (2007). "Evolution of a bacteriophytochrome from light to redox sensor." Embo Journal 26(14): 3322-3331.

Wagner, J. R., Brunzelle, J. S. *et al.* (2005). "A light-sensing knot revealed by the structure of the chromophore-binding domain of phytochrome." Nature 438(7066): 325-331.

Wang, H. Y. and Deng, X. W. (2002). "*Arabidopsis* FHY3 defines a key phytochrome A signaling component directly interacting with its homologous partner FAR1." Embo Journal 21(6): 1339-1349.

Wang, H. Y., Ma, L. G. *et al.* (2001). "Direct interaction of *Arabidopsis* cryptochromes with COP1 in light control development." Science 294(5540): 154-158.

Whitelam, G. C., Johnson, E. *et al.* (1993). "Phytochrome-a null mutants of *Arabidopsis* display a wild-type phenotype in white light." Plant Cell 5(7): 757-768.

Widdows, J., Brinsley, M. D. *et al.* (2000). "Influence of biota on spatial and temporal variation in sediment erodability and material flux on a tidal flat (Westerschelde, The Netherlands)." Marine Ecology-Progress Series 194: 23-37.

Wilde, A., Fiedler, B. *et al.* (2002). "The cyanobacterial phytochrome Cph2 inhibits phototaxis towards blue light." Molecular Microbiology 44(4): 981-988.

Williams, P. J. (1990). "The importance of losses during microbial growth: commentary on the physiology, measurement and ecology of the release of dissolved organic material." Marine Microbial Food Webs 4(175–206).

Wu, H., Cockshutt, A.M., McCarthy, A., Campbell, D.A. (2011). "Distinctive photosystem II photoinactivation and protein dynamics in marine diatoms." Plant Physiology 156: 2184–2195.

Wu, S. H. and Lagarias J. C. (2000). "Defining the bilin lyase domain: Lessons from the extended phytochrome superfamily." Biochemistry 39(44): 13487-13495.

Yamaguchi, R., Nakamura, M. *et al.* (1999). "Light-dependent translocation of a phytochrome B-GFP fusion protein to the nucleus in transgenic *Arabidopsis*." Journal of Cell Biology 145(3): 437-445.

Yang, H. Q., Tang, R. H. *et al.* (2001). "The signaling mechanism of *Arabidopsis* CRY1 involves direct interaction with COP1." Plant Cell 13(12): 2573-2587.

Yang, X., Stojkovic, E.A. *et al.* (2007). "Crystal structure of the chromophore binding domain of an unusual bacteriophytochrome, RpBphP3, reveals residues that modulate photoconversion." Proceedings of the National Academy of Sciences of the United States of America 104(30): 12571-12576.

Yang, Y. J., Zuo, Z. C. *et al.* (2008). "Blue-light-independent activity of *Arabidopsis* cryptochromes in the regulation of steady-state levels of protein and mRNA expression." Molecular Plant 1(1): 167-177.

Yeh, K. C. and Lagarias J. C. (1998). "Eukaryotic phytochromes: Light-regulated serine/threonine protein kinases with histidine kinase ancestry." Proceedings of the National Academy of Sciences of the United States of America 95(23): 13976-13981.

Yeh, K. C., Wu, S. H. *et al.* (1997a). "A cyanobacterial phytochrome two-component light sensory system." Science 277(5331): 1505-1508.

Yeh, K. C., Wu, S. H. *et al.* (1997b). "Cyanobacterial phytochrome: implication for mechanism of phytochrome action." Plant Physiology 114(3): 1464-1464.

Yoon, H. S., Hackett, J. D. *et al.* (2004). "A molecular timeline for the origin of photosynthetic eukaryotes." Molecular Biology and Evolution 21(5): 809-818.

Yoshida, K., Watanabe, C. *et al.* (2008). "Influence of chloroplastic photo-oxidative stress on mitochondrial alternative oxidase capacity and respiratory properties: A case study with *Arabidopsis* yellow variegated 2." Plant and Cell Physiology 49(4): 592-603.

Yoshihara, S., Katayama, M. *et al.* (2004). "Phytochrome-like PixJ1 holoprotein from *Synechocystis* shows novel reversible photoconversion between blue- and green-absorbing forms." Plant and Cell Physiology 45: S46-S46.

Yoshihara, S., Matsuoka, D. *et al.* (2006). "Manner of the chromophore-binding involved in the blue/green reversible photoconversion of a phytochrome-like photoreceptor." Plant and Cell Physiology 47: S157-S157.

Yoshihara, S., Suzuki, F. *et al.* (2000). "Novel putative photoreceptor and regulatory genes required for the positive phototactic movement of the unicellular motile cyanobacterium *Synechocystis* sp PCC 6803." Plant and Cell Physiology 41(12): 1299-1304.

Zatz, M. M. (1984). "Culture of animal-cells - a manual of basic technique - freshney,ri." American Scientist 72(2): 204-204.

Zhao, K. H., Ran, Y. *et al.* (2004). "Photochromic biliproteins from the cyanobacterium *Anabaena* sp PCC 7120: Lyase activities, chromophore exchange, and photochromism in phytochrome AphA." Biochemistry 43(36): 11576-11588.

Zhou, J., Mopper, K. *et al.* (1998). "The role of surface-active carbohydrates in the formation of transparent exopolymer particles by bubble adsorption of seawater." Limnology and Oceanography 43(8): 1860-1871.

Zhu, S. H., Green, B.R. (2010). "Photoprotection in the diatom *Thalassiosira pseudonana*: role of LI818-like proteins in response to high light stress." Biochimica et Biophysica Acta 1797: 1449–1457.

Phaeodactylum tricornutum

ID number Phatr2	Domain architecture	Predicted by Pfam	Predicted by SMART
44688	GAF domain only	Yes	Yes
36809	GAF domain only	Yes	Yes
45070	GAF-Ankyrin	Yes	Ankyrin insignificant match
44514	GAF-HiskA-RR (Lhk)	GAF: insignificant match	Yes
38264	GAF-HiskA-RR	GAF: insignificant match	Yes
54330	GAF-PHY-HiskA-HATPase-RR (DPh)	Yes	Yes
44448	GAF-HisKA-HATPase-RR	GAF: insignificant match	Yes

Thalasssiosira pseudonana

ID number Thaps3	Domain architecture	Predicted by Pfam	Predicted by SMART
38732	GAF-HisKA-HATPase-RR	All predicted but GAF: insignificant match	Yes
23423	GAF domain only	Yes	Yes
263128	GAF domain only	Yes	Yes
261065	GAF domain only	Yes	Yes
1565	GAF-PDEasel-HAMP-Guanylate cyclase	GAF and HAMP: insignificant matches	Yes
22848	PAS-GAF-PHY-HiskA-HATPase-RR (DPh)	Yes	Yes
8821	GAF-Guanylate cyclase (CYC)	GAF insignificant match	Yes

Fragilariopsis cylindricus

ID number Fracy	Domain architecture	Predicted by Pfam	Predicted by SMART
183709	GAF-HiskA-RR	Yes	Yes
18284	GAF-HATPase-RR	GAF: insignificant match	Yes
154516	GAF-HATPase-RR	GAF insignificant match	Yes
271509	GAF domain only	Yes	Yes

Annex 1: Table with GAF-containing proteins identified in three diatom species (*P. tricornutum*, *T. pseudonana* and *F. cylindricus*) by PFAM (pfam.sanger.ac.uk/) and SMART (smart.embl-heidelberg.de/) protein database predictions.

Annex 2: Review Article Depauw *et al.*, 2012 (see last pages of the thesis).

Annex 3: plasmid maps

A. PtDPh GAF RNAi knock-down plasmid

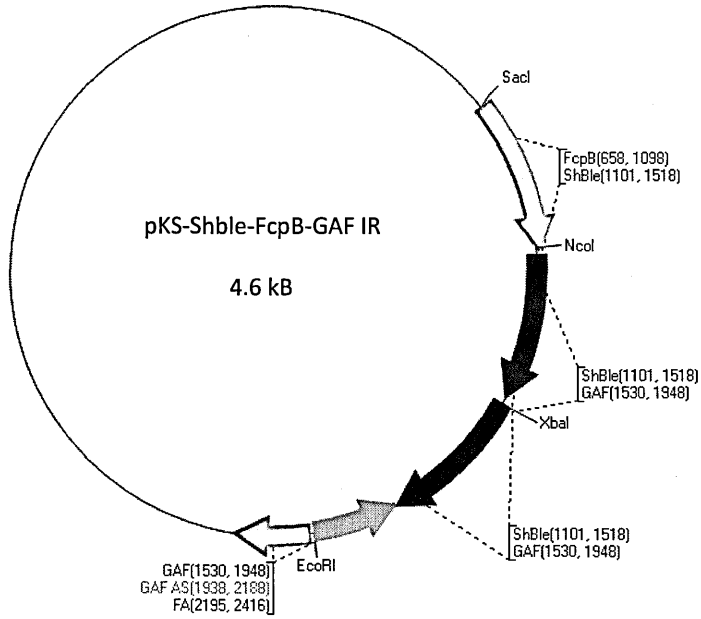

B. PtDPh GAF anti-sense knock-down plasmids

1/pKS FcpB-PHY AS long fragment

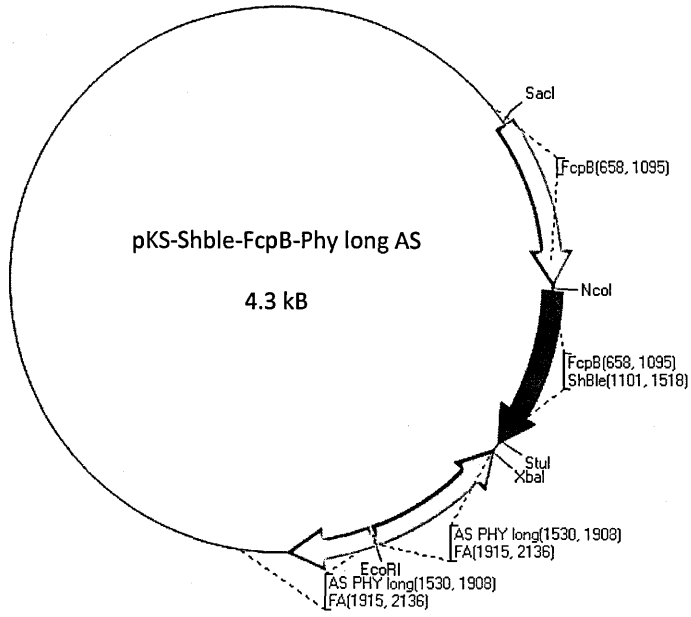

2/ pKS FcpB-PHY AS short fragment

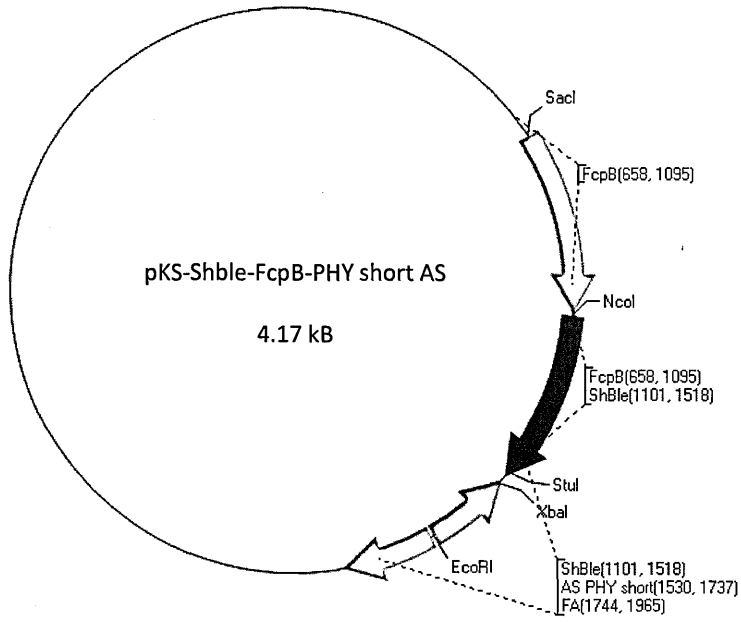

3/ pKS H4-PHY AS (long fragment)

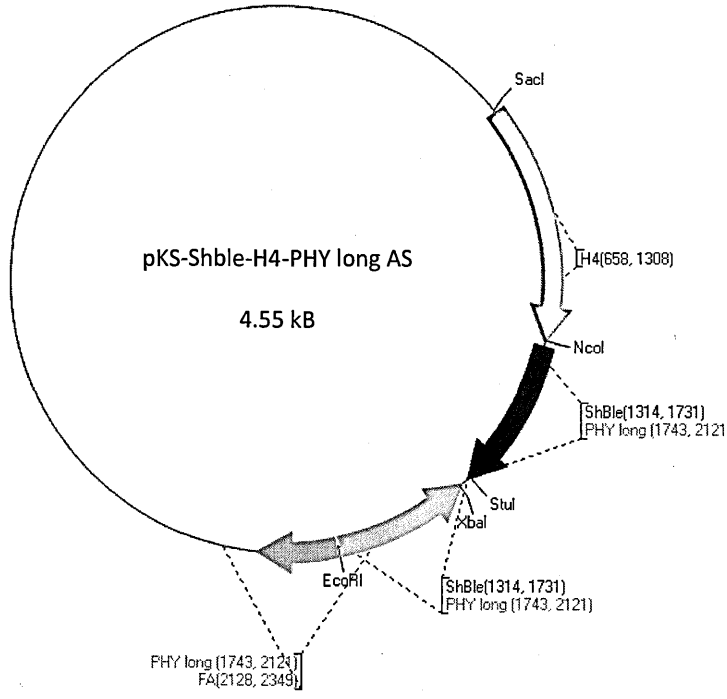

4/ pKS H4-PHY AS (short fragment)

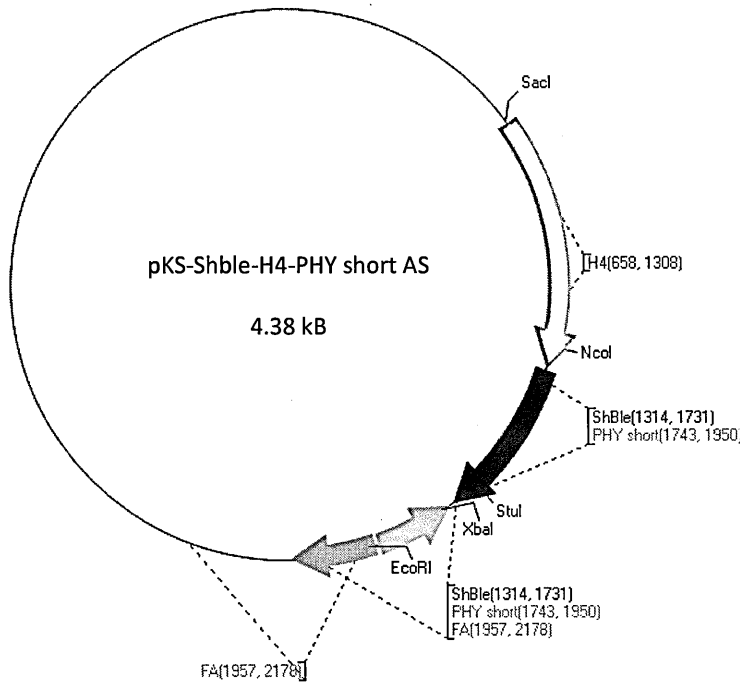

C. PtDPh 3'UTR anti-sense knock-down plasmids

1/ pKS FcpB-PHY 3'UTR AS (short fragment)

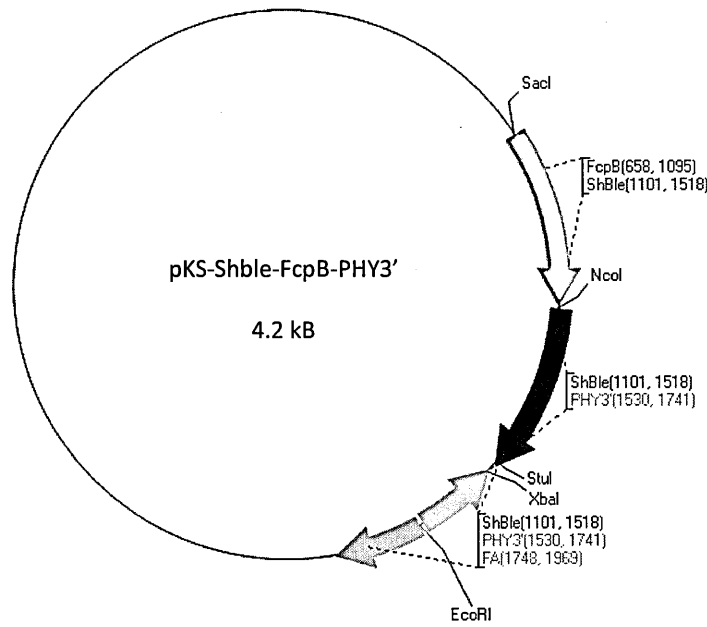

2/ pKS H4-PHY 3'UTR AS (short fragment)

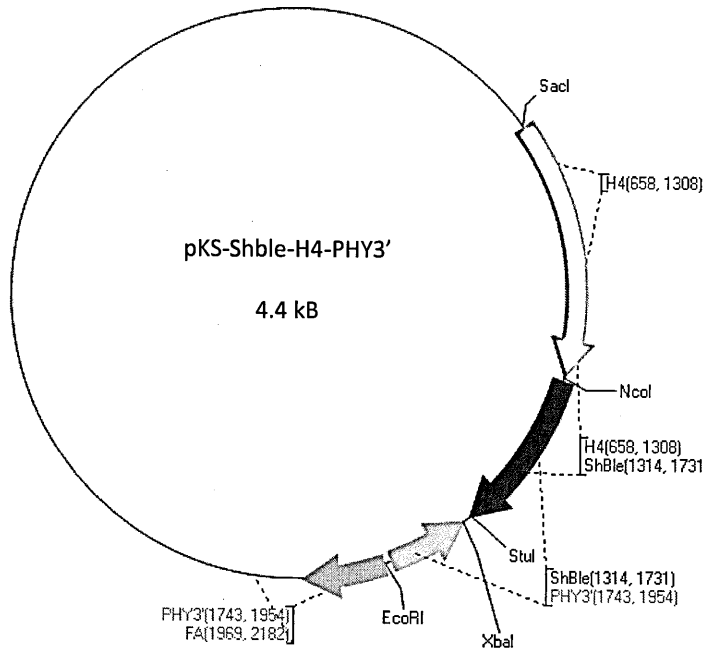

D. PtHO anti-sense knock-down plasmids

1/ pKS H4-PtHO

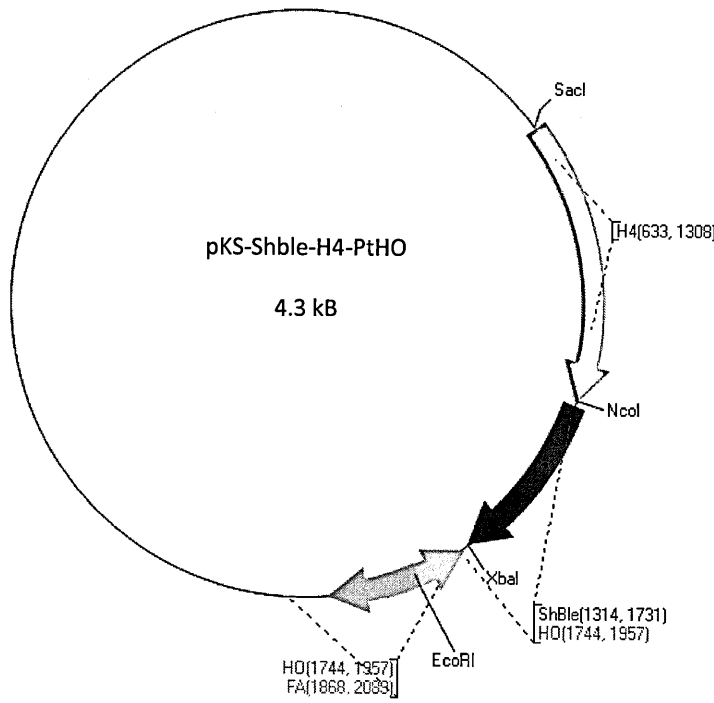

2/ pKS FcpB-PtHO

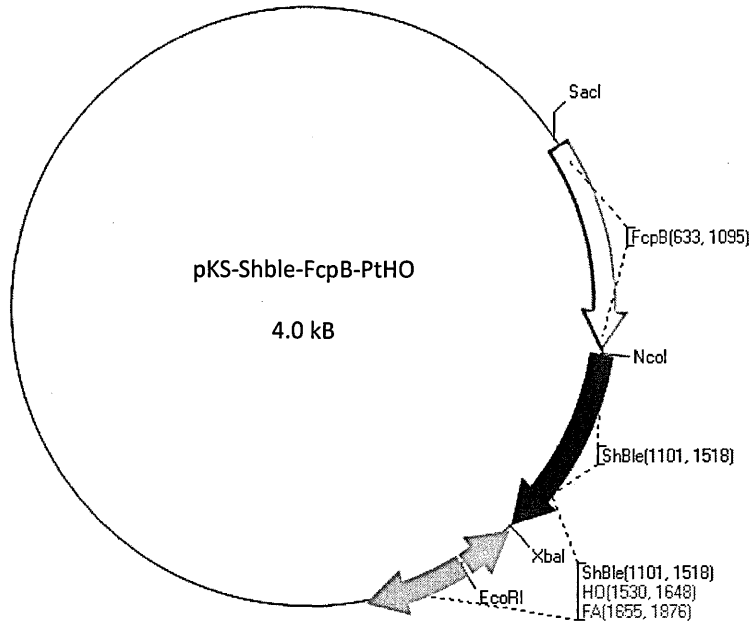

E. Tp DPh anti-sense knock-down plasmids

1/ pNR-TpPHY AS (short fragment) made by Amy Kirkham

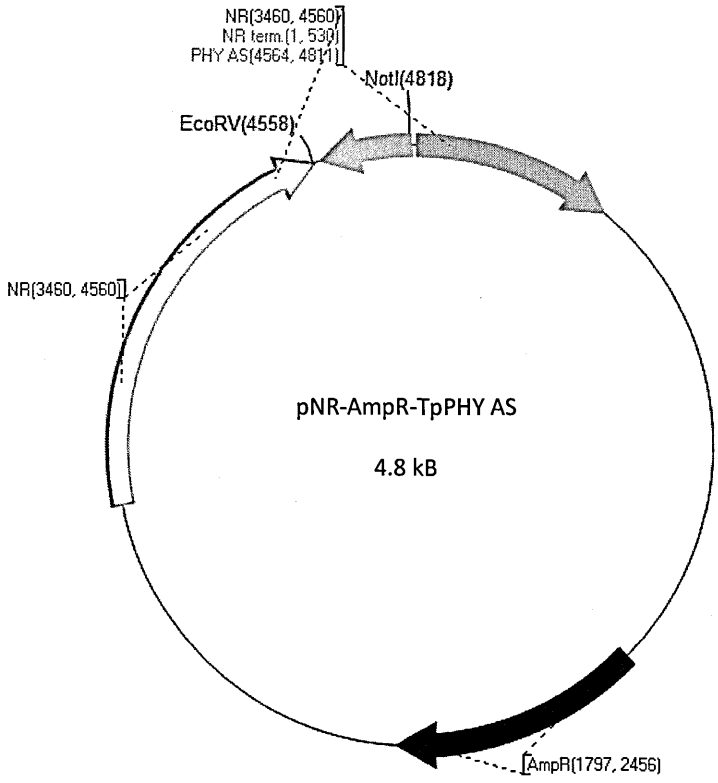

2/ pFcp-TpPHY AS (short fragment)

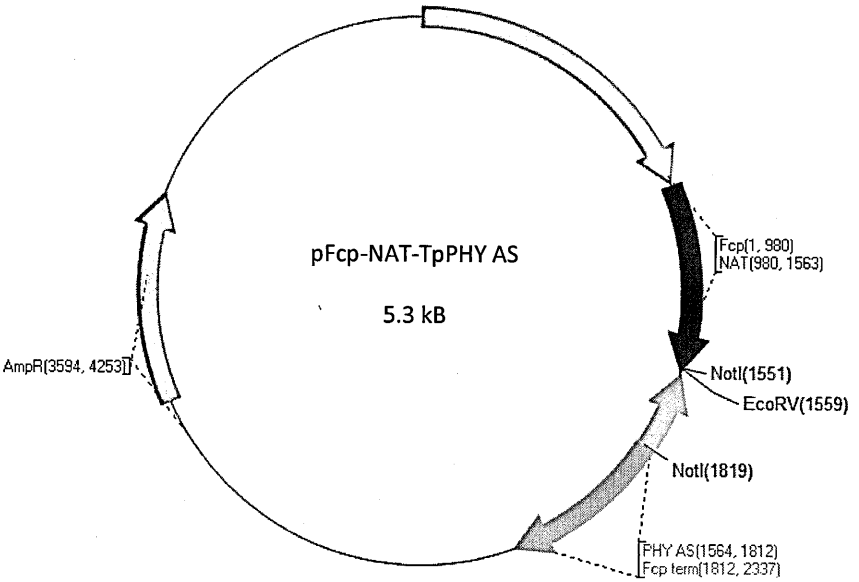

F. pBad-GAF-Myc-HisC expression plasmid

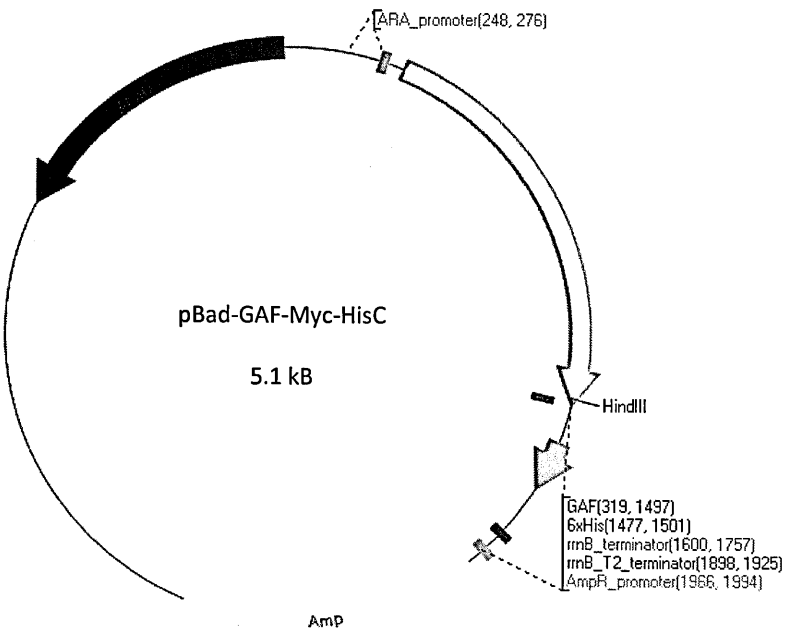

G. pKT270 PebB-PebA expression plasmid

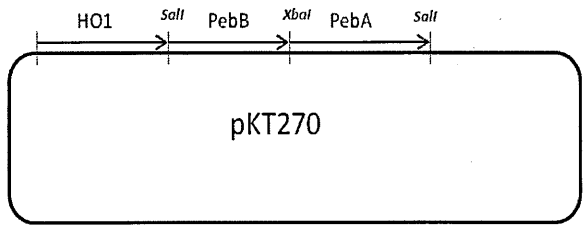

Plasmid map of pKT270 PebB-PebA for expression in *E. coli*. PebB and PebA fragments were amplified, digested with *Xba*I and *Sal*I and introduced into the *Sal*I-digested pKT270-HO1 plasmid.

Annex 4: Overview of DPh sequence, targeted regions for silencing, qPCR oligo's and antibody peptides

Nucleotide sequence of DPh from *Phaeodactylum tricornutum:*

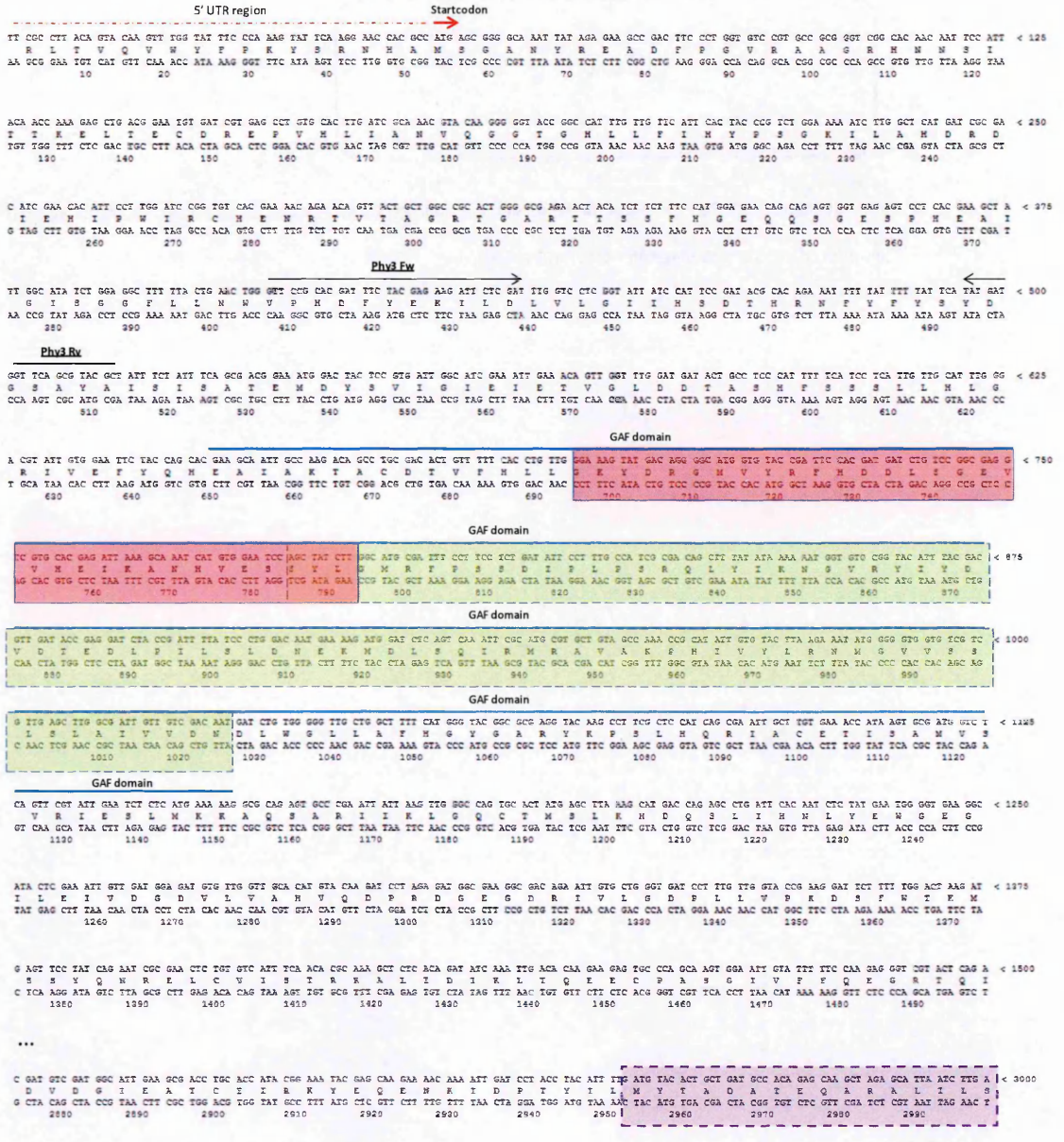

(Sequence continues on next page)

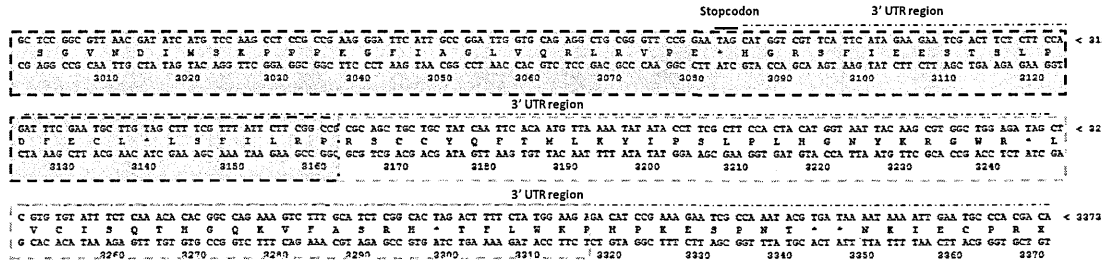
Stopcodon
3' UTR region
3' UTR region
3' UTR region

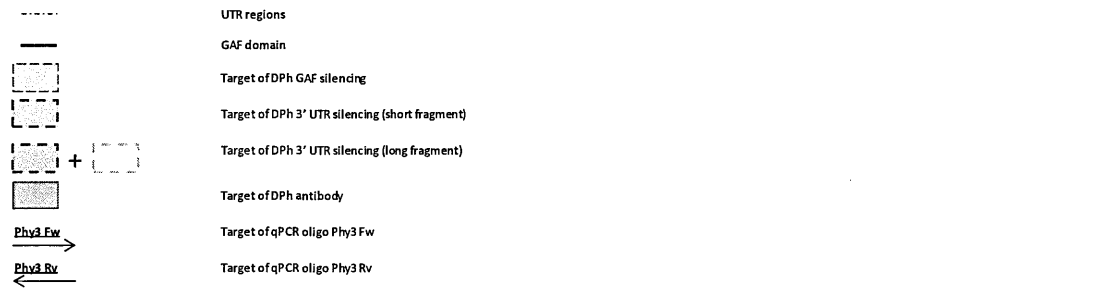
UTR regions
GAF domain
Target of DPh GAF silencing
Target of DPh 3' UTR silencing (short fragment)
Target of DPh 3' UTR silencing (long fragment)
Target of DPh antibody
Phy3 Fw
Target of qPCR oligo Phy3 Fw
Phy3 Rv
Target of qPCR oligo Phy3 Rv

Nucleotide sequence of DPh from *Thalassiosira pseudonana*

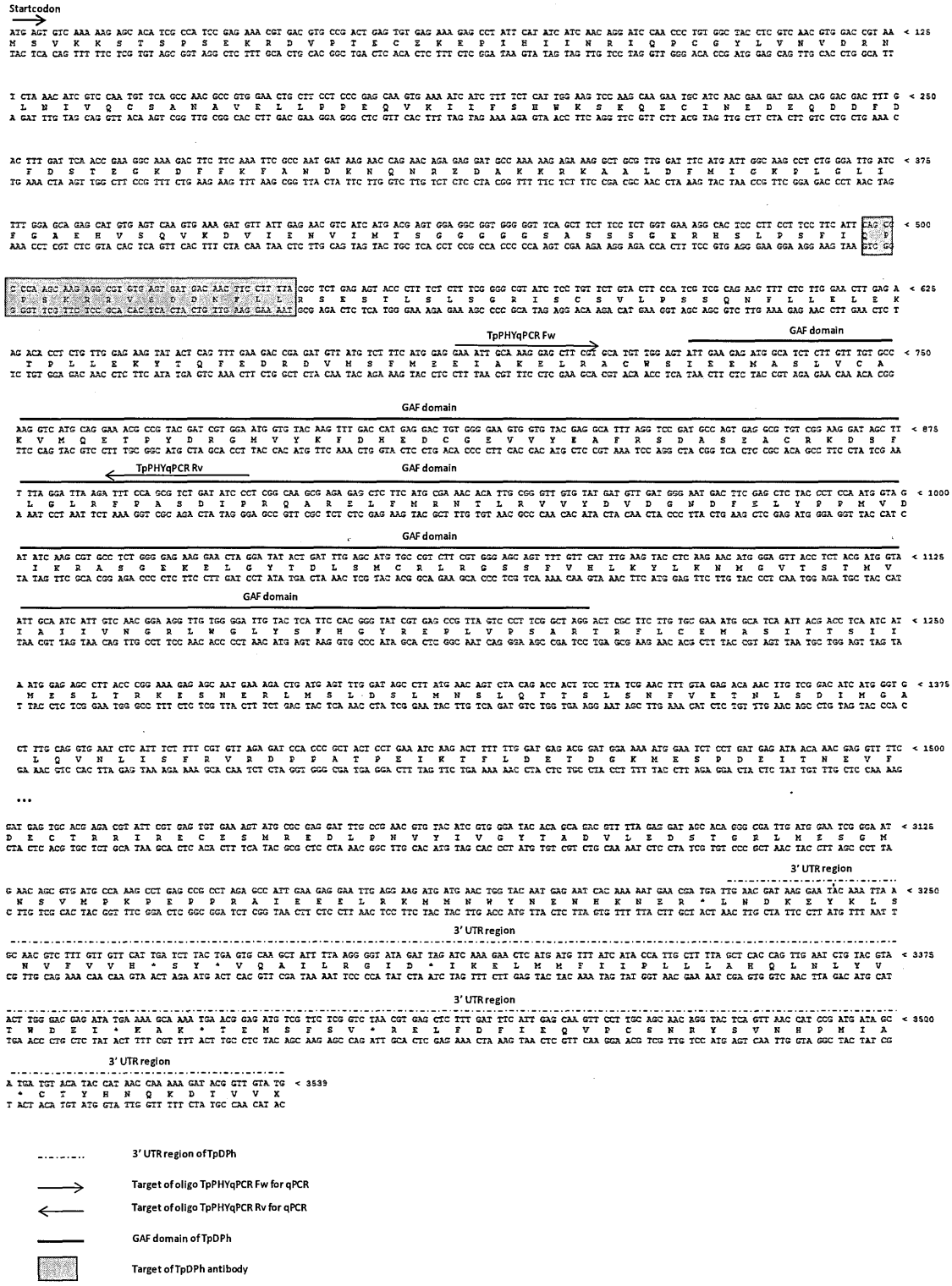

Annex 5: Ct values from qPCR analysis – chapter I

Figure 1.3.8 DPh WT

2 µE				20 µE			
RPS				RPS			
	Ct^1	Ct^2	Ct^3		Ct^1	Ct^2	Ct^3
Dark	27,51	27,29	27,1	Dark	27,81	28,07	27,92
30min	26,53	26,58	26,49	30min	27,16	26,94	26,97
1hr	26,92	26,67	26,66	1hr	26,01	25,91	25,8
2hrs	25,77	25,98	26,29	2hrs	25,44	25,19	25,33
DPh3				DPh3			
	Ct^1	Ct^2	Ct^3		Ct^1	Ct^2	Ct^3
Dark	31,28	31,41	31,13	Dark	31,58	31,62	31,57
30min	30,32	29,72	30,12	30min	30,58	30,28	30,62
1hr	30,55	31,16	30,58	1hr	30,15	30,38	30,26
2 hrs	30,31	29,93	30,07	2 hrs	29,61	29,67	30,33

Figure 1.3.8 HO WT

2 µE				20 µE			
RPS				RPS			
	Ct^1	Ct^2	Ct^3		Ct^1	Ct^2	Ct^3
Dark	27,68	27,69	27,5	Dark	27,96	27,78	27,56
30min	27,09	26,98	26,78	30min	27,09	27,02	27,16
1hr	27,11	27,04	27,06	1hr	26,14	25,94	25,93
2hrs	26	25,9	26,07	2hrs	25,26	25,22	25,24
HO				HO			
	Ct^1	Ct^2	Ct^3		Ct^1	Ct^2	Ct^3
Dark	28,46	28,23	28,13	Dark	28,73	28,94	28,95
30min	27,28	27,18	27,11	30min	27,71	27,54	27,5
1hr	29,07	27,56	27,74	1hr	26,71	26,92	26,71
2 hrs	27,13	27,07	27,22	2 hrs	26,39	26,36	26,44

Figure 1.3.8 PebA WT

2 µE				20 µE			
H4				H4			
	Ct^1	Ct^2	Ct^3		Ct^1	Ct^2	Ct^3
Dark	31,08	31,45	31,65	Dark	27,97	28,01	28
30min	31,5	35,31	30,98	30min	27,02	26,9	26,66
1hr	32,69	32,59	36,85	1hr	25,9	25,85	25,81
2hrs	33,74	32,71	32,58	2hrs	25,47	25,22	25,22
PebA				PebA			
	Ct^1	Ct^2	Ct^3		Ct^1	Ct^2	Ct^3
Dark	29,74	29,62	30,13	Dark	30,77	31,06	30,48
30min	28,58	28,54	28,95	30min	29,52	29,57	29,54
1hr	29,46	29,22	29,17	1hr	29,37	29,24	29,07
2 hrs	29,31	29,35	29,09	2 hrs	28,27	28,4	28,3

Figure 1.3.8 PebB WT

2 µE				20 µE			
H4				H4			
	Ct^1	Ct^2	Ct^3		Ct^1	Ct^2	Ct^3
Dark	31,08	31,45	31,65	Dark	27,97	28,01	28
30min	31,5	35,31	30,98	30min	27,02	26,9	26,66
1hr	34,06	35,13	34,87	1hr	25,9	25,85	25,81
2hrs	33,74	32,71	32,58	2hrs	25,47	25,22	25,22
PebB				PebB			
	Ct^1	Ct^2	Ct^3		Ct^1	Ct^2	Ct^3
Dark	32,09	32,4	32,01	Dark	32,29	32,4	32,7
30min	31,38	31,31	31,62	30min	28,02	27,87	27,69
1hr	31,77	32,25	31,57	1hr	25,42	25,39	25,41
2 hrs	31,28	31,41	31,7	2 hrs	23,86	23,94	24,08

Figure 1.3.8 AOX WT

2 µE				20 µE			
RPS				RPS			
	Ct^1	Ct^2	Ct^3		Ct^1	Ct^2	Ct^3
Dark	27,51	27,29	27,1	Dark	27,81	28,07	27,92
30min	26,53	26,58	26,49	30min	27,16	26,94	26,97
1hr	26,92	26,67	26,66	1hr	26,01	25,91	25,8
2hrs	25,77	25,98	26,29	2hrs	25,44	25,19	25,33
AOX				AOX			
	Ct^1	Ct^2	Ct^3		Ct^1	Ct^2	Ct^3
Dark	29,64	29,61	29,58	Dark	29,75	29,94	30,43
30min	27,12	27,16	27,03	30min	26,45	26,46	26,44
1hr	28,24	28,36	28,33	1hr	26,68	26,46	26,5
2 hrs	27,95	27,71	28	2 hrs	26,82	26,68	26,72

Figure 1.3.8 PDS WT

2 µE				20 µE			
RPS				RPS			
	Ct^1	Ct^2	Ct^3		Ct^1	Ct^2	Ct^3
Dark	27,68	27,69	27,5	Dark	27,96	27,78	27,56
30min	27,09	26,98	26,78	30min	27,09	27,02	27,16
1hr	27,11	27,04	27,06	1hr	26,14	25,94	25,93
2hrs	26	25,9	26,07	2hrs	25,26	25,22	25,24
PDS				PDS			
	Ct^1	Ct^2	Ct^3		Ct^1	Ct^2	Ct^3
Dark	31,86	32,28	34,03	Dark	32,81	33,49	34,19
30min	31,34	31,32	31,67	30min	31,98	31,7	32,23
1hr	30,64	30,77	30,64	1hr	30,65	30,4	30,15
2 hrs	29,74	29,88	29,83	2 hrs	29,03	29,33	28,89

Figure 1.3.8 VDL WT

2 µE				20 µE			
RPS				RPS			
	Ct^1	Ct^2	Ct^3		Ct^1	Ct^2	Ct^3
Dark	27,68	27,53	27,47	Dark	29,51	29,43	29,17
30min	27,02	26,76	26,72	30min	27,21	26,98	26,99
1hr	27,8	27,93	28,24	1hr	26,63	26,55	37,76
2hrs	29,52	25,96	26,03	2hrs	26,59	26,83	26,75
VDL1				VDL1			
	Ct^1	Ct^2	Ct^3		Ct^1	Ct^2	Ct^3
Dark	32,39	32,4	31,92	Dark	34,06	33,78	33,62
30min	31,09	31,24	31,15	30min	32,06	31,81	31,69
1hr	31,64	31,4	31,28	1hr	30,57	30,93	N/A
2 hrs	30,36	30,14	30,17	2 hrs	30,97	30,97	30,9

Figure 1.3.8 ZEP2 WT

2 µE				20 µE			
RPS				RPS			
	Ct^1	Ct^2	Ct^3		Ct^1	Ct^2	Ct^3
Dark	27,68	27,69	27,5	Dark	27,81	28,07	27,92
30min	27,09	26,98	26,78	30min	27,16	26,94	26,97
1hr	27,11	27,04	27,06	1hr	26,01	25,91	25,8
2hrs	26	25,9	26,07	2hrs	25,44	25,19	25,33
ZEP2				ZEP2			
	Ct^1	Ct^2	Ct^3		Ct^1	Ct^2	Ct^3
Dark	32,18	31,71	N/A	Dark	32,74	32,35	32,88
30min	30,09	30,27	29,18	30min	30,02	29,84	29,88
1hr	29,21	29,1	29,21	1hr	28,23	28,41	28,66
2 hrs	29	28,98	28,81	2 hrs	26,93	26,91	27,03

Figure 1.3.8 GSAT WT

2 µE				20 µE			
H4				H4			
	Ct^1	Ct^2	Ct^3		Ct^1	Ct^2	Ct^3
Dark	31,08	31,45	31,65	Dark	31,08	31,45	31,65
30min	31,5	35,31	30,98	30min	31,5	35,31	30,98
1hr	34,06	35,13	34,87	1hr	34,06	35,13	34,87
2hrs	33,74	32,71	32,58	2hrs	33,74	32,71	32,58
GSAT				GSAT			
	Ct^1	Ct^2	Ct^3		Ct^1	Ct^2	Ct^3
Dark	31,56	31,81	32,01	Dark	32,5	32,48	32,74
30min	27,72	27,84	27,54	30min	28,25	28,13	28,04
1hr	26,32	26,43	26,45	1hr	25,53	25,48	25,48
2 hrs	25,13	25,02	25,25	2 hrs	24,12	24,1	24,28

Figure 1.3.8 HEMA WT

2 µE				20 µE			
RPS				RPS			
	Ct^1	Ct^2	Ct^3		Ct^1	Ct^2	Ct^3
Dark	27,68	27,53	27,47	Dark	29,51	29,43	29,17
30min	27,02	26,76	26,72	30min	27,21	26,98	26,99
1hr	27,8	27,93	28,24	1hr	26,63	26,55	37,76
2hrs	29,52	25,96	26,03	2hrs	26,59	26,83	26,75
HEMA				HEMA			
	Ct^1	Ct^2	Ct^3		Ct^1	Ct^2	Ct^3
Dark	31,67	32,08	31,5	Dark	32,97	33,78	33,31
30min	28,69	28,93	29,16	30min	28,92	29,07	29,01
1hr	29,37	29,37	29,61	1hr	28,42	28,55	N/A
2 hrs	28,6	28,26	28,32	2 hrs	28,87	28,99	29,08

Figure 1.3.8 CHLH1 WT

2 µE				20 µE			
RPS				RPS			
	Ct^1	Ct^2	Ct^3		Ct^1	Ct^2	Ct^3
Dark	27,68	27,53	27,47	Dark	29,51	29,43	29,17
30min	27,02	26,76	26,72	30min	27,21	26,98	26,99
1hr	27,8	27,93	28,24	1hr	26,63	26,55	37,76
2hrs	29,52	25,96	26,03	2hrs	26,59	26,83	26,75
CHLH1				CHLH1			
	Ct^1	Ct^2	Ct^3		Ct^1	Ct^2	Ct^3
Dark	33,35	33,73	33,27	Dark	34,06	34,7	34,36
30min	30,51	30,93	30,89	30min	30,54	30,46	30,19
1hr	28,91	29,07	28,97	1hr	28,09	28	N/A
2 hrs	27,53	27,28	27,64	2 hrs	27,75	27,91	27,94

Figure 1.3.8 CHLH2 WT

2 µE				20 µE			
RPS				RPS			
	Ct^1	Ct^2	Ct^3		Ct^1	Ct^2	Ct^3
Dark	27,87	27,94	N/A	Dark	29,57	29,5	29,47
30min	27,26	26,99	27,07	30min	27,34	27,2	27,09
1hr	28,35	28,29	28,27	1hr	26,6	26,81	26,63
2hrs	26,28	26,3	26,35	2hrs	26,88	26,62	26,94
CHLH2				CHLH2			
	Ct^1	Ct^2	Ct^3		Ct^1	Ct^2	Ct^3
Dark	28,83	28,57	N/A	Dark	30,49	30,4	30,48
30min	27,04	27,01	26,83	30min	27,31	27,36	27,35
1hr	28,23	28,32	28,11	1hr	27,5	27,39	N/A
2 hrs	27,64	27,5	27,39	2 hrs	28,3	28,16	28,3

Figure 1.3.8 POR1 WT

2 µE				20 µE			
RPS				RPS			
	Ct^1	Ct^2	Ct^3		Ct^1	Ct^2	Ct^3
Dark	27,87	27,94	N/A	Dark	29,41	29,49	29,3
30min	27,26	26,99	27,07	30min	27,28	27,03	27,16
1hr	28,35	28,29	28,27	1hr	27,28	27,03	27,16
2hrs	26,28	26,3	26,35	2hrs	26,87	26,85	26,78
POR1				POR1			
	Ct^1	Ct^2	Ct^3		Ct^1	Ct^2	Ct^3
Dark	27,21	27,11	N/A	Dark	28,3	28,22	28,25
30min	26,36	26,24	26,29	30min	26,23	26,28	26,37
1hr	27,03	27,29	27,14	1hr	26,23	26,28	26,37
2 hrs	25,84	25,68	25,62	2 hrs	26,11	26,07	25,9

Figure 1.3.8 POR2 WT

2 µE				20 µE			
RPS				RPS			
	Ct^1	Ct^2	Ct^3		Ct^1	Ct^2	Ct^3
Dark	27,87	27,94	N/A	Dark	29,41	29,49	29,3
30min	27,26	26,99	27,07	30min	27,28	27,03	27,16
1hr	28,35	28,29	28,27	1hr	27,18	27	26,96
2hrs	26,28	26,3	26,35	2hrs	26,87	26,85	26,78
POR1				POR1			
	Ct^1	Ct^2	Ct^3		Ct^1	Ct^2	Ct^3
Dark	33,52	33,55	40,33	Dark	33,64	33,02	33,63
30min	29,48	29,23	29,38	30min	28,81	28,88	28,87
1hr	28,03	28,03	27,94	1hr	27,28	27,03	27,16
2 hrs	26,76	26,51	26,63	2 hrs	26,3	26,3	26,16

Figure 1.3.9 0,2 µE GSAT WT + DPh knock-down

H4	**Dark**					GSAT	**Dark**			
	WT	dph-1	dph1'	dph5'			WT	dph-1	dph1'	dph5'
Ct^1	23,14	24,01	23,12	25,21		Ct^1	30,99	33,6	33,85	34,52
Ct^2	23,1	23,89	23,14	23,32		Ct^2	29,93	32,96	34,03	33,29
Ct^3	23,08	23,99	23,21	22,56		Ct^3	30,15	31,74	33,87	35,11
H4	**10' Red 0,2**					GSAT	**10' Red 0,2**			
	WT	dph-1	dph1'	dph5'			WT	dph-1	dph1'	dph5'
Ct^1	21,78	23	23,13	22,45		Ct^1	30,17	31,62	35,09	33,29
Ct^2	21,89	22,39	22,72	22,43		Ct^2	30,67	31,09	34,23	33,78
Ct^3	24,28	25,49	24,21	22,34		Ct^3	30,98	31,3	34,13	34,08
H4	**30' Red 0,2**					GSAT	**30' Red 0,2**			
	WT	dph-1	dph1'	dph5'			WT	dph-1	dph1'	dph5'
Ct^1	22,66	26,17	23,29	23,65		Ct^1	29,48	31,46	33,86	34,39
Ct^2	21,68	23,24	22,68	24,78		Ct^2	29,55	31,8	33,69	34,32
Ct^3	21,57	22,25	23,68	24,77		Ct^3	29,62	32,2	34,2	34,09
H4	**1hr Red 0,2**					GSAT	**1hr Red 0,2**			
	WT	dph-1	dph1'	dph5'			WT	dph-1	dph1'	dph5'
Ct^1	27,57	23,45	25,66	23,76		Ct^1	28,52	30,33	31,16	28,94
Ct^2	22,23	23,93	22,01	22,28		Ct^2	28,3	30,32	31,14	30,14
Ct^3	23,16	22,95	22,74	28,65		Ct^3	28,82	30,79	30,51	N/A

Figure 1.3.9 0,2 µE ZEP2 WT + DPh knock-down

H4	**Dark**					ZEP2	**Dark**			
	WT	dph-1	dph1'	dph5'			WT	dph-1	dph1'	dph5'
Ct^1	23,14	24,01	23,12	25,21		Ct^1	28,49	28,94	28,34	30,19
Ct^2	23,1	23,89	23,14	23,32		Ct^2	28,26	28,87	28,63	29,98
Ct^3	23,08	23,99	23,21	22,56		Ct^3	28,44	28,43	28,53	30,07
H4	**10' Red 0,2**					ZEP2	**10' Red 0,2**			
	WT	dph-1	dph1'	dph5'			WT	dph-1	dph1'	dph5'
Ct^1	21,78	23	23,13	22,45		Ct^1	28,25	28,7	28,57	29,56
Ct^2	21,89	22,39	22,72	22,43		Ct^2	28,28	28,34	28,57	29,69
Ct^3	24,28	25,49	24,21	22,34		Ct^3	28,27	28,36	28,94	29,54
H4	**30' Red 0,2**					ZEP2	**30' Red 0,2**			
	WT	dph-1	dph1'	dph5'			WT	dph-1	dph1'	dph5'
Ct^1	22,66	26,17	23,29	23,65		Ct^1	28,34	28,99	28,64	30,09
Ct^2	21,68	23,24	22,68	24,78		Ct^2	28,31	28,63	28,82	30,21
Ct^3	21,57	22,25	23,68	24,77		Ct^3	28,29	28,73	28,88	30,28
H4	**1hr Red 0,2**					ZEP2	**1hr Red 0,2**			
	WT	dph-1	dph1'	dph5'			WT	dph-1	dph1'	dph5'
Ct^1	27,57	23,45	25,66	23,76		Ct^1	27,06	27,64	27,13	27,5
Ct^2	22,23	23,93	22,01	22,28		Ct^2	27,02	27,92	26,78	28
Ct^3	23,16	22,95	22,74	28,65		Ct^3	26,85	N/A	N/A	N/A

Figure 1.3.9 0,2 µE AOX WT + DPh knock-down

H4	**Dark**			
	WT	dph-1	dph1'	dph5'
Ct^1	23,14	24,01	23,12	25,21
Ct^2	23,1	23,89	23,14	23,32
Ct^3	23,08	23,99	23,21	22,56
H4	**10' Red 0,2**			
	WT	dph-1	dph1'	dph5'
Ct^1	21,78	23	23,13	22,45
Ct^2	21,89	22,39	22,72	22,43
Ct^3	24,28	25,49	24,21	22,34
H4	**30' Red 0,2**			
	WT	dph-1	dph1'	dph5'
Ct^1	22,66	26,17	23,29	23,65
Ct^2	21,68	23,24	22,68	24,78
Ct^3	21,57	22,25	23,68	24,77
H4	**1hr Red 0,2**			
	WT	dph-1	dph1'	dph5'
Ct^1	27,57	23,45	25,66	23,76
Ct^2	22,23	23,93	22,01	22,28
Ct^3	23,16	22,95	22,74	28,65

AOX	**Dark**			
	WT	dph-1	dph1'	dph5'
Ct^1	28,19	29,08	28,53	28,77
Ct^2	27,99	28,71	28,84	29,2
Ct^3	28,39	28,63	28,31	28,87
AOX	**10' Red 0,2**			
	WT	dph-1	dph1'	dph5'
Ct^1	27,72	28,36	28,59	29,09
Ct^2	27,49	28,06	28,47	28,61
Ct^3	27,5	28,11	28,9	28,83
AOX	**30' Red 0,2**			
	WT	dph-1	dph1'	dph5'
Ct^1	26,64	27,92	28,34	28,73
Ct^2	26,68	27,52	28,28	28,6
Ct^3	26,77	27,94	28,5	28,66
AOX	**1hr Red 0,2**			
	WT	dph-1	dph1'	dph5'
Ct^1	26,82	27,35	27,47	27,87
Ct^2	26,8	27,07	27,47	27,99
Ct^3	26,48	27,27	N/A	N/A

Figure 1.3.9 0,2 µE CHLH1 WT + DPh knock-down

H4	**Dark**			
	WT	dph-1	dph1'	dph5'
Ct^1	23,14	24,01	23,12	25,21
Ct^2	23,1	23,89	23,14	23,32
Ct^3	23,08	23,99	23,21	22,56
H4	**10' Red 0,2**			
	WT	dph-1	dph1'	dph5'
Ct^1	21,78	23	23,13	22,45
Ct^2	21,89	22,39	22,72	22,43
Ct^3	24,28	25,49	24,21	22,34
H4	**30' Red 0,2**			
	WT	dph-1	dph1'	dph5'
Ct^1	22,66	26,17	23,29	23,65
Ct^2	21,68	23,24	22,68	24,78
Ct^3	21,57	22,25	23,68	24,77
H4	**1hr Red 0,2**			
	WT	dph-1	dph1'	dph5'
Ct^1	27,57	23,45	25,66	23,76
Ct^2	22,23	23,93	22,01	22,28
Ct^3	23,16	22,95	22,74	28,65

CHLH1	**Dark**			
	WT	dph-1	dph1'	dph5'
Ct^1	27,76	29,47	32,46	31,63
Ct^2	27,66	29,47	33,13	32,86
Ct^3	27,73	29,63	31,8	32,34
CHLH1	**10' Red 0,2**			
	WT	dph-1	dph1'	dph5'
Ct^1	27,6	28,34	31,13	31,1
Ct^2	27,45	28,32	31,69	30,78
Ct^3	27,81	28,09	31,36	31,47
CHLH1	**30' Red 0,2**			
	WT	dph-1	dph1'	dph5'
Ct^1	27,86	29,81	32,81	31,15
Ct^2	28,08	29,05	32,01	31,41
Ct^3	27,97	29,4	31,7	30,6
CHLH1	**1hr Red 0,2**			
	WT	dph-1	dph1'	dph5'
Ct^1	27,15	28,16	30,42	29,16
Ct^2	27,15	28,42	30,15	29,24
Ct^3	27,2	27,81	30,18	29,54

Figure 1.3.9 2 µE GSAT WT + DPh knock-down

H4	**Dark**					GSAT	**Dark**			
	WT	dph-1	dph1'	dph5'			WT	dph-1	dph1'	dph5'
Ct^1	22,98	24,78	23,17	25,31		Ct^1	26,99	29,13	28,14	30,28
Ct^2	23,05	24,77	25,39	25,33		Ct^2	27,1	29,17	28,34	30,04
Ct^3	22,97	25,1	23,59	25,3		Ct^3	27,17	29	28,29	30,14
H4	**10' Red**						**10' Red**			
	WT	dph-1	dph1'	dph5'			WT	dph-1	dph1'	dph5'
Ct^1	25,09	24,21	23,69	24,62		Ct^1	28,8	28,27	27,98	29,23
Ct^2	25,26	24,32	23,87	24,35		Ct^2	29,04	28,22	28,3	29,31
Ct^3	25,22	24,08	24,19	24,48		Ct^3	28,58	28,42	28,04	29,29
H4	**30' Red**						**30' Red**			
	WT	dph-1	dph1'	dph5'			WT	dph-1	dph1'	dph5'
Ct^1	23,22	23,23	23,3	23,14		Ct^1	26,43	26,41	26,59	26,47
Ct^2	23,1	23,28	23,2	23,29		Ct^2	26,21	26,39	27,02	26,43
Ct^3	23,09	23,3	22,98	23,3		Ct^3	26,24	26,17	26,37	26,48
H4	**1hr Red**						**1hr Red**			
	WT	dph-1	dph1'	dph5'			WT	dph-1	dph1'	dph5'
Ct^1	24,03	23,64	23,18	22,68		Ct^1	26,33	26,45	24,92	24,66
Ct^2	23,89	23,59	23,08	22,66		Ct^2	26,25	26,35	24,48	24,77
Ct^3	23,56	23,21	23,3	22,87		Ct^3	26,29	26,52	24,82	25,06

Figure 1.3.9 2 µE ZEP2 WT + DPh knock-down

H4	**Dark**					ZEP2	**Dark**			
	WT	dph-1	dph1'	dph5'			WT	dph-1	dph1'	dph5'
Ct^1	22,98	24,78	23,17	25,31		Ct^1	29,39	30,97	29,61	32,13
Ct^2	23,05	24,77	25,39	25,33		Ct^2	29,29	31,04	30,38	31,73
Ct^3	22,97	25,1	23,59	25,3		Ct^3	29,21	30,99	30,51	32,17
H4	**10' Red**					ZEP2	**10' Red**			
	WT	dph-1	dph1'	dph5'			WT	dph-1	dph1'	dph5'
Ct^1	25,09	24,21	23,69	24,62		Ct^1	31,44	31,29	30,96	N/A
Ct^2	25,26	24,32	23,87	24,35		Ct^2	31,36	31,09	31,02	N/A
Ct^3	25,22	24,08	24,19	24,48		Ct^3	31,68	31,11	31,04	N/A
H4	**30' Red**					ZEP2	**30' Red**			
	WT	dph-1	dph1'	dph5'			WT	dph-1	dph1'	dph5'
Ct^1	23,22	23,23	23,3	23,14		Ct^1	29,22	29,06	29,37	29,96
Ct^2	23,1	23,28	23,2	23,29		Ct^2	29,46	29,32	29,47	29,95
Ct^3	23,09	23,3	22,98	23,3		Ct^3	29,23	29,06	29,32	29,63
H4	**1hr Red**					ZEP2	**1hr Red**			
	WT	dph-1	dph1'	dph5'			WT	dph-1	dph1'	dph5'
Ct^1	24,03	23,64	23,18	22,68		Ct^1	31,2	N/A	26,45	27,07
Ct^2	23,89	23,59	23,08	22,66		Ct^2	30,82	N/A	26,51	27,16
Ct^3	23,56	23,21	23,3	22,87		Ct^3	30,72	N/A	26,48	27,27

Figure 1.3.9 2 µE AOX WT + DPh knock-down

H4	**Dark**				AOX	**Dark**			
	WT	dph-1	dph1'	dph5'		WT	dph-1	dph1'	dph5'
Ct^1	22,98	24,78	23,17	25,31	Ct^1	27,73	29,22	29,12	29,14
Ct^2	23,05	24,77	25,39	25,33	Ct^2	27,38	29,24	29,32	28,69
Ct^3	22,97	25,1	23,59	25,3	Ct^3	27,64	29,5	29,22	28,3
H4	**10' Red**				AOX	**10' Red**			
	WT	dph-1	dph1'	dph5'		WT	dph-1	dph1'	dph5'
Ct^1	25,09	24,21	23,69	24,62	Ct^1	28,37	28,59	28,48	27,24
Ct^2	25,26	24,32	23,87	24,35	Ct^2	29,05	28,29	28,49	27,55
Ct^3	25,22	24,08	24,19	24,48	Ct^3	28,57	28,45	29,05	27,21
H4	**30' Red**				AOX	**30' Red**			
	WT	dph-1	dph1'	dph5'		WT	dph-1	dph1'	dph5'
Ct^1	23,22	23,23	23,3	23,14	Ct^1	29,19	25,53	25,46	25,13
Ct^2	23,1	23,28	23,2	23,29	Ct^2	29,49	25,48	25,5	25,31
Ct^3	23,09	23,3	22,98	23,3	Ct^3	29,51	25,37	25,34	25,2
H4	**1hr Red**				AOX	**1hr Red**			
	WT	dph-1	dph1'	dph5'		WT	dph-1	dph1'	dph5'
Ct^1	24,03	23,64	23,18	22,68	Ct^1	26,6	27,51	25,52	27,09
Ct^2	23,89	23,59	23,08	22,66	Ct^2	26,65	27,18	25,39	26,78
Ct^3	23,56	23,21	23,3	22,87	Ct^3	26,51	27,61	25,3	26,84

Figure 1.3.9 2 µE CHLH1 WT + DPh knock-down

H4	**Dark**				CHLH1	**Dark**			
	WT	dph-1	dph1'	dph5'		WT	dph-1	dph1'	dph5'
Ct^1	22,98	24,78	23,17	25,31	Ct^1	29,91	30,9	33,06	33,35
Ct^2	23,05	24,77	25,39	25,33	Ct^2	29,9	30,56	33,08	32,88
Ct^3	22,97	25,1	23,59	25,3	Ct^3	29,83	30,74	32,85	33,63
H4	**10' Red**				CHLH1	**10' Red**			
	WT	dph-1	dph1'	dph5'		WT	dph-1	dph1'	dph5'
Ct^1	25,09	24,21	23,69	24,62	Ct^1	31,13	31,02	33,09	N/A
Ct^2	25,26	24,32	23,87	24,35	Ct^2	31,57	30,54	33,32	N/A
Ct^3	25,22	24,08	24,19	24,48	Ct^3	31,76	31,34	32,37	N/A
H4	**30' Red**				CHLH1	**30' Red**			
	WT	dph-1	dph1'	dph5'		WT	dph-1	dph1'	dph5'
Ct^1	23,22	23,23	23,3	23,14	Ct^1	29,03	29,81	30,26	29,5
Ct^2	23,1	23,28	23,2	23,29	Ct^2	28,76	29,66	30,34	29,48
Ct^3	23,09	23,3	22,98	23,3	Ct^3	29,05	29,62	30,25	29,66
H4	**1hr Red**				CHLH1	**1hr Red**			
	WT	dph-1	dph1'	dph5'		WT	dph-1	dph1'	dph5'
Ct^1	24,03	23,64	23,18	22,68	Ct^1	27,27	N/A	26,31	25,55
Ct^2	23,89	23,59	23,08	22,66	Ct^2	27,31	N/A	26,33	25,74
Ct^3	23,56	23,21	23,3	22,87	Ct^3	27,12	N/A	26,22	25,52

Figure 1.3.9 20 µE GSAT WT + DPh knock-down

H4	**Dark**				GSAT	**Dark**			
	WT	dph-1	dph1'	dph5'		WT	dph-1	dph1'	dph5'
Ct^1	21,89	21,67	22,1	27,02	Ct^1	32,44	33,1	34,44	37,04
Ct^2	22,48	21,66	22,68	26,48	Ct^2	30,17	33,24	34,63	37,16
Ct^3	22,27	21,56	22,54	26,56	Ct^3	30,89	33,09	35,02	35,56
H4	**10' Red**				GSAT	**10' Red**			
	WT	dph-1	dph1'	dph5'		WT	dph-1	dph1'	dph5'
Ct^1	21,61	22,01	21,19	21,71	Ct^1	32,61	33,07	32,77	33,32
Ct^2	21,58	22,78	21,13	21,64	Ct^2	31,45	32,22	32,21	33,21
Ct^3	22,04	21,87	21,41	21,61	Ct^3	31,27	31,96	32,61	33,75
H4	**30' Red**				GSAT	**30' Red**			
	WT	dph-1	dph1'	dph5'		WT	dph-1	dph1'	dph5'
Ct^1	23,9	22,58	23,41	24,15	Ct^1	30,27	30,02	30,29	30,76
Ct^2	23,82	22,56	23,33	23,95	Ct^2	30,11	29,65	30,5	31,47
Ct^3	24,2	22,35	23,34	24,05	Ct^3	30,25	29,66	30,15	30,87
H4	**1hr Red**				GSAT	**1hr Red**			
	WT	dph-1	dph1'	dph5'		WT	dph-1	dph1'	dph5'
Ct^1	27,57	24,07	24,07	23,49	Ct^1	31,66	27,47	28,37	27,08
Ct^2	27,59	23,59	23,59	23,49	Ct^2	31,46	27,91	29,25	26,99
Ct^3	27,61	23,52	23,3	22,87	Ct^3	32,35	N/A	N/A	N/A

Figure 1.3.9 20 µE ZEP2 WT + DPh knock-down

H4	**Dark**				ZEP2	**Dark**			
	WT	dph-1	dph1'	dph5'		WT	dph-1	dph1'	dph5'
Ct^1	21,89	21,67	22,1	27,02	Ct^1	28,74	29,08	29,36	34,26
Ct^2	22,48	21,66	22,68	26,48	Ct^2	28,46	29,19	29,76	34,81
Ct^3	22,27	21,56	22,54	26,56	Ct^3	28,82	29,47	30,28	34,86
H4	**10' Red 0,2**				ZEP2	**' Red 0,2**			
	WT	dph-1	dph1'	dph5'		WT	dph-1	dph1'	dph5'
Ct^1	21,61	22,01	21,19	21,71	Ct^1	29,44	29,21	29,29	30,7
Ct^2	21,58	22,78	21,13	21,64	Ct^2	28,86	29,28	29,06	30,66
Ct^3	22,04	21,87	21,41	21,61	Ct^3	29,65	29,14	30,08	30,6
H4	**30' Red 0,2**				ZEP2	**' Red 0,2**			
	WT	dph-1	dph1'	dph5'		WT	dph-1	dph1'	dph5'
Ct^1	23,9	22,58	23,41	24,15	Ct^1	29,83	27,05	27,91	29,7
Ct^2	23,82	22,56	23,33	23,95	Ct^2	29,45	27,31	28,16	29,74
Ct^3	24,2	22,35	23,34	24,05	Ct^3	29,52	27,31	28,33	29,92
H4	**1hr Red 0,2**				ZEP2	**ır Red 0,2**			
	WT	dph-1	dph1'	dph5'		WT	dph-1	dph1'	dph5'
Ct^1	27,57	24,07	24,07	23,49	Ct^1	30,46	25,92	26,66	26,92
Ct^2	27,59	23,59	23,59	23,49	Ct^2	30,9	25,92	26,24	N/A
Ct^3	27,61	23,52	23,3	22,87	Ct^3	30,56	25,89	N/A	N/A

Figure 1.3.9 20 µE AOX WT + DPh knock-down

H4	**Dark**				AOX	**Dark**			
	WT	dph-1	dph1'	dph5'		WT	dph-1	dph1'	dph5'
Ct^1	21,89	21,67	22,1	27,02	Ct^1	26,14	26,27	27,84	30,82
Ct^2	22,48	21,66	22,68	26,48	Ct^2	26,79	27,51	28,02	30,4
Ct^3	22,27	21,56	22,54	26,56	Ct^3	26,96	27,59	28,03	31,16
H4	**10' Red 0,2**				AOX	**10' Red 0,2**			
	WT	dph-1	dph1'	dph5'		WT	dph-1	dph1'	dph5'
Ct^1	21,61	22,01	21,19	21,71	Ct^1	25,01	25,04	23,7	25,99
Ct^2	21,58	22,78	21,13	21,64	Ct^2	25,54	25,01	23,54	26,16
Ct^3	22,04	21,87	21,41	21,61	Ct^3	26,29	25,14	23,19	25,75
H4	**30' Red 0,2**				AOX	**30' Red 0,2**			
	WT	dph-1	dph1'	dph5'		WT	dph-1	dph1'	dph5'
Ct^1	23,9	22,58	23,41	24,15	Ct^1	21,77	21,02	20,48	24,38
Ct^2	23,82	22,56	23,33	23,95	Ct^2	21,95	20,86	20,97	24,22
Ct^3	24,2	22,35	23,34	24,05	Ct^3	21,54	21,42	20,79	24,27
H4	**1hr Red 0,2**				AOX	**1hr Red 0,2**			
	WT	dph-1	dph1'	dph5'		WT	dph-1	dph1'	dph5'
Ct^1	27,57	24,07	24,07	23,49	Ct^1	26,5	22,18	21,24	22,26
Ct^2	27,59	23,59	23,59	23,49	Ct^2	26,62	21,31	21,46	22,37
Ct^3	27,61	23,52	23,3	22,87	Ct^3	25,94	21,79	21,68	N/A

Figure 1.3.9 20 µE CHLH1 WT + DPh knock-down

H4	**Dark**				CHLH1	**Dark**			
	WT	dph-1	dph1'	dph5'		WT	dph-1	dph1'	dph5'
Ct^1	21,89	21,67	22,1	27,02	Ct^1	27,97	30,14	32,56	32,92
Ct^2	22,48	21,66	22,68	26,48	Ct^2	28,49	28,83	31,9	32,61
Ct^3	22,27	21,56	22,54	26,56	Ct^3	28,88	29,76	31,74	31,79
H4	**10' Red 0,2**				CHLH1	**10' Red 0,2**			
	WT	dph-1	dph1'	dph5'		WT	dph-1	dph1'	dph5'
Ct^1	21,61	22,01	21,19	21,71	Ct^1	28,83	30,59	31,44	32,82
Ct^2	21,58	22,78	21,13	21,64	Ct^2	28,86	30,61	32,06	32,35
Ct^3	22,04	21,87	21,41	21,61	Ct^3	28,11	30,61	31,55	31,78
H4	**30' Red 0,2**				CHLH1	**30' Red 0,2**			
	WT	dph-1	dph1'	dph5'		WT	dph-1	dph1'	dph5'
Ct^1	23,9	22,58	23,41	24,15	Ct^1	29,86	28,5	32,08	31,29
Ct^2	23,82	22,56	23,33	23,95	Ct^2	29,75	28,49	30,61	30,74
Ct^3	24,2	22,35	23,34	24,05	Ct^3	30,01	28,44	31,67	30,47
H4	**1hr Red 0,2**				CHLH1	**1hr Red 0,2**			
	WT	dph-1	dph1'	dph5'		WT	dph-1	dph1'	dph5'
Ct^1	27,57	24,07	24,07	23,49	Ct^1	29,33	25,87	25,53	27,25
Ct^2	27,59	23,59	23,59	23,49	Ct^2	30,05	25,79	27,36	25,62
Ct^3	27,61	23,52	23,3	22,87	Ct^3	30,13	NA	NA	NA

Figure 1.3.11 LHCF2 WT

	H4						LHCF2			
	Dark A	Dark B	Dark C	Dark D			Dark A	Dark B	Dark C	Dark D
Ct^1	26,15	25,01	26,92	25,31		Ct^1	28,96	31,07	31,33	32,54
Ct^2	25,62	25	26,16	25,49		Ct^2	28,89	31,16	30,8	33
Ct^3	26,01	25,09	26,31	25,64		Ct^3	29,2	31,2	31,38	32,06
	20' A	20' B	20' C	20' D			20' A	20' B	20' C	20' D
Ct^1	25,44	24,31	26,01	25,52		Ct^1	30,02	29,33	29,87	30,97
Ct^2	25,43	24,53	25,87	25,5		Ct^2	29,66	29,52	29,48	30,49
Ct^3	25,46	24,39	26,13	25,49		Ct^3	29,71	29,62	29,86	30,49
	1 hrs A	1 hrs B	1 hrs C	1 hrs D			1 hrs A	1 hrs B	1 hrs C	1 hrs D
Ct^1	26,65	24,75	26,34	24,54		Ct^1	29,11	28,87	30,64	30,12
Ct^2	26,29	24,94	25,99	25,04		Ct^2	29,62	28,86	31,03	30,39
Ct^3	26,6	25,1	26,32	24,99		Ct^3	29,28	29,08	30,71	29,32
	3 hrs A	3 hrs B	3 hrs C	3 hrs D			3 hrs A	3 hrs B	3 hrs C	3 hrs D
Ct^1	N/A	25,92	26,33	25,17		Ct^1	N/A	28,22	30	28,65
Ct^2	N/A	26,09	26,67	25,77		Ct^2	N/A	29,58	30,13	28,59
Ct^3	N/A	25,94	26,78	25,51		Ct^3	N/A	28,58	30,05	28,69
	5 hrs A	5 hrs B	5 hrs C	5 hrs D			5 hrs A	5 hrs B	5 hrs C	5 hrs D
Ct^1	25,15	26,33	26,28	30,49		Ct^1	26,62	27,98	28,07	29,55
Ct^2	25,05	26,5	29,4	33,11		Ct^2	26,71	27,91	27,59	29,44
Ct^3	25,05	26,85	30,3	31,58		Ct^3	26,73	28,19	28,02	29,38

Figure 1.3.11 GSAT WT

	H4						GSAT			
	Dark A	Dark B	Dark C	Dark D			Dark A	Dark B	Dark C	Dark D
Ct^1	26,15	25,01	26,92	25,31		Ct^1	32,71	33,69	33,6	33,69
Ct^2	25,62	25	26,16	25,49		Ct^2	32,48	33,79	34,15	33,01
Ct^3	26,01	25,09	26,31	25,64		Ct^3	32,41	33,6	33,12	33
	20' A	20' B	20' C	20' D			20' A	20' B	20' C	20' D
Ct^1	25,44	24,31	26,01	25,52		Ct^1	31,67	31,88	31,37	32,17
Ct^2	25,43	24,53	25,87	25,5		Ct^2	32,22	31,83	31,64	33,03
Ct^3	25,46	24,39	26,13	25,49		Ct^3	31,58	32,33	31,23	33,28
	1 hrs A	1 hrs B	1 hrs C	1 hrs D			1 hrs A	1 hrs B	1 hrs C	1 hrs D
Ct^1	26,65	24,75	26,34	24,54		Ct^1	31,13	32,13	32,23	31,01
Ct^2	26,29	24,94	25,99	25,04		Ct^2	31,86	33,19	31,88	31,25
Ct^3	26,6	25,1	26,32	24,99		Ct^3	31,37	32,07	33,84	31,38
	3 hrs A	3 hrs B	3 hrs C	3 hrs D			3 hrs A	3 hrs B	3 hrs C	3 hrs D
Ct^1	N/A	25,92	26,33	25,17		Ct^1	N/A	30,86	31,55	29,52
Ct^2	N/A	26,09	26,67	25,77		Ct^2	N/A	32,1	32,07	29,43
Ct^3	N/A	25,94	26,78	25,51		Ct^3	N/A	31,41	31,76	30,08
	5 hrs A	5 hrs B	5 hrs C	5 hrs D			5 hrs A	5 hrs B	5 hrs C	5 hrs D
Ct^1	25,15	26,33	26,28	30,49		Ct^1	28,55	29,64	29,72	31,07
Ct^2	25,05	26,5	29,4	33,11		Ct^2	28,72	30,17	29,87	30,86
Ct^3	25,05	26,85	30,3	31,58		Ct^3	28,62	30,25	29,64	31,34

Figure 1.3.11 CHLH1 WT

	H4						CHLH1			
	Dark A	Dark B	Dark C	Dark D			Dark A	Dark B	Dark C	Dark D
Ct^1	26,15	25,01	26,92	25,31		Ct^1	30,02	31,55	31,7	32,81
Ct^2	25,62	25	26,16	25,49		Ct^2	30,45	32,96	31,92	32,83
Ct^3	26,01	25,09	26,31	25,64		Ct^3	30,28	32,56	32,08	34,03
	20' A	20' B	20' C	20' D			20' A	20' B	20' C	20' D
Ct^1	25,44	24,31	26,01	25,52		Ct^1	31,32	29,8	30,21	30,15
Ct^2	25,43	24,53	25,87	25,5		Ct^2	30,99	30,1	30,38	31,01
Ct^3	25,46	24,39	26,13	25,49		Ct^3	31,09	30,38	30,38	31,55
	1 hrs A	1 hrs B	1 hrs C	1 hrs D			1 hrs A	1 hrs B	1 hrs C	1 hrs D
Ct^1	26,65	24,75	26,34	24,54		Ct^1	30,09	30,2	31,25	30,45
Ct^2	26,29	24,94	25,99	25,04		Ct^2	30,03	30,59	31,78	30,94
Ct^3	26,6	25,1	26,32	24,99		Ct^3	29,65	30	31,48	30,36
	3 hrs A	3 hrs B	3 hrs C	3 hrs D			3 hrs A	3 hrs B	3 hrs C	3 hrs D
Ct^1	N/A	25,92	26,33	25,17		Ct^1	N/A	29,46	31,06	29,63
Ct^2	N/A	26,09	26,67	25,77		Ct^2	N/A	29,71	31,2	29,78
Ct^3	N/A	25,94	26,78	25,51		Ct^3	N/A	30	31,27	30,06
	5 hrs A	5 hrs B	5 hrs C	5 hrs D			5 hrs A	5 hrs B	5 hrs C	5 hrs D
Ct^1	25,15	26,33	26,28	30,49		Ct^1	27,91	28,29	28,75	30,13
Ct^2	25,05	26,5	29,4	33,11		Ct^2	28,4	28,55	28,67	30,48
Ct^3	25,05	26,85	30,3	31,58		Ct^3	28,18	28,25	28,91	N/A

Figure 1.3.11 LHCF2 dph-2

	H4						LHCF2			
	Dark A	Dark B	Dark C	Dark D			Dark A	Dark B	Dark C	Dark D
Ct^1	25,19	25,41	25,17	28,61		Ct^1	29,35	30,74	30,53	31,72
Ct^2	25,02	25,49	25,13	29,05		Ct^2	29,01	30,99	30,53	32,25
Ct^3	25,19	25,58	25,2	28,92		Ct^3	30,23	29,46	30,44	32,39
	20' A	20' B	20' C	20' D			20' A	20' B	20' C	20' D
Ct^1	24,81	24,6	24,44	26,29		Ct^1	31,17	29,34	31,12	32,08
Ct^2	24,93	24,83	24,35	26,41		Ct^2	31,11	29,52	29,6	31,02
Ct^3	25,05	24,87	24,48	26,88		Ct^3	31,2	29,43	30,65	31,31
	1 hrs A	1 hrs B	1 hrs C	1 hrs D			1 hrs A	1 hrs B	1 hrs C	1 hrs D
Ct^1	27,31	26,66	27,81	26,11		Ct^1	32,54	31,22	N/A	30,56
Ct^2	27,49	26,65	27,52	26,31		Ct^2	31,94	31,23	31,43	30,13
Ct^3	27,46	26,86	27,48	26,3		Ct^3	31,66	30,82	33,15	30,7
	3 hrs A	3 hrs B	3 hrs C	3 hrs D			3 hrs A	3 hrs B	3 hrs C	3 hrs D
Ct^1	29,1	27,02	27,33	25,65		Ct^1	32,74	30,95	31,26	29,52
Ct^2	29,9	27,34	27,19	26,17		Ct^2	33,12	30,82	31,41	29,56
Ct^3	29,24	27,17	27,29	25,93		Ct^3	N/A	31,44	31,6	28,91
	5 hrs A	5 hrs B	5 hrs C	5 hrs D			5 hrs A	5 hrs B	5 hrs C	5 hrs D
Ct^1	25,26	26,01	25,74	N/A		Ct^1	27,97	30,33	29,12	N/A
Ct^2	25,37	25,96	25,48	N/A		Ct^2	29,03	29,77	29,08	N/A
Ct^3	25,28	26,27	25,32	N/A		Ct^3	28,23	29,15	28,89	N/A

Figure 1.3.11 GSAT dph-2

	H4						GSAT			
	Dark A	Dark B	Dark C	Dark D			Dark A	Dark B	Dark C	Dark D
Ct^1	25,19	25,41	25,17	28,61		Ct^1	41,78	39,74	44,34	43,5
Ct^2	25,02	25,49	25,13	29,05		Ct^2	39,57	40,82	N/A	N/A
Ct^3	25,19	25,58	25,2	28,92		Ct^3	42,44	41,91	42,15	43,01
	20' A	20' B	20' C	20' D			20' A	20' B	20' C	20' D
Ct^1	24,81	24,6	24,44	26,29		Ct^1	42,53	42,41	N/A	40,76
Ct^2	24,93	24,83	24,35	26,41		Ct^2	41,01	39,31	38,29	40,33
Ct^3	25,05	24,87	24,48	26,88		Ct^3	N/A	41,47	38,32	41,74
	1 hrs A	1 hrs B	1 hrs C	1 hrs D			1 hrs A	1 hrs B	1 hrs C	1 hrs D
Ct^1	27,31	26,66	27,81	26,11		Ct^1	N/A	40,2	N/A	N/A
Ct^2	27,49	26,65	27,52	26,31		Ct^2	40,43	N/A	N/A	N/A
Ct^3	27,46	26,86	27,48	26,3		Ct^3	N/A	N/A	N/A	39,58
	3 hrs A	3 hrs B	3 hrs C	3 hrs D			3 hrs A	3 hrs B	3 hrs C	3 hrs D
Ct^1	29,1	27,02	27,33	25,65		Ct^1	44,9	40,27	N/A	38,29
Ct^2	29,9	27,34	27,19	26,17		Ct^2	N/A	N/A	43,05	41,53
Ct^3	29,24	27,17	27,29	25,93		Ct^3	N/A	44,03	41,8	37,81
	5 hrs A	5 hrs B	5 hrs C	5 hrs D			5 hrs A	5 hrs B	5 hrs C	5 hrs D
Ct^1	25,26	26,01	25,74	N/A		Ct^1	42,41	N/A	N/A	N/A
Ct^2	25,37	25,96	25,48	N/A		Ct^2	38,68	N/A	N/A	N/A
Ct^3	25,28	26,27	25,32	N/A		Ct^3	42,14	N/A	N/A	N/A

Figure 1.3.11 CHLH1 dph-2

	H4						CHLH1			
	Dark A	Dark B	Dark C	Dark D			Dark A	Dark B	Dark C	Dark D
Ct^1	25,19	25,41	25,17	28,61		Ct^1	33,17	31,94	33,49	33,29
Ct^2	25,02	25,49	25,13	29,05		Ct^2	32,77	31,27	31,37	32,57
Ct^3	25,19	25,58	25,2	28,92		Ct^3	32,9	31,55	32,02	32,52
	20' A	20' B	20' C	20' D			20' A	20' B	20' C	20' D
Ct^1	24,81	24,6	24,44	26,29		Ct^1	32,9	31,96	31,5	32,11
Ct^2	24,93	24,83	24,35	26,41		Ct^2	32,47	31,51	31,39	32,39
Ct^3	25,05	24,87	24,48	26,88		Ct^3	31,57	31,49	31,44	34,97
	1 hrs A	1 hrs B	1 hrs C	1 hrs D			1 hrs A	1 hrs B	1 hrs C	1 hrs D
Ct^1	27,31	26,66	27,81	26,11		Ct^1	33,96	33,07	32,48	31,58
Ct^2	27,49	26,65	27,52	26,31		Ct^2	33,39	31,03	32,34	32,58
Ct^3	27,46	26,86	27,48	26,3		Ct^3	33,16	31,13	31,71	31,96
	3 hrs A	3 hrs B	3 hrs C	3 hrs D			3 hrs A	3 hrs B	3 hrs C	3 hrs D
Ct^1	29,1	27,02	27,33	25,65		Ct^1	33,89	32,81	32,43	31,48
Ct^2	29,9	27,34	27,19	26,17		Ct^2	32,92	33,17	32,37	31,03
Ct^3	29,24	27,17	27,29	25,93		Ct^3	33,15	31,9	31,54	32,74
	5 hrs A	5 hrs B	5 hrs C	5 hrs D			5 hrs A	5 hrs B	5 hrs C	5 hrs D
Ct^1	25,26	26,01	25,74	N/A		Ct^1	30,03	31,74	32,12	N/A
Ct^2	25,37	25,96	25,48	N/A		Ct^2	30,35	31,68	31,73	N/A
Ct^3	25,28	26,27	25,32	N/A		Ct^3	30,88	30,92	31,62	N/A

Figure 1.3.12 DPh 2 and 20 µE

2 µE				20 µE			
RPS + DCMU				RPS + DCMU			
	Ct^1	Ct^2	Ct^3		Ct^1	Ct^2	Ct^3
Dark	27,51	27,29	27,1	Dark	27,81	28,07	27,92
30min	30,01	29,94	30,09	30min	29,54	29,24	29,25
1hr	29,22	28,87	29,08	1hr	28,24	28,3	28,23
2hrs	29,1	29,19	29,1	2hrs	28,25	28,43	28,44
DPh + DCMU				DPh + DCMU			
	Ct^1	Ct^2	Ct^3		Ct^1	Ct^2	ct^3
Dark	31,92	31,79	31,79	Dark	31,58	31,62	31,57
30min	35,35	34,67	35,52	30min	35,2	33,33	35,3
1hr	32,94	33,43	34,28	1hr	33,47	34,33	33,12
2 hrs	33,23	32,95	32,2	2 hrs	32,89	34,27	34,06
RPS - DCMU				RPS-DCMU			
	Ct^1	Ct^2	Ct^3		Ct^1	Ct^2	Ct^3
Dark	27,51	27,29	27,1	Dark	27,81	28,07	27,92
30min	26,53	26,58	26,49	30min	27,16	26,94	26,97
1hr	26,92	26,67	26,66	1hr	26,01	25,91	25,8
2hrs	25,77	25,98	26,29	2hrs	25,44	25,19	25,33
DPh - DCMU				DPh - DCMU			
	Ct^1	Ct^2	Ct^3		Ct^1	Ct^2	Ct^3
Dark	31,92	31,79	31,79	Dark	31,58	31,62	31,57
30min	30,98	31,05	31,03	30min	30,58	30,28	30,62
1hr	31,22	31,74	31,47	1hr	30,15	30,38	30,26
2 hrs	30,94	31,06	31,22	2 hrs	29,61	29,67	30,33

Figure 1.3.12 AOX 2 and 20 µE

2 µE				20 µE			
RPS + DCMU				RPS + DCMU			
	Ct^1	Ct^2	Ct^3		Ct^1	Ct^2	Ct^3
Dark	27,51	27,29	27,1	Dark	27,81	28,07	27,92
30min	30,01	29,94	30,09	30min	29,54	29,24	29,25
1hr	29,22	28,87	29,08	1hr	28,24	28,3	28,23
2hrs	29,1	29,19	29,1	2hrs	28,25	28,43	28,44
AOX + DCMU				AOX + DCMU			
	Ct^1	Ct^2	Ct^3		Ct^1	Ct^2	Ct^3
Dark	29,64	29,61	29,58	Dark	29,75	29,94	30,43
30min	31,51	31,22	31,4	30min	30,44	30,57	30,66
1hr	31,32	31,17	30,76	1hr	29,88	29,44	29,46
2 hrs	29,99	29,88	29,9	2 hrs	30,02	29,85	29,84
RPS - DCMU				RPS-DCMU			
	Ct^1	Ct^2	Ct^3		Ct^1	Ct^2	Ct^3
Dark	27,51	27,29	27,1	Dark	27,81	28,07	27,92
30min	26,53	26,58	26,49	30min	27,16	26,94	26,97
1hr	26,92	26,67	26,66	1hr	26,01	25,91	25,8
2hrs	25,77	25,98	26,29	2hrs	25,44	25,19	25,33
AOX - DCMU				AOX - DCMU			
	Ct^1	Ct^2	Ct^3		Ct^1	Ct^2	Ct^3
Dark	29,64	29,61	29,58	Dark	29,75	29,94	30,43
30min	27,12	27,16	27,03	30min	26,45	26,46	26,44
1hr	28,24	28,36	28,33	1hr	26,68	26,46	26,5
2 hrs	27,95	27,71	28	2 hrs	26,82	26,68	26,72

Figure 1.3.12 CHLH1 2 and 20 µE

	2 µE				20 µE		
RPS + DCMU	Ct^1	Ct^2	Ct^3	RPS + DCMU	Ct^1	Ct^2	Ct^3
Dark	27,68	27,53	27,47	Dark	29,51	29,43	29,17
30min	27,93	27,85	27,8	30min	30,82	30,53	31,04
1 hr	27,98	29,19	29,16	1 hr	28,28	28,23	28,2
2 hrs	29,76	29,63	29,71	2 hrs	27,96	28,07	27,83
CHLH1+DCMU	Ct^1	Ct^2	Ct^3	CHLH1+DCMU	Ct^1	Ct^2	Ct^3
Dark	33,35	33,73	33,27	Dark	34,06	34,7	34,36
30min	33,64	34,01	33,35	30min	35,47	N/A	34,67
1hr	33,93	34,59	34	1hr	35,36	34,05	34,12
2hrs	36,15	42,28	36,76	2hrs	37,08	34,19	34,84
RPS - DCMU	Ct^1	Ct^2	Ct^3	RPS - DCMU	Ct^1	Ct^2	Ct^3
Dark	27,68	27,53	27,47	Dark	29,51	29,43	29,17
30min	27,02	26,76	26,72	30min	27,21	26,98	26,99
1 hr	27,8	27,93	28,24	1 hr	26,63	26,55	37,76
2 hrs	29,52	25,96	26,03	2 hrs	26,59	26,83	26,75
CHLH1 -DCMU	Ct^1	Ct^2	Ct^3	CHLH1 -DCMU	Ct^1	Ct^2	Ct^3
Dark	33,35	33,73	33,27	Dark	34,06	34,7	34,36
30min	30,51	30,93	30,89	30min	30,54	30,46	30,19
1hr	28,91	29,07	28,97	1 hr	28,09	28	N/A
2hrs	27,53	27,28	27,64	2 hrs	27,75	27,91	27,94

Figure 1.3.12 HEMA 2 and 20 µE

	2 µE				20 µE		
RPS + DCMU	Ct^1	Ct^2	Ct^3	RPS + DCMU	Ct^1	Ct^2	Ct^3
Dark	27,68	27,53	27,47	Dark	29,51	29,43	29,17
30min	27,93	27,85	27,8	30min	30,82	30,53	31,04
1 hr	27,98	29,19	29,16	1 hr	28,28	28,23	28,2
2 hrs	29,76	29,63	29,71	2 hrs	27,96	28,07	27,83
HEMA+DCMU	Ct^1	Ct^2	Ct^3	HEMA+DCMU	Ct^1	Ct^2	Ct^3
Dark	31,67	32,08	31,5	Dark	32,97	33,78	33,31
30min	31,94	32,32	32,18	30min	34,19	35,25	34,45
1hr	33,49	33,59	33,89	1hr	32,23	32,4	32,3
2hrs	33,9	34,53	33,26	2hrs	32,23	32,3	32,34
RPS - DCMU	Ct^1	Ct^2	Ct^3	RPS - DCMU	Ct^1	Ct^2	Ct^3
Dark	27,68	27,53	27,47	Dark	29,51	29,43	29,17
30min	27,02	26,76	26,72	30min	27,21	26,98	26,99
1 hr	27,8	27,93	28,24	1 hr	26,63	26,55	37,76
2 hrs	29,52	25,96	26,03	2 hrs	26,59	26,83	26,75
HEMA -DCMU	Ct^1	Ct^2	Ct^3	HEMA -DCMU	Ct^1	Ct^2	Ct^3
Dark	31,67	32,08	31,5	Dark	32,97	33,78	33,31
30min	28,69	28,93	29,16	30min	28,92	29,07	29,01
1hr	29,37	29,37	29,61	1 hr	28,42	28,55	N/A
2hrs	28,6	28,26	28,32	2 hrs	28,87	28,99	29,08

Figure 1.3.12 VDL1 2 and 20 µE

	2 µE				20 µE		
RPS+DCMU	Ct^1	Ct^2	Ct^3	RPS + DCMU	Ct^1	Ct^2	Ct^3
Dark	27,68	27,53	27,47	Dark	29,51	29,43	29,17
30min	27,93	27,85	27,8	30min	30,82	30,53	31,04
1 hr	27,98	29,19	29,16	1 hr	28,28	28,23	28,2
2 hrs	29,76	29,63	29,71	2 hrs	27,96	28,07	27,83
VDL1+DCMU	Ct^1	Ct^2	Ct^3	VDL1+DCMU	Ct^1	Ct^2	Ct^3
Dark	32,39	32,4	31,92	Dark	34,06	33,78	33,62
30min	33,01	33,04	33,25	30min	37,95	35,18	36,48
1hr	33,8	34,31	33,7	1hr	34,96	34,19	33,91
2hrs	33,87	33,67	33,86	2hrs	33,38	33,18	33,03
RPS - DCMU	Ct^1	Ct^2	Ct^3	RPS - DCMU	Ct^1	Ct^2	Ct^3
Dark	27,68	27,53	27,47	Dark	29,51	29,43	29,17
30min	27,02	26,76	26,72	30min	27,21	26,98	26,99
1 hr	27,8	27,93	28,24	1 hr	26,63	26,55	37,76
2 hrs	29,52	25,96	26,03	2 hrs	26,59	26,83	26,75
VDL1 -DCMU	Ct^1	Ct^2	Ct^3	VDL1 -DCMU	Ct^1	Ct^2	Ct^3
Dark	32,39	32,4	31,92	Dark	34,06	33,78	33,62
30min	31,09	31,24	31,15	30min	32,06	31,81	31,69
1 hr	31,64	31,4	31,28	1 hr	30,57	30,93	N/A
2 hrs	30,36	30,14	30,17	2 hrs	30,97	30,97	30,9

Figure 1.3.13 LHCF2 WT + DPh knock-down lines

	H4						LHCF2				
	WT 5 µmols						WT 5 µmols				
	Dark	30'	1hr	3hrs	5hrs		Dark	30'	1hr	3hrs	5hrs
Ct^1	26,72	26,39	34,45	25,83	26,03	Ct^1	32,04	31,37	N/A	31,19	31,19
Ct^2	27	26,71	34,6	26,06	25,75	Ct^2	32,34	32,5	37,85	32	32
Ct^3	27,03	26,45	34,46	25,73	25,5	Ct^3	32,66	31,82	N/A	31,56	31,56
	WT 100 µmols						WT 100 µmols				
	Dark	30'	1hr	3hrs	5hrs		Dark	30'	1hr	3hrs	5hrs
Ct^1	29,56	27,62	27,65	26,6	24,76	Ct^1	34,84	33,23	32,57	33,34	31,44
Ct^2	29,36	27,39	27,68	26,97	24,96	Ct^2	35,53	34,86	32,57	32,1	31,9
Ct^3	29,82	27,49	27,57	26,66	24,78	Ct^3	36,2	34	32,48	31,29	32,18
	WT control						WT control				
	Dark	30'	1hr	3hrs	5hrs		Dark	30'	1hr	3hrs	5hrs
Ct^1	26,71	27,7	27,73	25,46	25,26	Ct^1	32,14	34,33	33,83	31,77	30,27
Ct^2	26,95	27,79	27,8	25,75	25,43	Ct^2	31,9	32,86	33,19	31,13	31,02
Ct^3	27,18	28,02	27,9	25,54	25,39	Ct^3	32,18	33,77	34,02	30,84	34,39
	dph-2 5 µmols						dph-2 5 µmols				
	Dark	30'	1hr	3hrs	5hrs		Dark	30'	1hr	3hrs	5hrs
Ct^1	27,29	26,65	28,47	26,26	26,04	Ct^1	32,14	32,36	34,06	32,33	31,11
Ct^2	27,2	26,79	28,5	26,27	26,04	Ct^2	31,86	31,26	36,57	32,88	31,16
Ct^3	27,25	26,8	28,51	26,24	25,97	Ct^3	32,08	31,31	34,78	33,15	31,88
	dph-2 100 µmols						dph-2 100 µmols				
	Dark	30'	1hr	3hrs	5hrs		Dark	30'	1hr	3hrs	5hrs
Ct^1	26,58	27,24	26,82	26,66	26,91	Ct^1	30,35	29,56	29,77	30,17	31,49
Ct^2	26,64	27,28	26,69	26,48	27,48	Ct^2	30,16	30,02	29,68	30,04	33,11
Ct^3	27,08	27,29	27,15	26,32	27,05	Ct^3	31	29,6	29,85	29,49	32,2
	dph-5' 5 µmols						dph-5' 5 µmols				
	Dark	30'	1hr	3hrs	5hrs		Dark	30'	1hr	3hrs	5hrs
Ct^1	27,31	27,49	26,99	26,99	24,22	Ct^1	31,27	32,13	31,01	30,61	27,96
Ct^2	27,74	27,64	26,98	27,27	24,36	Ct^2	32,79	32,16	31,79	30,8	28,04
Ct^3	27,86	27,61	26,6	26,86	24,73	Ct^3	32,07	33,93	30,9	31,1	28,17
	dph-5' 100 µmols						dph-5' 100 µmols				
	Dark	30'	1hr	3hrs	5hrs		Dark	30'	1hr	3hrs	5hrs
Ct^1	28,11	27	26,49	26,33	26,59	Ct^1	30,31	29,97	30,97	30,14	29,73
Ct^2	28,13	27,05	26,67	26,46	26,58	Ct^2	30,5	29,54	30,54	30,07	31,58
Ct^3	28,21	27,92	26,87	26,5	26,74	Ct^3	30,9	29,5	31,5	29,83	30,46

Figure 1.3.13 CHLH1 WT + DPh knock-down lines

	H4							CHLH1				
	WT 5 µmols							WT 5 µmols				
	Dark	30'	1hr	3hrs	5hrs			Dark	30'	1hr	3hrs	5hrs
Ct^1	26,72	26,39	34,45	25,83	26,03		Ct^1	30,44	30,56	35,19	28,13	29,18
Ct^2	27	26,71	34,6	26,06	25,75		Ct^2	31,29	30,34	36,29	28,35	29,52
Ct^3	27,03	26,45	34,46	25,73	25,5		Ct^3	31,43	30,85	35,22	28,21	29,44
	WT 100 µmols							WT 100 µmols				
	Dark	30'	1hr	3hrs	5hrs			Dark	30'	1hr	3hrs	5hrs
Ct^1	29,56	27,62	27,65	26,6	24,76		Ct^1	32,49	30,46	28,68	29,43	27,14
Ct^2	29,36	27,39	27,68	26,97	24,96		Ct^2	33,69	30,36	28,24	29,74	27,2
Ct^3	29,82	27,49	27,57	26,66	24,78		Ct^3	33,32	30,88	28,01	29,95	27,44
	WT control							WT control				
	Dark	30'	1hr	3hrs	5hrs			Dark	30'	1hr	3hrs	5hrs
Ct^1	26,71	27,7	27,73	25,46	25,26		Ct^1	31,06	31,14	31,57	30,79	29,15
Ct^2	26,95	27,79	27,8	25,75	25,43		Ct^2	31,36	31,09	32,25	29,7	29,23
Ct^3	27,18	28,02	27,9	25,54	25,39		Ct^3	31,43	31,52	32,14	30,48	29,22
	dph-2 5 µmols							dph-2 5 µmols				
	Dark	30'	1hr	3hrs	5hrs			Dark	30'	1hr	3hrs	5hrs
Ct^1	27,29	26,65	28,47	26,26	26,04		Ct^1	30,78	30,68	29,12	29,16	29,71
Ct^2	27,2	26,79	28,5	26,27	26,04		Ct^2	31,62	30,74	29,9	29,08	30,16
Ct^3	27,25	26,8	28,51	26,24	25,97		Ct^3	31,67	30,33	29,18	29,15	29,88
	dph-2 100 µmols							dph-2 100 µmols				
	Dark	30'	1hr	3hrs	5hrs			Dark	30'	1hr	3hrs	5hrs
Ct^1	26,58	27,24	26,82	26,66	26,91		Ct^1	30,56	31,46	30,81	31,04	N/A
Ct^2	26,64	27,28	26,69	26,48	27,48		Ct^2	31,37	31,86	30,73	31,96	N/A
Ct^3	27,08	27,29	27,15	26,32	27,05		Ct^3	32,22	32,01	30,13	31,66	N/A
	dph-5' 5 µmols							dph-5' 5 µmols				
	Dark	30'	1hr	3hrs	5hrs			Dark	30'	1hr	3hrs	5hrs
Ct^1	27,31	27,49	26,99	26,99	24,22		Ct^1	31,94	32,15	31,63	32,5	31,63
Ct^2	27,74	27,64	26,98	27,27	24,36		Ct^2	32,53	34,03	32,01	32,52	31,87
Ct^3	27,86	27,61	26,6	26,86	24,73		Ct^3	32,64	33,21	31,87	32,61	32,14
	dph-5' 100 µmols							dph-5' 100 µmols				
	Dark	30'	1hr	3hrs	5hrs			Dark	30'	1hr	3hrs	5hrs
Ct^1	28,11	27	26,49	26,33	26,59		Ct^1	31,36	32,23	31,83	31,55	31,03
Ct^2	28,13	27,05	26,67	26,46	26,58		Ct^2	31,87	31,79	31,04	31,51	31,77
Ct^3	28,21	27,92	26,87	26,5	26,74		Ct^3	31,89	31,18	31,05	31,92	31,74

Figure 1.3.13 GSAT WT + DPh knock-down lines

	H4							GSAT				
	WT 5 µmols							WT 5 µmols				
	Dark	30'	1hr	3hrs	5hrs			Dark	30'	1hr	3hrs	5hrs
Ct^1	26,72	26,39	34,45	25,83	26,03		Ct^1	35,14	32,61	N/A	30,59	32,81
Ct^2	27	26,71	34,6	26,06	25,75		Ct^2	37,85	33,24	N/A	30,97	31,63
Ct^3	27,03	26,45	34,46	25,73	25,5		Ct^3	38,05	32,91	35,95	30,82	31,89
	WT 100 µmols							WT 100 µmols				
	Dark	30'	1hr	3hrs	5hrs			Dark	30'	1hr	3hrs	5hrs
Ct^1	29,56	27,62	27,65	26,6	24,76		Ct^1	39,79	34,99	33,17	31,73	31,65
Ct^2	29,36	27,39	27,68	26,97	24,96		Ct^2	39,29	33,41	32,9	32,09	32,11
Ct^3	29,82	27,49	27,57	26,66	24,78		Ct^3	N/A	32,50	33,53	32,12	32,05
	WT control							WT control				
	Dark	30'	1hr	3hrs	5hrs			Dark	30'	1hr	3hrs	5hrs
Ct^1	26,71	27,7	27,73	25,46	25,26		Ct^1	42,27	33,48	33,56	31,34	N/A
Ct^2	26,95	27,79	27,8	25,75	25,43		Ct^2	40,86	33,13	34,17	31,37	N/A
Ct^3	27,18	28,02	27,9	25,54	25,39		Ct^3	39,27	33,86	32,65	31,62	N/A
	dph-2 5 µmols							dph-2 5 µmols				
	Dark	30'	1hr	3hrs	5hrs			Dark	30'	1hr	3hrs	5hrs
Ct^1	27,29	26,65	28,47	26,26	26,04		Ct^1	39,35	34,57	35,26	32,38	32,66
Ct^2	27,2	26,79	28,5	26,27	26,04		Ct^2	39,4	33,94	37,02	33,04	32,73
Ct^3	27,25	26,8	28,51	26,24	25,97		Ct^3	39,92	34,75	N/A	32,4	32,44
	dph-2 100 µmols							dph-2 100 µmols				
	Dark	30'	1hr	3hrs	5hrs			Dark	30'	1hr	3hrs	5hrs
Ct^1	26,58	27,24	26,82	26,66	26,91		Ct^1	41,47	N/A	40,95	38,59	38,47
Ct^2	26,64	27,28	26,69	26,48	27,48		Ct^2	39,07	N/A	38,17	N/A	39,6
Ct^3	27,08	27,29	27,15	26,32	27,05		Ct^3	39,78	N/A	38,16	40,38	39,33
	dph-5' 5 µmols							dph-5' 5 µmols				
	Dark	30'	1hr	3hrs	5hrs			Dark	30'	1hr	3hrs	5hrs
Ct^1	27,31	27,49	26,99	26,99	24,22		Ct^1	40,88	38,84	N/A	44,26	39,9
Ct^2	27,74	27,64	26,98	27,27	24,36		Ct^2	39,4	38,39	N/A	39,48	39,12
Ct^3	27,86	27,61	26,6	26,86	24,73		Ct^3	39,15	39,63	N/A	37,49	37,43
	dph-5' 100 µmols							dph-5' 100 µmols				
	Dark	30'	1hr	3hrs	5hrs			Dark	30'	1hr	3hrs	5hrs
Ct^1	28,11	27	26,49	26,33	26,59		Ct^1	37,8	40,8	39,14	N/A	38,01
Ct^2	28,13	27,05	26,67	26,46	26,58		Ct^2	39,55	39,07	39,36	N/A	37,13
Ct^3	28,21	27,92	26,87	26,5	26,74		Ct^3	38,87	N/A	38,97	N/A	37,04

Figure 1.3.14 LHCF1WT

ACTIN				LHCF1			
Red	Ct^1	Ct^2	Ct^3	**Red**	Ct^1	Ct^2	Ct^3
Dark	27,63	27,28	27,78	Dark	25,03	24,81	25,13
3hrs	29,79	28,68	28,61	3hrs	26,45	26,4	27,24
5hrs	27,81	27,95	27,76	5hrs	24,43	24,49	24,84
FarRed				**FarRed**			
	Ct^1	Ct^2	Ct^3		Ct^1	Ct^2	Ct^3
Dark	29,14	29,18	28,98	Dark	26,45	25,71	26,15
3hrs	28,22	28,19	28,02	3hrs	25,79	25,26	25,31
5hrs	27,45	27,09	26,74	5hrs	25,1	25,77	26
Red+ Far-red				**Red+ Far-red**			
	Ct^1	Ct^2	Ct^3		Ct^1	Ct^2	Ct^3
Dark	27,1	27,44	27,85	Dark	24,67	24,24	25
3hrs	25,97	26,28	26,17	3hrs	22,93	23,01	23,54
5hrs	29,43	29,44	29,31	5hrs	26,34	25,71	25,64
Far-red+Red				**Far-red+Red**			
	Ct^1	Ct^2	Ct^3		Ct^1	Ct^2	Ct^3
Dark	30,18	29,14	29,46	Dark	26,6	27,03	26,95
3hrs	30,02	30,38	29,99	3hrs	27,22	27,41	27,98
5hrs	26,89	32,23	27,28	5hrs	23,74	23,56	24,01

Figure 1.3.14 LHCF2WT

ACTIN				LHCF2			
Red				**Red**			
	Ct^1	Ct^2	Ct^3		Ct^1	Ct^2	Ct^3
Dark	27,63	27,28	27,78	Dark	24,6	24,41	24,33
3hrs	29,79	28,68	28,61	3hrs	25,49	25,64	25,5
5hrs	27,81	27,95	27,76	5hrs	24,28	24,64	24,7
FarRed				**FarRed**			
	Ct^1	Ct^2	Ct^3		Ct^1	Ct^2	Ct^3
Dark	29,14	29,18	28,98	Dark	25,63	26,29	26,59
3hrs	28,22	28,19	28,02	3hrs	24,23	25,06	24,62
5hrs	27,45	27,09	26,74	5hrs	25,59	25,54	25,61
Red+ Far-red				**Red+ Far-red**			
	Ct^1	Ct^2	Ct^3		Ct^1	Ct^2	Ct^3
Dark	27,1	27,44	27,85	Dark	24,66	24,66	24,34
3hrs	25,97	26,28	26,17	3hrs	23,47	23,71	23,3
5hrs	29,43	29,44	29,31	5hrs	26,06	25,91	25,76
Far-red+Red				**Far-red+Red**			
	Ct^1	Ct^2	Ct^3		Ct^1	Ct^2	Ct^3
Dark	30,18	29,14	29,46	Dark	26,88	26,77	26,54
3hrs	30,02	30,38	29,99	3hrs	28,16	27,65	28,01
5hrs	26,89	32,23	27,28	5hrs	24,18	24,2	24,16